



# On QCD Corrections to Jet Functions and Deep Inelastic Scattering

On QCD Corrections to Jet Functions and Deep Inelastic Scattering

Avanish Prashan Basdew-Sharma

Avanish Prashan Basdew-Sharma

# On QCD Corrections to Jet Functions and Deep Inelastic Scattering

Avanish Prashan Basdew-Sharma

---

**Title:** On QCD Corrections to Jet Functions  
and Deep Inelastic Scattering  
**ISBN:** 978-94-6483-209-9  
**Cover and printed by:** Ridderprint, the Netherlands

Nikhef



UNIVERSITY OF AMSTERDAM

This work is supported by the NWO Vidi grant 680-47-551.  
NWO is the Dutch Research Council.

# On QCD Corrections to Jet Functions and Deep Inelastic Scattering

## ACADEMISCH PROEFSCHRIFT

ter verkrijging van de graad van doctor

aan de Universiteit van Amsterdam

op gezag van de Rector Magnificus

prof. dr. ir. P.P.C.C. Verbeek

ten overstaan van een door het College voor Promoties ingestelde commissie,

in het openbaar te verdedigen in de Aula der Universiteit

op vrijdag 30 juni 2023, te 14.00 uur

door Avanish Prashan Basdew-Sharma

geboren te Amsterdam



***Promotiecommissie***

<i>Promotor:</i>	prof. dr. E.L.M.P. Laenen	Universiteit van Amsterdam
<i>Copromotor:</i>	dr. F. Herzog	The University of Edinburgh
<i>Overige leden:</i>	prof. dr. M. Vreeswijk dr. M.E.J. Postma prof. dr. A. Vogt dr. J. de Vries dr. J. Rojo dr. W.J. Waalewijn	Universiteit van Amsterdam Nikhef University of Liverpool Universiteit van Amsterdam Vrije Universiteit Amsterdam Universiteit van Amsterdam

Faculteit der Natuurwetenschappen, Wiskunde en Informatica

---

*Dedicated to my grandparents Mama Nanie and Baab Nana,  
who both passed away in the four years that I spent conducting  
research to complete this thesis.*

---

The material presented in this thesis is based on the following publications:

- [1] A. Basdew-Sharma, F. Herzog, S. Schrijnder van Velzen and W. J. Waalewijn, *One-loop jet functions by geometric subtraction*, *JHEP* **10** (2020) 118 [2006.14627].
- [2] A. Basdew-Sharma, *Towards DIS at  $N_4LO$* , *SciPost Phys. Proc.* **8** (2022) 153 [2108.00459].
- [3] A. Basdew-Sharma, A. Pelloni, F. Herzog and A. Vogt, *Four-loop large- $n_f$  contributions to the non-singlet structure functions  $F_2$  and  $F_L$* , *JHEP* **03** (2023) 183 [2211.16485].

In [1] I worked on the application of the Geometric Subtraction scheme to one-loop jet functions. In order to do so, I modified the scheme and implemented it in MATHEMATICA. Subsequently I optimised the implementation. I tested the resulting procedure thoroughly on a range of known jet functions. Moreover, I used the scheme to calculate the angularity jet function including recoil effects, which has never been done before. I wrote a significant part of the paper.

In [2] I worked on the development of the recursive algorithm to calculate Mellin moments in Deep Inelastic Scattering (DIS). In particular I worked on the reduction of loop integrals to master integrals. I optimised this part of the workflow using FIRE and MATHEMATICA. I furthermore contributed to the calculation of the differential matrices and the recursive calculation of the master integrals. I wrote the paper.

In [3] the techniques described in [2] are applied to DIS. I generated the required scalar loop integrals and reduced them to master integrals, using my automated procedure. On top of that I mapped, when required, the original master integrals into a new basis of master integrals in which the  $\epsilon$ -dependence factorizes from the  $\omega$ -dependence. The factorized coefficients are crucial in order to be able to expand the differential matrices. I subsequently generated the differential matrices, which were used to recursively compute the DIS Mellin moments. I contributed to section 3 and section 6 of the paper.



# Contents

<b>Introduction</b>	<b>13</b>
<b>1 Background</b>	<b>21</b>
1.1 Quantum Chromo Dynamics . . . . .	21
1.1.1 The Standard Model . . . . .	21
1.1.2 Quantum Chromo Dynamics Fundamentals . . . . .	22
1.1.3 Asymptotic Freedom and Confinement . . . . .	27
1.2 Deep Inelastic Scattering . . . . .	35
1.2.1 The Hadronic Tensor . . . . .	36
1.2.2 The Parton Model . . . . .	39
1.2.3 Evolution of Parton Distributions . . . . .	44
1.3 IR Singularities . . . . .	46
1.4 Integration By Parts . . . . .	49
1.4.1 Dimensional regularization . . . . .	49
1.4.2 Applications of the IBP relation . . . . .	53
1.4.3 General structure of the reduction . . . . .	57
1.4.4 Laporta’s Algorithm . . . . .	59
1.4.5 Lorentz Identities . . . . .	60
1.4.6 FIRE . . . . .	61
<b>2 One-loop Jet Functions by Geometric Subtraction</b>	<b>65</b>
2.1 Introduction . . . . .	65
2.2 General Method . . . . .	67
2.2.1 Subtraction scheme . . . . .	68
2.2.2 Delta and theta functions . . . . .	74
2.2.3 Infrared safety and limitations on the observable . . . . .	76
2.2.4 Example: Angularities with the Winner-Take-All axis . . . . .	76
2.3 GOJET Program . . . . .	78
2.3.1 Functions . . . . .	78
2.3.2 Input format . . . . .	79
2.3.3 Example: $k_T$ clustering algorithms . . . . .	82

2.4	Applications . . . . .	83
2.4.1	Cone jet . . . . .	83
2.4.2	Angularities with recoil . . . . .	84
2.4.3	Jet shape . . . . .	88
2.5	Conclusions . . . . .	88
<b>3</b>	<b>Four-loop large-<math>n_f</math> contributions to the non-singlet structure functions <math>F_2</math> and <math>F_L</math></b>	<b>91</b>
3.1	Introduction . . . . .	92
3.2	Theoretical framework and notations . . . . .	93
3.3	Method and computations . . . . .	95
3.3.1	Topologies for the non-singlet $n_f^2$ structure functions .	97
3.3.2	Series expansion and differential equations . . . . .	98
3.3.3	Four-loop rescaling example . . . . .	101
3.4	Results in N-space . . . . .	106
3.4.1	A five-loop prediction . . . . .	119
3.5	The x-space coefficient functions . . . . .	120
3.6	Summary and outlook . . . . .	136
<b>4</b>	<b>Overall Conclusions</b>	<b>141</b>
<b>5</b>	<b>Outlook</b>	<b>145</b>
	<b>Appendices</b>	<b>149</b>
<b>A</b>	<b><math>G_2</math> Subtraction Term for Rapidity Divergences</b>	<b>151</b>
<b>B</b>	<b>Counterterm Mapping</b>	<b>153</b>
<b>C</b>	<b>Azimuthal Integral</b>	<b>157</b>
<b>D</b>	<b>Harmonic Sums</b>	<b>161</b>
<b>E</b>	<b>Harmonic Polylogarithms</b>	<b>163</b>
<b>F</b>	<b>One-loop Example Recursive Algorithm</b>	<b>165</b>
F.1	Master integrals . . . . .	165
F.2	Derivation of the differential equation . . . . .	166
F.3	Construction of the differential operators . . . . .	167
F.4	Series solution . . . . .	169
F.5	Full solution . . . . .	170
<b>G</b>	<b>The Larin Scheme for the Non-Singlet Axial Current</b>	<b>171</b>



## Contents

---

<b>H</b>	<b><math>N = 100</math> 3-loop DIS</b>	<b>175</b>
<b>I</b>	<b><math>C_3</math> at N<sup>4</sup>LO order <math>n_f^2</math></b>	<b>201</b>
<b>J</b>	<b>Order <math>\epsilon</math> coefficient functions at N<sup>3</sup>LO</b>	<b>213</b>
	<b>Summary</b>	<b>231</b>
	<b>Samenvatting</b>	<b>237</b>
	<b>Acknowledgements</b>	<b>243</b>
	<b>Bibliography</b>	<b>249</b>



# Introduction

This year marks the 11<sup>th</sup> anniversary of the discovery of the Higgs particle at the Large Hadron Collider (LHC) at CERN, Geneva. The Higgs particle was the last ingredient required to construct a consistent theory that describes the interactions between all the known elementary particles in Nature: it provides the masses to the quarks and leptons in the Standard Model of particle physics (SM). However, there are still many open questions left in physics and I will elaborate on some of them in the following.

First of all, we do not know how to combine the other significant theory in physics, the theory of gravity, with the Standard Model. Indeed, the Standard Model only describes one side of all the physical phenomena in Nature. It is very successful in predicting the outcome of physical processes at (sub)atomic length scales. However, large length-scale physics obeys the rules of General Relativity. The theory of particle physics is a quantum physical theory and results in probabilities, whereas General Relativity is deterministic. So far physicists have been unable to join these two theories with each other. Yes, there are proposals which result in a unified theory, such as String Theory or Emergent Gravity, but we lack the experimental and observational evidence to validate these theories.

Secondly, we do not know to what we should ascribe dark matter and dark energy. Let us focus on the former quantity, dark matter. Discrepancies between observed and predicted rotational velocity curves in galaxies hint to unseen amounts of matter. Unseen in the sense that it is a kind of matter which, for now, we are unable to detect directly. There are two kinds of solutions proposed to solve this problem, either the theory of gravity has to be modified to account for this discrepancy, or the dark matter content is a (new) particle. In the particle physics community the latter solution is more favourable.

Lastly, even within the domain of particle physics there remain open questions. For instance, how do we account for the observed neutrino mass through neutrino oscillations, even though it should be zero according to the Standard Model? How do we explain the asymmetry between baryonic

matter and antimatter? Why do we not observe charge-parity-violation in the theory which describes the strong interactions? I hope that the reader is convinced by now that there is much unknown about the Universe. Thus, how does one proceed?

In order to understand the challenges in searches for new physics, we will first review the current theory of particle physics. The elementary particles are the fundamental building blocks of the Universe at the smallest length scale. They are described by the Standard Model of particle physics, which is defined within the framework of Quantum Field Theory. At high energies, the Standard Model can be divided into two sections, the strong sector and the electroweak sector. The former sector, also known as Quantum Chromodynamics (QCD), describes the quarks and gluons which are the constituents of the hadrons such as the protons and neutrons. Massless gluons are the mediating particles of the strong force. Quarks and gluons are also collectively called the partons. The latter sector describes the electromagnetic and weak interactions. Electromagnetic interactions affect electrically charged particles such as the electrons. The corresponding force is mediated by massless photons. Weak interactions act on the left-handed fermions in the Standard Model. These include the leptons and their corresponding neutrinos, and the quarks. The force is mediated by the massive  $W^\pm$  and  $Z$  bosons, of which the former are electrically charged and the latter is electrically neutral. As mentioned before, the inclusion of the Higgs particle, which provides the masses to the quarks and leptons, renders the Standard Model self-consistent. However, one might argue for an extension of the theory if hints of new physics were to be found.

One way to search for hints of new physics, is by conducting collision experiments in which particles such as protons or electrons are collided into each other. In order to do so, the theoretical predictions have to be calculated and the results of the experiments have to be analysed. These two are then compared against each other. If both agree, the correctness of the Standard Model is confirmed and some of its parameters are constrained. However, if there exists a discrepancy, this would indicate a modification of the Standard Model. In order to compare the predictions against the results, it is imperative that the predictions are calculated to a sufficiently high accuracy. Unfortunately, this is not the case for the predictions of some processes. For example, the current experimental uncertainty of Higgs production at the LHC (run 2) is 8% and it is expected to decrease to 3% with the high luminosity upgrade [4]. However, in order to obtain the desired theoretical precision for the predictions of the processes, one requires to perform calculations at  $N^3\text{LO}$  precision in perturbation theory (more on that later on). Some of these calculations have yet to be performed.

Now, even though most of the calculations require the usage of powerful computers, the calculations are so complex, that an extra set of CPU cores or more RAM is not sufficient to successfully perform the calculations at the required accuracy. In the following I will briefly elaborate on some of the intricacies in the calculations of these predictions.

To start, the theoretical predictions can be dissected into many ingredients such as parton showers, parton distribution functions, partonic cross sections, soft functions, beam functions, jet functions, coefficient functions, structure functions, etc. To reach the required accuracy for the final predictions, each of the ingredients should be calculated at the same required accuracy. Most of the ingredients are calculated in the framework of perturbative Quantum Field Theory. This framework allows one to systematically organise the calculations according to the complexity of the process under consideration. The correlations between the interacting particles are calculated as a Taylor series in the coupling constants. These coupling constants describe the interaction strengths between the interacting particles. One is only allowed to calculate the Taylor series if the coupling constants are sufficiently small, such that the series converges. The coefficients of the Taylor series are organised in terms of Feynman diagrams. These diagrams visualise the interactions between the particles. The first, leading order (LO), term in the series is given by the simplest Feynman diagrams one can draw for the process at the lowest power order in the corresponding coupling constant. To obtain a more precise result for the correlation, one has to include the next-to-leading order (NLO) term at the next power order in the coupling constant. The corresponding Feynman diagrams are more numerous and also more complex, because they either include a loop correction or they account for the emission of a massless particle on top of the diagrams which were drawn at LO<sup>1</sup>. At next-to-next-to-leading order (NNLO) one has to account for terms including two loop diagrams, diagrams including a loop correction and an emission, or diagrams with two emissions<sup>2</sup>. In general, at an N<sup>k</sup>LO accuracy one requires all the diagrams that contribute up to the  $k^{th}$ -power order in the expansion in the coupling constants.

Unfortunately, the calculations for the predictions get increasingly complicated at each order. As mentioned before, both the number of diagrams and their complexity increase. On top of that difficulties arise due to the ultraviolet (UV) and infrared (IR) divergences in the calculations. The former type of divergences are well understood and are dealt with by using the method of renormalization. For the latter type of divergences, especially for

---

<sup>1</sup>At least in Quantum Chromo Dynamics, which will be explained a later paragraph.

<sup>2</sup>Again, all on top of the LO diagrams.

final state emissions graphs, there are many methods to choose from, each with its own benefits and drawbacks. We will elaborate on both types in this thesis.

One of the crucial ingredients in the predictions for collisions between the elementary particles, are the Altarelli-Parisi splitting functions [5]. The leading order splitting functions describe the probability to find a parton  $i$  in a parton  $j$  at a certain momentum fraction of the parent parton. Not only are they required for the evolution of the parton distribution functions, which describe the splitting of initial state hadrons and partons, but they are also needed for the computation of other theoretical constructs such as the jet functions. We will elaborate on the jet functions in a later section of the introduction. The NLO contributions to the splitting functions followed not long after their invention and were calculated in [6–11]. After that it took roughly twenty years until Moch, Vermaseren and Vogt were able to calculate the NNLO contributions in [12, 13]. Fast forward in time, it is 2022 and so far only some parts of the N<sup>3</sup>LO splitting functions are known [14–16]. As mentioned before, there is a large demand for the N<sup>3</sup>LO contributions, therefore it is of high importance that new methods are developed in order to obtain the complete four-loop splitting functions. But how does one calculate these splitting functions?

One way to obtain the splitting functions is from Deep Inelastic Scattering (DIS). DIS is interesting to study on itself, not only does it contain the splitting functions, but high precision DIS calculations are also required to extract DIS data for the parton distribution functions [17]. In DIS a lepton is scattered off a hadron to produce a new hadronic final state. For a sufficiently large lepton energy, one can probe the inner structure of the hadron. The shattered target hadron will break up into its constituents, the quarks and gluons. However, due to confinement the partons will hadronise. The resulting hadrons are detected in the colliders. By tracing these hadrons and by investigating their properties, one can retrieve information about the constituent partons. Some of the earliest DIS experiments were conducted for electron-proton scattering at the Stanford Linear Accelerator Center (SLAC) in the late 60's of the previous century [18, 19] in which electrons were scattered on hydrogen. As of today, most of the datasets used to describe DIS result from experiments at the Hadron-Electron Ring Accelerator (HERA) at DESY [20–35] at which electrons and protons were collided into each other. The first theoretical calculations, which accounted for the observed scaling violations at the experiments, were performed in the late 70's [36–38]. It then took theorists ten years to include perturbative corrections at NNLO accuracy in the QCD coupling constant  $\alpha_s$  [39–41]. Subsequently it took another decade to obtain the DIS coefficient functions at N<sup>3</sup>LO [42–44]. These coeffi-

cient functions allow one to obtain the hadronic contribution to the DIS cross section. Note however that the full analysis at N<sup>3</sup>LO only has been completed in 2016 by computing the coefficient functions for  $F_2$ ,  $F_3$  and  $F_L$  in  $\nu - \bar{\nu}$  charged-current DIS [45]. The computations were performed in Mellin space. The Mellin transform of a function is an integral transformation similar to the Laplace and Fourier transforms. The Mellin moments are functions of  $N$ , the frequency parameter of the transformation. By obtaining results for a sufficient amount of moments, the authors in the papers were able to construct results for general  $N$ . Subsequently the results were translated back to momentum space. Before the work of this thesis, only a few low Mellin moments were known for the coefficient functions at N<sup>4</sup>LO [46]. A part of this thesis is dedicated to the description of a new algorithm to calculate the DIS cross section, using the optical theorem, integration-by-parts relations and the method of differential equations. Even though each of these methods have been well studied and applied in the past, we are the first ones to combine them in a unique way in order to obtain results at N<sup>4</sup>LO accuracy for DIS.

We will use the optical theorem to relate the DIS cross section to the forward scattering amplitude. This simplifies the problem, since it is less complicated to deal with Feynman loop integrals in the amplitude than to calculate the full cross section and integrate over the complete phase space. This method has been applied to DIS in the past in e.g. [42–44], but also to the Drell-Yan cross section in [47].

The second method allows one to obtain the integration-by-parts relations (IBPs) in loop momentum space. With the IBPs one can reduce a set of complex Feynman loop integrals to a smaller set of simpler master integrals<sup>3</sup>. The resulting set of relations which simplify the complex loop integrals to the master integrals are stored in the reduction tables. The IBPs were first applied in [48], however they have been modified to their currently used form in [49]. In the past, the reduction tables were constructed by hand for a fixed set of propagator-type (or self-energy) loop integrals. The corresponding program was called MINCER [50] and it was implemented in the computer algebra program SCHOONSCHIP [51]. Its FORM<sup>4</sup> [52,53] implementation was introduced in [54] and used to calculate 2-loop DIS coefficient functions [55] and 3-loop moments [56]. Later the program was extended to the 4<sup>th</sup> loop order in FORCER [57]. FORCER was a crucial ingredient to obtain the low moments for the 4-loop splitting functions [16] and coefficient

---

<sup>3</sup>At N<sup>3</sup>LO we reduced a million loop integrals to 3000 master integrals.

<sup>4</sup>FORM is a modern computer algebra program which is continuously being updated. SCHOONSCHIP is not supported anymore.



functions [46]. In this thesis we will use a different type of reduction procedure, called Laporta's algorithm [58, 59], implemented in KIRA [60] and FIRE [61]. The upside of this algorithm is that it is a procedure which can process generic loop integrals, instead of a fixed set of integrals. However, one still has to solve the resulting master integrals (unlike in the MINCER case). Since the master integrals at three and four loops turn out to be relatively complex, we will apply the sophisticated method of differential equations to solve them.

The last step in our algorithm is the construction and solving of the system of differential equations (DEs) for the resulting master integrals. After being developed by Kotikov [62–66] and Remiddi [67], the first remarkable application of the method of DEs was in [68]. In this paper the authors calculated the master integrals for 2-loop 4-point functions with massless propagators. Subsequently they constructed a linear system of differential equations (in the external variables) for the master integrals and solved them. In other words, this method bypasses the necessity to directly compute the loop integrals. It has been used extensively in high precision calculations such as [69–71] and many others. In 2013 Henn made significant progress to the method of differential equations [72]. He showed that the solutions to the differential equations simplify if one chooses the masters such that the equations can be cast into canonical (or  $\epsilon$ ) form. One can then obtain answers to the DEs in terms of Chen's iterated integrals or Goncharov polylogarithms. However, even though it might be possible, we will not apply Henn's technique<sup>5</sup>. Instead, we will solve the DEs recursively using a power series ansatz for the master integrals. This technique will grant us the ability to obtain a large number of Mellin moments in a very efficient way. Consequently, the large number of moments allows us reconstruct the full DIS coefficient functions by using Gaussian elimination.

As mentioned before, in this thesis we will also try to improve on the calculation of final state real emission graphs. These are Feynman diagrams in which a massless particle is emitted from the final state. We will do so using a new subtraction scheme in the context of Soft-Collinear Effective Theory (SCET) in QCD [73–77]. Note that the IR singularities cancel out for total inclusive quantities, such as the cross section due to the Kinoshita-Lee-Nauenberg (KLN) theorem [78, 79]. However, in differential quantities, where one integrates over an IR safe region of phase space, this is not necessarily the case. Hence a subtraction procedure is required to render the quantities IR finite. There exist two different kinds of subtraction procedures: subtraction methods and slicing methods.

---

<sup>5</sup>Possible, but very hard and not guaranteed to work.

In the former method one subtracts counterterms from the singular integrands in the quantity under consideration. These counterterms mimic the singular behaviour of the integrands in the IR. Afterwards one adds the integrated counterterms back to the quantity to obtain an IR finite solution. Some well known subtraction methods are the Catani-Seymour (CS) dipole method [80, 81], the Frixione-Kunszt-Signer (FKS) subtraction method [82, 83] and the Antenna subtraction method [84–86]. The construction of the counterterms in these methods depends on the factorisation of the amplitudes in the soft and collinear limits, which are parametrisation dependent. It can be very challenging to find suitable parametrisations and might not be possible in some cases.

Slicing methods, on the other hand, slice out the IR singular regions in phase space using a measurement function. These regions are subsequently added back in integrated form [87]. Two modern implementations are the kt-subtraction [88] method and the N-jettiness [89, 90] method. The singular limits of the amplitudes are obtained from general factorisation theorems, which are parametrisation independent. However, in order for the factorisation theorems to be valid, one has to choose sufficiently small slicing parameters. Unfortunately, the integrated counterterms may exhibit numerical instabilities at such small values for the parameters [91, 92].

In this thesis we will apply the Geometric Subtraction scheme [93]. This subtraction scheme combines the two aforementioned methods. By parametrising the IR infinite integrals in the space of Mandelstam variables, the soft and/or collinear singularities are sliced away in a geometrical manner. This produces relatively simple counterterms to be integrated and added back. The simplicity of this new subtraction scheme allows one to automate it for a large class of observables. In particular, we will automate the subtraction scheme in the context of one-loop jet functions. These functions describe the collinear regime of final state particles in SCET. Apart from observable dependent measurement functions, these jet functions also depend on the splitting functions. This is an example of the universality and importance of the splitting functions.

The thesis will be structured as follows: we will first explain all the necessary theory and set up the frameworks in chapter 1 to get familiarised with the topics described in the thesis. Then we will apply the Geometric Subtraction scheme to a range of one-loop jet functions and automate the procedure for generic jet functions in chapter 2. Subsequently we will calculate the 4-loop non-singlet DIS coefficient functions at order  $n_f^2$  in chapter 3. We will demonstrate our new algorithm which involves the optical theorem, IBP relations, the method of DEs and Gaussian elimination. Notice that these calculations also verify for the first time the 4-loop non-singlet splitting func-

tions at order  $n_f^2$ . The thesis concludes in chapter 4. Lastly we will give an outlook in chapter 5 towards the calculation of the  $O(n_f C_F^3)$  splitting functions using our new algorithm. Complementary material is provided in the appendices, in order to keep the flow of reading intact. A layman summary is included at the end of the thesis, both in English and Dutch.

# Chapter 1

## Background

### 1.1 Quantum Chromo Dynamics

As mentioned in the introduction, the Standard Model of Particle Physics (SM) represents our current understanding of the interactions amongst the fundamental particles in Nature. In this chapter we will briefly discuss the SM, and in particular, focus on the sector which describes the strong interactions, Quantum Chromo Dynamics (QCD). This chapter is based on [94] and [95].

#### 1.1.1 The Standard Model

The Standard Model of Particle Physics describes the fundamental interactions in Nature. Before spontaneous symmetry breaking the Standard Model can be written as

$$\mathcal{L} = \mathcal{L}_{\text{vct}} + \mathcal{L}_{\text{Higgs}} + \mathcal{L}_{\text{lep}} + \mathcal{L}_{\text{quark}}. \quad (1.1.1)$$

The Lagrangian possesses an  $SU(3)_C \times SU(2)_L \times U(1)_Y$  symmetry. In this the subscript  $C$  stands for colour,  $L$  stands for left-handed, meaning that it only acts on left-handed fermions and  $Y$  stands for hypercharge. The first term in eq. (1.1.1) corresponds to the gauge bosons, which includes the  $SU(3)_C$  Gluon fields and the  $SU(2)_L \times U(1)_Y$  electroweak gauge fields. The second term corresponds to the Higgs sector, which, when spontaneously broken, generates masses for the leptons and quarks through Yukawa interactions. And finally, the last two terms correspond, respectively, to the fermionic lepton and quark terms. In terms of its constituent theories, the Lagrangian is

$$\mathcal{L} = \mathcal{L}_{\text{QCD}} + \mathcal{L}_{\text{EW}} + \mathcal{L}_{\text{Higgs}}. \quad (1.1.2)$$

The first term includes the quarks and gluons. The second term describes the electroweak interactions. These include the electromagnetically charged particles such as the electrons. Their electromagnetic force is mediated by the photon. The term also includes the weak interactions, which act on the fermions such as the leptons and their corresponding neutrinos, and the quarks. The weak force is mediated by the electrically neutral Z boson for all fermions and by the electrically charged  $W^\pm$  bosons for left-handed fermions. Spontaneous symmetry breaking reduces the electroweak symmetry as  $SU(2)_L \times U(1)_Y \rightarrow U(1)_{EM}$  where  $EM$  stands for electromagnetic. This gives rise to the massless photon and additionally the Z and  $W^\pm$  bosons obtain a mass.

### 1.1.2 Quantum Chromo Dynamics Fundamentals

In this thesis, we will be particularly interested in the sector which describes the strong fundamental interactions, Quantum Chromo Dynamics. Its constituents are the quarks and gluons which adhere a colour<sup>1</sup>  $SU(3)_C$  symmetry. The colour singlet states of quarks correspond to the baryons and mesons, which are composite objects that contain an odd or even number of quarks respectively. The QCD Lagrangian in eq. (1.1.2) can be divided into three terms

$$\mathcal{L}_{\text{QCD}} = \mathcal{L}_{\text{classical}} + \mathcal{L}_{\text{gauge-fixing}} + \mathcal{L}_{\text{ghost}}. \quad (1.1.3)$$

The first terms corresponds to the classical Lagrangian, similar to the one in QED. The second term fixes a gauge, which allows us to define a gluon propagator. The last term follows from the Faddeev-Popov procedure, which is necessary if one picks a covariant gauge in a non-Abelian field theory.

Let us start with the classical Lagrangian,

$$\mathcal{L}_{\text{classical}} = -\frac{1}{4}F_{\alpha\beta}^A F_A^{\alpha\beta} + \sum_{n_f} \bar{q}_a (i\not{D} - m)_{ab} q_b, \quad (1.1.4)$$

in which we ignored the spinor indices. Here  $q$  stands for a spin- $\frac{1}{2}$  quark with mass  $m$  (see table 1.1),  $n_f$  is the number of flavours,  $g$  is a coupling constant, and  $\not{D} = \gamma_\mu D^\mu$  the covariant derivative. The covariant derivative uses two different representations of the same  $SU(3)$  generators when acting on quark and gluon fields, namely:

$$\begin{aligned} (D_\alpha)_{ab} &= \partial_\alpha \delta_{ab} + ig(t^C A_\alpha^C)_{ab} \\ (D_\alpha)_{AB} &= \partial_\alpha \delta_{AB} + ig(T^C A_\alpha^C)_{AB}, \end{aligned} \quad (1.1.5)$$

---

<sup>1</sup>Hence the name Quantum *Chromo* Dynamics.

## 1.1. Quantum Chromo Dynamics

---

Quark	Mass	Charge
Up	2.16 MeV	+2/3
Down	4.67 MeV	-1/3
Strange	83.4 MeV	-1/3
Charm	1.27 GeV	+2/3
Bottom	4.18 GeV	-1/3
Top	173 GeV	+2/3

Table 1.1: Shown are the quark masses and charges in the  $\overline{\text{MS}}$  subtraction scheme [96].

respectively.  $A$  is the massless spin-1 gluon. The generators  $t$  and  $T$  are in the fundamental and adjoint representation of the colour group, respectively, obeying the *non-abelian* algebra

$$\begin{aligned}
[t^A, t^B] &= if^{ABC}t^C \\
[T^A, T^B] &= if^{ABC}T^C \\
(T^A)_{BC} &= -if^{ABC},
\end{aligned}
\tag{1.1.6}$$

with totally antisymmetric structure constants  $f^{ABC}$ . The field strength tensor is

$$F_{\alpha\beta}^A = \partial_\alpha A_\beta^A - \partial_\beta A_\alpha^A - gf^{ABC}A_\alpha^B A_\beta^C, \tag{1.1.7}$$

where the last term is due to the non-abelian nature of the algebra as described in eq. (1.1.6). This term generates the self-interacting gluon Feynman rules. The self-interactions involve the colour indices in a non-trivial way as can be seen in table 1.2. One can also see that the gluon propagator demands colour conservation. This behaviour differs from QED, where the photon propagator is not electromagnetically charged. Additionally we have the following relations in  $SU(N)$  (and for  $N = 3$ ):

$$\begin{aligned}
\text{tr}(t^A t^B) &= T_R \delta^{AB} = \frac{1}{2} \delta^{AB} \\
\sum_A t_{ab}^A t_{bc}^A &= C_F \delta_{ac} = \frac{N^2 - 1}{2N} \delta_{ac} = \frac{4}{3} \delta_{ac} \\
\text{tr}(T^C T^D) &= \sum_{A,B} f^{ABC} f^{ABD} = C_A \delta^{CD} = N \delta^{CD} = 3 \delta^{CD} \\
\{t^A, t^B\} &= \frac{1}{N} \delta^{AB} I + d^{ABC} t^C = \frac{1}{3} \delta^{AB} I + d^{ABC} t^C \\
\sum_{A,B} d^{ABC} d^{ABD} &= \frac{N^2 - 4}{N} \delta^{CD} = \frac{5}{3} \delta^{CD},
\end{aligned}
\tag{1.1.8}$$

in which  $d^{ABC}$  is the symmetric structure constant and we defined  $d^{AAC} \equiv 0$ . The relations in eq. (1.1.8) can be useful when one wants to simplify expressions resulting from Feynman diagrams. And finally, by combining eq. (1.1.5) and eq. (1.1.7) we can obtain the Ricci identity

$$[D_\alpha, D_\beta] = i g t \cdot F_{\alpha\beta}, \quad (1.1.9)$$

where the colour indices are contracted. From the Ricci identity it becomes clear why the field strength alternatively is known as the curvature tensor [97]. If the right hand side of eq. (1.1.9) were to be zero, then two successive covariant translations in the  $\hat{\alpha}$  and  $\hat{\beta}$  directions would amount to the same result as two successive covariant translations in the  $\hat{\beta}$  and  $\hat{\alpha}$  directions. However, since the field strength is non-zero, the two covariant translations do not commute. This is analogous to the situation where one applies two successive translations on a curved space-time. Hence the analogy between the non-abelian nature of the field strength tensor and the curvature in space-time<sup>2</sup>.

The classical Lagrangian in eq. (1.1.4) allows for local gauge transformations. Acting on the quark field and covariant derivative, the transformations are

$$q_a(x) \rightarrow q'_a(x) = e^{(it \cdot \theta(x))_{ab}} q_b(x) \equiv \Omega(x)_{ab} q_b(x) \quad (1.1.10)$$

and

$$D_\alpha q(x) \rightarrow D'_\alpha q'(x) \equiv \Omega(x) D_\alpha q(x). \quad (1.1.11)$$

The transformation rule for the gluon field is obtained by combining eq. (1.1.5), eq. (1.1.10) and eq. (1.1.11), resulting in

$$t \cdot A'_\alpha = \Omega(x) t \cdot A_\alpha \Omega^{-1}(x) + \frac{i}{g} (\partial_\alpha \Omega(x)) \Omega^{-1}(x), \quad (1.1.12)$$

from which we also can derive the transformation rule for  $F_{\alpha\beta}$ ,

$$t \cdot F'_{\alpha\beta}(x) = \Omega(x) t \cdot F_{\alpha\beta}(x) \Omega^{-1}(x). \quad (1.1.13)$$

Another way to prove this transformation rule is by making use of the Ricci identity in eq. (1.1.9), given the transformation properties of the covariant derivative in eq. (1.1.11). Notice that a quadratic gluon term  $A^\alpha A_\alpha$  is not gauge invariant, unlike the term  $\bar{q}q$ , forbidding a mass term for the gluons<sup>3</sup>.

<sup>2</sup>For more on the geometrical aspects of QCD see section 10.3.4 and onwards of [98].

<sup>3</sup>Although the quark mass term  $m\bar{q}q$  is still forbidden in the Standard Model due to electroweak interactions. The quarks obtain a mass term through the Higgs mechanism.



## 1.1. Quantum Chromo Dynamics

---

Let us consider the latter two terms in eq. (1.1.3). As mentioned before, one needs to include a gauge-fixing term to the Lagrangian in order to define the gluon propagator. A choice is the class of covariant gauges

$$\mathcal{L}_{\text{gauge-fixing}} = -\frac{1}{2\lambda}(\partial^\alpha A_\alpha^A)^2, \quad (1.1.14)$$

where  $\lambda$  is the gauge parameter. The gauge-fixing term explicitly breaks the gauge invariance. Covariant gauges allow for unphysical degrees of freedom in non-abelian theories. To cancel those degrees of freedom we require an additional term

$$\mathcal{L}_{\text{ghost}} = \partial_\alpha \eta^{A\dagger} (D_{AB}^\alpha \eta^B), \quad (1.1.15)$$

in which the ghost  $\eta^A$  is a complex anti-commuting scalar field. This is sufficient to derive the Feynman rules in a covariant gauge, as illustrated in table 1.2. Notice that the gluon propagator depends on the gauge parameter  $\lambda$ . However, the final physical observables will always be independent of the gauge parameter. Some common gauge choices are  $\lambda = 1$ , called the Feynman gauge and  $\lambda = 0$ , the Landau gauge. It is also possible to introduce a different class of gauges to fix the gauge, namely the axial gauges

$$\mathcal{L}_{\text{gauge-fixing}} = -\frac{1}{2\lambda}(n^\alpha A_\alpha^A)^2, \quad (1.1.16)$$

with  $n$  an auxiliary four-vector. By choosing this class of gauges, one does not require a ghost Lagrangian. The downside of this particular class of gauges is the complexity of the gluon propagator

$$\Delta_{(BC,\beta\gamma)} = \delta_{BC} \left( \frac{i}{p^2 + i\epsilon} \right) \left[ -g_{\beta\gamma} + \frac{n_\beta p_\gamma + p_\beta n_\gamma}{n \cdot p} - \frac{(n^2 + \lambda p^2) p_\beta p_\gamma}{(n \cdot p)^2} \right], \quad (1.1.17)$$

which is singular at  $n \cdot p = 0$ . The propagator simplifies in the so-called light-cone gauge in which  $\lambda = 0$  and  $n^2 = 0$ ,

$$\begin{aligned} \Delta_{(BC,\beta\gamma)} &= \delta_{BC} \left( \frac{i}{p^2 + i\epsilon} \right) d_{\beta\gamma}(p, n), \\ d_{\beta\gamma} &= -g_{\beta\gamma} + \frac{n_\beta p_\gamma + p_\beta n_\gamma}{n \cdot p}. \end{aligned} \quad (1.1.18)$$

By taking the dot products of  $n$  and  $p$  with  $d$ , one obtains

$$\begin{aligned} n^\beta d_{\beta\gamma}(p, n) &\stackrel{p^2 \rightarrow 0}{\longrightarrow} 0 \\ p^\beta d_{\beta\gamma}(p, n) &\stackrel{p^2 \rightarrow 0}{\longrightarrow} 0, \end{aligned} \quad (1.1.19)$$

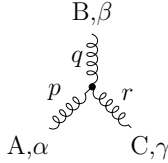
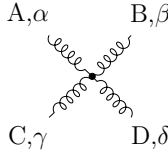
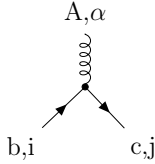
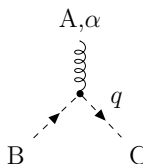
$A, \alpha \quad \text{---} \quad B, \beta$	$\delta^{AB} \left[ -g^{\alpha\beta} + (1-\lambda) \frac{p^\alpha p^\beta}{p^2 + i\epsilon} \right] \frac{i}{p^2 + i\epsilon}$
	$-g f^{ABC} [(p-q)^\gamma g^{\alpha\beta} + (q-r)^\alpha g^{\beta\gamma} + (r-p)^\beta g^{\gamma\alpha}]$
	$  \begin{aligned}  &-ig^2 f^{XAC} f^{XBD} [g^{\alpha\beta} g^{\gamma\delta} - g^{\alpha\delta} g^{\beta\gamma}] \\  &-ig^2 f^{XAD} f^{XBC} [g^{\alpha\beta} g^{\gamma\delta} - g^{\alpha\gamma} g^{\beta\delta}] \\  &-ig^2 f^{XAB} f^{XCD} [g^{\alpha\gamma} g^{\beta\delta} - g^{\alpha\delta} g^{\beta\gamma}]  \end{aligned}  $
$a, i \quad \text{---} \quad b, j$	$\delta^{ab} \frac{i}{(p-m+i\epsilon)_{ji}}$
	$-ig (t^A)_{cb} (\gamma^\alpha)_{ji}$
$A \quad \text{---} \quad B$	$\delta^{AB} \frac{i}{(p^2 + i\epsilon)}$
	$g f^{ABC} q^\alpha$

Table 1.2: Depicted are the QCD Feynman rules in a covariant gauge. From top to bottom we have: the gluon propagator, the gluon 3-vertex, the gluon 4-vertex, the quark propagator, the quark-quark-gluon vertex, the ghost propagator, the ghost-ghost-gluon vertex.

resulting in two propagating states orthogonal to  $n$  and  $p$ . It now becomes clear why these classes of gauges are called the physical gauges, since the two resulting states are the physical polarization states. Furthermore,  $d$  can be decomposed in terms of the two polarizations as

$$d_{\alpha\beta} \stackrel{p^2 \rightarrow 0}{=} \sum_i \epsilon_\alpha^{(i)}(p) \epsilon_\beta^{(i)}(p). \quad (1.1.20)$$

Here the two polarizations are defined as

$$\begin{aligned} \epsilon^+ &= \frac{1}{\sqrt{2}}(0, 1, i, 0) \\ \epsilon^- &= \frac{1}{\sqrt{2}}(0, 1, -i, 0) \end{aligned} \quad (1.1.21)$$

at a fixed momentum  $p = (p^0, 0, 0, p^0)$ . Lastly, in axial gauges one can simplify the calculations using the constraint  $\epsilon_\beta^{(i)}(p)n^\beta = 0$  on top of the gauge-independent constraint  $\epsilon_\beta^{(i)}(p)p^\beta = 0$ . This could correspond to the choice  $n = (p^0, 0, 0, -p^0)$ .

#### 1.1.3 Asymptotic Freedom and Confinement

First of all I would like to mention the concept of factorization in QCD, which allows us to perform calculations for the predictions of physical observables. To calculate hadronic observables, one can factorize the hadronic cross sections as

$$\begin{aligned} d\sigma_{pp \rightarrow X} &= \sum_{i,j} \int_0^1 dx_1 dx_2 \phi_{i/p}(x_1, \mu_F) \phi_{j/p}(x_2, \mu_F) \times d\sigma_{ij \rightarrow X}(x_1, x_2, \alpha_s, \mu_R, \mu_F) \\ &\quad + O\left(\frac{\Lambda^2}{Q^2}\right). \end{aligned} \quad (1.1.22)$$

Here  $\phi_{i/p}(x_1, \mu_F)$  and  $\phi_{j/p}(x_2, \mu_F)$  are the parton distribution functions which describe the long-distance dynamics,  $d\sigma_{ij \rightarrow X}$  is the partonic cross section which, as we will see, is calculable in perturbation theory and  $O(\Lambda^2/Q^2)$  are non-perturbative power corrections. The factorization scale at which the long- and short-distance dynamics separate is  $\mu_F$  and  $\mu_R$  is the renormalization scale. In section 1.2.2 we will elaborate on factorization in the context of deep inelastic scattering. Renormalization is required to remove ultraviolet divergences in perturbative calculations and will be further explained in this section.

The last term in eq. (1.1.7) is responsible for two key features of QCD: *asymptotic freedom* and *confinement*. The latter feature can be described as the phenomenon which explains why one does not see individual quarks in Nature. The former allows one to perform calculations for partonic cross sections perturbatively in QCD at high energy scales. To explain the features, we will introduce concepts such as the running coupling constant, the  $\beta$  function and scheme dependence. Let us start with the running coupling constant.

We will begin with a dimensionless physical observable  $R$ , depending solely on the scale  $Q$ . In the case that  $Q$  is sufficiently large, one can neglect the quark masses. As mentioned before one needs to renormalize the theory to remove the ultraviolet (UV) divergences which emerge in perturbative calculations. Two well-known examples of renormalization schemes are *minimal subtraction* (MS) and *modified minimal subtraction* ( $\overline{\text{MS}}$ ). In both schemes *dimensional regularization* is used to regularise the resulting Feynman integrals. Here the dimension  $d$  is re-expressed as  $d = 4 - 2\epsilon$ . This requires the introduction of an additional scale  $\mu$  at which one performs the necessary subtractions. We will explore dimensional regularization in more detail in section 1.4.1. Consequently, the theory (and in particular the couplings) depend on the renormalization scale  $\mu$ . In QCD one performs computations as a series expansion in the strong coupling constant  $\alpha_s = g^2/4\pi$ , which depends on  $\mu^2$ . The dimensionless physical observable  $R$  depends on the dimensionless ratio  $Q^2/\mu^2$ . A careful reader will now probably object to the introduction of the new parameter  $\mu$ , since the bare QCD Lagrangian in eq. (1.1.3) does not mention this extra scale. This reader would be right, even though the scale is necessary at intermediate steps in the calculation, the final physical observable should be independent of the choice of the renormalization scale. This independence is manifest in the renormalization group equation (RGE) for the physical observable<sup>4</sup>,

$$\mu^2 \frac{d}{d\mu^2} R\left(\frac{Q^2}{\mu^2}, \alpha_s\right) \equiv \left[ \mu^2 \frac{\partial}{\partial \mu^2} + \mu^2 \frac{\partial \alpha_s}{\partial \mu^2} \frac{\partial}{\partial \alpha_s} \right] R = 0. \quad (1.1.23)$$

Introducing the  $\beta$  function and parameter  $\tau$  as

$$\begin{aligned} \beta(\alpha_s) &= \mu^2 \frac{\partial \alpha_s}{\partial \mu^2} \Big|_{\alpha_s, \text{bare fixed}} \\ \tau &= \log \left( \frac{Q^2}{\mu^2} \right), \end{aligned} \quad (1.1.24)$$

---

<sup>4</sup>For convenience we perform the calculation in the Landau gauge. Had the gauge not been fixed, one would also need to consider variations in the gauge parameter.

eq. (1.1.23) becomes

$$\left[ -\frac{\partial}{\partial \tau} + \beta(\alpha_s) \frac{\partial}{\partial \alpha_s} \right] R(e^\tau, \alpha_s) = 0. \quad (1.1.25)$$

To solve this differential equation, one defines a *running coupling*  $\alpha_s(Q^2)$

$$\tau = \int_{\alpha_s}^{\alpha_s(Q^2)} \frac{dx}{\beta(x)} \quad (1.1.26)$$

$$\alpha_s(\mu^2) \equiv \alpha_s.$$

Using the fundamental theorem of calculus, one obtains for the derivative of  $\tau$

$$\frac{\partial \alpha_s(Q^2)}{\partial \tau} = \beta(\alpha_s(Q^2)). \quad (1.1.27)$$

At  $Q^2 = \mu^2$  we also have from eq. (1.1.24)

$$\frac{\partial \alpha_s(Q^2)}{\partial \alpha_s} = \frac{\beta(\alpha_s(Q^2))}{\beta(\alpha_s)}. \quad (1.1.28)$$

By combining eq. (1.1.25), eq. (1.1.27) and eq. (1.1.28) for  $\tau = 0$  one finds that  $R(1, \alpha_s(Q^2))$  is a solution to the differential equation. Thus, the ability to solve the running of the coupling, allows us to predict the dependence of  $R$  on  $Q$ .

To investigate the running of the coupling constant, one needs to know the  $\beta$  function. In the UV this is determined by

$$\beta(\alpha_s) = Q^2 \frac{\partial \alpha_s}{\partial Q^2}, \quad (1.1.29)$$

which can be perturbatively expanded as

$$\beta(\alpha_s) = -b\alpha_s^2(1 + b'\alpha_s + b''\alpha_s^2 + O(\alpha_s^3)). \quad (1.1.30)$$

The first term corresponds to the one-loop graphs as seen in figure 1.1 and its coefficient  $b$  is given by [99, 100]

$$b = \frac{(11C_A - 2n_f)}{12\pi} = \frac{33 - 2n_f}{12\pi}. \quad (1.1.31)$$



Figure 1.1: Illustrated are some Feynman diagrams which contribute to the  $\beta$  function at one-loop order.

The higher order coefficients in  $\overline{\text{MS}}$  are (two-loop [101] and three-loop [102, 103] respectively)

$$\begin{aligned}
 b' &= \frac{(17C_A^2 - 5C_A n_f - 3C_F n_f)}{2\pi(11C_A - 2n_f)} = \frac{(153 - 19n_f)}{2\pi(33 - 2n_f)} \\
 b'' &= \frac{1}{288\pi^2(11C_A - 2n_f)} \left[ 2857C_A^3 + (54C_F^2 - 615C_F C_A - 1415C_A^2)n_f + \right. \\
 &\quad \left. + (66C_F + 79C_A)n_f^2 \right] \\
 &= \frac{(77139 - 15099n_f + 325n_f^2)}{288\pi^2(33 - 2n_f)}.
 \end{aligned} \tag{1.1.32}$$

Only the one- and two-loop coefficients are renormalization scheme independent, the higher order coefficients are not. The one-, two- and three-loop results are shown in figure 1.2 for four light flavours. As one can see, the value of the  $\beta$  function changes significantly (in a converging manner) by including higher order loop corrections. This marks the importance of higher order calculations in QCD. At the time of writing this thesis, the QCD  $\beta$  function is known up till five loops [104–108]. Notice that the diagrams in figure 1.1 are one-loop corrections to the gluon propagator. For the complete computation one also needs to consider the one-loop corrections to the quark propagator using quark-quark-gluon vertices (and a gluon 3-vertex self-interaction) and the one-loop correction to the gluon propagator using the gluon 4-vertex self-interaction. In general  $\beta$  functions describe the quantum corrections to 2-point correlation functions for a given Lagrangian. In fact, the  $\beta$  function for QED can be expanded as

$$\beta_{\text{QED}}(\alpha) = \frac{1}{3\pi}\alpha^2 + \dots, \tag{1.1.33}$$

where we omitted higher order terms. Pay attention to the sign difference between the first order QED and QCD coefficients, for it is of crucial im-

## 1.1. Quantum Chromo Dynamics

---

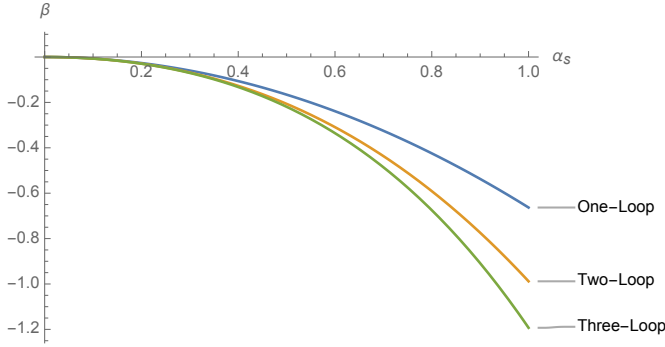


Figure 1.2: The one-, two- and three-loop results for the  $\beta$  function are illustrated for  $n_f = 4$ . As one can see, the value of the  $\beta$  function changes significantly (in a converging manner) by including higher order loop corrections. This marks the importance of higher order calculations in QCD.

portance to the predictions that QCD provides to high energy collisions at colliders. One can now rewrite eq. (1.1.29) as

$$Q^2 \frac{\partial \alpha_s}{\partial Q^2} = -b \alpha_s^2(Q^2) (1 + b' \alpha_s(Q^2) + O(\alpha_s^2)). \quad (1.1.34)$$

Neglecting the higher order terms and focussing on the first-order term (for the time being), the differential equation can be rewritten as

$$\int_{\alpha_s(\mu^2)}^{\alpha_s(Q^2)} \frac{d\alpha_s'}{\alpha_s'^2} = -b \int_{\mu^2}^{Q^2} \frac{dQ'^2}{Q'^2}, \quad (1.1.35)$$

which results in

$$\alpha_s(Q^2) = \frac{\alpha_s(\mu^2)}{1 + \alpha_s(\mu^2) b \tau}, \quad (1.1.36)$$

where we used the logarithmic definition for  $\tau$  as given in eq. (1.1.24). Now, notice that the coupling constant decreases for increasing values of  $\tau$ . For large values of  $\tau$ , thus at a high energy scale, the coupling constant is at such a small value, that it is justified to perform perturbative calculations. The phenomenon of  $\alpha_s$  decreasing to zero for increasing energy scales is called *asymptotic freedom*. Here I would like to highlight the aforementioned importance of the sign of the first order coefficient of the  $\beta$  function. If the sign were to be positive as in QED, the coupling constant would increase



with energy scale. At a sufficiently large energy scale it would be impossible to perform perturbative calculations. Note however that the value of the QED coupling still allows to perform perturbative calculations at the LHC.

If one were to expand the solution to eq. (1.1.25) in terms of  $\alpha_s$  as  $R = R_1\alpha_s + O(\alpha_s^2)$ , one can re-express  $R(1, \alpha_s(Q^2))$  using the geometric series for  $\alpha_s(Q^2)$  as

$$\begin{aligned} R(1, \alpha_s(Q^2)) &= R_1\alpha_s(\mu^2) \sum_{i=0}^{\infty} (-\alpha_s(\mu^2)b\tau)^i \\ &= R_1\alpha_s(\mu^2)(1 - \alpha_s(\mu^2)b\tau + \alpha_s^2(\mu^2)b^2\tau^2 + \dots), \end{aligned} \quad (1.1.37)$$

where we used eq. (1.1.36). So, by using the running coupling constant, one automatically re-sums logarithms of  $Q^2/\mu^2$ .

So far we have ignored the quark masses. However, we are now in the position to justify this choice. Let us consider a quark flavour with renormalized mass  $m$ . Following similar arguments as previously described, one can again construct a RGE for the physical observable  $R$ , including variations of the mass,

$$\left[ \mu^2 \frac{\partial}{\partial \mu^2} + \beta(\alpha_s) \frac{\partial}{\partial \alpha_s} - \gamma_m(\alpha_s) m \frac{\partial}{\partial m} \right] R(Q^2/\mu^2, \alpha_s, m/Q) = 0. \quad (1.1.38)$$

Here  $\gamma_m$  is the mass anomalous dimension, which only depends on  $\alpha_s$ ,

$$\gamma_m(\alpha_s) = c\alpha_s(1 + c'\alpha_s + O(\alpha_s^2)). \quad (1.1.39)$$

In contrary to the  $\beta$  function, all the coefficients of  $\gamma_m$  are renormalization scheme dependent. In  $\overline{\text{MS}}$  the first two coefficients are [109, 110]

$$\begin{aligned} c &= \frac{1}{\pi} \\ c' &= \frac{303 - 10n_f}{72\pi}. \end{aligned} \quad (1.1.40)$$

Owing to the dimensionlessness of  $R$ , one also has that

$$\left[ \mu^2 \frac{\partial}{\partial \mu^2} + Q^2 \frac{\partial}{\partial Q^2} + m^2 \frac{\partial}{\partial m^2} \right] R(Q^2/\mu^2, \alpha_s, m/Q) = 0. \quad (1.1.41)$$

Consequently, by subtracting eq. (1.1.38) from eq. (1.1.41), one can fix the  $Q$ -dependence of  $R$  using the resulting relation

$$\left[ Q^2 \frac{\partial}{\partial Q^2} - \beta(\alpha_s) \frac{\partial}{\partial \alpha_s} + \left( \frac{1}{2} + \gamma_m(\alpha_s) \right) m \frac{\partial}{\partial m} \right] R(Q^2/\mu^2, \alpha_s, m/Q) = 0. \quad (1.1.42)$$

This equation can be solved by using a running mass  $m(Q^2)$

$$\begin{aligned}
Q^2 \frac{\partial m}{\partial Q^2} &= -\gamma_m(\alpha_s) m(Q^2) \\
&\implies \\
m(Q^2) &= m(\mu^2) \exp \left[ - \int_{\mu^2}^{Q^2} \frac{dQ^2}{Q^2} \gamma_m(\alpha_s(Q^2)) \right] \\
&= m(\mu^2) \exp \left[ - \int_{\alpha_s(\mu^2)}^{\alpha_s(Q^2)} d\alpha_s \frac{\gamma(\alpha_s)}{\beta(\alpha_s)} \right].
\end{aligned} \tag{1.1.43}$$

With this, the scale-dependence of  $R$  is transferred not only to the running of the coupling, but also to the running of the mass, such that

$$R(Q^2/\mu^2, \alpha_s, m/Q) \rightarrow R(1, \alpha_s(Q^2), m(Q^2)/Q). \tag{1.1.44}$$

Notice that the mass is suppressed by a factor of  $1/Q$ . Due to asymptotic freedom at high energies, one can now perturbatively calculate the running of the mass

$$m(Q^2) = \hat{m}[\alpha_s(Q^2)]^{c/b} \left\{ 1 + \frac{c(c' - b')}{b} \alpha_s(Q^2) + O(\alpha_s^2) \right\}, \tag{1.1.45}$$

in which  $\hat{m}$  is a RG invariant integration constant. The factor of  $\alpha_s(Q^2)^{c/b}$  introduces a logarithmic suppression (due to the geometric series of  $\alpha_s(Q^2)$  in  $\tau$ ) in the running of the mass for  $c/b > 0$  coming from the anomalous dimension  $\gamma_m$ . It is now clear why it is justified to neglect the mass term at high energy. At large  $Q^2$  for  $Q \gg m(Q^2)$  the mass dependence in  $R$  is suppressed by the factor  $1/Q$  and by the logarithm in  $Q$  which stems from the anomalous dimension, due to the asymptotic freedom of the theory. In cases where the quark masses are much larger than the probed energy scales, the mass scales and their contributions to the cross section are suppressed by inverse powers of  $m$ . That explains why we for instance choose  $n_f = 4$  in figure 1.2 at the energy scale  $Q^2 \sim 50 \text{ GeV}^2$  (with  $\alpha_s = 0.2$ ) in anticipation of unpolarized deep inelastic scattering further on in this thesis.

When  $Q^2 \sim m^2$  one has to include the mass of the quarks in the predictions. The functions of  $\alpha_s$  in the regimes  $Q \gg m$  and  $Q \ll m$  have to be related to each other by matching the full theory with the effective theory, including the light quarks, which goes beyond the scope of this thesis.

In the previous sections one has to fix the renormalization scale  $\mu$  at a conveniently high reference scale (such that one can perform perturbative calculations) in order to extract an absolute value for  $\alpha_s$  from experiments,

for instance at  $\mu = M_Z$ , the mass of the Z-boson. By knowing the value of  $\alpha_s$  at this scale, one can evolve the coupling constant to other energy scales with the renormalization group equation. An alternative description of  $\alpha_s$  requires the introduction of the scale  $\Lambda$  at which the coupling diverges, defined by

$$\log\left(\frac{Q^2}{\Lambda^2}\right) = - \int_{\alpha_s(Q^2)}^{\infty} \frac{dx}{\beta(x)} = \int_{\alpha_s(Q^2)}^{\infty} \frac{dx}{bx^2(1+b'x+\dots)}. \quad (1.1.46)$$

Roughly speaking one usually takes  $\Lambda = 200$  MeV. Observe now that  $\alpha_s(Q^2)$  is very large for values of the light quarks (around  $Q \approx 1$  GeV). We thus see that the coupling constant increases for low energy scales. This hints towards *confinement* of the quarks and gluons in the hadrons. At leading order, truncating higher order coefficients, one obtains from the latter equation

$$\alpha_s(Q^2) = \frac{1}{b \log(Q^2/\Lambda^2)}, \quad (1.1.47)$$

which is in agreement with eq. (1.1.36) for  $Q \gg \Lambda$ . At NLO eq. (1.1.46) becomes

$$\frac{1}{\alpha_s(Q^2)} + b' \log\left(\frac{b'\alpha_s(Q^2)}{1+b'\alpha_s(Q^2)}\right) = b \log\left(\frac{Q^2}{\Lambda^2}\right), \quad (1.1.48)$$

with the solution

$$\alpha_s(Q^2) = \frac{1}{b \log(Q^2/\Lambda'^2)} \left[ 1 - \frac{b'}{b} \frac{\log(\log(Q^2/\Lambda'^2))}{\log(Q^2/\Lambda'^2)} \right]. \quad (1.1.49)$$

The parameters  $\Lambda$  and  $\Lambda'$  at this order are related to each other as

$$\Lambda \approx \left(\frac{b}{b'}\right)^{\frac{b'}{2b}} \Lambda' \quad (1.1.50)$$

for the same value of  $\alpha_s(Q^2)$ .

Lastly I would like to describe the renormalization scheme dependence of  $\Lambda$ . When renormalizing a quantum field theory, one always has the freedom to choose a particular scheme. In our case, for instance, starting with the bare coupling constant  $\alpha_s^0$ , consider the renormalization of  $\alpha_s$  using two different schemes  $A$  and  $B$ ,

$$\begin{aligned} \alpha_s^A &= Z^A \alpha_s^0 \\ \alpha_s^B &= Z^B \alpha_s^0. \end{aligned} \quad (1.1.51)$$

## 1.2. Deep Inelastic Scattering

---

The infinite parts in  $Z^A$  and  $Z^B$  are equal, thus the differences are manifest in the finite pieces of the renormalization constants,

$$\alpha_s^B = \alpha_s^A(1 + c_1\alpha_s^A + O((\alpha_s^A)^2)). \quad (1.1.52)$$

Notice that the one- and two-loop coefficients in 1.1.30 are invariant under such a transformation. By using 1.1.46 we can relate the values for the scale  $\Lambda$  in the different schemes as

$$\begin{aligned} \log\left(\frac{\Lambda^B}{\Lambda^A}\right) &= \frac{1}{2} \int_{\alpha_s^A(Q^2)}^{\alpha_s^B(Q^2)} \frac{dx}{bx^2(1+..)} \stackrel{Q \rightarrow \infty}{=} \frac{c_1}{2b} \vee Q^2 \\ &\implies \Lambda^B = \Lambda^A e^{\frac{c_1}{2b}}. \end{aligned} \quad (1.1.53)$$

This is a very useful relation, because one only requires to perform the one-loop calculations to fix  $c_1$  in order to obtain a relation which relates the two  $\Lambda$ 's at all orders in perturbation theory. The UV poles are manifest as poles in the Feynman integrals as  $\epsilon \rightarrow 0$ . The poles usually appear in the form

$$\frac{\Gamma(1+\epsilon)}{\epsilon}(4\pi)^\epsilon = \frac{1}{\epsilon} + \log(4\pi) - \gamma_E + O(\epsilon), \quad (1.1.54)$$

where  $\gamma_E$  is the Euler-Mascheroni constant and the gamma-function  $\Gamma(1+\epsilon)$  is

$$\Gamma(1+\epsilon) = 1 - \gamma_E\epsilon + \left(\frac{\pi^2}{12} - \frac{1}{2}\gamma_E^2\right)\epsilon^2 + O(\epsilon^3). \quad (1.1.55)$$

In  $\overline{\text{MS}}$  the poles of  $1/\epsilon$  are subtracted and  $\alpha_s^0$  is replaced by  $\alpha_s(\mu^2)$ . In  $\overline{\text{MS}}$ , additionally, one also subtracts the constant terms in eq. (1.1.54). The relation in eq. (1.1.53) thus becomes

$$\Lambda_{\overline{\text{MS}}}^2 = \Lambda_{\text{MS}}^2 e^{[\log(4\pi) - \gamma_E]}. \quad (1.1.56)$$

This concludes our chapter on QCD. In later sections of the thesis we will examine interactions which involve quarks and gluons at higher orders in perturbative quantum chromo dynamics.

## 1.2 Deep Inelastic Scattering

In this section we will describe *Deep Inelastic Scattering* (DIS). In DIS a lepton scatters off a hadron through the interchange of a vector boson. We will be primarily interested in the QCD corrections to this process. DIS is interesting for a number of reasons. For instance the factorization between

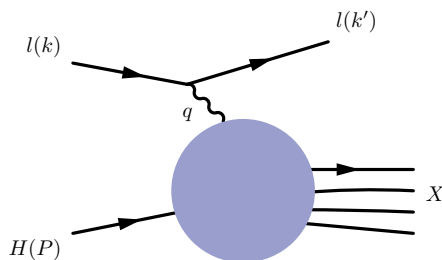


Figure 1.3: The DIS Feynman diagram is illustrated. A lepton with momentum  $k$  scatters a vector boson with momentum  $q$  off a hadron with momentum  $P$  resulting in a final state hadron with momentum  $X$  and lepton with momentum  $k'$ .

long-distance and short-distance effects is manifest in the calculation, and one can relate the evolution of the momentum transfer to the renormalization group. However, with the forthcoming high-luminosity upgrade of the LHC, the most relevant application is the extraction of the splitting functions from the DIS cross section. In order to explain the splitting functions, we will first describe the hadronic tensor. This is followed by an introduction of the coefficient functions and finally we will elaborate on the evolution of the parton densities. This section is based on [47, 94, 95].

### 1.2.1 The Hadronic Tensor

The DIS Feynman diagram is illustrated in figure 1.3. In this a lepton with momentum  $k$  scatters via the exchange of a virtual gauge boson with momentum  $q$  off a hadron with momentum  $P$ , resulting in a final (multi-particle) hadronic state with momentum  $X$  and lepton with momentum  $k'$ . The vertex on the top depicts the tree-level electro-weak interaction between the leptons and vector boson. The purple blob represents not only the tree-level interaction, but also includes quantum corrections between the scattered hadron (including constituents) and the vector boson. It is convenient to choose  $Q^2 = -q^2$ , since the vector boson is off-shell space-like. One can factorise the cross section in leptonic and hadronic tensors as

$$d\sigma = \frac{1}{2sQ^4} L^{\mu\nu}(k, k') W_{\mu\nu}(P, q) \frac{d^3 k'}{|k'|} \quad (1.2.1)$$

## 1.2. Deep Inelastic Scattering

---

for a hadron with momentum  $P$ . Here  $s$  is the invariant mass in the process,  $L$  is the leptonic tensor and  $W$  is the hadronic tensor. They are defined as

$$\begin{aligned} L_{\mu\nu}(k, k') &= \frac{e^2}{8\pi^2} (k_\mu k'_\nu + k_\nu k'_\mu - \eta_{\mu\nu} k \cdot k'), \\ W_{\mu\nu}(P, q) &= \frac{1}{8\pi} \sum_X \langle H(P) | J_\mu^\dagger(0) | X \rangle (2\pi)^4 \delta^4(P_X - P - q) \langle X | J_\nu(0) | H(P) \rangle. \end{aligned} \quad (1.2.2)$$

The sum in the hadronic tensor is over final hadronic states and is fully inclusive in QCD with momenta  $P$  and  $q$  incoming. The spin is implicitly summed over in the external states.

We define the Bjorken  $x$  variable as  $x \equiv \frac{Q^2}{2P \cdot q}$ , such that the hadronic final state momentum  $P_X$  can be written as

$$P_X^2 = (P + q)^2 = m^2 + (2P \cdot q)(1 - x). \quad (1.2.3)$$

For  $x = 1$  the process is elastic and the invariant mass of the incoming and final state hadrons are equal. As such,  $x \rightarrow 1$  is known as the threshold limit. For  $x \rightarrow 0$  the process is deeply inelastic, since  $P_X^2 \gg P^2$ . This limit corresponds to a large momentum transfer between the lepton and the hadron, therefore it is known as the high-energy limit. By imposing current conservation  $q^\mu W_{\mu\nu} = W_{\mu\nu} q^\nu = 0$ , we can express the hadronic tensor as

$$\begin{aligned} W_{\mu\nu}(P, q) &= - \left( \eta_{\mu\nu} - \frac{q_\mu q_\nu}{q^2} \right) W_1(x, Q^2) + \\ &+ \left( P_\mu - \frac{q_\mu P \cdot q}{q^2} \right) \left( P_\nu - \frac{q_\nu P \cdot q}{q^2} \right) W_2(x, Q^2), + \\ &- \left( \frac{i\epsilon_{\mu\nu}{}^{\lambda\sigma}}{2m^2} \right) q_\lambda P_\sigma W_3(x, Q^2), \end{aligned} \quad (1.2.4)$$

in which  $\epsilon_{\mu\nu\lambda\sigma}$  is totally antisymmetric. The last line, which breaks the parity invariance, is only present in the case of charged-current exchange. For simplicity of the description we will restrict ourselves to neutral-current exchange and choose  $J$  in eq. (1.2.2) to be the electromagnetic current coupled to an exchanged photon, such that parity is preserved. It is common to parametrise the energy loss of the lepton as  $\nu = P \cdot q$ , such that the scalar functions  $W_1$  and  $W_2$  can be related to the structure functions as

$$\begin{aligned} F_1(x, Q^2) &= W_1(x, Q^2), \\ F_2(x, Q^2) &= \nu W_2(x, Q^2). \end{aligned} \quad (1.2.5)$$

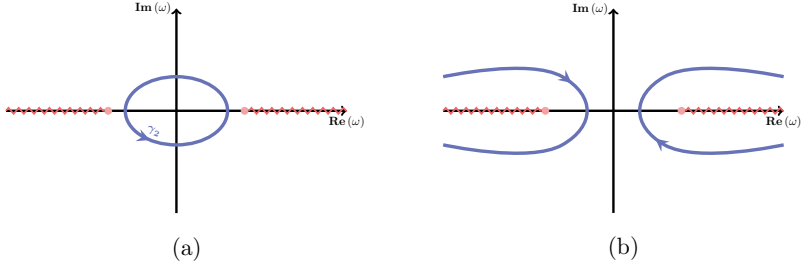


Figure 1.4: The contour in (a) around the origin can be deformed into two contours in (b) around the branch cuts.

Because the sum in eq. (1.2.2) is fully inclusive, we can apply the optical theorem to the hadronic tensor

$$W_{\mu\nu}(P, q) = 2 \text{Im} T_{\mu\nu}(P, q), \quad (1.2.6)$$

in which  $T_{\mu\nu}$  is the Compton scattering amplitude. This results in

$$\begin{aligned} T_{\mu\nu}(P, q) = & - \left( \eta_{\mu\nu} - \frac{q_\mu q_\nu}{q^2} \right) T_1(\omega, Q^2) + \\ & + \left( P_\mu - \frac{q_\mu P \cdot q}{q^2} \right) \left( P_\nu - \frac{q_\nu P \cdot q}{q^2} \right) T_2(\omega, Q^2), \end{aligned} \quad (1.2.7)$$

with  $\omega \equiv x^{-1}$ . There are normal thresholds at  $(P \pm q)^2 > 0$ , which correspond to the branch points at  $x \pm 1$ . The scalar functions in the hadronic tensor then possess a cut, running from  $x = -1$  to  $x = 1$ , and the scalar functions in the forward scattering amplitude possess a cut along  $(-\infty, -1]$  and  $[1, \infty)$ . Using Cauchy's theorem, one can relate the derivatives at  $\omega = 0$  to a contour integral around it (figure 1.4a) as

$$T_i^{(n)}(Q^2) = \frac{1}{n!} \frac{d^n T_i(\omega, Q^2)}{d\omega^n} \Big|_{\omega=0} = \oint_{C_0} \frac{d\omega}{2\pi i} \frac{T_i(\omega, Q^2)}{\omega^{n+1}}. \quad (1.2.8)$$

However, the contour around the origin can be deformed into two contours (figure 1.4b) around the branch cuts. Now we can use the fact that the functions  $T_1$  and  $T_2$  are symmetric in  $\omega$ , so that we obtain

$$T_i^{(n)}(Q^2) = \frac{(1 + (-1)^n)}{2\pi i} \int_1^\infty d\omega \frac{\text{Disc}_\omega T_i(\omega, Q^2)}{\omega^{n+1}}. \quad (1.2.9)$$

The discontinuity is defined as

$$\text{Disc}_\omega f(\omega) = \lim_{\epsilon \rightarrow 0} [f(\omega + i\epsilon) - f(\omega - i\epsilon)]. \quad (1.2.10)$$

## 1.2. Deep Inelastic Scattering

---

Notice that the discontinuity across the branch cuts is the imaginary part of the forward scattering amplitude. Therefore, by again using the optical theorem for even  $n$ , we can go back to  $x$ -space to obtain the Mellin moments as

$$T_i^{(n)}(Q^2) = \frac{1}{\pi} \int_0^1 dx x^{n-1} W_i(x, Q^2) = \frac{1}{\pi} \mathcal{M}_n[W_i(Q^2)]. \quad (1.2.11)$$

By knowing a sufficient amount of Mellin moments, one can construct the full  $\omega$  dependence of the coefficient functions. This has been used extensively in the past to calculate splitting functions [12, 13, 111]. We will elaborate on the coefficient- and splitting functions in the next section.

### 1.2.2 The Parton Model

The previous section described DIS at the hadronic level, in which the lepton scatters off the hadron. However, in section 1.1.3 we argued that the hadron possesses quarks and gluons as its constituents. Due to the decreasing value of the QCD coupling (with respect to energy), one is allowed to calculate the cross section between the photon and partons in a perturbative manner at a sufficiently high energy scale. Notice that this is not a physically measurable cross section, since the partons are confined at lower (relevant) energy scales. Nonetheless we will obtain a useful result which is universally applicable to different processes.

Let us first consider the cross section for massless quark with momentum  $p$  and charge  $Q_f e$  with a photon. At tree level the hadronic<sup>5</sup> scalar functions become

$$\begin{aligned} W_1^{(f,0)} &= \frac{Q_f^2}{2} \delta(1-x) \\ W_2^{(f,0)} &= \frac{Q_f^2}{\nu} \delta(1-x). \end{aligned} \quad (1.2.12)$$

The structure functions in eq. (1.2.5) then become

$$2F_1^{(f,0)}(x, Q^2) = F_2^{(f,0)}(x, Q^2) = Q_f^2 \delta(1-x). \quad (1.2.13)$$

Notice that both structure functions only depend on the dimensionless Bjorken  $x$  variable. This behaviour is known as *scaling*. The scaling will be broken when we include quantum corrections, as this will reintroduce the  $Q^2$  dependence to the cross section.

---

<sup>5</sup>It would make more sense to call these *partonic* scalar functions. Nonetheless I will follow Serman and refer to them as hadronic.



At one loop, it will be convenient to calculate contractions with the hadronic tensor

$$\begin{aligned} -g^{\mu\nu}W_{\mu\nu} &= (1-\epsilon)(F_2/x) - (3-2\epsilon)[(F_2/2x) - F_1] \\ p^\mu p^\nu W_{\mu\nu} &= (Q^2/4x^2)[(F_2/2x) - F_1] \equiv (Q^2/4x^2)\frac{1}{2x}F_L, \end{aligned} \quad (1.2.14)$$

where we defined the longitudinal structure function  $F_L$ <sup>6</sup>. Then, after including the real and virtual contributions, we obtain for the first term

$$\begin{aligned} (\alpha_s/\pi)[-g^{\mu\nu}W_{\mu\nu}^{(1)}] &= (1-\epsilon)(\alpha_s/2\pi)Q_f^2(4\pi\mu^2/Q^2)^\epsilon \times \\ &\times \left[ -\epsilon^{-1}P_{qq}(x)\frac{\Gamma(1-\epsilon)}{\Gamma(1-2\epsilon)} + C_2(F)\left((1+x^2)\left\{\frac{\log(1-x)}{(1-x)}\right\}_+ + \right. \right. \\ &\left. \left. - \frac{3}{2}[1/(1-x)]_+ - (1+x^2)\frac{\log x}{(1-x)} + 3-x - \left[\frac{9}{2} + \frac{\pi^2}{3}\right]\delta(1-x)\right) \right], \end{aligned} \quad (1.2.15)$$

in which  $C_2(F)$  is a colour factor.  $P_{qq}(x)$  is an Altarelli-Parisi *splitting function* defined as

$$P_{qq}(x) \equiv C_2(F)\{(1+x^2)[1/(1-x)]_+ + \frac{3}{2}\delta(1-x)\}. \quad (1.2.16)$$

In these formulas we used the so-called plus distributions. Given a differentiable function  $f(x)$ , then

$$\int_z^1 dx f(x)[1/(1-x)]_+ = \int_z^1 dx [f(x) - f(1)][1/(1-x)] + f(1)\log(1-z). \quad (1.2.17)$$

By expanding the term  $4\pi\mu^2/Q^2$  eq. (1.2.15) we obtain a term  $(\alpha_s/\pi)C_2(F) \times \log(Q^2/\mu^2)P_{qq}(x)$  which is responsible for the previously mentioned scale breaking. The second term in eq. (1.2.14) becomes

$$\frac{\alpha_s}{\pi}[p^\mu p^\nu W_{\mu\nu}^{(1)}] = Q_f^2 C_2(F) \frac{\alpha_s}{4\pi} \frac{Q^2}{2x}. \quad (1.2.18)$$

---

<sup>6</sup> $F_L$  only becomes non-zero at  $O(\alpha_s)$ . By neglecting partonic corrections to the structure functions, one obtains the Callan-Gross relation  $F_2 = 2xF_1$ .

## 1.2. Deep Inelastic Scattering

---

In terms of structure functions, the contributions can be summarised as

$$\begin{aligned}
\frac{\alpha_s}{\pi} F_2^{(f,1)}(x, Q^2) &= \frac{\alpha_s}{2\pi} Q_f^2 x \left[ - (4\pi\mu^2/Q^2)^\epsilon \epsilon^{-1} P_{qq}(x) \frac{\Gamma(1-\epsilon)}{\Gamma(1-2\epsilon)} + \right. \\
&\quad + C_2(F) \left( (1+x^2) \left\{ \frac{\log(1-x)}{(1-x)} \right\}_+ - \frac{3}{2} [1/(1-x)]_+ + \right. \\
&\quad \left. \left. - (1+x^2) \frac{\log x}{(1-x)} + 3 + 2x - \left[ \frac{9}{2} + \frac{\pi^2}{3} \right] \delta(1-x) \right) \right], \\
\frac{\alpha_s}{\pi} F_1^{(f,1)}(x, Q^2) &= \frac{\alpha_s}{\pi} F_2^{(f,1)}(x, Q^2)/2x - Q_f^2 C_2(F) \frac{\alpha_s}{2\pi} x.
\end{aligned} \tag{1.2.19}$$

Neither  $F_1^{(f,1)}$  nor  $F_2^{(f,1)}$  is infrared safe, but their difference is. This means that we can calculate the difference in a meaningful way. Moreover, if one were to measure one of the structure functions experimentally, one could predict the value for the other one. However, experimentalists usually measure the hadronic structure functions, as the partons are inaccessible after hadronization. Luckily it is possible to relate the hadronic and partonic structure functions to each other.

The hadronic and partonic cross sections, differential in energy and solid angle, can be related to each other as

$$\frac{d\sigma^{(lh)}}{dE_{k'} d\Omega_{k'}} = \sum_f \int_0^1 d\xi \frac{d\sigma^{(lf)}(\xi)}{dE_{k'} d\Omega_{k'}} \phi_{f/h}(\xi), \tag{1.2.20}$$

where the sum runs over the quark flavours in the hadron  $h$  and  $\phi_{f/h}(\xi)$  is the distribution of these quarks in the hadron. In figure 1.5 this splitting is visualised. Note that the lepton-quark cross section includes an extra factor of  $\xi^{-1}$  when compared to the lepton-hadron cross section. The quark with momentum fraction  $\xi$  escapes the hadron and interacts with the photon. At tree level, the hadronic tensor then becomes

$$W_{\mu\nu}^{(h)}(P, q) = \sum_f \int_0^1 \frac{d\xi}{\xi} W_{\mu\nu}^{(f,0)}(\xi p, q) \phi_{f/h}(\xi), \tag{1.2.21}$$

and likewise for the structure functions

$$\begin{aligned}
F_1^{(h)}(x) &= \sum_f \int_0^1 \frac{d\xi}{\xi} F_1^{(f,0)}(x/\xi) \phi_{f/h}(\xi) \\
F_2^{(h)}(x) &= \sum_f \int_0^1 d\xi F_2^{(f,0)}(x/\xi) \phi_{f/h}(\xi).
\end{aligned} \tag{1.2.22}$$

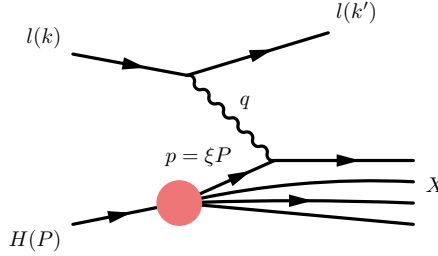


Figure 1.5: Illustrated is the partonic interaction of the quark with momentum fraction  $\xi$  with the photon. Only the tree-level interaction is drawn.

One can extend this *factorization* theorem to include quantum corrections. Generalising to the case that  $h$  can be either a nucleon or parton, the theorem states

$$\begin{aligned}
 F_1^{(h)}(x, Q^2) &= \sum_i \int_0^1 \frac{d\xi}{\xi} C_1^{(i)}(x/\xi, Q^2/\mu^2, \alpha_s(\mu^2)) \phi_{i/h}(\xi, \epsilon, \alpha_s(\mu^2)) + O(m^2/Q^2) \\
 F_2^{(h)}(x, Q^2) &= \sum_i \int_0^1 d\xi C_2^{(i)}(x/\xi, Q^2/\mu^2, \alpha_s(\mu^2)) \phi_{i/h}(\xi, \epsilon, \alpha_s(\mu^2)) + O(m^2/Q^2),
 \end{aligned}
 \tag{1.2.23}$$

in which  $\mu$  is a factorization scale. Note that the factorization scale  $\mu_F$  in principle is different than the renormalization scale  $\mu_R$ , however one is free to choose  $\mu_F = \mu_R$ <sup>7</sup>. For simplicity we will use  $\mu = \mu_R = \mu_F$ . The new functions  $C_1^{(i)}$  and  $C_2^{(i)}$ , called the *coefficient functions*<sup>8</sup>, describe the short-distance physics and can be calculated perturbatively. The hadronic distribution functions  $\phi_{i/h}$ , which describe the long-distance correlations, are, on the other hand, non-perturbative objects. However, if we restrict ourselves to the cases in which we consider partonic interactions, i.e.  $h = j = \text{parton}$ , one can calculate the distributions in a perturbative manner. At tree level we obtain the trivial relation

$$\phi_{i/j}(\xi, \epsilon, \alpha_s(\mu^2)) = \delta_{ij} \delta(1 - \xi) + O(\alpha_s).
 \tag{1.2.24}$$

<sup>7</sup>Formally the factorization scale is introduced in the renormalization of the bi-local operators which define the PDFs, however this goes beyond the scope of this thesis. For further reading see [94] or [112].

<sup>8</sup>Do not confuse them with the colour factor  $C_2(F)$ .

## 1.2. Deep Inelastic Scattering

---

$$\begin{aligned}
P_{qq}(x) &= P_{\bar{q}\bar{q}}(x) = C_2(F)[(1+x^2)[1/(1-x)]_+ + \frac{3}{2}\delta(1-x)] \\
P_{\bar{q}\bar{q}}(x) &= P_{q\bar{q}}(x) = 0 \\
P_{qg}(x) &= P_{\bar{q}g}(x) = T(F)[z^2 + (1-z)^2] \\
P_{gq}(x) &= P_{g\bar{q}}(x) = C_2(F)(x^{-1}[1 + (1-x)^2]) \\
P_{gg}(x) &= 2C_2(A)(x[1/(1-x)]_+ + (z^{-1} + z)(1-z)) + \\
&\quad + (\frac{11}{6}C_2(A) - \frac{2}{3}n_f T(F))\delta(1-z)
\end{aligned}$$

Table 1.3: Shown are the leading-order splitting functions in QCD.  $T(F)$  is a colour factor.

At one-loop the distributions are defined as

$$\frac{\alpha_s}{\pi} \phi_{i/j}^{(1)}(x) = \frac{\alpha_s}{2\pi} (-\epsilon)^{-1} P_{ij}(x), \quad (1.2.25)$$

according to the  $\overline{\text{MS}}$  subtractions scheme (as described in section 1.1.3), in which the  $\epsilon$  pole corresponds to the collinear pole in eq. (1.2.19) (for quarks). Here  $P_{ij}(x)$  are the leading-order splitting functions, summarised in table 1.3. The distribution functions are *universal*, in the sense that they are the same for the cross sections for other scattering processes, like Drell-Yan. Finally, it is possible to express the coefficient functions in terms of splitting functions and higher order terms in  $\epsilon$ . For quarks we obtain

$$\begin{aligned}
\frac{\alpha_s}{\pi} C_2^{(f,1)}(x, Q^2) &= \frac{\alpha_s}{2\pi} Q_f^2 x \left[ \left\{ \log \left[ \frac{Q^2}{\mu^2} \right] + \gamma_E - \log[4\pi] \right\} P_{qq}(x) + \right. \\
&\quad + C_2(F) \left( (1+x^2) \left\{ \frac{\log(1-x)}{(1-x)} \right\}_+ - \frac{3}{2} [1/(1-x)]_+ + \right. \\
&\quad \left. \left. - (1+x^2) \frac{\log[x]}{(1-x)} + 3 + 2x - \left( \frac{9}{2} + \frac{\pi^2}{3} \right) \delta(1-x) \right) \right] + O(\epsilon), \\
\frac{\alpha_s}{\pi} C_1^{(f,1)}(x, Q^2) &= \frac{\alpha_s}{2x \cdot \pi} C_2^{(f,1)}(x, Q^2) - \frac{\alpha_s}{2\pi} Q_f^2 C_2(F) x + O(\epsilon).
\end{aligned} \quad (1.2.26)$$

A later chapter of this thesis will be devoted to the calculation of the coefficient functions at higher orders in perturbation theory. As we mentioned before, the PDFs are non-perturbative whose central values must be extracted from experiments, but the knowledge of the splitting function allows us to evolve them from one energy scale to another. We will dedicate the details of this application to the following section.

### 1.2.3 Evolution of Parton Distributions

The parton distributions obey evolution equations reminiscent of the renormalization group equation, described in section 1.1.3. It is convenient to define the *flavour non-singlet* structure function

$$F_a^{(p-n)}(x, Q^2) \equiv F_a^{(p)}(x, Q^2) - F_a^{(n)}(x, Q^2), \quad (1.2.27)$$

for  $p$  proton and  $n$  neutron. Only diagrams in which the external quark line flows uninterrupted to the electromagnetic vertex contribute to the flavour non-singlet structure function. All other diagrams contribute to the flavour *singlet* structure functions. Similarly to what has been done in the previous section, one can factorize the non-singlet structure function

$$\begin{aligned} F_1^{(p-n)}(x, Q^2) &= \sum_f \int_0^1 \frac{d\xi}{\xi} C_1^{(ns,f)}(x/\xi, Q^2/\mu^2, \alpha_s(Q^2)) \times \\ &\times [\phi_{f/p}^{(val)}(\xi, \epsilon, \alpha_s(\mu^2)) - \phi_{f/n}^{(val)}(\xi, \epsilon, \alpha_s(\mu^2))] + O(m^2/Q^2), \end{aligned} \quad (1.2.28)$$

in which the flavour-dependence of the coefficient function only stems from an overall constant  $Q_f^2$ . The *valence* distributions are defined as

$$\phi_{f/h}^{(val)}(\xi, \epsilon, \alpha_s(\mu^2)) \equiv \phi_{f/h}(\xi, \epsilon, \alpha_s(\mu^2)) - \phi_{\bar{f}/h}(\xi, \epsilon, \alpha_s(\mu^2)). \quad (1.2.29)$$

The convolutions described above reduce to simple products in Mellin space. For a given function  $F(x)$ , the transform is given by

$$\bar{F}(n) = \int_0^1 dx \, dx^{n-1} F(x), \quad (1.2.30)$$

where  $n$  is the Mellin moment. Using eq. (1.2.30), we obtain

$$\bar{F}_1^{(ns,f)}(n, Q^2) = \bar{C}_1^{(ns,f)}(n, \alpha_s(\mu^2), Q^2/\mu^2) \bar{\phi}^{(ns)}(n, \epsilon, \alpha_s(\mu^2)), \quad (1.2.31)$$

in which  $F_1^{(ns,f)}$  measures the valence distributions of flavour  $f$  and  $\bar{\phi}^{(ns)}$  corresponds to the combination of valence distribution functions in eq. (1.2.28).

Since the moments  $\bar{F}_a^{(ns,f)}$  can be measured experimentally, they have to be independent of  $\mu^2$ . This translates into the requirement

$$\mu \frac{d}{d\mu} \bar{F}_a^{(ns,f/h)}(n, Q^2) = 0. \quad (1.2.32)$$

## 1.2. Deep Inelastic Scattering

---

For  $\bar{F}_1^{(ns,f)}$  we then obtain

$$\mu \frac{d}{d\mu} \log \left( \bar{\phi}^{(ns)}(n, \epsilon, \alpha_s(\mu^2)) \right) = -\mu \frac{d}{d\mu} \log \left( \bar{C}_1^{(ns)}(n, \alpha_s(\mu^2), Q^2/\mu^2) \right). \quad (1.2.33)$$

Notice that this relation is independent of the flavour and external hadron. We define the right hand side of eq. (1.2.33) as the anomalous dimension

$$\gamma_n(\alpha_s(\mu^2)) \equiv \mu \frac{d}{d\mu} \log \left( \bar{C}_1^{(ns)}(n, \alpha_s(\mu^2), Q^2/\mu^2) \right), \quad (1.2.34)$$

which only depends on  $\alpha_s(\mu^2)$ . In the singlet case one obtains a matrix  $[\gamma_n^{(s)}]_{ij}$  for partons  $i$  and  $j$ ,

$$\mu \frac{d}{d\mu} \bar{\phi}_{i/h}(n, \epsilon, \alpha_s(\mu^2)) = -[\gamma_n^{(s)}]_{ij} \bar{\phi}_{j/h}(n, \epsilon, \alpha_s(\mu^2)). \quad (1.2.35)$$

Often the terms 'splitting function' and 'anomalous dimension' are used interchangeably, since they are related by a Mellin transform. For instance, if we consider the non-singlet structure function for only one quark flavour at one loop order, we can relate  $\gamma_n^{(1)}$  to  $P_{qq}(x)$  as

$$\begin{aligned} \frac{\alpha_s}{\pi} \gamma_n^{(1)} &= -\frac{\alpha_s}{\pi} \int_0^1 dx x^{n-1} P_{qq}(x) \\ &= \frac{\alpha_s}{2\pi} C_2(F) \left( 4 \sum_{m=2}^n \frac{1}{m} - \frac{2}{n(n+1)} + 1 \right). \end{aligned} \quad (1.2.36)$$

Similar relations exist for the other anomalous dimensions and splitting functions.

The solution to eq. (1.2.33) in terms of  $\gamma_n$  becomes

$$\begin{aligned} \bar{\phi}^{(val)}(n, \epsilon, \alpha_s(Q^2)) &= \bar{\phi}^{(val)}(n, \epsilon, \alpha_s(m^2)) \times \\ &\times \exp \left( -\frac{1}{2} \int_0^{\log(Q^2/m^2)} dt \gamma_n(\alpha_s(m^2 e^t)) \right), \end{aligned} \quad (1.2.37)$$

in which  $m$  is a reference mass. By plugging this into eq. (1.2.31) we obtain for the moments of the structure function

$$\begin{aligned} \bar{F}_1^{(ns)}(n, Q^2) &= \bar{C}_1^{(ns)}(n, \alpha_s(Q^2)) \bar{\phi}^{(val)}(n, \epsilon, \alpha_s(m^2)) \times \\ &\times \exp \left( -\frac{1}{2} \int_0^{\log(Q^2/m^2)} dt \gamma_n(\alpha_s(m^2 e^t)) \right). \end{aligned} \quad (1.2.38)$$

Again, notice the scale breaking  $Q^2$  dependence in the structure function.

Now we finally arrive at the evolution of the parton distribution functions. By applying the inverse Mellin transformation to eq. (1.2.33), we obtain the Dokshitzer-Gribov-Lipatov-Altarelli-Parisi (DGLAP) evolution equation

$$\mu \frac{d}{d\mu} \phi_{f/h}^{val}(x, \epsilon, \alpha_s(\mu^2)) = \int_x^1 \frac{d\xi}{\xi} P_f(x/\xi, \alpha_s(\mu^2)) \phi_{f/h}^{(val)}(\xi, \epsilon, \alpha_s(\mu^2)), \quad (1.2.39)$$

in which

$$P_f(\zeta, \alpha_s) = \int_{-i\infty}^{i\infty} \frac{dn'}{2\pi i} \zeta^{-n'+1} \gamma^{(ns)}(n', \alpha_s), \quad (1.2.40)$$

with  $\text{Re } n > 0$ . It is an RGE which allows one to evolve known parton distribution functions at a certain energy scale to a different energy scale. Likewise one can obtain similar evolution equations for the other parton distribution functions, in which case one obtains a  $(2n_f + 1)$ -dimensional matrix equation in the space of partons.

This concludes our section on DIS. The coefficient functions which we will calculate later on in the thesis are required to extract DIS data from experiments to describe the parton distribution functions to high precision. Moreover, the evolution of the parton distribution functions is governed by the splitting functions, which will also be included in our calculations.

### 1.3 IR Singularities

In section 1.1 we discussed UV divergences in the context of the  $\beta$  functions, but in section 1.2 we implicitly also dealt with IR singularities when we calculated the cross section. It is useful to study IR singularities in more detail. We will see that the IR singularities cancel when one sums over all possible final and initial states in the cross section. To this end we will introduce the concepts of final state radiation and jets, which will be elaborated upon in chapter 2. This section is based on [113].

It is sufficiently insightful to take a step back and consider the abelian gauge theory QED. In particular, it is interesting to study the process  $e^+e^- \rightarrow \mu^+\mu^-$  (figure 1.6). At tree level, the cross section, in the high energy limit  $Q \gg m_e$  and  $Q \gg m_\mu$ , is

$$\sigma_0 = \frac{e_R^4}{12\pi Q^2}, \quad (1.3.1)$$

### 1.3. IR Singularities

---

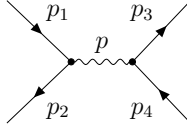


Figure 1.6: Illustrated is the process  $e^+e^- \rightarrow \mu^+\mu^-$  at tree level.

with  $E_{CM} = Q$  and  $e_R$  is the renormalized electric charge<sup>9</sup>. Let us now consider higher-order corrections to this cross section. First, we will take a look at the vertex correction (figure 1.7). We call this a *virtual* contribution to

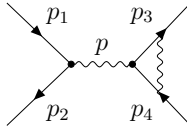


Figure 1.7: Illustrated is the vertex correction to the final state particles of  $e^+e^- \rightarrow \mu^+\mu^-$ .

the process. By including its counterterm to renormalize the UV divergence, we obtain at order  $e_R^6$

$$\sigma_V = \sigma_0 \frac{e_R^2}{8\pi^2} \left( -\log^2 \left[ \frac{m_\gamma^2}{Q^2} \right] - 3 \log \left[ \frac{m_\gamma^2}{Q^2} \right] - \frac{7}{2} + \frac{\pi^2}{3} \right), \quad (1.3.2)$$

in which we have used a Pauli-Villars cutoff to regulate the UV divergence and  $m_\gamma$  regulates the IR divergence. Notice that this cross section is IR divergent, because it blows up when we take  $m_\gamma \rightarrow 0$ . The first term in the brackets is characteristic of IR divergences, known as the Sudakov double logarithm.

To cancel the IR divergence which emerge from the virtual graphs, we need to add the *real* emission graphs  $e^+e^- \rightarrow \mu^+\mu^-\gamma$  at tree level (figure 1.8). The cross section becomes

$$\sigma_R = \sigma_0 \frac{e_R^2}{8\pi^2} \left( \log^2 \left[ \frac{m_\gamma^2}{Q^2} \right] + 3 \log \left[ \frac{m_\gamma^2}{Q^2} \right] - \frac{\pi^2}{3} + 5 \right). \quad (1.3.3)$$

Notice that this also contains IR divergences, regulated by  $m_\gamma$ . If we would not have regulated the divergences with a fictitious mass for the outgoing

---

<sup>9</sup>In the following the on-shell subtraction scheme is used together with a Pauli-Villars regulator to render the UV divergences finite. This results in simpler intermediate expressions, such that we can focus on the IR singularities. The final cross section is regulator and scheme independent.





Figure 1.8: Illustrated are the final state real emission corrections  $e^+e^- \rightarrow \mu^+\mu^-\gamma$ .

photon, the phase space integrand for the cross section would involve the denominators  $E_3 E_\gamma (1 - \cos \theta)$  and  $E_4 E_\gamma (1 - \cos \theta)$ , corresponding to the first and second diagram in figure 1.8. Let us focus on the first term. Here  $\theta$  is the angle between the muon with momentum  $p_3$  and the outgoing photon. Notice that the term diverges if  $E_3 = 0$  or  $E_\gamma = 0$ , and also if  $\theta = 1$ . The first type of divergence is called a *soft singularity* and the second one is called a *collinear singularity* or *mass singularity*. In chapter 2 we will consider a new way to render these kinds of singularities finite. By adding the virtual and real emission cross sections, we obtain

$$\sigma_{tot} = \sigma_V + \sigma_R = \sigma_0 \left( 1 + \frac{3e_R^2}{16\pi^2} \right), \quad (1.3.4)$$

which does not depend on  $m_\gamma$  anymore. The total cross section is IR finite and therefore we call it an *IR safe* observable.

So far we have only described the IR divergences due to final state radiation (and the vertex correction to the final state muons). Equivalently one has to consider the IR divergences due to initial state radiation. In a similar manner, the vertex correction to the incoming electrons has to be added to photons radiating from the electrons. The sum of their cross sections will be IR finite. The collinear singularities are absorbed in electron distribution functions, the QED analog to the PDFs described in section 1.2. In general, the IR singularities will cancel out if one sums over all initial and final states in a finite energy range. This is known as the Kinoshita-Lee-Nauenberg (KLN) theorem.

Lastly, let us introduce jets. Jets are collimated collections of particles. Going back to QCD, consider the production of a hard particle at a collider. As the parton moves through the collider, it will radiate gluons (collinear to its moving direction). These gluons in turn produce gluons and quark-antiquark pairs. At some point the particles will have lost enough energy to hadronize into hadrons, which in turn decay into (meta)stable particles. These are the particles that one detects at the colliders. The collection of radiated particles, moving collinearly to the initial hard parton, constitute

a jet. The momentum of the initial hard parton can then be approximated by adding the momenta of the particles in the jet. In figure 2.4 a jet for a sophisticated jet observable is illustrated.

This concludes brief description on IR singularities. In chapter 2 we will study functions related to jets. In particular, we will apply a new subtraction method to render the jet functions IR finite and to parametrise their poles.

## 1.4 Integration By Parts

In this section we will explain the *Integration By Parts* (IBP) technique for the reduction of scalar integrals to master integrals. First will derive the relation in the context of dimensional regularization, then we will apply it to a simple example and finally we will discuss an algorithm to automate the procedure. This section is based on [114, 115].

### 1.4.1 Dimensional regularization

Often one encounters UV and IR divergencies in Feynman graphs. There are many ways to regulate them, such as imposing a fixed cut-off to regulate the divergencies. However, in QCD it is convenient to regularize the divergent integrals by using the method of dimensional continuation. This is based on the observation that the divergencies are eliminated by changing the dimension of the integrals. The main advantage of the method is that the gauge and Poincaré symmetries of the theory are preserved, which isn't necessarily true in other regularization schemes.

In dimensional regularization one works with integrals in  $d$  finite non-integer dimensions. On the contrast, in ordinary integration the dimension is either finite and integer or infinite. Therefore one cannot assume that the properties for ordinary integration also hold in  $d$ -dimensional integrals. Thus there is a need to proof that the required properties of the integrals (with which we are familiar in ordinary integration) also hold in  $d$  dimensions. Among many existing useful properties, we are interested in one particular, which we will come to call the *integration by parts* identity. In order to derive the identity, we will first need to establish a definition for  $d$ -dimensional integration. To do that, we will first explain the setup.

Suppose that  $f$  is a function of a finite set of vectors, e.g. a scalar  $f(p^2, p \cdot q_1, q_1^2, \dots)$  or a tensor

$$f^{ij}(p, q) = p^i q^j f_1(p^2, p \cdot q, q^2) + g^{ij} f_2(p^2, p \cdot q, q^2), \quad (1.4.1)$$

in which  $p$  and  $q_i$  are vectors in a  $d$ -dimensional space. We would then like to split our  $d$ -dimensional space as a finite integer subspace containing all the  $q$ 's and the remainder, calling them *parallel* space and *transverse* space respectively,

$$\begin{aligned} p &= p_{||} + p_T \\ &= \sum_{i=1}^J p^i e_i + p_T, \end{aligned} \quad (1.4.2)$$

in which the  $e_i$ 's span an orthonormal basis containing all the  $q_i$ 's with  $i = \{1, \dots, J\}$ . One is now able to express the  $d$ -dimensional integral in terms of an ordinary integral as

$$\int d^d p f(p) = \frac{2\pi^{(d-J)/2}}{\Gamma((d-J)/2)} \int d^J p_{||} \int_0^\infty dp_T p_T^{d-J-1} f(p). \quad (1.4.3)$$

However, notice that this definition is problematic at  $p_T = 0$  for small  $d$ . In order to derive an adequate definition for the continuation to small  $d$ , we will consider a function  $f(p^2)$  that vanishes as  $p \rightarrow \infty$  and is analytic at  $p = 0$  such that

$$\int d^d p f(p^2) = \frac{2\pi^{d/2}}{\Gamma(d/2)} \int_0^\infty dp p^{d-1} f(p^2), \quad (1.4.4)$$

converges at  $p \rightarrow \infty$  for  $d > 0$ . By adding and subtracting the leading behaviour at the  $p \rightarrow 0$  limit<sup>10</sup>, one obtains expressions for the dimensional continuation for  $d \leq d_{\max}$ . For  $-2 < d < d_{\max}$  we can split the integral at a fixed constant  $C$  as

$$\begin{aligned} \int d^d p f(p^2) &= \frac{2\pi^{d/2}}{\Gamma(d/2)} \left\{ \int_C^\infty dp p^{d-1} f(p^2) + \int_0^C dp p^{d-1} f(p^2) \right\} \\ &= \frac{2\pi^{d/2}}{\Gamma(d/2)} \left\{ \int_C^\infty dp p^{d-1} f(p^2) + \right. \\ &\quad \left. + \int_0^C dp p^{d-1} \left( [f(p^2) - f(0)] + f(0) \right) \right\}. \end{aligned} \quad (1.4.5)$$

Subsequently we integrate over the last term as

$$\int_0^C dp p^{d-1} f(0) = f(0) \frac{p^d}{d} \Big|_0^C = f(0) \frac{C^d}{d}, \quad (1.4.6)$$

---

<sup>10</sup>By expanding  $f(p^2)$  as  $f(p^2) = f(0) + f'(0)p^2 + \frac{f''(0)}{2!}p^4 + \dots$

#### 1.4. Integration By Parts

---

such that eq. (1.4.5) becomes

$$\int d^d p f(p^2) = \frac{2\pi^{d/2}}{\Gamma(d/2)} \left\{ \int_C^\infty dp p^{d-1} f(p^2) + \int_0^C dp p^{d-1} [f(p^2) - f(0)] + f(0) \frac{C^d}{d} \right\}, \quad (1.4.7)$$

which is independent of the choice of  $C$ . In the case that  $d_{\max} = 0$  we can use this freedom to choose  $C \rightarrow \infty$  to obtain

$$\int d^d p f(p^2) = \frac{2\pi^{d/2}}{\Gamma(d/2)} \int_0^\infty dp p^{d-1} [f(p^2) - f(0)]. \quad (1.4.8)$$

At  $d = 0$  we first rewrite the gamma function as

$$\frac{1}{\Gamma(\frac{d}{2})} = \frac{d}{2} \frac{1}{\Gamma(\frac{d}{2} + 1)}. \quad (1.4.9)$$

This term will contribute a factor of zero at  $d = 0$  to the expression. Then we choose  $C = 1$ , such that the  $\log(C)$  terms vanish in the  $d$ -expansion of the last term in eq. (1.4.7),

$$f(0) \frac{C^d}{d} = \frac{f(0)}{d}. \quad (1.4.10)$$

This results in

$$\int d^d p f(p^2) = d \left( \int_{C=1}^\infty dp p^{d-1} f(p^2) + \int_0^{C=1} dp p^{d-1} [f(p^2) - f(0)] \right) + d \frac{f(0)}{d}. \quad (1.4.11)$$

Notice that the first term on the right hand side vanishes, since the terms inside the brackets are finite (because the first integral does not contain a divergence and in the second integral we subtract the divergent behaviour at  $p \rightarrow 0$ ). In the second term the zero from the gamma function (eq. (1.4.9)) cancels the pole in  $d$  (eq. (1.4.10)). Finally we obtain

$$\int d^0 p f(p^2) = f(0). \quad (1.4.12)$$

This procedure can be extended to lower  $d$ , for  $-2l - 2 < d < -2l$  with  $l$  a positive integer,

$$\int d^d p f(p^2) = \frac{2\pi^{\frac{d}{2}}}{\Gamma(\frac{d}{2})} \int_0^\infty dp p^{d-1} \left( f(p^2) - f(0) - p^2 f'(0) - \dots - \frac{p^{2l}}{l!} f^{(l)}(0) \right), \quad (1.4.13)$$

with

$$\int d^{-2l}p f(p^2) = (-\pi)^{-l} f^{(l)}(0). \quad (1.4.14)$$

But what if eq. (1.4.4) diverges at  $p = \infty$  for  $d > 0$  as a power-law? This occurs often in Feynman integrals at  $d = 4$ . Well, in this case one can again use eq. (1.4.3) to apply dimensional continuation in order to regulate the integral with  $d - 4$  perpendicular dimensions. This is a negative number of dimensions, thus one can apply eq. (1.4.4) to the  $p_T$ -integral in which  $d$  is replaced by  $(d - J)$ .

Because we systematically related  $d$ -dimensional integration to ordinary integration and showed that dimensional continuation is not problematic, we can extend the property of translational invariance, which holds for ordinary integration, to  $d$ -dimensional integration,

$$\int d^d p f(p + q) = \int d^d p f(p), \quad (1.4.15)$$

in which  $q$  is included in the parallel space. By considering an infinitesimal translation, one can expand the left hand side to the first order as

$$\int d^d p \left( f(p) + q^i \frac{\partial}{\partial p^i} f(p) \right), \quad (1.4.16)$$

which suggests that<sup>11</sup>

$$\int d^d p \frac{\partial}{\partial p^i} f(p) = 0. \quad (1.4.17)$$

Here we assumed  $f$  to be a scalar function, but of course the same also holds for tensor functions. Replacing  $f(p) \rightarrow f^i(p) = k^i f(p)$  with  $k^i \in \{p, q^i\}$ , we obtain

$$\int d^d p \frac{\partial}{\partial p^i} \left( k^i f(p) \right) = 0. \quad (1.4.18)$$

This is our desired result. Historically it has been called the *integration-by-parts* (IBP) relation, because it is reminiscent of the surface term in the integration-by-parts relation of calculus.

---

<sup>11</sup>By Gauss's law this was to be expected, since we assumed that  $f \rightarrow 0$  for  $p \rightarrow \infty$ .

### 1.4.2 Applications of the IBP relation

To demonstrate the method, we will first apply the identity to the simple case of one-loop vacuum massive Feynman integrals

$$F(\alpha) = \int \frac{d^d p}{(p^2 - m^2)^\alpha}. \quad (1.4.19)$$

Let us start with the IPB relation

$$\int d^d p \frac{\partial}{\partial p} \cdot p \frac{1}{(p^2 - m^2)^\alpha} = 0, \quad (1.4.20)$$

in which the dot product sums over the indices  $\mu = 1, 2, \dots, d$ . The integrand becomes

$$\begin{aligned} & \frac{d(p^2 - m^2)^\alpha - p \cdot \partial_p ((p^2 - m^2)^\alpha)}{(p^2 - m^2)^{2\alpha}} \\ &= \frac{d}{(p^2 - m^2)^\alpha} - \frac{2\alpha p^2}{(p^2 - m^2)^{\alpha+1}} \\ &= \frac{d}{(p^2 - m^2)^\alpha} - \frac{2\alpha}{(p^2 - m^2)^\alpha} - \frac{2\alpha m^2}{(p^2 - m^2)^{\alpha+1}}, \end{aligned} \quad (1.4.21)$$

such that the relation results in

$$(d - 2\alpha) F(\alpha) - 2\alpha m^2 F(\alpha + 1) = 0, \quad (1.4.22)$$

or

$$F(\alpha) = \frac{d - 2\alpha + 2}{2(\alpha - 1)m^2} F(\alpha - 1). \quad (1.4.23)$$

Using the fact that the integrals with integer  $\alpha < 0$  vanish here<sup>12</sup>, one can reduce all the integrals to a single *master integral* (MI)  $F(1) = I_1$  as

$$F(\alpha) = \frac{(-1)^\alpha (1 - d/2)_{\alpha-1}}{(\alpha - 1)! (m^2)^{\alpha-1}} I_1 \quad (1.4.24)$$

for integer positive  $\alpha$ . The master integral  $I_1$  is

$$I_1 = -i\pi^{d/2} \Gamma(1 - d/2) (m^2)^{(\frac{d}{2}-1)}. \quad (1.4.25)$$

---

<sup>12</sup>One way to see this, is to apply eq. (1.4.13) to eq. (1.4.19) with  $-2\beta - 2 < d \leq -2\beta$ , in which  $\beta = -\alpha$ . This results in  $\int d^d p f(p^2) = \int d^d p (f(p^2) - (p^2)^\beta / m^2)$ , which implies that  $\int d^d p (p^2)^\beta = 0$ , for every  $\beta$ . For negative values of  $\alpha$  eq. (1.4.19) will consist of linear combinations of such integrals and will therefore vanish.

Here  $(x)_\alpha$  is the Pochhammer symbol, which is defined as

$$(x)_\alpha = \frac{\Gamma(\alpha + x)}{\Gamma(x)}. \quad (1.4.26)$$

Let us now consider a slightly more realistic and complicated example, a massless one-loop propagator

$$F(\alpha_1, \alpha_2) = \int \frac{d^d k}{(k^2)^{\alpha_1} ((q-k)^2)^{\alpha_2}}. \quad (1.4.27)$$

Notice that these integrals vanish if  $\alpha_1$  and/or  $\alpha_2 \leq 0$ , because the integrals will be scaleless or have an odd power in  $k$ . The corresponding IBP relation is

$$\int d^d k \frac{\partial}{\partial k} \cdot k \frac{1}{(k^2)^{\alpha_1} ((q-k)^2)^{\alpha_2}} = 0. \quad (1.4.28)$$

The left hand side becomes

$$\begin{aligned} &= dF(\alpha_1, \alpha_2) + \int d^d k \left( -\frac{2\alpha_1}{(k^2)^{\alpha_1} ((q-k)^2)^{\alpha_2}} + 2\alpha_2 \frac{k}{(q-k)} \frac{1}{(k^2)^{\alpha_1} ((q-k)^2)^{\alpha_2}} \right) \\ &= dF(\alpha_1, \alpha_2) - 2\alpha_1 F(\alpha_1, \alpha_2) - \alpha_2 F(\alpha_1, \alpha_2) - \alpha_2 F(\alpha_1 - 1, \alpha_2 + 1) + \\ &\quad + \alpha_2 q^2 F(\alpha_1, \alpha_2 + 1), \end{aligned} \quad (1.4.29)$$

in which we rewrote

$$2 \frac{k}{(q-k)} = -1 - \frac{k^2}{(q-k)^2} + \frac{q^2}{(q-k)^2}. \quad (1.4.30)$$

Adopting the definition  $n^\pm F(\alpha_n) \equiv F(\alpha_n \pm 1)$ , the IBP can be written as

$$d - 2\alpha_1 - \alpha_2 - \alpha_2 2^+(1^- - q^2) = 0, \quad (1.4.31)$$

in which we implicitly act on  $F(\alpha_1, \alpha_2)$ . To obtain a recursive relation one can isolate the term proportional to  $q^2$ , shift  $\alpha_2 \rightarrow \alpha_2 - 1$  and divide by  $q^2$ , such that one obtains

$$\begin{aligned} F(\alpha_1, \alpha_2) = & -\frac{1}{q^2(\alpha_2 - 1)} \left( (d - 2\alpha_1 - \alpha_2 + 1) F(\alpha_1, \alpha_2 - 1) + \right. \\ & \left. - (\alpha_2 - 1) F(\alpha_1 - 1, \alpha_2) \right). \end{aligned} \quad (1.4.32)$$

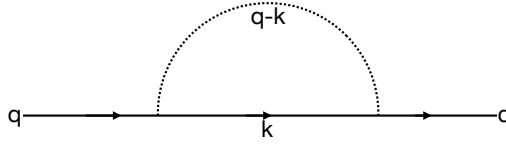


Figure 1.9: The one-loop self energy graph of a massive propagator is illustrated. The dashed line corresponds to the propagator with  $\alpha_2$ , the solid line with momentum  $k$  corresponds to  $\alpha_1$ .

Notice that this relation only is valid if  $\alpha_2 > 1$  due to the pole on the right hand side. Now, you might wonder how far we can reduce an integral with respect to  $\alpha_1$ . Say we reduced an integral to the form  $F(\alpha_1, \alpha_2 = 1)$ , then one can use the symmetry  $F(x, y) = F(y, x)$  for this specific family of integrals, because we are free to shift  $k \rightarrow k - q$ . Thus, by interchanging  $\alpha_1 \leftrightarrow \alpha_2$  on the left and right hand side of eq. (1.4.32) and using the identity on the right hand side, we obtain

$$F(\alpha_1, \alpha_2) = -\frac{1}{q^2(\alpha_1 - 1)} \left( (d - 2\alpha_2 - \alpha_1 + 1)F(\alpha_1 - 1, \alpha_2) + (\alpha_1 - 1)F(\alpha_1, \alpha_2 - 1) \right), \quad (1.4.33)$$

with  $\alpha_2 = 1 \Rightarrow$

$$F(\alpha_1, 1) = -\frac{1}{q^2(\alpha_1 - 1)} (d - \alpha_1 - 1)F(\alpha_1 - 1, 1).$$

Subsequently it is possible to reduce  $\alpha_1$  to  $\alpha_1 = 1$ , such that one obtains an expression in terms of the master integral  $I_1 = F(1, 1)$ .

Lastly, let us take a look at the one-loop self energy graph of a massive propagator (see figure 1.9)

$$F(\alpha_1, \alpha_2) = \int \frac{d^d k}{(k^2 - m^2)^{\alpha_1} ((q - k)^2)^{\alpha_2}}. \quad (1.4.34)$$

Again, for values of  $\alpha_1 \leq 0$  the integral is scaleless and will therefore vanish. Also, the integral can be evaluated in terms of gamma functions for  $\alpha_2 \leq 0$  (see [115] for all the formulae required). After taking the corresponding derivatives, we obtain the following set of integration by parts relations,

$$\begin{aligned} d - 2\alpha_1 - \alpha_2 - 2m^2\alpha_1 1^+ - 2\alpha_2 2^+(1^- - q^2 + m^2) &= 0 \\ \alpha_2 - \alpha_1 - \alpha_1 1^+(q^2 + m^2 - 2^-) - \alpha_2 2^+(1^- - q^2 + m^2) &= 0. \end{aligned} \quad (1.4.35)$$



By multiplying the first equality in eq. (1.4.35) by  $(q^2 + m^2)$  and the second one by  $2m^2$  and by taking the difference of the two resulting relations, we obtain

$$(q^2 - m^2)^2 \alpha_2 2^+ = (q^2 - m^2) \alpha_2 1^- 2^+ + (d - 2\alpha_1 - \alpha_2) q^2 - (d - 3\alpha_2) m^2 + 2m^2 \alpha_1 1^+ 2^-. \quad (1.4.36)$$

We see that this relation allows us to reduce the index  $\alpha_2$ , as the values of  $\alpha_2$  on the right hand side will be smaller than or equal to the value of  $\alpha_2$  on the left hand side. It is convenient to rewrite the equation as

$$F(\alpha_1, \alpha_2) = \frac{1}{(\alpha_2 - 1)(q^2 - m^2)^2} \left[ (\alpha_2 - 1)(q^2 - m^2) F(\alpha_1 - 1, \alpha_2) + \{ (d - 2\alpha_1 - \alpha_2 + 1) q^2 + (d - 3\alpha_2 + 3) m^2 \} F(\alpha_1, \alpha_2 - 1) + 2m^2 \alpha_1 F(\alpha_1 + 1, \alpha_2 - 2) \right]. \quad (1.4.37)$$

By repeatedly applying the relation, one can reduce  $\alpha_2$  to one (due to the pole in  $\alpha_2 = 1$  on the right hand side) or a value  $\leq 0$ . Notice that the first term on the right hand side also reduces  $\alpha_1$ .

Now, one might wonder whether the integrals with  $\alpha_2 = 1$  will be problematic (unlike the integrals with  $\alpha_2 \leq 0$  which can be expressed in terms of gamma functions). It turns out that these integrals can be re-expressed by using eq. (1.4.35). Taking the difference of the two relations with  $\alpha_2 = 1$ , we obtain

$$(q^2 - m^2) \alpha_1 1^+ = \alpha_1 + 2 - d + \alpha_1 1^+ 2^-, \quad (1.4.38)$$

which either lowers the index  $\alpha_1$  keeping  $\alpha_2 = 1$  fixed or keeps  $\alpha_1$  fixed and lowers  $\alpha_2$ . By repeatedly applying the relation, one will obtain a solution which will be a linear combination of the master integral  $I_1 = F(1, 1)$  and integrals with  $\alpha_2 \leq 0$  and  $\alpha_1 > 0$ . Naturally the question arises whether one can obtain a minimal set of irreducible master integrals. I.e. can we reduce the sum of integrals with  $\alpha_2 \leq 0$  to a set of master integrals? The answer is yes: by applying the first relation in eq. (1.4.35) to the integral, we can reduce the index  $\alpha_1$  to one. Subsequently we multiply the same relation by  $2^-$  to re-express the last term in eq. (1.4.36), resulting in

$$(d - \alpha_2 - 1) 2^- = (q^2 - m^2)^2 \alpha_2 2^+ + (q^2 + m^2)(d - 2\alpha_2 - 1). \quad (1.4.39)$$

This relation allows us to increase  $\alpha_2$  to either zero or one. Therefore we are left with two master integrals  $I_1 = F(1, 1)$  and  $I_2 = F(1, 0)$ , meaning that we

can express  $F(\alpha_1, \alpha_2)$  as a linear combination of both, including coefficients which depend on  $d, q^2$  and  $m^2$ . Notice that it is impossible to relate  $I_1$  and  $I_2$  to each other at general  $d$ , because the former integral depends on  $q^2$  whereas the latter does not.

### 1.4.3 General structure of the reduction

In this section we will discuss the general structure of the IBP reduction process. Our starting point will be a family of scalar Feynman integrals parametrised as

$$F(q_1, \dots, q_n; \alpha_1, \dots, \alpha_N) = \int \dots \int \prod_{i=1}^h d^d k_i \frac{1}{\prod_{j=1}^N E_j^{\alpha_j}}, \quad (1.4.40)$$

in which we have  $n$  external momenta and  $N$  integer indices for general  $d$ . The denominators in eq. (1.4.40) are defined as

$$E_l = \sum_{i \geq j \geq 1} A_l^{ij} r_i \cdot r_j - m_l^2, \quad (1.4.41)$$

where the momenta  $r_i$  either are loop momenta ( $k_i$  with  $i = 1, \dots, h$ ) or externals  $r_{h+1} = q_1$  until  $r_{h+n} = q_l$  and  $N = h + n$ . The integration by parts relation will then be of the form

$$\int \dots \int \prod_{i'=1}^h d^d k_{i'} \frac{\partial}{\partial k_i} \left( r_j \prod_{j'=1}^N E_j^{-\alpha_{j'}} \right) = 0. \quad (1.4.42)$$

Subsequently one takes the required derivatives. The resulting scalar products can be rewritten in terms of the denominators using eq. (1.4.41), such that the IBP relations can be expressed as

$$\sum a_i F(\alpha_1 + b_{i,1}, \dots, \alpha_N + b_{i,N}) = 0, \quad (1.4.43)$$

in which we omitted the external momenta from the arguments. The  $b_{i,j}$  are integers and the coefficients  $a_i$  are polynomials which depend on  $\alpha_i$ , masses, dimension  $d$  and kinematic invariants. By explicitly substituting all values for  $(\alpha_1, \dots, \alpha_N)$ , one obtains a large set of relations between the Feynman integrals in the family. Of course, one should not forget about the shift symmetries amongst the integrals,

$$F(\alpha_1, \dots, \alpha_N) = (-1)^{\sum d_i \alpha_i} F(\alpha_{\pi(1)}, \dots, \alpha_{\pi(N)}), \quad (1.4.44)$$

in which the  $\pi_i$  depicts a permutation and  $d_i$  is a fixed integer that can either be zero or one. We encountered this symmetry in the example of the massless one-loop propagator<sup>13</sup>. Moreover, parity conditions can constrain the number of non-vanishing integrals in the family. The boundary conditions

$$F(\alpha_1, \dots, \alpha_N) = 0 \text{ for } \alpha_{i_1} \leq 0, \dots, \alpha_{i_k} \leq 0, (i_1, \dots, i_k) \subset (1, \dots, N), \quad (1.4.45)$$

are related to the scaleless integrals, as discussed in the previous section.

On the more formal mathematical side of this discussion, the Feynman integrals and the relations amongst them can be viewed as follows: each integral is an element of the field of functions  $\mathcal{F}$  with  $N$  integer arguments. The previously described relations are then elements in the adjoint space  $\mathcal{F}^*$ , such that for each  $r \in \mathcal{F}^*$  and  $f \in \mathcal{F}$  there exists a  $\langle r, f \rangle$ . A trivial example in the adjoint space is the set of elements  $H_{\alpha_1, \dots, \alpha_N}^*$ ,

$$\langle H_{\alpha_1, \dots, \alpha_N}^*, f \rangle = f(\alpha_1, \dots, \alpha_N). \quad (1.4.46)$$

By fixing a set of IBPs and relations, one generates the subspace  $\mathcal{R} \subset \mathcal{F}^*$ . One can relate an integral  $F(\alpha_1, \dots, \alpha_N)$  to other integral(s)  $F(\alpha'_1, \dots, \alpha'_N)$  given that there exists an element  $r \in \mathcal{R}$  such that

$$\langle r, F \rangle = F(\alpha_1, \dots, \alpha_N) + \sum k_{\alpha'_1, \dots, \alpha'_N} F(\alpha'_1, \dots, \alpha'_N) = 0. \quad (1.4.47)$$

In particular, we are interested in the set of solutions of all the elements in  $\mathcal{R}$ , since all the independent solutions correspond to the master integrals of the given family. This finite set  $\mathcal{S}$  is defined as

$$\mathcal{S} = \{f \in \mathcal{F} : \langle r, f \rangle = 0 \ \forall \ r \in \mathcal{R}\}. \quad (1.4.48)$$

Now, you might wonder how one chooses these master integrals. Indeed, there is some freedom in choosing them<sup>14</sup>. We will define an ordering scheme between different points  $(\alpha_1, \dots, \alpha_N)$ . They will be ranked according to the simplicity of the integrals, using the *lower* symbol  $\prec$ . Notice that integrals in section 1.4.2 simplified if (some of) the indices reduced to a non-positive value, since these resulted in vanishing integrals or known expressions. It is convenient to decompose the space of integer indices in *sectors*. For  $N$  indices there are  $2^N$  sectors, labeled by  $\nu \subseteq \{1, \dots, N\}$  in which  $\sigma_\nu = \{(\alpha_1, \dots, \alpha_N) : \alpha_i > 0 \text{ if } i \in \nu, \text{ else } \alpha_i \leq 0\}$ . In this way  $\sigma_\nu \prec \sigma_\mu$  if  $\nu \subset \mu$ , i.e. having more non-positive indices. Moreover, on the level of the integrals, if the sector of

<sup>13</sup>The righthand side of eq. (1.4.44) could become a sum of integrals if the topology definition includes numerators.

<sup>14</sup>For instance if two integrals are equivalent to each other by symmetry.

the indices in  $F(\alpha_1, \dots, \alpha_N) \prec$  the sector of the indices in  $F(\alpha'_1, \dots, \alpha'_N)$ , then  $F(\alpha_1, \dots, \alpha_N) \prec F(\alpha'_1, \dots, \alpha'_N)$ .

An alternative way to define sectors, is by making use of the sets of *directions*  $\nu = \{d_1, \dots, d_N\}$ . Each element can either be -1 or 1. The sectors are then defined as  $\sigma_\nu = \{(\alpha_1, \dots, \alpha_N) : (\alpha_i - 1/2)d_i > 0\}$ . The corner point  $\alpha_i = (d_i + 1)/2$  for  $i = 1, \dots, N$  is the lowest point in the sector  $\sigma_\nu$ . After one has introduced an ordering scheme inside the sectors, the masters can be chosen as the integrals  $F(\alpha_1, \dots, \alpha_N)$  for which there exists no relation that produces an integral  $F'$  lower than  $F$ .

### 1.4.4 Laporta's Algorithm

Laporta's Algorithm [59] is a method that is frequently used in automated reduction programs which implement integration by parts relations. Consider a set  $\mathcal{F}_M \subset \mathcal{F}$  generated by  $H_{\alpha_1, \dots, \alpha_n}$  with  $\sum_i |\alpha_i| \leq M$ . In the adjoint space we consider  $\mathcal{R}_M = \mathcal{R} \cap (\text{subset of } \mathcal{F}^* \text{ generated by } H_{\alpha_1, \dots, \alpha_n}^*)$ , with again  $\sum_i |\alpha_i| \leq M$ . Then,

$$\lim_{M \rightarrow \infty} |\dim(\mathcal{F}_M) - \dim(\mathcal{R}_M)| = \dim(\mathcal{S}), \quad (1.4.49)$$

which is exactly the number of masters in the system. The trick is then, to find the value of  $M$  for which  $\mathcal{R}_M$  is sufficiently large to express any integral in the family in terms of its masters and only its masters. Indeed, at any value of  $M$  one can express an integral in terms of other integrals. However, these 'other integrals' only tend to stabilise to a fixed set of integrals, the masters, once a certain value of  $M$  has been reached. Starting from a minimal value of  $M$ , one repeatedly solves the system of linear equations, until the solutions remain unchanged, i.e. until all the integrals have been expressed in terms of the master integrals of the system.

Let us apply the algorithm to the one-loop self energy graph of a massive propagator eq. (1.4.34). It is convenient to rewrite eq. (1.4.35) as

$$\begin{aligned} L_1(\alpha_1, \alpha_2) &= 0 \\ L_2(\alpha_1, \alpha_2) &= 0, \end{aligned} \quad (1.4.50)$$

with

$$\begin{aligned} L_1(\alpha_1, \alpha_2) &= (d - 2\alpha_1 - \alpha_2)F(\alpha_1, \alpha_2) - 2m^2\alpha_1 F(\alpha_1 + 1, \alpha_2) + \\ &\quad - \alpha_2(F(\alpha_1 - 1, \alpha_2 + 1) + (m^2 - q^2)F(\alpha_1, \alpha_2 + 1)) \\ L_2(\alpha_1, \alpha_2) &= -\alpha_1((m^2 + q^2)F(\alpha_1 + 1, \alpha_2) - F(\alpha_1 + 1, \alpha_2 - 1)) \times \\ &\quad \times (\alpha_2 - \alpha_1)F(\alpha_1, \alpha_2) - \alpha_2(F(\alpha_1 - 1, \alpha_2 + 1) + \\ &\quad + (m^2 - q^2)F(\alpha_1, \alpha_2 + 1)). \end{aligned} \quad (1.4.51)$$

Following the terminology of the previous section, we will consider the sector with  $\alpha_1 > 0$  and  $\alpha_2 \leq 0$ . The values allowed for  $M$  are then dictated by  $\alpha_1 + |\alpha_2| \leq M$ . Thus we will start to solve the system at  $M = 1$  with  $\alpha_1 = 1$  and  $\alpha_2 = 0$ , i.e.  $L_{\{1,2\}}(1, 0) = 0$  to obtain

$$\begin{aligned} F(2, -1) &= \frac{d(m^2 + q^2) - 2q^2}{2m^2} F(1, 0) \\ F(2, 0) &= \frac{(d-2)}{2m^2} F(1, 0). \end{aligned} \quad (1.4.52)$$

If we increase  $M$  by one, we have to solve  $L_{\{1,2\}}(1, 0) = 0$ ,  $L_{\{1,2\}}(2, 0) = 0$  and  $L_{\{1,2\}}(1, -1) = 0$ , which results in

$$\begin{aligned} F(2, -2) &= \frac{(d+2)m^4 + 2(d+2)m^2q^2 + (d-2)q^4}{2m^2} F(1, 0) \\ F(3, -1) &= \frac{(d-2)(-4q^2 + d(m^2 + q^2))}{8m^4} F(1, 0) \\ F(3, 0) &= \frac{(d-4)(d-2)}{8m^4} F(1, 0) \\ F(1, -1) &= (m^2 + q^2) F(1, 0) \end{aligned} \quad (1.4.53)$$

and the two solutions from eq. (1.4.52). Now, notice that all the integrals can be expressed in terms of  $F(1, 0)$ . This means that we have found the master integral corresponding to this sector. In this example the solution stabilised early on, but it could happen that one needs to proceed to higher values of  $M$  for more complicated problems.

### 1.4.5 Lorentz Identities

Apart from the IBP relations, there exists another class of identities used by reduction programs, called the Lorentz Identities (LI). The Lorentz Identities result from the fact that all the Feynman integrals are invariant under Lorentz transformations. The Lorentz identities are of the form

$$q_i^\mu q_j^\nu \left( \sum_s q_{s[\nu} \frac{\partial}{\partial q_s^{\mu]} \right) F(\alpha_1, \dots, \alpha_N) = 0. \quad (1.4.54)$$

They can be expanded as

$$\sum_{i=1}^{h+n} r_{i[\nu} \frac{\partial}{\partial r_i^{\mu]} = \sum_{i=1}^h k_{i[\nu} \frac{\partial}{\partial k_i^{\mu]} + \sum_{i=1}^n q_{i[\nu} \frac{\partial}{\partial q_i^{\mu]}. \quad (1.4.55)$$

## 1.4. Integration By Parts

---

We are then able to show that the Lorentz Identities can be derived from the IBP relations. To this end, let us rewrite eq. (1.4.54) as

$$\begin{aligned}
q_i^\mu q_j^\nu \sum_{s=1}^n q_{s[\mu} \frac{\partial}{\partial q_{s]^\nu]} F &= q_i^\mu q_j^\nu \sum_{s=1}^{h+n} r_{s[\nu} \frac{\partial}{\partial r_{s]^\mu]} F - q_i^\mu q_j^\nu \sum_{s=1}^h k_{s[\nu} \frac{\partial}{\partial k_{s]^\mu]} F \\
&= -q_i^\mu q_j^\nu \sum_{s=1}^h k_{s[\nu} \frac{\partial}{\partial k_{s]^\mu]} F \\
&= \sum_{s=1}^h \left[ (q_i \cdot k_s) q_j \cdot \frac{\partial}{\partial k_s} - (q_j \cdot k_s) q_i \cdot \frac{\partial}{\partial k_s} \right] F \\
&= \sum_{s=1}^h \left[ \frac{\partial}{\partial k_s} \cdot q_j (q_i \cdot k_s) - \frac{\partial}{\partial k_s} \cdot q_i (q_j \cdot k_s) \right] F,
\end{aligned} \tag{1.4.56}$$

where we used eq. (1.4.55) to go from the first to the second line. By expressing  $(q_i \cdot k_s)$  and  $(q_j \cdot k_s)$  linearly in the denominators of the Feynman integrals, and by identifying the generators of the IBP relations as

$$O_{ij} = \frac{\partial}{\partial k_i} \cdot r_j, \tag{1.4.57}$$

we conclude that the Lorentz Identities can be derived from the IBP relations.

### 1.4.6 FIRE

The DIS calculations in the latter part of this thesis relied on the program FIRE [61], which implements Laporta's algorithm. We initially used KIRA [60] to reduce the integrals required for DIS up till three loops. However, FIRE seemed better suited for the type of integrals we encountered, where only a small subset involves the most complicated combinations of risen propagators and numerators. This allowed us to push the calculations to the 4<sup>th</sup>-loop order. The downside of FIRE, when compared to KIRA, is the manual labor required. Indeed, KIRA is more automated and requires less manual interference. However, to streamline the process, all the individual steps which require human interference have been chained together and automated by the author of this thesis. I'll briefly describe the steps required in order to obtain reductions for a set of integrals in FIRE.

We will describe the reduction for the one-loop topology as depicted in figure F.1. We can define the topology as

$$F(\alpha_1, \alpha_2, \alpha_3) = \int d^d k \left( \frac{1}{(k^2)^{\alpha_1}} \right) \left( \frac{1}{(P-k)^{\alpha_2}} \right) \left( \frac{1}{(Q+k)^{\alpha_3}} \right). \tag{1.4.58}$$

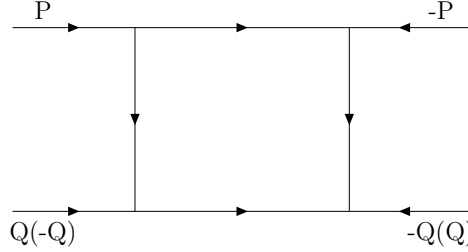


Figure 1.10: The one-loop DIS forward scattering diagram is illustrated.

For the generation of the so-called 'startfile', FIRE requires the parametrisation of each topology. In our case the topology is supplemented as

$$\text{Propagators} = \{\{1, \{k^2, (P - k)^2, (Q + k)^2\}\}\}$$

in the corresponding MATHEMATICA file. One also needs to define the variables of the problem, which in our case are the dimension  $d$  and the inverse Bjorken variable  $w = \frac{2P \cdot Q}{Q^2}$ . The startfile now contains all the necessary IBP relations as well as information on zero-sectors. However, for more complicated problems it is useful to include the program LITERED [116], which generates all the internal symmetries and external symmetries in the corresponding topology. The internal symmetries correspond to the mappings inside sectors and the external symmetries correspond to mappings between different sectors. The LITERED inputfiles require no additional information of the topology. In our experience this decreased the reduction time by a significant amount. For example, the reduction of topology 30 of the N<sup>3</sup>LO DIS non-singlet coefficient function took two weeks to finish using KIRA. However, using FIRE and LITERED, the computation time reduced to two days. Moreover, in some cases it uncovered symmetries among masters, such that we obtained reductions in terms of the minimal set of masters. Not only does this mean that we had to solve less master integrals (manifesting itself in a smaller differential system), but it was also crucial to obtain the minimal set of master integrals for the expansions of the solutions of the master integrals<sup>15</sup>. The expansions rely on the fact that coefficients of the masters in the differential equations are factorised in terms of  $\epsilon$  and  $\omega$ . If there exist relations among some masters in the reduction table, the coefficients in the differential equations turn out to be algebraically involved and unfactorised.

<sup>15</sup>See app. F for a one-loop example of this algorithm.

## 1.4. Integration By Parts

---

In principle one can still expand the coefficients of the master integrals in the case of unfactorised expressions in the differential matrix, but one then needs to take care of spurious poles in  $\epsilon$  in the expansions of the differential matrix.

As a next step, one needs to supplement the integrals to be reduced. Let us for now choose just one integral,  $F(-1, 2, 1)$ . It is possible to supplement a preferred list of master integrals to FIRE, however this is not necessary. The configuration file "ties" all the different files together, includes optional functionalities (such as the inclusion of LITERED generation files, specifying the number of cores to use, usage of a hints folder, using a larger bucket size, etc.) and enjoins FIRE the location to save the results. The results are saved as a .tables file, in which the integrals are identified with unique 10 + - digit numbers. One need to convert the .tables file to a more convenient format by using MATHEMATICA. In our case we obtain

$$\{F[1, \{-1, 2, 1\}] - > ((2 - 2 * w + d * w) * F[1, \{0, 1, 1\}]) / (2 * (1 + w))\}$$

If one were to include more integrals to be reduced, their reductions would be appended to this list. Notice that the reduction is performed in C++, while the start files are generated in MATHEMATICA, as is the conversion of the .tables file to a MATHEMATICA reduction table.

I would briefly like to mention that there exist programs which search for an optimal basis of master integrals [117, 118]. Sometimes the reduction tables include coefficients in which the kinematical invariants mix with the dimension  $d$ , resulting in unfactorised expressions in the differential equations. This can happen due to a degeneracy in the minimal set of master integrals. These programs then search for a different basis of master integrals, such that the denominators are decomposed in products of polynomials of the kinematical variables, which do not depend on the dimension, and polynomials up till order  $O(d^1)$  in which the coefficients are rational numbers. This always resulted in factorised expressions for the differential equations. It is not guaranteed that these procedures result in factorised expressions<sup>16</sup>. Nonetheless the program in [118] performed well when we required its usage.

This concludes our section on IBP relations. We will exhaust the method to reduce all the Feynman integrals required to calculate three- and four-loop DIS amplitudes.

---

<sup>16</sup>There could still exist hidden relations amongst the master integrals, independent of the IBP relations.





## Chapter 2

# One-loop Jet Functions by Geometric Subtraction

This chapter is based on [1]. We will study the GOJET program, which is an automated implementation of the Geometric Subtraction scheme in the class of one-loop jet functions. As explained in section 1.3, physical observables are IR finite if one sums over all the final (and initial) states in a finite energy range. The IR divergences from the virtual contributions cancel against the IR poles which result from real radiation. In Soft-Collinear Effective Theory (SCET) the collinear regime of the final state particles is described by jet functions. In this chapter we will focus on the subtraction of the IR divergences of final state radiation in jet functions at one-loop order in the QCD coupling  $\alpha_s$ . As a result we will obtain regularized jet functions in which the IR poles are identified and the finite contribution is calculated.

### 2.1 Introduction

Experimental studies at the Large Hadron Collider (LHC) impose restrictions on QCD radiation in the final state, to stress test the Standard Model and search for New Physics. If these restrictions are tight, they lead to large logarithms in the corresponding cross section. For example, for Higgs plus one jet production with a veto on additional jets with transverse momentum above  $p_T^{\text{veto}}$ , the cross section takes the following form

$$\sigma(p_T^{\text{veto}}) = \sigma_0 \left[ 1 + \sum_{\substack{n \geq 1 \\ 2n \geq m \geq 0}} c_{n,m} \alpha_s^n \ln^m \left( \frac{m_H}{p_T^{\text{veto}}} \right) + \mathcal{O} \left( \frac{p_T^{\text{veto}}}{m_H} \right) \right], \quad (2.1.1)$$

where  $\sigma_0$  is the leading-order cross section, and the coefficients  $c_{n,m}$  are independent of  $p_T^{\text{veto}}$ . For a tight veto  $p_T^{\text{veto}} \ll m_H \sim p_T^{\text{jet}}$ , the expansion

in  $\alpha_s$  deteriorates due to the large logarithms and resummation is crucial to improve convergence and reduce the theory uncertainty. Resummation captures the dominant effect of higher-order corrections, effectively treating  $\ln(m_H/p_T^{\text{veto}}) \sim 1/\alpha_s$ .

Large logarithms arise because the cross section involves multiple scales that are widely separated. Resummation of these logarithms can be achieved by factorizing the cross section into components that each involve a single scale, using diagrammatic methods in QCD, see e.g. [119–126], or Soft-Collinear Effective Theory (SCET) [73–77]. For exclusive Higgs plus one jet production, discussed in eq. (2.1.1), this takes on the following (schematic) form  $\sigma \sim HSBBJ$  [127, 128]. The hard function  $H$  describes hard scattering, the soft function  $S$  encodes the effect of soft radiation, and the beam functions  $B$  and jet function  $J$  account for initial- and final-state collinear radiation. The structure of this factorization not only depends on the process, but also on the observable and can involve convolutions between ingredients (though it is simply a product in the above example). Because each ingredient in the factorization involves a single scale, the large logarithms can be resummed by evaluating each ingredient at its natural scale and using the renormalization group to evolve them to a common scale. Alternatively, an automated approach to resummation was pursued in refs. [129, 130].

In this chapter we focus on calculating one-loop jet functions, which enter in resummed cross sections starting at next-to-leading logarithmic (NLL') accuracy. Resummation at NLL' includes the two-loop cusp anomalous dimension and one-loop (non-cusp) anomalous dimensions. Jet functions have been calculated for a wide range of observables, including the invariant mass [131–136], the family of  $e^+e^-$  event shapes called angularities with respect to the thrust axis [137–139] or Winner-Take-All axis [140, 141], Sterman-Weinberg jets [142, 143], the cone and the  $k_T$  family of jet algorithms for exclusive [143, 144] and inclusive [145, 146] jet production. Jet functions have also been considered for a range of jet substructure observables, such as the jet shape [147–149]. In our calculations we treat quarks as massless and restrict to infrared-safe observables. An example of a massive quark (initiated) jet function is given in refs. [150, 151], and an example of an infrared-unsafe jet observable is the electric charge of the jet [152, 153].

We briefly comment on the other ingredients in the factorization: A general approach to calculating soft functions has been developed in refs. [154–157]. In particular, the `SOFTSERVE` package [157] provides two-loop soft functions for processes with two collinear directions (i.e. two jets in  $e^+e^-$  or 0 jets in  $pp$  collisions), and an extension to  $N$  jets is in progress [158]. Hard functions can be obtained from the IR finite part of helicity amplitudes, as long as the color of the initial (final) particles is not averaged (summed) over,

see e.g. ref. [159].

The difficulty in calculating jet functions lies in the phase-space integration, which depends on the observable. When feasible, an analytic approach is superior. However, there are observables for which even the one-loop jet function is highly nontrivial, such as jet broadening [138] and the jet shape [149], for which fully analytic results are difficult to obtain or have not been obtained yet. The numerical approach we develop here offers a promising alternative, addressing the collinear and soft divergences in a general way, thereby automating the calculation of one-loop jet functions for a broad range of observables. At minimum, our work provides a valuable cross check for analytic calculations.

The poles in the dimensional regulator are obtained analytically, possibly up to an integral over the azimuthal angle, and depend on the collinear and soft behavior of the observable. This soft behavior is described by a power law, and therefore simply characterized by the exponent and coefficient. Extracting these parameters may require solving non-trivial algebraic equations, and we develop a procedure to simplify this step. The full details/complications of the measurement only enter in the finite term, which can be integrated numerically. We have implemented our approach in a MATHEMATICA package, Geometric One-loop Jet functions (GOJET), which accompanies the GOJET paper [1]. GOJET can handle a large class of infrared-safe observables, including all the observables listed above.

Using GOJET we provide explicit examples of the method for the angularities with respect to the Winner-Take-All axis, the cone and  $k_T$ -clustering jet algorithms and the jet shape. Furthermore we calculate for the first time the one-loop jet function for angularities with respect to the thrust axis including recoil. We cross check our result against existing results in the literature for the specific case of jet broadening [138] and for the case of no recoil [137, 160].

The remainder of the chapter is structured as follows: In section 2.2 we discuss how we use geometric subtraction to calculate jet functions, including a simple example. The GOJET package, which provides a MATHEMATICA implementation, is discussed in section 2.3. In section 2.4, we use our package to calculate several one-loop jet functions, and we conclude in section 2.5.

## 2.2 General Method

In section 2.2.1 we will discuss geometric subtraction and how we apply it to calculate one-loop jet functions. Technical aspects related to the treatment of Heaviside theta functions in our calculation and infrared safety are discussed

in sections 2.2.2 and 2.2.3, respectively. We illustrate our method by calculating the jet function for the  $e^+e^-$  angularity event shapes in section 2.2.4, with further examples in section 2.4.

### 2.2.1 Subtraction scheme

The jet function depends on the flavor  $i = q, g$  of the initiating parton and the jet observable, and has a perturbative expansion in  $\alpha_s$

$$\mathcal{J}_{i,\text{obs}} = \sum_n \left( \frac{\alpha_s}{2\pi} \right)^n \mathcal{J}_{i,\text{obs}}^{(n)}. \quad (2.2.1)$$

At tree level the jet consists of a single quark or gluon, and in general  $\mathcal{J}_i^{(0)} = 1$  in the appropriate units.<sup>1</sup> The one-loop contribution is given by the collinear limit of two final-state partons

$$\begin{aligned} \mathcal{J}_{i,\text{obs}}^{(1)} &= \int_0^\pi d\phi \int_0^\infty ds \int_0^1 dz Q_i(s, z, \phi) M_{\text{obs}}(s, z, \phi), \\ Q_i(s, z, \phi) &= \frac{(\mu^2 e^{\gamma_E})^\epsilon}{\sqrt{\pi} \Gamma(\frac{1}{2} - \epsilon)} \left( \frac{\nu}{\omega} \right)^\eta \frac{P_i(z) (\sin \phi)^{-2\epsilon}}{z^{\epsilon+\eta} (1-z)^{\epsilon+\eta} s^{1+\epsilon}}, \\ P_q(z) &= C_F \left[ \frac{1+z^2}{1-z} - \epsilon(1-z) \right], \\ P_g(z) &= n_f T_R \left[ 1 - \frac{2z(1-z)}{1-\epsilon} \right] + C_A \left[ \frac{z}{1-z} + \frac{1-z}{z} + z(1-z) \right]. \end{aligned} \quad (2.2.2)$$

Here  $s$  denotes the invariant mass of the two partons, and  $z$  and  $1-z$  the momentum fractions of the partons. The squared matrix element is contained in  $Q_i(s, z, \phi)$ , with  $P_i(z)$  the (sum of) splitting function(s). The calculation is performed in  $d = 4 - 2\epsilon$  dimensions and the  $\overline{\text{MS}}$ -renormalization scheme with renormalization scale  $\mu$  is employed. For certain observables an additional rapidity regulator  $\eta$  and corresponding rapidity scale  $\nu$  are required [161–166], which is included in eq. (2.2.2) for generality. This arises when the collinear and soft functions have the same invariant mass scale  $\mu$ , with transverse momentum measurements being the typical example. We will use [162], but at one loop this is essentially equivalent to almost all other choices. For the extension of eq. (2.2.2) to a two-loop example, see ref. [167].

The measurement in a jet function can often be written as  $\delta[\mathcal{O} - f(s, z, \phi)]$ . To avoid distributions, we require the user to rewrite the measurement as

<sup>1</sup>An exception is the jet shape, discussed in section 2.4.3, which contains a theta function that sets it to zero if the recoil from soft radiation is too large.

## 2.2. General Method

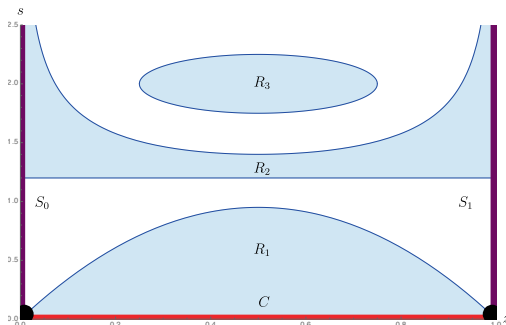


Figure 2.1: For an example of a generic observable the phase space can be constrained to several representative regions (blue). The collinear singularity  $C$  (red line), soft singularities  $S_0$  and  $S_1$  (purple lines), and soft-collinear singularities (black dots) are indicated.

a Heaviside theta function by integrating, i.e.  $\Theta[\mathcal{O} - f(s, z, \phi)]$ , where we are now cumulative in  $\mathcal{O}$ .<sup>2</sup> We therefore assume that the measurement  $M_{\text{obs}}(s, z, \phi)$  is a Heaviside theta function, which cuts out a certain region of the collinear phase space, as illustrated in figure 2.1 (suppressing  $\phi$  dependence). An advantage of cumulative distributions is that they involve logarithms rather than plus distributions:

$$\int_0^{t^c} dt \left[ \frac{\theta(t) \ln^n t}{t} \right]_+ = \frac{1}{n+1} \ln^{n+1} t^c. \quad (2.2.3)$$

In section 2.2.2, a technical point related to rewriting measurement delta functions in terms of theta functions will be discussed. There are also measurements that are naturally theta functions. For example, the  $k_T$ -family of jet algorithms requires both particles to be clustered into a jet with radius parameter  $R$ ,  $M_{k_T}(s, z, \phi) = \Theta(s \leq z(1-z)p_T^2 R^2)$ , where  $p_T$  is the transverse momentum of the jet. In principle these phase-space constraints  $M_{\text{obs}}$  can depend on the azimuthal angle  $\phi$  as well, but since there is no singularity associated with the  $\phi$  integration, we will only include  $\phi$  when needed.

The jet function in eq. (2.2.2) has divergences as  $s \rightarrow 0$  (collinear divergence), and  $z \rightarrow 0$  and  $z \rightarrow 1$  (soft divergences), which occur at the phase-space boundaries in figure 2.1. Infrared-safe observables must always either include or exclude the entire collinear divergence (the red line in figure 2.1), as will be discussed more in section 2.2.3. From the point of view of

<sup>2</sup>Alternatively, one can consider a conjugate space, as was employed in automated calculations of soft functions [155, 156].

collinear subtraction, one can consider the jet function (as long as it contains the collinear divergence) as a collinear counterterm. Different observables can then be viewed as different schemes, differing in the extent that soft and soft-collinear divergences are included in the observable. For instance, region 1 of the generic observable illustrated in figure 2.1 only contains the collinear and part of the soft-collinear singularities. By contrast, region 2 only contains part of the soft and none of the collinear divergence. Region 3 does not contain any soft or collinear divergent parts of phase space and does therefore not have to be regulated. Another possibility would be to consider an observable which corresponds to the complement of region 1, which naively causes problems because it develops a logarithmic singularity for  $s \rightarrow \infty$ . However, its one-loop jet function is given by minus the jet function for region 1, because the integral over the full collinear phase space results in a scaleless integral.

To define a general subtraction scheme for calculating jet functions for infrared-safe observables, we follow the approach of geometric subtraction [93]. We would like to define a finite part of the jet function as follows:

$$\text{Finite}(\mathcal{J}_{i,\text{obs}}^{(1)}) = \left[ \int_0^\pi d\phi \int_{B\mu^2}^\infty ds \int_A^{1-A} dz Q_{i \rightarrow j}(s, z, \phi) M_{\text{obs}}(s, z, \phi) \right]_{A,B \rightarrow 0}, \quad (2.2.4)$$

where we introduced the dimensionless slicing parameters  $A$  and  $B$ , that remove the soft and collinear divergence, and which we subsequently want to take to zero. The central idea of geometric subtraction rests on the identity:

$$\begin{aligned} \left[ \int_a^1 dx \frac{f(x)}{x} \right]_{a \rightarrow 0} &= \left[ \int_0^1 dx \frac{f(x) - f(x)\Theta(x < a)}{x} \right]_{a \rightarrow 0} \\ &= \int_0^1 dx \frac{f(x) - f(0)\Theta(x < a)}{x}, \end{aligned} \quad (2.2.5)$$

where we exploited that  $a$  is small on the second line to replace  $f(x)$  by  $f(0)$  in the second term. However, the expression on the second line is now regulated for any  $0 < a \leq 1$ , leading to a duality between slicing and subtraction schemes. To obtain the full jet function from the above finite part, counterterms need to be added to reinstate the part of the integral that is removed by the cuts. The counterterms generated in this way are added back in integrated form, regulated dimensionally and if needed also with a rapidity regulator, and may give a finite contribution to the jet function. While a subtlety arises in general when different limits do not commute, here we do not face this problem as the collinear and soft singularities are factorized. For the small  $A$  limit in eq. (2.2.4) we can then straightforwardly

## 2.2. General Method

---

apply eq. (2.2.5). However for the parameter  $B$  nothing is gained from this procedure, because the jet function is already in the limit of small  $s$  and the counterterm generated is the original integral itself.

To obtain a simpler counterterm in the  $s < B$  region, we can however use a simpler observable, which we choose to be the jet mass, as a collinear counterterm. (This was also used in the geometric subtraction scheme [93].) Since the region of the  $s$ - $z$  plane corresponding to the jet mass is box-shaped, we will refer to this collinear counterterm as the *box*. A subtlety now appears due to the difference of soft and soft-collinear divergences included in the box counterterm and the given observable  $M_{\text{obs}}$ , which as discussed above may not be the same. To deal with this problem we introduce separate soft counterterms for both the box counterterm and the  $M_{\text{obs}}$  term in the region  $s < B\mu^2$ , as discussed in detail below.

These considerations lead us to the following final decomposition of the jet-function into finite and divergent parts:

$$\begin{aligned}
 \mathcal{J}_{i,\text{obs}}^{(1)} &= G_{i,\text{obs},1} + G_{i,\text{obs},2} + G_{i,\text{obs},3}, \\
 G_{i,\text{obs},1} &\equiv \int_0^\pi d\phi \int_0^1 dz \int_{B\mu^2}^\infty ds \left[ Q_i M_{\text{obs}} - Q_{i,0} M_{\text{obs},0} \Theta(z < A) - Q_{i,1} M_{\text{obs},1} \Theta(1 - z < A) \right] \\
 &\quad + \int_0^\pi d\phi \int_0^1 dz \int_0^{B\mu^2} ds \left[ Q_i (M_{\text{obs}} - 1) - Q_{i,0} (M_{\text{obs},0} - 1) \Theta(z < A) \right. \\
 &\quad \left. - Q_{i,1} (M_{\text{obs},1} - 1) \Theta(1 - z < A) \right], \\
 G_{i,\text{obs},2} &\equiv \int_0^\pi d\phi \int_0^1 dz \int_0^\infty ds \left[ Q_{i,0} M_{\text{obs},0} \Theta(z < A) + Q_{i,1} M_{\text{obs},1} \Theta(1 - z < A) \right], \\
 G_{i,\text{obs},3} &\equiv \int_0^\pi d\phi \int_0^1 dz \int_0^{B\mu^2} ds \left[ Q_i - Q_{i,0} \Theta(z < A) - Q_{i,1} \Theta(1 - z < A) \right],
 \end{aligned} \tag{2.2.6}$$

where the arguments  $s, z, \phi$  are suppressed and  $A, B$  are positive real numbers with  $A \leq 1$ . The first term in  $G_{i,\text{obs},1}$  corresponds to the finite part defined in eq. (2.2.4), and the other terms correspond to integrated counterterms. The box counterterm  $G_{i,\text{obs},3}$  leads to  $M_{\text{obs}} \rightarrow (M_{\text{obs}} - 1)$  in the box region  $s < B\mu^2$  in  $G_{i,\text{obs},1}$ . It is straightforward to check that the sum of  $G_1$ ,  $G_2$  and  $G_3$  is equal to the original one-loop jet function.

The advantage of the above decomposition is that  $G_3$  is observable independent,  $G_2$  only depends on the soft limit of the observable (which can be encoded by a few parameters at one-loop order, see eq. (2.2.8)) and  $G_1$  is finite. In eq. (2.2.6),  $Q_0$  and  $Q_1$  denote the soft  $z \rightarrow 0$  and  $z \rightarrow 1$  limit of  $Q$ .



Explicitly,

$$\begin{aligned}
 Q_{q,0}(s, z, \phi) &= Q_q(s, z, \phi)|_{z \rightarrow 0} = 0, \\
 Q_{q,1}(s, z, \phi) &= Q_q(s, z, \phi)|_{z \rightarrow 1} = \frac{(\mu^2 e^{\gamma_E})^\epsilon}{\sqrt{\pi} \Gamma(\frac{1}{2} - \epsilon)} \left(\frac{\nu}{\omega}\right)^\eta \frac{2C_F(\sin \phi)^{-2\epsilon}}{(1-z)^{1+\eta+\epsilon} s^{1+\epsilon}}, \\
 Q_{g,1}(s, z, \phi) &= \frac{(\mu^2 e^{\gamma_E})^\epsilon}{\sqrt{\pi} \Gamma(\frac{1}{2} - \epsilon)} \left(\frac{\nu}{\omega}\right)^\eta \frac{C_A(\sin \phi)^{-2\epsilon}}{(1-z)^{1+\eta+\epsilon} s^{1+\epsilon}} = Q_{g,0}(s, 1-z, \phi).
 \end{aligned} \tag{2.2.7}$$

Similarly,  $M_{\text{obs},0}$  and  $M_{\text{obs},1}$  denote the soft  $z \rightarrow 0$  and  $z \rightarrow 1$  limit of the measurement  $M_{\text{obs}}$ . The soft limit can contain multiple boundary conditions on the phase space, which we account for by writing  $M_{\text{obs},0}$  and  $M_{\text{obs},1}$  as a sum of Heaviside theta functions that constrain the integration over  $s$  as a function of  $z$ . Moreover, they will follow a power-law behavior parametrized by

$$M_{\text{obs}}(s, z, \phi)|_{z \rightarrow 0} = \Theta(\Phi) \sum_r M_{\text{obs}}^r = \Theta(\Phi) \sum_r \Theta\left(\frac{c_{0r}^+ \mu^2}{z^{\alpha_{0r}^+}} - s\right) \Theta\left(s - \frac{c_{0r}^- \mu^2}{z^{\alpha_{0r}^-}}\right), \tag{2.2.8}$$

$$M_{\text{obs}}(s, z, \phi)|_{z \rightarrow 1} = \Theta(\Phi) \sum_r M_{\text{obs}}^r = \Theta(\Phi) \sum_r \Theta\left(\frac{c_{1r}^+ \mu^2}{(1-z)^{\alpha_{1r}^+}} - s\right) \Theta\left(s - \frac{c_{1r}^- \mu^2}{(1-z)^{\alpha_{1r}^-}}\right),$$

where the sum on  $r$  is over different regions (see figure 2.1), and the parameters  $c_i$ ,  $\alpha_i$  depend on the observable, and can depend on  $\phi$  as well.<sup>3</sup> We also allow for a constraint  $\Phi$  on the azimuthal angle, as will be discussed in section 2.2.3. Depending on the observable, each soft boundary condition will therefore follow one out of three distinct behaviors shown in figure 2.1: the upper boundary of  $R_1$  corresponds to  $\alpha < 0$ , the lower boundary of  $R_2$  to  $\alpha = 0$ , the upper boundary to  $\alpha > 0$  and  $R_3$  does not extend into the soft region. Finding  $c_{0,1}$  and  $\alpha_{0,1}$  can be nontrivial, and we will discuss a strategy to do so for an involved example in section 2.4.2.

We will now discuss the decomposition in eq. (2.2.6) in more detail, using the graphical representation in figure 2.2 for the  $k_T$  algorithm. In order to get a finite  $G_1$  in figure 2.2a, we subtracted the collinear singularity and the soft singularities. The collinear singularity is removed by the box, replacing  $M_{\text{obs}}$  by  $M_{\text{obs}} - 1$  when  $s \leq B\mu^2$ , such that  $M_{\text{obs}}(s = 0, z, \phi) - 1 = 0$ . The soft singularities get accounted for by subtracting the  $z \rightarrow 0$  and/or  $z \rightarrow 1$

<sup>3</sup>In general  $c_0 = c_1$  and  $\alpha_0 = \alpha_1$ , but we will show examples where this is no longer true because the observable depends on the azimuthal angle, which differs by  $\pi$  between the two partons.

## 2.2. General Method

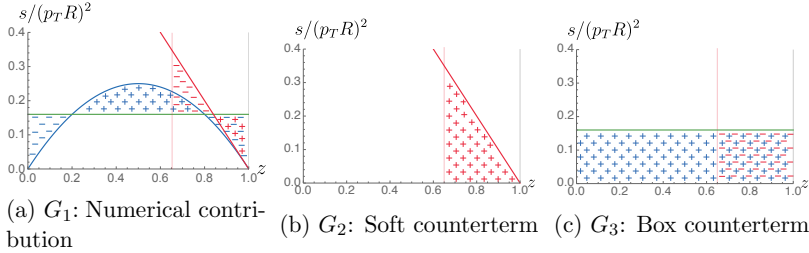


Figure 2.2: A graphical representation of our subtraction scheme in eq. (2.2.6). We have only included the soft counterterms for  $z \rightarrow 1$  for legibility. Shown are the restrictions on the measurement from the observable  $M_{obs}$  (blue line), the soft limit of the observable  $M_{obs,1}$  (red line), the box  $s < B\mu^2$  (green line) and the cut on  $z$  arising from  $A$  (pink line). Blue plus (minus) areas correspond to positive (negative) contributions of the full integrand  $Q_i$ , while red plus (minus) areas correspond to positive (negative) contributions of  $Q_{i,1}$ .

limits of the integrand. Indeed, one can see that in figure 2.2a the blue plusses and red minuses cancel as  $z \rightarrow 1$ . The resulting integral  $G_1$  is now finite. For general observables,  $G_1$  in eq. (2.2.6) may be hard to calculate analytically, and one has to resort to numerical integration techniques. In the examples in section 2.4, we will use the CUBA implementation of VEGAS [168] to perform the integrations. Convergence problems in the numerical integration may arise due to the mismatch of the observable and its soft approximation, which generally can lead to integrable singularities. If these problems are severe it can help to find an explicit remapping of the counterterm, which decreases the mismatch between the observable and its soft limit. We present a method for how this can be achieved with a worked through example in app. B.

Let us now discuss the integrated counterterms. Due to their simplicity, the counterterms can be calculated analytically, which we discuss for a single region  $r$  in the sum in eq. (2.2.8). Let us first focus on the soft counterterms, which are contained in  $G_2$  shown in figure 2.2b. The soft limits of the integrand  $Q_i M_{obs}$  are given by  $Q_{i,0} M_{obs,0}$  and  $Q_{i,1} M_{obs,1}$ , see eqs. (2.2.7) and (2.2.8). The constants  $c_i$  and  $\alpha_i$  are user input in our code, see section 2.3. For values  $\alpha \neq 1$ , no rapidity regulator is needed and  $\eta$  can be set to 0, leading to the following soft counterterm

$$G_{q,2} = \frac{2C_F}{\epsilon^2} \frac{e^{\gamma_E \epsilon}}{\sqrt{\pi} \Gamma(\frac{1}{2} - \epsilon)} \int_0^\pi d\phi \Theta(\Phi) (\sin \phi)^{-2\epsilon} \left[ \frac{(c_1^+)^{-\epsilon}}{(1 - \alpha_1^+)} A^{-\epsilon(1 - \alpha_1^+)} - \frac{(c_1^-)^{-\epsilon}}{(1 - \alpha_1^-)} A^{-\epsilon(1 - \alpha_1^-)} \right],$$

$$G_{g,2} = \frac{C_A}{\epsilon^2} \frac{e^{\gamma_E \epsilon}}{\sqrt{\pi} \Gamma(\frac{1}{2} - \epsilon)} \int_0^\pi d\phi \Theta(\Phi) (\sin \phi)^{-2\epsilon} \left[ \frac{(c_0^+)^{-\epsilon}}{(1 - \alpha_0^+)} A^{-\epsilon(1 - \alpha_0^+)} - \frac{(c_0^-)^{-\epsilon}}{(1 - \alpha_0^-)} A^{-\epsilon(1 - \alpha_0^-)} + \frac{(c_1^+)^{-\epsilon}}{(1 - \alpha_1^+)} A^{-\epsilon(1 - \alpha_1^+)} - \frac{(c_1^-)^{-\epsilon}}{(1 - \alpha_1^-)} A^{-\epsilon(1 - \alpha_1^-)} \right]. \quad (2.2.9)$$

For  $\alpha = 1$  one needs a rapidity regulator and the corresponding expression is given in app. A. The box counterterm  $G_3$  in figure 2.2c is given by

$$G_{q,3} = C_F I(\phi^+, \phi^-; \epsilon) \frac{e^{\gamma_E \epsilon} B^{-\epsilon}}{\sqrt{\pi} \Gamma(\frac{1}{2} - \epsilon)} \left( \frac{(4 - \epsilon)(1 - \epsilon) \Gamma^2[1 - \epsilon]}{2\Gamma[2 - 2\epsilon]} - 2A^{-\epsilon} \right), \quad (2.2.10)$$

$$G_{g,3} = I(\phi^+, \phi^-; \epsilon) \frac{e^{\gamma_E \epsilon} B^{-\epsilon}}{\sqrt{\pi} \Gamma(\frac{1}{2} - \epsilon)} \left( - \left( \frac{3}{2} C_A (3\epsilon - 4) + 2\epsilon n_f T_R \right) \times \right. \\ \left. \times \frac{(1 - \epsilon) \Gamma^2[1 - \epsilon]}{(3 - 2\epsilon) \Gamma[2 - 2\epsilon]} - 2C_A A^{-\epsilon} \right).$$

The integral over  $\phi$  has been carried out for  $\Theta(\Phi) = \Theta(\phi^+ - \phi) \Theta(\phi - \phi^-)$  leading to the function

$$I(a, b; \epsilon) = \int_a^b d\phi \sin^{-2\epsilon} \phi. \quad (2.2.11)$$

The evaluation of this integral and its expansion to order  $\epsilon^2$  is presented in app. C.

The chosen subtraction bears fruit in the simplicity of the integrated counterterms. The corresponding Laurent series in  $\epsilon$  can be expressed solely in terms of the Riemann zeta function at integer values, given that only pure Gamma functions appear. From an analytic point of view, the potentially more complicated pieces are instead captured in the finite part, which depends on the details of the observable and can be calculated numerically to arbitrary high order in  $\epsilon$ . Notice that the soft counterterm  $G_{i,2}$  can give rise to more complicated integrals if the coefficients  $c_i^\pm$  depend on the azimuthal angle  $\phi$ . One may be able to carry out this integral analytically in certain cases, but this can certainly not be done in general. This is not a problem, because one can expand in  $\epsilon$  and  $\eta$  before integrating over  $\phi$ .

## 2.2.2 Delta and theta functions

In our subtraction scheme we assume that the observables restrict the integration to certain regions of phase space via Heaviside theta functions. However,

## 2.2. General Method

---

many observables  $\mathcal{O}$  are naturally expressed in terms of Dirac delta functions, requiring one to rewrite it using

$$\delta[\mathcal{O} - f(s, z, \phi)] = \pm \frac{d}{d\mathcal{O}} \Theta[\pm(\mathcal{O} - f(s, z, \phi))], \quad (2.2.12)$$

where  $f$  is a function of the kinematics of the collinear splitting, and possibly external parameters. The sign  $\pm$  should be chosen such that the theta function does not vanish at tree-level, which ensures that the poles are included in the one-loop jet function. For example, if  $\mathcal{O} \geq 0$  and at tree-level  $\mathcal{O} = 0$ , one needs to choose the plus sign in eq. (2.2.12).

In perturbative QCD one often works with the following convention for the Dirac delta function,

$$g(0) = \int_0^c dx \, g(x) \delta(x) \quad \text{for } c > 0. \quad (2.2.13)$$

This differs from the definition given in standard math literature

$$g(0) = \int_b^c dx \, g(x) \delta(x) \quad \text{for } c > 0 > b, \quad (2.2.14)$$

where the lower boundary  $b$  must be strictly less than zero. If the delta function that encodes the measurement satisfies eq. (2.2.13), this has implications for the definition of the Heaviside function on the right-hand side of eq. (2.2.12). In particular, one must demand then that  $\Theta(0) = 0$ . To see this, consider a function  $g(x)$  with  $0 \leq x \leq 1$ . From

$$\begin{aligned} g(0) &= \int_0^1 dx \, g(x) \delta(x) = \int_0^1 dx \, g(x) \frac{d}{dx} \Theta(x) = [g(x) \Theta(x)]_0^1 - \int_0^1 dx \, \frac{d}{dx} g(x) \\ &= g(1) \Theta(1) - g(0) \Theta(0) - (g(1) - g(0)) = g(0) (1 - \Theta(0)), \end{aligned} \quad (2.2.15)$$

we conclude that  $\Theta(0) = 0$ . While this is not of much concern when a theta function is integrated over, there are situations where it must be taken into account. As an example, the jet shape calculation involves a jet function describing the energy fraction  $z$  inside a cone, see section 2.4.3. Switching to a cumulant variable for  $z$ , we need to choose  $\delta(z - \dots) = -d/dz[-(z - \dots)]$ , because  $0 \leq z \leq 1$  and  $z = 1$  at tree-level. If we now want to calculate the average momentum fraction from the cumulant tree-level result

$$\begin{aligned} \int_0^1 dz \, z \delta(z - 1) &= - \int_0^1 dz \, z \frac{d}{dz} \theta(1 - z) \\ &= -z \theta(1 - z)|_0^1 + \int_0^1 dz \, \theta(1 - z) = 1 - \theta(0) = 1, \end{aligned} \quad (2.2.16)$$

we have to take  $\theta(0) = 0$  to find agreement with the direct evaluation using the delta function.

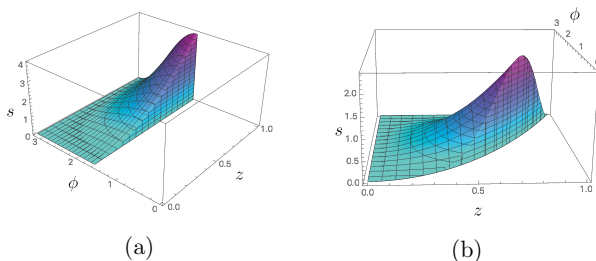


Figure 2.3: IR unsafe observables that our code (a) can and (b) can't handle.

### 2.2.3 Infrared safety and limitations on the observable

While so far our discussion was mostly based on the  $s$ - $z$  plane, there are observables which depend also on the azimuthal angle  $\phi$ . The integration domain is then parametrized by coordinates  $(s, z, \phi)$  and IR safety requires the full  $s = 0$  plane to be included or excluded by the observable, i.e. the set of points

$$\{(s, z, \phi) | s = 0, 0 \leq z \leq 1, 0 \leq \phi \leq \pi\}. \quad (2.2.17)$$

However, our method allows for a special class of IR-unsafe observables, where only subdomains of the collinear plane with the azimuthal angle bounded between constant values are included/excluded by the observable, i.e.

$$\{(s, z, \phi) | s = 0, 0 \leq z \leq 1, \phi^- \leq \phi \leq \phi^+\}, \quad (2.2.18)$$

with  $0 \leq \phi^- < \phi^+ \leq \pi$ . This is illustrated in figure 2.3a. An IR-unsafe observable which is not of this form, and currently not supported by GOJET, is illustrated in figure 2.3b. Here  $\phi^\pm$  vary as functions of  $z$  across the collinear plane in such a way that not the full  $s = 0$  plane is included in the integration domain. For  $s > 0$  the bounds on  $\phi$  can depend on  $z$ . GOJET can also handle IR-unsafe observables that include just  $z = 0$  and/or  $z = 1$  of the  $s = 0$  plane, which only require soft counterterms.

### 2.2.4 Example: Angularities with the Winner-Take-All axis

We will now illustrate our scheme by considering the family of  $e^+e^-$  event shapes called angularities [169]

$$e_b \equiv \frac{1}{Q} \sum_i E_i (\sin \theta_i)^{1-b} (1 - |\cos \theta_i|)^b \stackrel{\theta_i \ll 1}{\approx} \frac{2^{-b}}{Q} \sum_i E_i \theta_i^{b+1}, \quad (2.2.19)$$

## 2.2. General Method

parametrized by  $b^4$ . Here  $Q$  is the center-of-mass energy, and the sum runs over all particles  $i$  in the final state with energy  $E_i$  and angle  $\theta_i$  with respect to some axis. The final expression is only valid in the small-angle limit, which is appropriate for the jet function calculation, highlighting that  $e_b$  probes the angular distribution with exponent  $1 + b > 0$ . While angles were originally taken with respect to the thrust axis, we will here use the Winner-Take-All axis [140]. For the one-loop jet function this axis is simply along the most energetic particle in the jet, so the only non-zero contribution in the sum on  $i$  in eq. (2.2.19) comes from the least energetic particle, with  $\theta_i$  the angle between the two partons in the jet. Noting that  $s = 2p_1 \cdot p_2 = \frac{1}{2}z(1-z)(1-\cos\theta)Q^2 \approx \frac{1}{4}z(1-z)\theta^2Q^2$ , we obtain the following measurement function for a cut on the angularity  $e_b \leq e_b^c$ ,

$$M_b(s, z) = \Theta \left[ z(1-z)Q^2 \left( \frac{e_b^c}{\min[z, 1-z]} \right)^{2/(b+1)} - s \right]. \quad (2.2.20)$$

For angularity exponent  $b < 1$ , the observable is unbounded from above, similar to the top curve of region 2 in figure 2.1. In the notation of eq. (2.2.8), we see that the soft limit of the observable is characterized by  $c_0 = c_1 = Q^2(e_b^c)^{2/(b+1)}/\mu^2$  and  $\alpha_0 = \alpha_1 = 2/(1+b) - 1$ . The one-loop contribution to the jet function is obtained by plugging in these constants in eqs. (2.2.9) and (2.2.10) to calculate  $G_2$ , performing the integration over  $s$  and  $z$  for  $G_1$ , and adding these contributions to the box  $G_3$ . Performing the integration over  $s$  analytically and the integration over  $z$  numerically for  $b = 2$ , we obtain using GOJET

$$\mathcal{J}_{q,e_2}^{(1)} = \frac{\alpha_s C_F}{2\pi} \left( \frac{\mu^2}{Q^2(e_2^c)^{2/3}} \right)^\epsilon \left( \frac{3}{2\epsilon^2} + \frac{3}{2\epsilon} - 1.909961286856877 \right), \quad (2.2.21)$$

where we used  $\mu = Q(e_2^c)^{1/3}$  to calculate the constant contribution and re-instated the logarithmic behaviour afterwards. Our result agrees with the expression in refs. [140, 141] up to order  $10^{-11}$ .<sup>5</sup> For  $b = 0$  the rapidity regulator is required. In that case we find

$$\mathcal{J}_{q,e_0}^{(1)} = \frac{\alpha_s C_F}{2\pi} \left( \frac{2\nu}{Q} \right)^\eta \left( \frac{\mu^2}{Q^2(e_0^c)^2} \right)^\epsilon \left( \frac{2}{\epsilon\eta} + \frac{3 - 4\log 2}{2\epsilon} - 1.8693096781349734 \right), \quad (2.2.22)$$

in agreement with ref. [140].

<sup>4</sup>Our  $b$  is related to the parameter  $a$  in ref. [169] by  $b = 1 - a$ .

<sup>5</sup>Refs. [140, 141] both use  $\beta = 1 + b$  instead of  $b$ , and ref. [140] also removes the  $2^{-b}$  from the definition in eq. (2.2.19) and takes  $Q$  to be the jet energy.

## 2.3 GOJet Program

The **GOJET** **MATHEMATICA**-package automatically performs the subtraction, given the observable and its soft limit (see eq. (2.2.8)) as input. One can either let **MATHEMATICA** perform the numerical integration or choose to export the integrand. The latter feature may be useful if **NIntegrate** either has difficulty converging or is not fast enough. In such cases it can be advantageous to use algorithms such as **VEGAS**, that are faster due to their implementation in C++ or Fortran. A general overview of the various functions included in the package is given in section 2.3.1. A detailed description of their input is given in section 2.3.2, with a worked-out example in section 2.3.3.

### 2.3.1 Functions

There are a total of 12 different functions, listed in section 2.3.2, which the user can access. As indicated by their names half of these are for calculating gluon jet functions while the other half are for calculating quark jet functions. Restricting to the former, **PolesGluon** returns the pole terms in  $\epsilon$  and  $\eta$  for the gluon jet function and **GluonJet** returns the integrand of the finite terms, by which we here refer to the  $\epsilon^0\eta^0$ -term. In addition, **GluonJetN** performs the numerical integration over the cube  $0 \leq s, z, \phi \leq 1$  of this integrand. This integration domain is the result of mapping  $s \rightarrow s/(1-s)$  and  $\phi \rightarrow \pi\phi$ , which also stabilizes the integration over  $s$ . Note that **GluonJet** also contains the  $\epsilon^0\eta^0$ -pieces of the counterterms  $G_2$  and  $G_3$ , which are already integrated over analytically. For the convenience of the user these pieces are simply added in integrated form since they are not altered by the trivial numerical integration over the unit cube.

Let us now discuss the arguments of the functions in general terms. The first arguments encode the measurement  $\mathcal{O}$  and its soft limit  $\mathcal{O}_0$  and  $\mathcal{O}_1$  corresponding to the limits  $z \rightarrow 0$  and  $z \rightarrow 1$ , respectively. The observable should generally be IR safe, with some exceptions discussed in section 2.2.3. Furthermore, we require certain restrictions on the form of the soft limits. Specifically, it is not possible to restrict the  $\phi$ -integration boundaries via  $\mathcal{O}_0$  and  $\mathcal{O}_1$ , whose format is fixed. It is however possible to apply  $s, z$ -independent constraints on the boundaries of the  $\phi$ -integration through the separate argument  $\Phi$ , which are the same for the finite part as well as the counterterms.

The next set of arguments specify the regularization and IR scheme: the need of a rapidity regulator or collinear regulator is controlled by the switches **rr** and **box**, respectively. The explicit cut for the soft limits and box is specified by **A** and **B** (see eq. (2.2.6)). The independence of the final result on

### 2.3. GOJET Program

---

these parameters provides a useful cross-check for the calculation. A specific choice of these parameters can also be used to improve the convergence of the numerical integration. For the gluon jet function, the number of quark flavors is specified through the argument `nf`. The number of colors has been fixed to three, but the full dependence on the Casimirs can be easily reconstructed from the answer. The final set of arguments enables the user to specify the integration method or output format for the integrand.

Finally, we also allow for more complicated observables, where the phase-space restriction due to the measurement breaks up into more than one region. The corresponding functions have “Regions” appended to their name, and contain additional arguments specifying possible dependence on external parameters in the regions.

#### 2.3.2 Input format

Here we specify the syntax of each of the functions:

```
GluonJet[O, O0, O1, Φ, rr, box, A, B, s, z, φ, nf, format, file]
GluonJetRegions[R, O, R0, O0, R1, O1, Φ, rr, box, A, B, s, z, φ, nf,
format, file]
GluonJetN[O, O0, O1, Φ, rr, box, A, B, s, z, φ, nf, method]
GluonJetRegionsN[R, O, R0, O0, R1, O1, Φ, rr, box, A, B, s, z, φ, nf,
method]
PolesGluon[O0, O1, Φ, rr, box, A, B, φ, nf]
PolesGluonRegions[O0, O1, Φ, rr, box, A, B, φ, nf]

QuarkJet[O, O0, O1, Φ, rr, box, A, B, s, z, φ, format, file]
QuarkJetRegions[R, O, R0, O0, R1, O1, Φ, rr, box, A, B, s, z, φ, format,
file]
QuarkJetN[O, O0, O1, Φ, rr, box, A, B, s, z, φ, method]
QuarkJetRegionsN[R, O, R0, O0, R1, O1, Φ, rr, box, A, B, s, z, φ, method]
PolesQuark[O0, O1, Φ, rr, box, A, B, φ]
PolesQuarkRegions[O0, O1, Φ, rr, box, A, B, φ]
```

The variables used to describe the input are:

- `O`: The list of argument(s) of the Heaviside theta function encoding the bounds imposed by the measurement. More specifically, `O` contains the arguments of the Heaviside theta functions  $M_{\text{obs}}$  in eq. (2.2.2). For



the case of a single region, the elements of the list correspond to the arguments of Heaviside theta functions, whose product constrain the region. In the case of multiple regions,  $\mathbf{0}$  is a list of lists. The entries of the outer list correspond to the different regions, each entry is again a list of constraints containing the arguments of the Heaviside theta functions  $M_{\text{obs}}^r$  constraining the particular region. This allows the user to implement arbitrary sums of products of Heaviside theta functions.

- $\mathbf{R}_1$  ( $\mathbf{R}_0$ ): List of lists which contain arguments of Heaviside theta functions which depend *only* on external parameters for each region in the limit  $z \rightarrow 1$  ( $z \rightarrow 0$ ). The length of this list is therefore equal to the number of soft regions that emerge in the soft limit. Regions that do not depend on external parameters need  $\{1\}$  as input in their respective position in the list. The number of soft regions can be less than the number of regions, but should match with the lists for  $\mathbf{0}_0$  and  $\mathbf{0}_1$  below. In particular, regions may merge or disappear in the soft limit.  $\mathbf{R}_1$  ( $\mathbf{R}_0$ ) can also be used in cases with just one region where there is dependence on external parameters in the soft limits.
- $\mathbf{0}_1$  ( $\mathbf{0}_0$ ): List  $\{\{c_1^-, \alpha_1^-\}, \{c_1^+, \alpha_1^+\}\}$  describing the lower and upper boundary of the region in the limit where  $z \rightarrow 1$  (and similarly for  $z \rightarrow 0$ ), see eq. (2.2.8). If there is no lower boundary,  $c_1^-$  is just 0. When considering multiple regions,  $\mathbf{0}_1$  ( $\mathbf{0}_0$ ) is a list of lists where each region has an upper and a lower boundary of the aforementioned format.
- $\Phi$ : List of arguments of the Heaviside theta functions that impose constraints on the azimuthal angle  $\phi$ , i.e., the input  $\{\phi^+ - \phi, \phi - \phi^-\}$  will constrain  $\phi^- < \phi < \phi^+$ . In the case of multiple regions that contain collinear and/or soft divergences we require the range on  $\phi$  to be the same for all regions. (Arbitrary constraints on  $\phi$  can of course be encoded in  $\mathbf{0}$ ; but these are not allowed to survive singular limits; that is they should match the boundaries imposed by  $\Phi$  in these limits; see section 2.2.3 for more details.)
- **rr**: Boolean variable specifying whether a rapidity regulator should be included, which we implemented as

$$(2(1-z)z))^{-\eta} \quad (2.3.1)$$

This corresponds to the more conventional factor  $(\nu/((1-z)z\omega))^\eta$ , for the scale choice  $\nu = \frac{1}{2}\omega$ . The user can always reconstruct the full dependence on the scale  $\nu$  a posteriori, given the knowledge of the  $1/\eta$  pole.

### 2.3. GOJET Program

---

- **box**: Boolean controlling whether a box is needed to handle the collinear divergence. It should be included when the region of phase space includes  $s = 0$  and not otherwise (in line with the restrictions outlined in section 2.2.3).
- **A**: Real number specifying the region where the soft counterterms are subtracted. Explicitly, the  $z \rightarrow 0$  ( $z \rightarrow 1$ ) counterterms are subtracted in the phase-space region where  $z < A$  ( $1 - z < A$ ), and therefore  $0 < A \leq 1$ .
- **B**: Postive real number specifying the size of the box.
- **s**: Variable used to describe the invariant mass of the parton that initiates the jet. In the code we have made this variable dimensionless by rescaling with the renormalisation scale  $\mu^2$ , i.e.,  $\mathbf{s} = \frac{s}{\mu^2}$ .
- **z**: Variable encoding the momentum fraction  $z$  of one of the partons in the collinear splitting.
- $\phi$ : Variable corresponding to the azimuthal angle of the collinear splitting.
- **nf**: Variable specifying the number of (massless) quark flavors. This variable does not need to be set to an integer, but can be left in symbolic form.
- **format**: String specifying the output form of this function. One can choose between “Mathematica”, “Fortran” and “C”. Note that when performing the numerical integration in Fortran or C, the user needs to provide a function `HeavisideTheta` that satisfies  $\Theta(0) = 0$ , as described in section 2.2.2. In addition, for exporting to C, one needs to include the MATHEMATICA header file `mdefs.h` provided by MATHEMATICA in the directory<sup>6</sup> `$InstallationDirectory/SystemFiles/IncludeFiles/C`.
- **file**: String with the filename to which the integrand will be exported. For an empty string the integrand will be printed to the screen.
- **method**: This string can specify which method `NIntegrate` uses in MATHEMATICA, and we refer the reader to the MATHEMATICA documentation for the available options. For an empty string the default method of `NIntegrate` will be used.

---

<sup>6</sup>The installation directory can be determined by running `$InstallationDirectory` in MATHEMATICA.

### 2.3.3 Example: $k_T$ clustering algorithms

To illustrate the use of our code we now calculate the jet function for the family of  $k_T$  clustering algorithms. At one-loop order, where there are at most two particles in the final state, they are clustered into a single jet if the angle between them is less than the jet radius parameter  $R$ , which for the case of an  $e^+e^-$  collider corresponds to a single region<sup>7</sup>

$$s \leq z(1-z)E^2R^2, \quad (2.3.2)$$

where  $E$  is the jet energy. The  $z \rightarrow 0$  and  $z \rightarrow 1$  limits of eq. (2.3.2) are described by

$$\begin{aligned} z \rightarrow 0: \quad s &= zE^2R^2 & \longrightarrow & \quad c_0^+ = E^2R^2/\mu^2, \alpha_0^+ = -1, \\ z \rightarrow 1: \quad s &= (1-z)E^2R^2 & \longrightarrow & \quad c_1^+ = E^2R^2/\mu^2, \alpha_1^+ = -1. \end{aligned} \quad (2.3.3)$$

These are no lower constraints, i.e.  $c_i^- = 0$ . Calculating this observable requires a box since the  $s = 0$  line is inside the domain of integration. Since  $\alpha_i \neq 1$ , a rapidity regulator is not needed. The constraint in eq. (2.3.2) due to the measurement does not depend on  $\phi$ , and so we take  $\Phi = \{\}$ .

We now calculate the quark jet function. As eq. (2.2.8) is a relatively simple expression, for which the jet function can be easily calculated analytically, we will use MATHEMATICA to perform the numerical integration over the subtracted integral by using **QuarkJetN** with the the ‘LocalAdaptive’ integration method. In the following we set  $\mu = ER$  for simplicity. Note how this, since the variable  $s$  corresponds to  $\frac{s}{\mu^2}$ , cancels the factor  $E^2R^2$  in the observable.

```
In[1]:= O = z(1 - z) - s;
O0 = {{0,0},{1,-1}};
O1 = {{0,0},{1,-1}};
method = "LocalAdaptive";
box = True;
rr = False;
A=0.6;
B=20;

In[2]:= QuarkJetN[O, O0, O1, {}, rr, box, A, B, s, z, phi, method]

Out[2]= -1.2029367022'

In[3]:= PolesQuark[O0, O1, {}, rr, box, A, B, phi]
```

---

<sup>7</sup>The corresponding result for  $pp$  collisions can be obtained by simply replacing the jet energy  $E$  by the jet transverse momentum  $p_T$ , and  $R$  then corresponds to a distance in  $(\eta, \phi)$  instead of an angle.

## 2.4. Applications

---

$$\text{Out}[3]=\frac{4}{3\epsilon^2}+\frac{2}{\epsilon}$$

From this answer it is straight forward to reconstruct that the full color-dependence of the regulated one-loop quark jet function is given by:

$$\mathcal{J}_q^{k_T} = C_F \left( \frac{1}{\epsilon^2} + \frac{3}{2\epsilon} - 0.9022033008 \right). \quad (2.3.4)$$

The poles match exactly with the result by [144] and the finite term agrees up to order  $10^{-6}$ . Similar agreement is found for the gluon jet function:

$$\mathcal{J}_g^{k_T} = C_A \left( 0.0422426 + \frac{1}{\epsilon^2} + \frac{11}{6\epsilon} \right) - n_f T_R \left( \frac{2}{3\epsilon} + 2.55555 \right). \quad (2.3.5)$$

The accompanying MATHEMATICA notebook contains several hands-on examples to further illustrate the use of the different functions.

## 2.4 Applications

To validate the method and corresponding code, the jet functions for several known examples have been checked. Some of these were used throughout the chapter to explain our approach, namely the  $k_T$  family of clustering algorithms (section 2.3.3), and angularities with respect to the WTA axis (section 2.2.4). In addition, we provide results in section 2.4.1 for the cone algorithm and in section 2.4.3 for the jet shape. The latter is more challenging due to its azimuthal-angular dependence, which arises because the jet axis is along the total jet momentum and thus sensitive to recoil of soft radiation. In section 2.4.2 we present, for the first time, the one-loop jet functions for angularities with respect to the thrust axis, taking into account recoil. Although for  $b > 0$  this recoil is formally power-suppressed, it can be numerically large [160].

### 2.4.1 Cone jet

At one-loop order, the condition that both partons are within a cone jet in an  $e^+e^-$  collisions is that their angle with the jet axis is less than  $R$  (for  $pp^7$ ). Since the jet axis is along the total jet momentum, one simply needs to consider the angle with the parton that initiates the jet, leading to the following condition

$$s \leq E^2 R^2 \min \left[ \frac{1-z}{z}, \frac{z}{1-z} \right]. \quad (2.4.1)$$

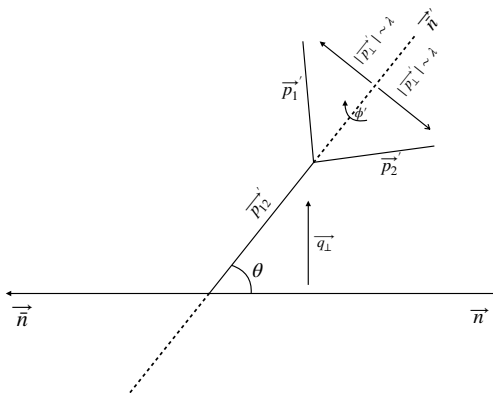


Figure 2.4: The setup of our calculation. The recoil is quantified by  $\theta$ .

As we focus on the finite term in the jet function, we fix  $\mu = ER$  finding

$$\begin{aligned}\mathcal{J}_q^{\text{Cone}} &= C_F \left( 1.46711 + \frac{1}{\epsilon^2} + \frac{3}{2\epsilon} \right), \\ \mathcal{J}_g^{\text{Cone}} &= C_A \left( 2.23477 + \frac{1}{\epsilon^2} + \frac{11}{6\epsilon} \right) - n_f T_R \left( \frac{2}{3\epsilon} + 2.20197 \right),\end{aligned}\quad (2.4.2)$$

which agrees up to order  $10^{-6}$  with ref. [144].

### 2.4.2 Angularities with recoil

In this section we determine, for the first time, the one-loop angularity jet function that includes the recoil of the thrust axis due soft radiation. While this recoil is power-suppressed for  $b > 0$ , ref. [160] noted that it has a numerically large effect and presented a factorization framework to include it. The one-loop jet function we calculate here will start to contribute at NLL' accuracy. This should be contrasted with the calculation in section 2.2.4, where we considered the angularity with respect to the WTA axis. To clearly distinguish these two cases in the notation, we will use  $\tau_n$  instead of  $e_b$ , where  $n$  refers to the thrust axis.

The setup underpinning our calculation is illustrated in figure 2.4. Here  $\theta$  is the angle between the thrust axis  $\vec{n}$  and the direction  $\vec{n}'$  of the initial collinear parton due to the recoil from soft radiation, which is treated as an external parameter in our calculation. The momenta of the two massless

## 2.4. Applications

partons in the jet are denoted by  $\vec{p}_1$  and  $\vec{p}_2$ , where we use (un)primed coordinates to denote light-cone components with respect to the  $\vec{n}'$  ( $\vec{n}$ ) direction. Explicitly,

$$\begin{aligned} p_1'^\mu &= zQ \frac{n'^\mu}{2} + \frac{(1-z)s}{Q} \frac{\bar{n}'^\mu}{2} + p_{1\perp}'^\mu \equiv p_1'^-\frac{n'^\mu}{2} + p_1'^+\frac{\bar{n}'^\mu}{2} + p_{1\perp}'^\mu, \\ p_1^\mu &= p_1^-\frac{n^\mu}{2} + p_1^+\frac{\bar{n}^\mu}{2} + p_{1\perp}^\mu, \quad p_1^\pm = p_1^0 \mp p_1^3, \end{aligned} \quad (2.4.3)$$

and similarly for  $p_2$ . Here we chose  $n^\mu = (1, 0, 0, 1)$  and  $\bar{n}^\mu = (1, 0, 0, -1)$ ,  $z$  is the momentum fraction of the parton,  $s$  the invariant mass of the jet, and  $Q$  the center-of-mass energy of the  $e^+e^-$  collision. The expression in the recoiled frame follows from the definition of  $z$  and  $s$  through  $p_1'^- = zQ$  and  $s = (p_1' + p_2')^2$ , as well as  $p_{1\perp}'^\mu = -p_{2\perp}'^\mu$  and the on-shell condition  $p_1'^2 = p_2'^2 = 0$ . Note that  $|p_{i\perp}'|^2 = z(1-z)s$ .

The rotation between the two frames is described by

$$\vec{p}_1 = \begin{pmatrix} \cos \theta & 0 & -\sin \theta \\ 0 & 1 & 0 \\ \sin \theta & 0 & \cos \theta \end{pmatrix} \vec{p}_1', \quad (2.4.4)$$

implying  $|p_\perp|^2 = |p_\perp'|^2 + \theta^2(p_1^3)^2 - 2\theta \cos \phi' |p_\perp'| |p_1^3|$  in the small  $\theta$  approximation, where  $\phi'$  is the azimuthal angle around the  $\vec{n}'$  axis. The large momentum components are the same in both frames,  $p_i^- = p_i'^-$ . The expression for the angularity  $\tau_n$  becomes

$$\begin{aligned} \tau_n &= \frac{1}{Q} \sum_i |p_{i\perp}| \left( \frac{p_i^+}{p_i^-} \right)^{\frac{b}{2}} = \frac{1}{Q} \sum_i \left( \frac{|p_{i\perp}|^{1+b}}{(p_i^-)^b} \right) \\ &= \frac{1}{(2Q)^{1+b}} z^{-b} \left( 4z(1-z)s + (\theta Q)^2 z^2 - 4\theta Q \cos \phi' z^{\frac{3}{2}} \sqrt{(1-z)s} \right)^{\frac{1+b}{2}} \\ &\quad + \frac{1}{(2Q)^{1+b}} (1-z)^{-b} \left( 4z(1-z)s + (\theta Q)^2 (1-z)^2 + 4\theta Q \cos \phi' (1-z)^{\frac{3}{2}} \sqrt{zs} \right)^{\frac{1+b}{2}}, \end{aligned} \quad (2.4.5)$$

where  $b > -1$ . Using the delta function trick (see section 2.2.2), we switch to a cumulative measurement, writing the observable as

$$M_{\text{obs}} = \Theta[\tau_n^c - \tau_n]. \quad (2.4.6)$$

Unfortunately it is not possible to invert eq. (2.4.6) to obtain an analytic solution for  $s$  and subsequently extract the soft limit  $z \rightarrow 0$ . We can, however, use the power-law ansatz in eq. (2.2.8) to find the soft behavior of the

observable. Since the equation is symmetric in  $z \rightarrow 1 - z$ , we focus on finding the soft behavior in the  $z \rightarrow 0$  limit. Using

$$s|_{z \rightarrow 0} = c_0(\phi) z^{-\alpha_0} \mu^2, \quad (2.4.7)$$

in eq. (2.4.5) and taking the  $z \rightarrow 0$  soft limit, we find

$$\begin{aligned} \tau_n^c \left( \frac{2Q}{\mu} \right)^{1+b} &= z^{-b} \left( 4c_0 z^{1-\alpha_0} + \left( \frac{\theta Q}{\mu} \right)^2 z^2 - 4\sqrt{c_0} \left( \frac{\theta Q}{\mu} \right) \cos \phi' z^{\frac{3-\alpha_0}{2}} \right)^{\frac{1+b}{2}} \\ &\quad + \left( 4c_0 z^{1-\alpha_0} + \left( \frac{\theta Q}{\mu} \right)^2 + 4\sqrt{c_0} \left( \frac{\theta Q}{\mu} \right) \cos \phi'(z) z^{\frac{1-\alpha_0}{2}} \right)^{\frac{1+b}{2}}. \end{aligned} \quad (2.4.8)$$

There is a single solution for  $s$  in either of the soft limits and therefore this observable only has an upper boundary over the full range of  $b$ , i.e.  $c_0^- = 0$ . The leading terms in eq. (2.4.8) are used to solve for  $\alpha_0^+$  and  $c_0^+$ , and differ for  $-1 < b < 0$ ,  $b = 0$  and  $b > 0$ . We will analyze the last case in some detail and only provide the solutions for the others.

Assuming  $b > 0$ , the leading behavior in the  $z \rightarrow 0$  limit of eq. (2.4.8) is

$$\tau_n^c \left( \frac{2Q}{\mu} \right)^{1+b} = c_0^{\frac{1+b}{2}} z^{-b+(1-\alpha_0)(1+b)/2} + \left( \frac{\theta Q}{2\mu} \right)^{1+b}, \quad (2.4.9)$$

and from this we infer

$$c_0^+ = \frac{Q^2 (\tau_n^c)^{2/(1+b)}}{\mu^2} (1 - k^{1+b})^{\frac{2}{1+b}}, \quad \alpha_0^+ = \frac{1-b}{1+b}, \quad (2.4.10)$$

where

$$k \equiv \frac{1}{2} \theta (\tau_n^c)^{-1/(1+b)}. \quad (2.4.11)$$

Similarly, for  $b = 0$  we obtain

$$c_0^+ = \frac{Q^2 (\tau_n^c)^{2/(1+b)}}{\mu^2} \frac{1 - k^2}{(2 + 2k \cos \phi)^2}, \quad \alpha_0^+ = 1. \quad (2.4.12)$$

For  $-1 < b < 0$  the solution is a bit more difficult and reads

$$\begin{aligned} c_0^+ &= \frac{Q^2 (\tau_n^c)^{2/(1+b)}}{\mu^2} \left[ 1 + k^2 \cos 2\phi - 2k |\cos \phi| \sqrt{1 - k^2 \sin^2 \phi} \right], \\ \alpha_0^+ &= 1. \end{aligned} \quad (2.4.13)$$

## 2.4. Applications

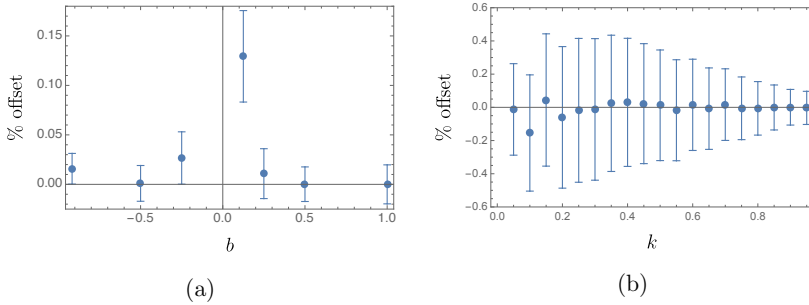


Figure 2.5: The offset between our results for (a) different values of  $b$  with  $\theta = 0$  and (b) different values of the recoil parameter  $k$  with  $b = 0$  and the known results from the literature is shown.

In order to use GOJET, we rescale  $s$  and choose an energy scale  $\mu$ . To be able to smoothly turn off the recoil, we choose  $\mu$  in terms of the angularity,  $\mu = Q(\tau_n^c)^{1/(1+b)}$ . The only independent variable left is then given by  $k$  in eq. (2.4.11). To be complete we also give the resulting observable input for GOJET:

$$0 = 1 - z^{-b} \left( z(1-z)s + k^2 z^2 - 2k \cos \phi' z^{\frac{3}{2}} \sqrt{(1-z)s} \right)^{\frac{1+b}{2}} - (1-z)^{-b} \left( z(1-z)s + k^2(1-z)^2 + 2k \cos \phi'(1-z)^{\frac{3}{2}} \sqrt{zs} \right)^{\frac{1+b}{2}}. \quad (2.4.14)$$

The jet function for  $\theta = 0$  (without recoil) was calculated analytically in refs. [137, 160] and we obtain the same results as can be seen in figure 2.5a. The error bars indicate the uncertainty from our numerical integration. Ref. [160] includes a zero-bin subtraction [170] to avoid double counting with the soft function in their factorization, which we do not include. The zero-bin subtraction depends on the details of the factorization theorem (indeed it vanishes in ref. [137]), so we do not offer this as a standard functionality of GOJET. The numerical integration for small values of  $b$  is particularly challenging (as can be seen for  $b = \frac{1}{8}$ ), because the sub-leading terms with respect to the leading soft behavior of the observable in eq. (2.4.10) are particularly large in this case. A more detailed discussion of this issue and a method to cope with it is presented in app. B. In figure 2.5b we reproduce the known results for  $b = 0$  (broadening) and general recoil [165]. Our new results for general  $b$  including the effect of recoil, are shown in figure 2.6. The error bars are not shown in this plot as they are



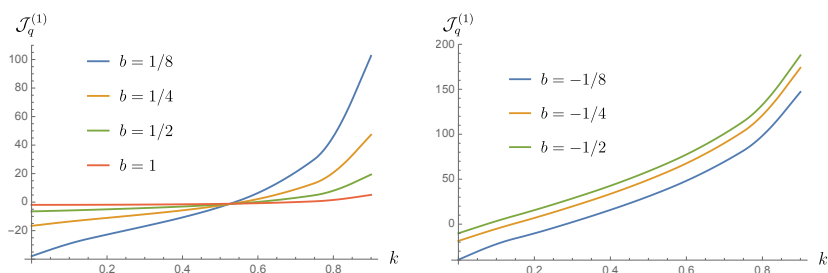


Figure 2.6: The results for the finite part of  $\mathcal{J}_q^1$  for different values of  $b$  as a function of  $k$ .

negligibly small.

### 2.4.3 Jet shape

As another nontrivial example, we calculate the jet function for the classic jet shape observable, reproducing the one-loop result of ref. [149]. The jet shape describes the average energy fraction  $z_r$  inside a cone of angular size  $r$  around the jet axis. As in section 2.4.2, recoil from soft radiation displaces the jet axis from the initial parton by an angle  $\theta$ . This breaks the azimuthal symmetry, requiring one to integrate over  $\phi$ . We have checked that our poles match exactly with the poles in [149] for all values of  $\theta$  and  $r$ . The difference between the finite term is always below 0.5%. This has been illustrated in figure 2.7a for gluon jets and figure 2.7b for quark jets. We note that run time is not an issue, as less precision is needed in phenomenological results and the distribution can be interpolated. Our calculation represents the second independent calculation of this observable and thereby delivers a useful cross check of the results of ref. [149].

## 2.5 Conclusions

In this chapter we developed an automated approach for calculating one-loop jet functions, and provide an implementation in the accompanying MATHEMATICA package called GOJET. We use geometric subtraction [93] to isolate the soft and collinear singularities. The collinear counterterm does not depend on the details of the observable, except that certain observables do not require it. We find that the soft counterterm depends on the behavior of the

## 2.5. Conclusions

---

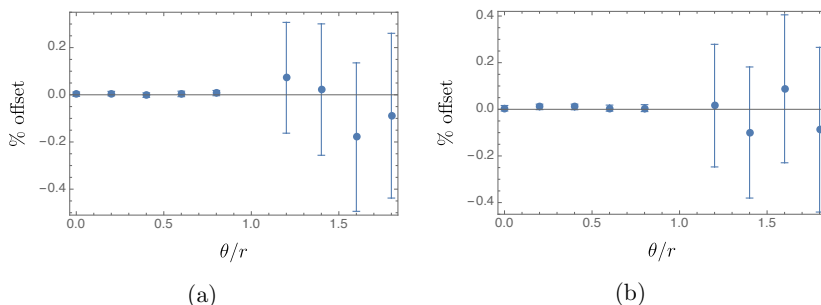


Figure 2.7: The offset between our finite result of the (a) gluon and (b) quark jet function and [149] for several values of  $\frac{\theta}{r}$ .

observable in the soft limits, which can be described by a power law. While the user must provide GOJET with this power law as input, we present a strategy to extract this in a highly nontrivial example. We employed cumulative distributions, such that observables correspond to integrating over certain regions of phase space, and thereby avoiding plus distributions. We have demonstrated our approach by reproducing the known one-loop jet function for a range of observables, and calculating, for the first time, the jet function for angularities including recoil. For broadening ( $b = 0$  in our conventions) the effect of recoil must be kept [138], while for  $b > 0$  it is formally power suppressed but can be numerically large [160]. For  $b$  close to 0, we encountered numerical convergence issues, due to an integrable divergence. We addressed this problem by substantially improving the counterterm through a remapping.

Our approach focusses on IR-safe observables, and we did not address the IR-unsafe case. Jet functions containing IR divergences are sensitive to nonperturbative physics, and our purely partonic calculation must be supplemented by a (universal) nonperturbative function that subtracts these divergences. A prime example is initial-state jets, which are described by beam functions [171]. Beam functions contain infrared divergences, which are removed by matching onto parton distribution functions, leaving finite matching coefficients.

The automated approach and code presented here provides a very useful tool, calculating jet functions at one-loop order. Very few two-loop jet functions are known, and an automated approach would allow many resummation calculations to be extended to NNLL' or N<sup>3</sup>LL accuracy. At this order the singular limits become more complicated, the order of subtractions matter, and the parametrization of the observable in these limits will no longer be a

simple power law, complicating the counterterms.

# Chapter 3

## Four-loop large- $n_f$ contributions to the non-singlet structure functions $F_2$ and $F_L$

In section 1.2 we described the process of inclusive Deep Inelastic Scattering (DIS) in which a hadron scatters against a lepton by exchanging a vector boson to produce a new lepton-hadron final state. The total cross section can be factorized into a leptonic tensor and a hadronic tensor. Corrections to the hadronic tensor involve higher powers of the strong coupling constant  $\alpha_s$  and are dominant in comparison to the electro-weak corrections required for the leptonic tensor. The hadronic tensor can be written in terms of structure functions, which include both perturbative contributions from small-scale dynamics and non-perturbative contributions from large-scale dynamics. We will focus on the coefficient functions at N<sup>4</sup>LO which perturbatively describe the partonic interactions in the hadronic tensor. As a byproduct we will also obtain the N<sup>3</sup>LO splitting functions, the same functions which we already have encountered (at LO) in the previous chapter, cf. eq. (2.2.2), to describe the jet functions. Moreover, the splitting functions are required to evolve the non-perturbative parton distribution functions (PDFs) with respect to the energy scale. These PDFs and splitting functions are universal objects and essential to the factorization of other processes in QCD. In fact, the PDFs also require the coefficient functions to evaluate experimental data for DIS. We will obtain the first ever analytic 4-loop results for DIS at order  $n_f^2$  in both Mellin-moments space and Bjorken- $x$  space by using an algorithm based on the optical theorem, the integration-by-parts technique and the method

of differential equations<sup>1</sup>. This chapter is based on [3].

## 3.1 Introduction

Inclusive deep-inelastic lepton-nucleon scattering (DIS) via the exchange of an electro-weak gauge boson is an experimental and theoretical benchmark process of perturbative QCD.

Data on its main structure functions provide a rather direct determination of (linear combinations of) the quark momentum distributions of the nucleon. The structure function  $F_2(x, Q^2)$ , in particular, has been determined in the past decades over a wide range of the scale  $Q^2$  ( $= -q^2$ , where  $q$  is the momentum of the exchanged boson) and the Bjorken variable  $x$  ( $= Q^2/(2p \cdot q)$ , where  $p$  is the momentum of the nucleon) in fixed-target experiments and at the electron-proton collider HERA, see ref. [96] and references therein. Further measurements of inclusive DIS are planned for future facilities, in particular the Electron Ion Collider (EIC) at Brookhaven National Lab [172, 173] and the Large Hadron Electron Collider (LHeC) [174, 175].

Precise determinations of the quark momentum distributions  $q_i(\xi, Q^2)$  (with  $\xi = x$  at the leading-order of perturbative QCD) as well as, less directly, of the gluon distribution  $g(\xi, Q^2)$  and the strong coupling  $\alpha_s$  from structure-function data require higher-order calculations of the corresponding coefficient functions (partonic structure functions). These coefficient functions are of relevance also beyond the cross sections for inclusive DIS, see, e.g., refs. [176, 177] on Higgs production in vector-boson fusion and ref. [178] on jet production in DIS.

For the quantities under consideration in this chapter, the flavour non-singlet contributions to  $F_2$  and the longitudinal structure function  $F_L$ , the second-order corrections have been calculated and verified long ago [39, 111, 179, 180]. The corresponding three-loop expressions were obtained in ref. [43] and recently re-calculated in ref. [181]. At the fourth order, only the lowest five Mellin- $N$  moments have been computed so far [46, 182, 183] using the FORCER program [184], in addition to the leading terms in the limit of a large number of flavours  $n_f$  [185, 186].

In the present chapter, we take the next step towards the determination of the fourth-order non-singlet coefficient functions  $c_{2,ns}^{(4)}(x)$  and  $c_{L,ns}^{(4)}(x)$  and compute their doubly fermionic  $n_f^2$  contributions. These results are obtained by a new method which allows the determination of their moments up to very high (even) values of  $N$ , beyond  $N = 1000$ , from which the analytic

<sup>1</sup>The integration-by-parts technique is explained in section 1.4. In app. F I provide a one-loop example of the recursive algorithm.

dependence on  $N$ , and hence on  $x$ , can be re-constructed in terms of harmonic sums [187] and harmonic polylogarithms (HPLs) [188], respectively. As a by-product, we have checked the  $n_f^2$ -contributions to the four-loop non-singlet splitting function  $P_{\text{ns}}^{(3)+}(x)$  of ref. [14].

The remainder of this chapter is organized as follows: In section 3.2 we briefly recall the theoretical framework for the coefficient functions in inclusive DIS and their determination to the fourth order in  $\alpha_s$ . In section 3.3 we describe our method of the calculation based on iteratively solving a system of recurrence relations which is derived via the method of differential equations [62, 64, 67, 68]. The analytic results for the coefficient functions in  $N$ -space are presented in section 3.4, which also includes a resulting partial prediction for the five-loop non-singlet splitting function  $P_{\text{ns}}^{(4)}(N)$ . The corresponding  $x$ -space coefficient functions and their threshold and high-energy limits are written down and discussed in section 3.5. We summarize our method and results and give a brief outlook in section 3.6.

## 3.2 Theoretical framework and notations

The subject of our computations is unpolarized inclusive lepton-nucleon DIS

$$\text{lepton}(k) + \text{nucleon}(p) \rightarrow \text{lepton}(k') + X \quad (3.2.1)$$

at the lowest order of QED (i.e., via the exchange of one photon with momentum  $q = k - k'$ ).  $X$  stands for all hadronic states allowed by quantum number conservation. The double-differential cross section in  $Q^2 = -q^2$  and  $x = Q^2/(2p \cdot q)$  for this process can be expressed as the product of a calculable and well-known leptonic tensor and the hadronic tensor

$$W_{\mu\nu}(p, q) = \left( \frac{q_\mu q_\nu}{q^2} - g_{\mu\nu} \right) F_1(x, Q^2) - (q_\mu + 2xp_\mu)(q_\nu + 2xp_\nu) \frac{1}{2xq^2} F_2(x, Q^2). \quad (3.2.2)$$

Neglecting contributions that are suppressed at large scales by powers of  $1/Q^2$ , the structure functions  $\mathcal{F}_2 = 1/x F_2$  and  $\mathcal{F}_L = 1/x (F_2 - 2xF_1)$  can be expressed in terms of the universal but perturbatively incalculable quark and gluon parton distribution functions (PDFs),  $q_i(\xi, Q^2)$  and  $g(\xi, Q^2)$ , and the perturbative coefficient functions  $\mathcal{C}_{a,p}(x, Q^2)$ . In the present chapter, we are specifically interested in non-singlet (combinations of) structure functions  $F_{a,\text{ns}}$ , such as  $F_a^{\text{proton}} - F_a^{\text{neutron}}$ , which decouple from the gluon distribution, viz

$$\mathcal{F}_{a,\text{ns}}(x, Q^2) = [\mathcal{C}_{a,\text{ns}} \otimes q_{\text{ns}}](x, Q^2) \quad (3.2.3)$$

where  $\otimes$  abbreviates the Mellin convolution. The non-singlet combinations  $q_{\text{ns}}$  of quark distributions are normalized such that the expansion of the coefficient functions in powers of  $a_s \equiv \alpha_s(Q^2)/(4\pi)$  is given by

$$\mathcal{C}_{a,\text{ns}}(x, Q^2) = (1 - \delta_{aL}) \delta(1-x) + \sum_{n=1} a_s^n c_{a,\text{ns}}^{(n)}(x) . \quad (3.2.4)$$

Here and below we identify the  $\overline{\text{MS}}$  renormalization and mass-factorization scales  $\mu_r^2$  and  $\mu_f^2$ , at which the strong coupling and the PDFs are evaluated, with  $Q^2$ . The dependence on  $\mu_r^2$  and  $\mu_f^2$  can be readily reconstructed a posteriori, see, e.g., eqs. (2.17) and (2.18) of ref. [189].

In terms of the general framework, our determination of the coefficient functions uses the method set out (and applied to the lowest moments at the third order) in refs. [56, 190], see also refs. [43, 111, 181]: The cross section for inclusive DIS for quark external states, projected onto the structure functions  $\mathcal{F}_a$ , is related by the optical theorem to the imaginary parts of the corresponding amplitudes for photon-quark forward scattering. Via a dispersion relation the coefficients of  $[(2p \cdot q)/Q^2]^N = 1/x^N$  lead to the even-integer (see also ref. [191]) Mellin- $N$  moments

$$\tilde{\mathcal{F}}_{a,\text{ns}}(N, Q^2) = \int_0^1 dx x^{N-1} \tilde{\mathcal{F}}_{a,\text{ns}}(x, Q^2) , \quad (3.2.5)$$

of the bare partonic structure functions. These are computed from Feynman diagrams in dimensional regularization with  $D = 4 - 2\varepsilon$  dimensions.

After the  $\overline{\text{MS}}$  renormalization of the coupling constant to the fourth order,

$$a_s^{\text{bare}} = a_s \left( 1 - \frac{\beta_0}{\varepsilon} a_s + \left( \frac{\beta_0^2}{\varepsilon^2} - \frac{\beta_1}{2\varepsilon} \right) a_s^2 - \left( \frac{\beta_0^3}{\varepsilon^3} - \frac{7\beta_1\beta_0}{6\varepsilon^2} + \frac{\beta_2}{3\varepsilon} \right) a_s^3 + \dots \right) \quad (3.2.6)$$

with  $\beta_0 = 11 - 2/3 n_f$  etc. in QCD [102, 103], the left-hand-side of eq. (3.2.5) can be written as

$$\tilde{\mathcal{F}}_{a,\text{ns}}(N, Q^2) = \tilde{\mathcal{C}}_{a,\text{ns}}(N, a_s) Z_{\text{ns}}(N, a_s) . \quad (3.2.7)$$

The  $D$ -dimensional coefficient function  $\tilde{\mathcal{C}}_{a,\text{ns}}$  includes additional terms with positive powers of  $\varepsilon$  on top of the Mellin transform of eq. (3.2.4), i.e.,

$$\tilde{\mathcal{C}}_{a,\text{ns}}^{(n)}(N) = c_{a,\text{ns}}^{(n)}(N) + \varepsilon a_{a,\text{ns}}^{(n)}(N) + \varepsilon^2 b_{a,\text{ns}}^{(n)}(N) + \varepsilon^3 d_{a,\text{ns}}^{(n)}(N) + \dots \quad (3.2.8)$$

The quantity  $Z_{\text{ns}}$  which renormalizes the non-singlet quark distributions is

### 3.3. Method and computations

---

given by

$$\begin{aligned}
Z_{\text{ns}} = & 1 + a_s \frac{1}{\varepsilon} \gamma_{\text{ns}}^{(0)} + a_s^2 \left[ \frac{1}{2\varepsilon^2} \{ (\gamma_{\text{ns}}^{(0)} - \beta_0) \gamma_{\text{ns}}^{(0)} \} + \frac{1}{2\varepsilon} \gamma_{\text{ns}}^{(1)} \right] \\
& + a_s^3 \left[ \frac{1}{6\varepsilon^3} \{ (\gamma_{\text{ns}}^{(0)} - 2\beta_0) (\gamma_{\text{ns}}^{(0)} - \beta_0) \gamma_{\text{ns}}^{(0)} \} \right. \\
& \quad \left. + \frac{1}{6\varepsilon^2} \{ (3\gamma_{\text{ns}}^{(0)} - 2\beta_0) \gamma_{\text{ns}}^{(1)} - 2\beta_1 \gamma_{\text{ns}}^{(0)} \} + \frac{1}{3\varepsilon} \gamma_{\text{ns}}^{(2)} \right] \\
& + a_s^4 \left[ \frac{1}{24\varepsilon^4} \{ (\gamma_{\text{ns}}^{(0)} - 3\beta_0) (\gamma_{\text{ns}}^{(0)} - 2\beta_0) (\gamma_{\text{ns}}^{(0)} - \beta_0) \gamma_{\text{ns}}^{(0)} \} \right. \\
& \quad + \frac{1}{12\varepsilon^3} \{ ((3\gamma_{\text{ns}}^{(0)} - 7\beta_0) \gamma_{\text{ns}}^{(0)} + 3\beta_0^2) \gamma_{\text{ns}}^{(1)} - 2(2\gamma_{\text{ns}}^{(0)} - 3\beta_0) \beta_1 \gamma_{\text{ns}}^{(0)} \} \\
& \quad \left. + \frac{1}{24\varepsilon^2} \{ 2(4\gamma_{\text{ns}}^{(0)} - 3\beta_0) \gamma_{\text{ns}}^{(2)} + 3(\gamma_{\text{ns}}^{(1)} - 2\beta_1) \gamma_{\text{ns}}^{(1)} - 6\beta_2 \gamma_{\text{ns}}^{(0)} \} + \frac{1}{4\varepsilon} \gamma_{\text{ns}}^{(3)} \right]
\end{aligned} \tag{3.2.9}$$

to the fourth order. Here  $\gamma_{\text{ns}}^{(n)}(N)$  – the arguments  $N$  have been suppressed in eq. (3.2.9) for brevity – are the  $N^n$ LO non-singlet anomalous dimensions related by

$$\gamma_{\text{ns}}^{(n)}(N) = - \int_0^1 dx x^{N-1} P_{\text{ns}}^{+(n)}(x) \tag{3.2.10}$$

to the expansion coefficients of the  $\overline{\text{MS}}$ -scheme splitting function for the evolution of flavour differences of the sums (hence ‘+’) of quark and antiquark PDFs,

$$P_{\text{ns}}^{+}(x, a_s) = \sum_{n=0} a_s^{n+1} P_{\text{ns}}^{+(n)}(x) . \tag{3.2.11}$$

Inserting the expansions (3.2.4), (3.2.8) and (3.2.9) into eq. (3.2.7), the anomalous dimension and ( $D$ -dimensional) coefficient functions can be extracted order by order from the results of the diagram calculations. In order to obtain the fourth-order coefficient functions  $c_{a,\text{ns}}^{(4)}$ , the lower-order calculations need to include terms up to  $\varepsilon^{4-n}$  at order  $\alpha_s(n)$ . In particular, the determination of the  $n_f^2$  contributions to  $c_{a,\text{ns}}^{(4)}$  requires the  $n_f$  parts of  $a_{a,\text{ns}}^{(3)}$  which were beyond the scope of ref. [43] – at the time only the integrals required for one simpler Lorentz projection of  $W_{\mu\nu}$  were extended to this accuracy for ref. [192].

## 3.3 Method and computations

In terms of the diagram sets and the treatment to the point at which the Feynman integrals are evaluated, our computation is closely related to that



of third-order fermionic ( $n_f$  and  $n_f^2$ ) contributions in ref. [193] and the non-singlet part of ref. [14]. Our evaluation of the Feynman integrals is entirely different, though, from both. In ref. [193] the analytic  $N$ -dependence was determined by setting up and solving, in a far from fully automated manner, complicated systems of difference equations. In ref. [14] the even moments were computed to  $N=22$  for the  $C_F C_A n_f^2$  terms and to  $N=42$  for the  $C_F^2 n_f^2$  terms using FORCER [184]. From these it was possible, just, to reconstruct the analytic  $N$ -dependence of the four-loop anomalous dimensions using all available physics constraints and systems of Diophantine equations.

Below we give details on the methods used in the present computation. We believe that some of the techniques we have used here have been employed for the first time in a multi-loop calculation, and that these should be useful not only for tackling DIS at four loops but also for other multi-loop calculations. Using these techniques we have been able to generate a very large number of Mellin moments, up to  $N = 1500$ , by evaluating the series expansion of the forward scattering amplitude around  $1/x \equiv \omega = 0$ , recall the discussion above eq. (3.2.5). With that many moments, it is possible to reconstruct the analytic  $N$ -dependence of the fourth-order coefficient functions by a direct (and over-constrained) Gaussian elimination for a sufficiently general ansatz in terms of harmonic sums.

Our basic setup relies on QGRAF [194] and FORM [52, 53, 195], employing the program MINOS [196] as a diagram database tool. Many of the FORM libraries we use have been employed in a substantial number of earlier calculations, e.g., in refs. [14, 43, 46, 111, 193] and have been highly optimized for multi-loop perturbative QCD calculations. In particular, as in refs. [14, 46], the database combines diagrams whose underlying graph topology is equivalent and whose colour factors are the same. Such sets of diagrams lead to faster evaluation times as they allow to realize algebraic cancellations between the individual diagrams.

As the  $n_f$  contributions at three loops, the present  $n_f^2$  contributions at four loops are special since they do not yet involve the more difficult topologies in their respective orders. In fact, the most difficult four-loop cases derive from the hardest three-loop diagrams shown in fig. 3.1 by simply inserting an additional quark loop into one of the gluon propagators, i.e., no ‘genuine’ (non-insertion) four-loop self-energy topologies are required [46].

The best route to determine the all- $N$  expressions for the  $n_f^2$  four-loop contributions is via the large- $n_c$  limits and the  $C_F^2 n_f^2$  terms. The former do not involve alternating harmonic sums, as even and odd  $N$ -values must lead to the same  $x$ -space function. For the latter one expects a somewhat simpler form than for the  $C_F C_A n_f^2$  terms, since only two-loop diagrams with two one-loop or one two-loop self-energy insertion(s) contribute. In practice,

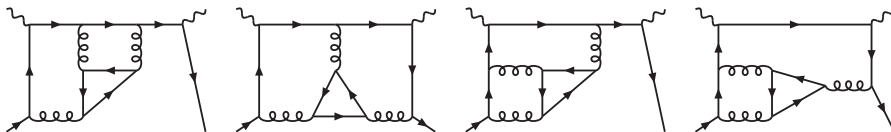


Figure 3.1: The hardest diagrams contributing to the  $n_f$  contributions to the third-order coefficient functions for  $F_{2,\text{ns}}$  and  $F_{L,\text{ns}}$ . In the notation of MINCER [50, 54], the two on the left are of the BE topology and the two on the right are O4 cases. All four diagrams have the colour factor  $C_F C_A n_f$ .

the non- $\zeta$  part of  $c_{2,\text{ns}}^{(4)}$  was the most difficult case, which we solved in FORM using an ansatz with a little less than 600 even- $N$  coefficients. All other cases required fewer than 400 coefficients.

#### 3.3.1 Topologies for the non-singlet $n_f^2$ structure functions

As discussed at the end of section 3.2, we also need the lower-order corrections to a sufficient power in  $\varepsilon$ ; in particular we have to compute the  $\varepsilon^1$  terms for the  $n_f$  parts at three loops.

The diagrams contributing to the final result are organized into topologies, and described in terms of a linear independent set of propagators and scalar products ready to be reduced to a smaller set of master integrals [59]. In order to obtain a more efficient reduction, especially at four loops, we build our topologies by keeping the number of propagators within a topology as low as possible. In practice, a four-loop DIS topology has 18 linearly independent scalar products; instead of describing them in terms of as many linearly independent propagators, we opt for at most 12 propagators and 6 scalar products that will appear only in the numerator. At three-loop, this results in a topology described by 10 propagators and 2 scalar products.

We further simplify the expressions of the diagrams by rewriting multi-loop self-energy corrections in terms of chained bubbles which has the additional benefit of keeping all the propagator powers as whole numbers more suited for the Laporta reductions,

$$q \text{ --- } \text{Bubble}(\Pi_L(q^2)) \text{ --- } q = \frac{\Pi_L(q^2)}{[\text{Bub}(q^2)]^L} \quad q \text{ --- } \text{Chain of bubbles (1, 2, ..., L)} \text{ --- } q. \quad (3.3.1)$$

In fig. 3.2 we show the range of topologies that are required for the non-singlet  $n_f^2$  correction at the fourth order, with diagrams ranging from 12 to 9

distinct scalar propagators, one propagator short from the most complicated case one can encounter at four loops.

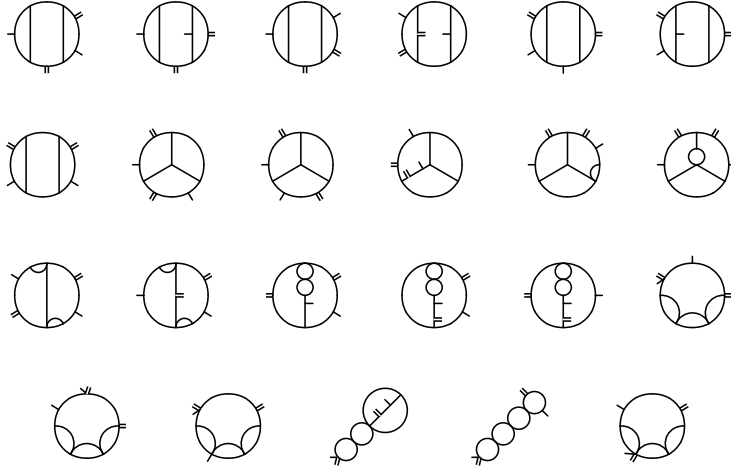


Figure 3.2: Three- and four-loop propagator topologies used for the reduction to master integrals and the expansion in  $\omega$  using differential equations. The external double line represent the off-shell photon while the simple lines the parton. Each diagram allows for two independent flows of the external momenta resulting in the same topology up to a sign inversion  $\omega \leftrightarrow -\omega$ .

The number of scalar propagators in the definition of each topology is not the only factor to take into account when considering the problem of reducing our integrals to master integrals (very important is also, for example, the dimensionality of the numerator). However, it remains a key aspect since it drastically reduces the degrees of freedom one has to consider during the reductions by effectively vetoing some of the sectors. To perform the reductions to master integrals we have used both the FIRE [61] and KIRA [197] programs.

### 3.3.2 Series expansion and differential equations

Once all the diagrams appearing in the process are reduced to master integrals, we build a system of differential equations by acting on them with the differential operator  $\partial/\partial\omega$  and further reduce the resulting integrals. This step may also involve extending the initial set of master integrals to achieve

### 3.3. Method and computations

---

a closed system. The resulting differential equations can be written as

$$\frac{\partial}{\partial \omega} \vec{M}(\omega, \varepsilon) = A(\omega, \varepsilon) \cdot \vec{M}(\omega, \varepsilon), \quad (3.3.2)$$

where  $A \in \mathbb{Q}^{n \times n}(\omega, \varepsilon)$  is a square matrix whose elements are rational functions in  $\omega$  and the dimensional regulator  $\varepsilon$  over the field  $\mathbb{Q}$ , with  $n$  being the number of master integrals. The general ansatz for this system of differential equations can be written as a linear combination of meromorphic functions,

$$\vec{M}(\omega, \varepsilon) = \omega^{\vec{\alpha}} \sum_{s \in \mathbb{Z}} \sum_{k=0}^{\infty} \vec{m}_k^{(s)}(\omega, \varepsilon) \omega^{k+s\varepsilon}, \quad \vec{\alpha} \in \mathbb{Z}^n, \quad (3.3.3)$$

where  $\vec{\alpha}$  defines the leading power of each master and the sum over  $s$  goes over a finite set of integers which multiply  $\varepsilon$  in the power of  $\omega$ , and represent independent (not necessarily physical) solutions to the differential equations. The space of solutions is reduced by noticing that the boundary conditions for the master integrals in the limit  $\omega = 0$  are finite ( $\alpha \geq 0$ ) and support only the regular sector  $s = 0$ . This may in fact not be true for individual integrals, but it is well known that the forward amplitudes for DIS are regular at  $p = 0$  and hence  $w = 0$ . We can thus safely ignore solutions with  $s \neq 0$ . The general problem of obtaining series expansions from differential equations is of course not new in the context of Feynman integrals and indeed has been employed successfully in, e.g., refs. [59, 181, 198–206], and public implementations exist [207–209].

Here we present a new method which takes advantage of the specific analytic properties of the problem and which is well suited for obtaining many coefficients in the expansion, while at the same time being simple enough to be implemented purely in FORM. We describe this procedure in the following.

We make use of the information coming from the boundary conditions to simplify the ansatz for the master integral expansion, and at the same time we consider the differential matrix to contain at most simple poles at  $\omega = 0$ , viz.

$$M_i = \omega^{\alpha_i} \sum_{k=0}^{\infty} m_{ik} \omega^k, \quad A = \frac{A_{-1}}{w} + \sum_{k=0}^{\infty} A_k \omega^k. \quad (3.3.4)$$

In general, the matrix  $A$  can contain higher order poles around  $\omega = 0$ , depending on the choice of master integrals. While it is known in the Mathematics literature since the 1950s that a basis transformation to remove higher poles exists [210], finding the transformation to bring the differential equations into a so-called canonical form is non-trivial in practice. By now there exist

nevertheless several strategies/algorithms to solve this problem [72, 211], and some implementations are now publicly available [212–214]. The feasibility to run these algorithms on systems containing hundreds master integrals is however questionable. For our purpose, we do not actually require the complete reduction of the system into the canonical form – as it is sufficient to simply remove higher order poles at  $\omega = 0$ .

We achieve this by applying a rescaling transformation  $T$  to the master integrals,

$$M \rightarrow T \cdot M, \quad A \rightarrow \frac{\partial T}{\partial \omega} T^{-1} + T \cdot A \cdot T^{-1}, \quad (3.3.5)$$

with the transformation matrix taking the form

$$T = \text{diag}(\omega^\beta), \quad \beta \in \mathbb{N}_0^n \Rightarrow A_{ij} \rightarrow \delta_{ij} \frac{\beta_i}{\omega} + \omega^{\beta_i - \beta_j} A_{ij}. \quad (3.3.6)$$

In general we found that the form of  $T$  required to remove all poles is not unique. We explored several algorithms allowing to construct a suitable  $T$ ; the probably simplest was based on constructing  $T$  by iteratively removing a pole of order  $k$  in the  $j^{\text{th}}$  row by setting  $\beta_j = \omega^{k-1}$ . While this particular pole would be removed, new poles could be created in other rows in the transformed matrix  $A$ . In all cases we found that iterating this procedure allowed to eventually remove all non-simple poles from  $A$ . We actually have no proof for this simple procedure to terminate and it remains to be seen whether it will also work for even more complicated cases. The advantage of the procedure in comparison to the much more involved algorithms to bring  $A$  into a Fuchsian form is that it is computationally far simpler and can be applied with ease also to comparably large systems of sizes around the 100s or even 1000s. It is not clear to us that the same holds for the algorithms mentioned above.

By using the definitions in eq. (3.3.4) it is possible to rewrite eq. (3.3.2) into a recursive expression that allows for an efficient extraction of the expansion coefficients of the master integrals,

$$\underbrace{((k+1)\mathbb{1} - A_{-1})}_{:= B_k} \cdot \vec{m}_{k+1} = \sum_{j=0}^k A_j \vec{m}_{k-j} \quad (3.3.7)$$

where  $\mathbb{1}$  is the identity matrix. Note that we can have at most  $n$  cases where  $\det(B_k) = 0$ , corresponding to positive integer values of the eigenvalue of  $A_{-1}$ . In these cases the system cannot be inverted and is solved by means of Gaussian elimination. For high enough  $k$  we have  $\det(B_k) \neq 0$  and we can write

$$\vec{m}_{k+1} = B_k^{-1} \cdot \left( \sum_{j=0}^k A_j \vec{m}_{k-j} \right). \quad (3.3.8)$$

### 3.3. Method and computations

---

The inversion of the matrix  $B$  is performed for generic values of  $k$ , avoiding the expensive procedure of performing a new inversion for every step of the expansion, especially for high values of  $k$ .

We have implemented the Gaussian elimination for the arbitrary steps of eq. (3.3.7) in C++ while the case of non-singular  $B_k$  matrices in eq. (3.3.8) has been implemented in FORM. The required boundary conditions have been computed using FORCER in the limit of  $\omega = 0$  for all the master integrals, where the external parton is taken to be soft. The performances of eq. (3.3.8) can be further improved by truncating the expansion in the dimensional regulator to the required order to obtain an amplitude known up to  $\varepsilon^{4-n}$  at the  $n$ -th order.

One can benefit from the combined expansion only when the two limits  $\varepsilon, \omega = 0$  of the differential matrix  $A$  commute. For example, the series expansion in  $\omega$  of a denominator of the form  $(\omega - \varepsilon)$  has a convergence radius that goes to zero as  $\varepsilon$  vanishes. These kind of poles are unphysical and will lead to arbitrary high poles in  $\varepsilon$  when expanding the differential matrix and will cancel in the final expression of the expansion coefficients  $\vec{m}_{k+1}$ .

To circumvent this problem one can transform to a basis of master integrals in which the reduction coefficients – and therefore also the coefficients of the differential equation matrix  $A$  – have the property that their dependence on  $\varepsilon$  factorizes from their dependence on  $\omega$ . The existence of such a basis was proven in ref. [215], and two independent implementations which construct the corresponding basis of master integrals have been published [117,118] as complementary codes to both the FIRE and KIRA reduction programs respectively. We used the former one in our reductions with FIRE.

With this implementation, and after obtaining a factorized form for the differential equations, we were able to push the recursive algorithm in eq. (3.3.8) up to  $\mathcal{O}(\omega^{1500})$  within no more than a few days for all of the masters. Such a large number of coefficients was necessary to be certain to fully constrain the expression of the coefficient functions in  $N$ -space from an ansatz in terms of harmonic sums and rational coefficients.

#### 3.3.3 Four-loop rescaling example

Here we expand on the method used to bring the differential system into the form with at most simple poles in  $\omega$ . We will illustrate this method with one of the four-loop topologies we encountered in our computation.

$$\begin{array}{c} \text{Diagram: A circle with four external lines (two on the left, two on the right) and a central vertex connected to four internal vertices forming a square.} \end{array} : \quad \mathcal{I}_{[\nu_1, \nu_2, \nu_3, \dots, \nu_{18}]} := \int \left( \prod_{j=1}^4 \frac{d^d k_j}{(2\pi)^d} \right) \frac{1}{\prod_{n=1}^{18} D_n^{\nu_n}} \quad (3.3.9a)$$



### 3.3. Method and computations

---

row-wise, where we rescale each master whose row contains at least one of the deepest poles by a factor of  $\omega$ . In the current example the iterative rescaling procedure leads to the following sequence of transformations:

$$\begin{pmatrix} \text{Matrix 1} \end{pmatrix} \xrightarrow{T_1} \begin{pmatrix} \text{Matrix 2} \end{pmatrix}$$

The diagram illustrates a transformation  $T_1$  applied to a sparse matrix. The matrix is represented within large parentheses. It contains a pattern of dots: yellow dots form a large triangular shape along the main diagonal and some off-diagonal elements; green dots are scattered along the diagonal and in some off-diagonal positions; and red dots are concentrated in a small cluster in the middle-left region. The transformation  $T_1$  is indicated by an arrow pointing from the first matrix to the second matrix, which shows a modified distribution of these colored dots, particularly an increase in the red dots in the central cluster.





### 3.3. Method and computations

---

where the transformation map is defined as

$$A \xrightarrow{T_a} T_a \cdot \left( A \cdot T_a^{-1} - \frac{\partial T_a^{-1}}{\partial \omega} \right) \quad (3.3.10)$$

with

$$(T_a)_{ij} = \delta_{ij} \times \begin{cases} \omega, & a = 1, i \in \{39, 40, 41\} \\ \omega, & a = 2, i \in \{25, 39, 40, 41\} \\ \omega, & a = 3, i \in \{23, 24, 25, 27, 32, 34, \dots, 41, 47, 52, 53\} \\ \omega, & a = 4, i \in \{38\} \\ 1. & \end{cases} \quad (3.3.11)$$

Here we use  $\dots$  as a short-hand for sequence of consecutive integers. The complete transformation for the matrix  $A$  can then be build by combining the intermediate steps

$$T = T_4 \cdot T_3 \cdot T_2 \cdot T_1 = \text{diag} \left( 1, \omega, \omega, \right. \\ \left. \omega^2, 1, \omega, 1, 1, 1, 1, \omega, 1, \omega, \omega, \omega, \omega^2, \omega^3, \omega^3, \omega^3, 1, 1, 1, \right. \\ \left. 1, 1, \omega, 1, 1, 1, 1, \omega, \omega, 1, 1 \right). \quad (3.3.12)$$

Alternatively, one could decide remove the deepest pole by rescaling column-wise, where each master, whose column contains one of the deepest poles, is rescaled by a factor of  $\omega^{-1}$  or, equivalently, all the others are rescaled by  $\omega$ . We use the latter because it does not affect the ability to express each master integral as a Taylor expansion.

If we were to start with the same matrix but cancel all the poles column-wise, the resulting transformation matrix would have been

$$(T_a)_{ij} = \delta_{ij} \times \begin{cases} \omega, & a = 1, i \notin \{9, 10\} \\ \omega, & a = 2, i \notin \{39, 40, 41\} \\ \omega, & a = 3, i \notin \{1, \dots, 6, 9, \dots, 19, 21, 22, 23, 24, 26, \dots, 30, 37, 42, 44\} \\ 1 & \end{cases} \quad (3.3.13)$$

and  $T = T_3 \cdot T_2 \cdot T_1$  with

$$T = \text{diag} \left( \omega^2, \omega^2, \omega^2, \omega^2, \omega^2, \omega^2, \omega^3, \omega^3, 1, 1, \omega^2, \omega^2, \omega^2, \omega^2, \omega^2, \omega, \omega, \omega^2, \right. \\ \left. \omega^3, \omega^2, \omega^2, \omega^2, \omega^2, \omega^3, \omega^2, \omega^2, \omega^2, \omega^2, \omega^2, \omega^3, \omega^3, \omega^3, \omega^3, \omega^3, \omega^2, \right. \\ \left. \omega^3, \omega^3, \omega^3, \omega^3, \omega^2, \omega^3, \omega^2, \omega^3, \omega^3, \omega^3, \omega^3, \omega^3, \omega^3, \omega^3, \omega^3, \omega^3, \omega^3 \right). \quad (3.3.14)$$

In general, one could combine the two approaches by alternating between column- and row-wise rescaling at any step of the procedure. Such a combination will generate different rescaling matrices  $T$ . We have observed that a column-wise approach is generally preferred for our computation because it requires the rescaling of fewer integrals, resulting in the ability to truncate the expansion for a larger set of master integrals.

### 3.4 Results in N-space

We are now ready to present our new analytic even- $N$  expressions for the  $n_f^2$  contributions to the fourth-order coefficient functions  $c_{2,\text{ns}}^{(4)}$  and  $c_{L,\text{ns}}^{(4)}$  in eq. (3.2.4). The corresponding  $n_f^3$  results were derived long ago [185, 186]. We confirm those results and include them below for completeness; for the case of  $\mathcal{C}_2$  in a more transparent form than given in ref. [186].

The quantities under consideration can be expressed in terms of harmonic sums. Following the notation of ref. [187], these sums are recursively defined by

$$\mathbf{S}_{\pm m}(M) = \sum_{i=1}^M \frac{(\pm 1)^i}{i^m} \quad (3.4.1)$$

and

$$\mathbf{S}_{\pm m_1, m_2, \dots, m_k}(M) = \sum_{i=1}^M \frac{(\pm 1)^i}{i^{m_1}} S_{m_2, \dots, m_k}(i) . \quad (3.4.2)$$

The sum of the absolute values of the indices  $m_k$  defines the weight  $w$  of the harmonic sum. In the  $n$ -loop coefficient functions one encounters sums up to weights  $2n$  for  $\mathcal{C}_2$  and  $2n-1$  for  $\mathcal{C}_L$ . The present non-singlet  $n_f^2$  contributions only include sums up to  $w = 6$  for  $\mathcal{C}_2$  and  $w = 5$  for  $\mathcal{C}_L$ , for the  $n_f^3$  terms the corresponding maximal weights are lower by 1. Below all harmonic sums have the argument  $N$ , which is omitted in the formulae for brevity, and we use the short-hand

$$D_a = (N + a)^{-1} . \quad (3.4.3)$$

We first present the result for the coefficient function for  $F_L$  which we write as

$$\begin{aligned} c_{L,\text{ns}}^{(4)}(N) &= n_f^0 \text{ and } n_f^1 \text{ contributions} \\ &+ C_F C_A n_f^2 \frac{16}{9} c_{L,\text{ns}}^{(4)\text{L}}(N) + C_F (C_F - \frac{1}{2} C_A) n_f^2 \frac{16}{9} c_{L,\text{ns}}^{(4)\text{N}}(N) \\ &+ C_F n_f^3 \frac{16}{27} c_{L,\text{ns}}^{(4)\text{F}}(N) \end{aligned} \quad (3.4.4)$$

### 3.4. Results in N-space

where  $C_A = n_c$  and  $C_F = (n_c - n_c^{-1})/2$  in  $SU(n_c)$ , with  $n_c = 3$  colours in QCD. For compactness, we have decomposed the  $n_f^2$  part into leading (L) and non-leading (N) contributions in the large- $n_c$  limit. The factors 16/9 and 16/27 have been put in order to shorten, on average, the lengths of the fractions in the expressions below. The  $n_f^2$  contributions are given by

$$\begin{aligned}
c_{L,ns}^{(4)L}(N) = & \\
& + \mathbf{S}_{1,4} (-80 D_{-2} + 40 D_{-1} - 40 D_1 + 80 D_2 - 120 D_3) + \mathbf{S}_{2,3} (-32 D_{-2} + 16 D_{-1} \\
& - 16 D_1 + 32 D_2 - 48 D_3) + \mathbf{S}_{3,2} (32 D_{-2} - 16 D_{-1} + 16 D_1 - 32 D_2 + 48 D_3) \\
& + \mathbf{S}_{4,1} (80 D_{-2} - 40 D_{-1} + 40 D_1 - 80 D_2 + 120 D_3) + \mathbf{S}_{1,1,3} (40 D_{-2} - 20 D_{-1} \\
& + 20 D_1 - 40 D_2 + 60 D_3) + \mathbf{S}_{1,2,2} (8 D_{-2} - 4 D_{-1} + 4 D_1 - 8 D_2 + 12 D_3) \\
& + \mathbf{S}_{1,3,1} (-8 D_{-2} + 4 D_{-1} - 4 D_1 + 8 D_2 - 12 D_3) + \mathbf{S}_{2,1,2} (8 D_{-2} - 4 D_{-1} \\
& + 4 D_1 - 8 D_2 + 12 D_3) + \mathbf{S}_{2,2,1} (-8 D_{-2} + 4 D_{-1} - 4 D_1 + 8 D_2 - 12 D_3) \\
& + \mathbf{S}_{3,1,1} (-40 D_{-2} + 20 D_{-1} - 20 D_1 + 40 D_2 - 60 D_3) + \mathbf{S}_{1,1,2,1} (-18 D_1 + 72 D_2 \\
& - 60 D_3) + \mathbf{S}_{1,2,1,1} (18 D_1 - 72 D_2 + 60 D_3) + \mathbf{S}_4 (120 D_{-2} - 40 D_{-1} - 55/3 D_1 \\
& - 80 D_2 + 180 D_3) + \mathbf{S}_{1,3} (-40 D_{-2} + 32 D_{-1} - 16 D_0 + 65 D_1 - 24 D_2 + 12 D_3 \\
& - 48 D_{-2}^2 + 24 D_{-1}^2) + \mathbf{S}_{2,2} (-12 D_{-2} + 4 D_{-1} + 38 D_1 + 8 D_2 - 18 D_3) \\
& + \mathbf{S}_{3,1} (-8 D_{-2} - 16 D_{-1} + 16 D_0 + 9 D_1 + 56 D_2 - 84 D_3 + 48 D_{-2}^2 - 24 D_{-1}^2) \\
& + \mathbf{S}_{1,1,2} (-34 D_1 + 16 D_2 - 8 D_3) + \mathbf{S}_{1,2,1} (-38 D_1 - 72 D_2 + 90 D_3) \\
& + \mathbf{S}_{2,1,1} (-46 D_1 + 56 D_2 - 82 D_3) + 36 D_1 \mathbf{S}_{1,1,1,1} + \mathbf{S}_3 (-30 D_{-2} - 4 D_{-1} \\
& - 26 D_0 + 1097/9 D_1 + 56 D_2 - 108 D_3 + 72 D_{-2}^2 - 24 D_{-1}^2 - 18 D_1^2) \\
& + \mathbf{S}_{1,2} (-10 D_{-2} + 4 D_{-1} + 65/3 D_0 - 895/6 D_1 + 56 D_2 - 116/3 D_3 + 29 D_1^2) \\
& + \mathbf{S}_{2,1} (10 D_{-2} - 4 D_{-1} + 91/3 D_0 - 913/6 D_1 - 163/3 D_3 + 25 D_1^2) \\
& + \mathbf{S}_{1,1,1} (-25 D_0 + 293/2 D_1 - 25 D_1^2) + \mathbf{S}_2 (-30 D_{-2} + 16 D_{-1} + 410/3 D_0 \\
& - 1493/4 D_1 - 16 D_2 - 11/2 D_3 - 35 D_0^2 + 263/3 D_1^2 - 27 D_1^3) + \mathbf{S}_{1,1} (45 D_{-2} \\
& - 20 D_{-1} - 140 D_0 + 14351/36 D_1 + 16 D_2 - 5 D_3 + 39 D_0^2 - 99 D_1^2 + 25 D_1^3) \\
& + \mathbf{S}_1 (135/2 D_{-2} - 20 D_{-1} - 4045/12 D_0 + 1030465/1296 D_1 - 152 D_2 \\
& + 2431/12 D_3 - 54 D_{-2}^2 + 24 D_{-1}^2 + 911/6 D_0^2 - 75/2 D_0^3 - 10565/36 D_1^2 \\
& + 245/3 D_1^3 - 37/2 D_1^4) - 75/2 D_{-2} - 714425/1296 D_0 + 3332269/2592 D_1 \\
& - 935/12 D_3 + 18 D_{-2}^2 + 3355/12 D_0^2 - 3661/36 D_0^3 + 115/6 D_0^4 \\
& - 785749/1296 D_1^2 + 3491/18 D_1^3 - 125/36 D_1^4 - 115/6 D_1^5 \\
& + \zeta_3 \left[ \mathbf{S}_2 (112 D_{-2} - 56 D_{-1} + 56 D_1 - 112 D_2 + 168 D_3) + \mathbf{S}_{1,1} (-80 D_{-2} + 40 D_{-1} \right. \\
& \left. + 32 D_1 - 208 D_2 + 120 D_3) + \mathbf{S}_1 (80 D_{-2} - 64 D_{-1} + 32 D_0 - 254/3 D_1 \right.
\end{aligned}$$

$$\begin{aligned}
& + 368 D_2 - 400 D_3 + 96 D_{-2}^2 - 48 D_{-1}^2 + 32 D_{-1} - 14/3 D_0 - 253/3 D_1 \\
& + 356 D_3 - 144 D_{-2}^2 + 48 D_{-1}^2 + 50/3 D_1^2 \Big] \\
& + \zeta_5 \left[ -240 D_{-2} + 120 D_{-1} + 240 D_1 - 1200 D_2 + 840 D_3 \right]
\end{aligned} \tag{3.4.5}$$

and

$$\begin{aligned}
c_{L,ns}^{(4)N}(N) = & + 288 D_1 \mathbf{S}_{-5} - 288 D_1 \mathbf{S}_5 - 256 D_1 \mathbf{S}_{-3,-2} - 288 D_1 \mathbf{S}_{-2,-3} - 576 D_1 \mathbf{S}_{1,-4} \\
& - 560 D_1 \mathbf{S}_{2,-3} - 72 D_1 \mathbf{S}_{2,3} - 368 D_1 \mathbf{S}_{3,-2} + 112 D_1 \mathbf{S}_{3,2} + 344 D_1 \mathbf{S}_{4,1} \\
& + 192 D_1 \mathbf{S}_{-2,-2,1} + 128 D_1 \mathbf{S}_{1,-2,-2} + 544 D_1 \mathbf{S}_{1,1,-3} + 88 D_1 \mathbf{S}_{1,1,3} \\
& + 352 D_1 \mathbf{S}_{1,2,-2} + 64 D_1 \mathbf{S}_{1,2,2} - 184 D_1 \mathbf{S}_{1,3,1} + 352 D_1 \mathbf{S}_{2,1,-2} + 56 D_1 \mathbf{S}_{2,1,2} \\
& - 16 D_1 \mathbf{S}_{2,2,1} - 168 D_1 \mathbf{S}_{3,1,1} - 320 D_1 \mathbf{S}_{1,1,1,-2} - 72 D_1 \mathbf{S}_{1,1,1,2} \\
& + 32 D_1 \mathbf{S}_{1,1,2,1} + 40 D_1 \mathbf{S}_{1,2,1,1} + \mathbf{S}_{-4} (576/5 D_{-2} + 576 D_0 - 664 D_1 \\
& + 864/5 D_3 - 432 D_1^2) + \mathbf{S}_4 (1138/3 D_1 - 144 D_1^2) + \mathbf{S}_{-3,1} (-224/5 D_{-2} \\
& + 112 D_{-1} - 224 D_0 + 224 D_2 - 336/5 D_3 + 224 D_1^2) + \mathbf{S}_{-2,-2} (-64/5 D_{-2} \\
& - 32 D_{-1} - 64 D_0 + 336 D_1 - 64 D_2 - 96/5 D_3 - 32 D_1^2) + \mathbf{S}_{-2,2} (-144/5 D_{-2} \\
& + 72 D_{-1} - 144 D_0 + 144 D_2 - 216/5 D_3 + 144 D_1^2) + \mathbf{S}_{1,-3} (-272/5 D_{-2} \\
& - 136 D_{-1} - 272 D_0 + 1040 D_1 - 272 D_2 - 408/5 D_3 - 16 D_1^2) + \mathbf{S}_{1,3} (-16/5 D_{-2} \\
& - 8 D_{-1} - 16 D_0 + 126 D_1 - 72 D_2 - 724/5 D_3 + 72 D_1^2) + \mathbf{S}_{2,-2} (-176/5 D_{-2} \\
& - 88 D_{-1} - 176 D_0 + 688 D_1 - 176 D_2 - 264/5 D_3 - 16 D_1^2) + \mathbf{S}_{2,2} (-32/5 D_{-2} \\
& - 16 D_{-1} - 32 D_0 + 176 D_1 - 32 D_2 - 48/5 D_3 + 8 D_1^2) + \mathbf{S}_{3,1} (64/5 D_{-2} \\
& + 32 D_{-1} + 64 D_0 - 370 D_1 + 120 D_2 + 796/5 D_3) + \mathbf{S}_{-2,1,1} (128/5 D_{-2} - 64 D_{-1} \\
& + 128 D_0 - 128 D_2 + 192/5 D_3 - 128 D_1^2) + \mathbf{S}_{1,1,-2} (32 D_{-2} + 80 D_{-1} + 160 D_0 \\
& - 672 D_1 + 160 D_2 + 48 D_3 + 32 D_1^2) + \mathbf{S}_{1,1,2} (16/5 D_{-2} + 8 D_{-1} + 16 D_0 \\
& - 188 D_1 + 48 D_2 + 544/5 D_3 - 32 D_1^2) + \mathbf{S}_{1,2,1} (-16/5 D_{-2} - 8 D_{-1} - 16 D_0 \\
& + 8 D_1 - 16 D_2 - 24/5 D_3 - 8 D_1^2) + \mathbf{S}_{2,1,1} (-56 D_1 - 32 D_2 - 104 D_3 + 40 D_1^2) \\
& + 72 D_1 \mathbf{S}_{1,1,1,1} + \mathbf{S}_{-3} (-1576/25 D_{-2} + 136 D_{-1} - 1384 D_0 + 2492/3 D_1 \\
& + 272 D_2 - 2724/25 D_3 + 576/5 D_{-2}^2 + 576 D_0^2 + 824 D_1^2 - 240 D_1^3) \\
& + \mathbf{S}_3 (24/5 D_{-2} + 8 D_{-1} - 48 D_0 - 2672/9 D_1 + 72 D_2 + 1086/5 D_3 + 160 D_1^2 \\
& - 48 D_1^3) + \mathbf{S}_{-2,1} (1232/25 D_{-2} - 160 D_{-1} + 448 D_0 - 48 D_1 - 368 D_2 \\
& + 1968/25 D_3 - 192/5 D_{-2}^2 + 96 D_{-1}^2 - 192 D_0^2 - 352 D_1^2 + 96 D_1^3) \\
& + \mathbf{S}_{1,-2} (32/25 D_{-2} + 80 D_{-1} + 432 D_0 - 2200/3 D_1 + 208 D_2 + 168/25 D_3
\end{aligned}$$

$$\begin{aligned}
 & -192/5 D_{-2}^2 - 96 D_{-1}^2 - 192 D_0^2 + 16 D_1^2) + \mathbf{S}_{1,2} (-24/5 D_{-2} - 8 D_{-1} \\
 & + 178/3 D_0 - 319/3 D_1 + 100 D_2 - 8/15 D_3 - 34 D_1^2 + 24 D_1^3) + \mathbf{S}_{2,1} (24/5 D_{-2} \\
 & + 8 D_{-1} + 134/3 D_0 + 5/3 D_1 - 132 D_2 - 2332/15 D_3 + 106 D_1^2 - 24 D_1^3) \\
 & + \mathbf{S}_{1,1,1} (-50 D_0 + 73 D_1 - 50 D_1^2) + \mathbf{S}_{-2} (5432/375 D_{-2} - 136 D_{-1} \\
 & + 3856/3 D_0 - 2194/3 D_1 - 320 D_2 + 3606/125 D_3 - 944/25 D_{-2}^2 + 384/5 D_{-2}^3 \\
 & + 96 D_{-1}^2 - 928 D_0^2 + 384 D_0^3 - 1828/3 D_1^2 + 344 D_1^3 - 96 D_1^4) \\
 & + \mathbf{S}_2 (-12 D_{-2} - 56 D_{-1} + 244/3 D_0 + 801/2 D_1 - 276 D_2 - 98 D_3 - 30 D_0^2 \\
 & - 320/3 D_1^2 + 6 D_1^3) + \mathbf{S}_{1,1} (96/5 D_{-2} + 64 D_{-1} - 82 D_0 - 3721/18 D_1 + 96 D_2 \\
 & - 506/5 D_3 + 34 D_0^2 - 34 D_1^2 + 42 D_1^3) + \mathbf{S}_1 (924/25 D_{-2} + 208 D_{-1} \\
 & - 499/6 D_0 - 418193/648 D_1 + 244 D_2 - 21269/150 D_3 - 144/5 D_{-2}^2 - 96 D_{-1}^2 \\
 & + 65/3 D_0^2 - 15 D_0^3 + 4699/18 D_1^2 + 46/3 D_1^3 + 3 D_1^4) + 10663/125 D_{-2} \\
 & - 1031/648 D_0 - 421403/1296 D_1 + 153647/750 D_3 - 2388/25 D_{-2}^2 + 288/5 D_{-2}^3 \\
 & + 307/6 D_0^2 - 1285/18 D_0^3 + 115/3 D_0^4 + 256829/648 D_1^2 - 2269/9 D_1^3 \\
 & + 2251/18 D_1^4 - 115/3 D_1^5 \\
 & + \zeta_3 \left[ -192 D_1 \mathbf{S}_{-2} - 432 D_1 \mathbf{S}_2 + 288 D_1 \mathbf{S}_{1,1} + \mathbf{S}_1 (-48 D_{-2} - 120 D_{-1} \right. \\
 & - 240 D_0 + 1964/3 D_1 - 64 D_2 + 416 D_3 - 192 D_1^2) - 1776/25 D_{-2} \\
 & - 40 D_{-1} - 3916/3 D_0 + 3196/3 D_1 + 584 D_2 + 3076/25 D_3 + 576/5 D_{-2}^2 \\
 & \left. + 96 D_{-1}^2 + 576 D_0^2 + 172/3 D_1^2 \right] + \zeta_5 \left[ 180 D_1 \right] . \tag{3.4.6}
 \end{aligned}$$

The  $C_F^2$  contribution (3.4.6) includes, as the corresponding lower-order quantities, only the denominator  $D_1 = 1/(N+1)$  at the maximal overall weight  $w = 5$  of the sums and Riemann  $\zeta$ -values. The  $C_F C_A$  part, and hence the large- $n_c$  coefficient (3.4.5), does not have this expected property, but instead involves the linear combinations

$$2D_{-2} - D_{-1} + D_1 - 2D_2 + 3D_3 \quad \text{and} \quad 3D_1 - 12D_2 + 10D_3 .$$

The presence of terms with  $D_{-2} = 1/(N-2)$  and  $D_{-1} = 1/(N-1)$  does not imply poles at  $N = 2$  or  $N = 1$ , as the corresponding numerators also vanish at this point. This feature already occurred in the second-order coefficient functions of refs. [39, 111, 179, 180]. At  $N=2$  these functions are given by

$$c_{L,ns}^{(4)L}(N=2) = \frac{1058755}{2916} - \frac{6713}{135} \zeta_3 - 32 \zeta_5 + 24 \zeta_3^2 , \tag{3.4.7}$$

$$c_{L,ns}^{(4)N}(N=2) = \frac{1720051}{29160} + \frac{247}{270} \zeta_3 + 30 \zeta_5 . \tag{3.4.8}$$

Note the  $\zeta_3^2$  term which does not occur at higher  $N$ . The  $n_f^3$  contribution to eq. (3.4.4) reads

$$c_{L,ns}^{(4)F}(N) = -12 D_1 \mathbf{S}_3 + 12 D_1 \mathbf{S}_{1,2} + 12 D_1 \mathbf{S}_{2,1} - 12 D_1 \mathbf{S}_{1,1,1} + \mathbf{S}_2 (-12 D_0 + 50 D_1 - 12 D_1^2) + \mathbf{S}_{1,1} (12 D_0 - 50 D_1 + 12 D_1^2) + \mathbf{S}_1 (38 D_0 - 317/3 D_1 - 12 D_0^2 + 50 D_1^2 - 12 D_1^3) + 203/3 D_0 - 8609/54 D_1 - 38 D_0^2 + 12 D_0^3 + 317/3 D_1^2 - 50 D_1^3 + 12 D_1^4. \quad (3.4.9)$$

The corresponding result for  $\mathcal{C}_2$  can be decomposed as

$$c_{2,ns}^{(4)}(N) = n_f^0 \text{ and } n_f^1 \text{ contributions} \\ + C_F C_A n_f^2 \frac{16}{9} c_{2,ns}^{(4)L}(N) + C_F (C_F - \frac{1}{2} C_A) n_f^2 \frac{16}{9} c_{2,ns}^{(4)N}(N) \\ + C_F (C_F - C_A) n_f^2 \frac{1}{3} \zeta_4 c_{2,ns}^{(4)Z}(N) + C_F n_f^3 \frac{16}{27} c_{2,ns}^{(4)F}(N) \quad (3.4.10)$$

In addition to the structures present in eq. (3.4.4), the  $n_f^2$  coefficient function for  $F_2$  includes a  $\zeta_4$  contribution, which is proportional to  $(C_F - C_A)$  and hence vanishes for  $C_A = C_F$  which is part of the choice of the colour factors that leads to a  $\mathcal{N} = 1$  supersymmetric theory. The three  $n_f^2$  coefficients in eq. (3.4.10) read

$$c_{2,ns}^{(4)L}(N) = -1951/12 \mathbf{S}_6 + 671/6 \mathbf{S}_{1,5} + 352/3 \mathbf{S}_{2,4} + 335/2 \mathbf{S}_{3,3} + 643/3 \mathbf{S}_{4,2} + 1445/6 \mathbf{S}_{5,1} \\ - 265/3 \mathbf{S}_{1,1,4} - 89 \mathbf{S}_{1,2,3} - 117 \mathbf{S}_{1,3,2} - 412/3 \mathbf{S}_{1,4,1} - 119 \mathbf{S}_{2,1,3} - 125 \mathbf{S}_{2,2,2} \\ - 137 \mathbf{S}_{2,3,1} - 169 \mathbf{S}_{3,1,2} - 188 \mathbf{S}_{3,2,1} - 688/3 \mathbf{S}_{4,1,1} + 71 \mathbf{S}_{1,1,1,3} + 81 \mathbf{S}_{1,1,2,2} \\ + 98 \mathbf{S}_{1,1,3,1} + 103 \mathbf{S}_{1,2,1,2} + 108 \mathbf{S}_{1,2,2,1} + 135 \mathbf{S}_{1,3,1,1} + 109 \mathbf{S}_{2,1,1,2} + 122 \mathbf{S}_{2,1,2,1} \\ + 139 \mathbf{S}_{2,2,1,1} + 176 \mathbf{S}_{3,1,1,1} - 70 \mathbf{S}_{1,1,1,1,2} - 82 \mathbf{S}_{1,1,1,2,1} - 94 \mathbf{S}_{1,1,2,1,1} - 114 \mathbf{S}_{1,2,1,1,1} \\ - 115 \mathbf{S}_{2,1,1,1,1} + 80 \mathbf{S}_{1,1,1,1,1,1} + \mathbf{S}_5 (20567/36 - 671/12 D_0 + 671/12 D_1) \\ + \mathbf{S}_{1,4} (-9995/36 - 20 D_{-2} + 265/6 D_0 - 505/6 D_1 + 120 D_2 - 180 D_3) \\ + \mathbf{S}_{2,3} (-13373/36 - 8 D_{-2} + 89/2 D_0 - 121/2 D_1 + 48 D_2 - 72 D_3) \\ + \mathbf{S}_{3,2} (-9817/18 + 8 D_{-2} + 117/2 D_0 - 85/2 D_1 - 48 D_2 + 72 D_3) \\ + \mathbf{S}_{4,1} (-12343/18 + 20 D_{-2} + 206/3 D_0 - 86/3 D_1 - 120 D_2 + 180 D_3) \\ + \mathbf{S}_{1,1,3} (8495/36 + 10 D_{-2} - 71/2 D_0 + 111/2 D_1 - 60 D_2 + 90 D_3) + \mathbf{S}_{1,2,2} (803/3 \\ + 2 D_{-2} - 81/2 D_0 + 89/2 D_1 - 12 D_2 + 18 D_3) + \mathbf{S}_{1,3,1} (12263/36 - 2 D_{-2} - 49 D_0 \\ + 45 D_1 + 12 D_2 - 18 D_3) + \mathbf{S}_{2,1,2} (4283/12 + 2 D_{-2} - 103/2 D_0 + 111/2 D_1$$

$$\begin{aligned}
 & -12 D_2 + 18 D_3) + \mathbf{S}_{2,2,1} (4835/12 - 2 D_{-2} - 54 D_0 + 50 D_1 + 12 D_2 - 18 D_3) \\
 & + \mathbf{S}_{3,1,1} (19967/36 - 10 D_{-2} - 135/2 D_0 + 95/2 D_1 + 60 D_2 - 90 D_3) \\
 & + \mathbf{S}_{1,1,1,2} (-1279/6 + 35 D_0 - 35 D_1) + \mathbf{S}_{1,1,2,1} (-1511/6 + 41 D_0 - 71 D_1 + 108 D_2 \\
 & - 90 D_3) + \mathbf{S}_{1,2,1,1} (-605/2 + 47 D_0 - 17 D_1 - 108 D_2 + 90 D_3) + \mathbf{S}_{2,1,1,1} (-2135/6 \\
 & + 57 D_0 - 57 D_1) + \mathbf{S}_{1,1,1,1,1} (226 - 40 D_0 + 40 D_1) + \mathbf{S}_4 (-152383/144 + 30 D_{-2} \\
 & + 5929/36 D_0 - 1906/9 D_1 - 120 D_2 + 270 D_3 - 319/6 D_0^2 + 20 D_1^2) \\
 & + \mathbf{S}_{1,3} (3800/9 - 13 D_{-2} + 6 D_{-1} - 4369/36 D_0 + 7735/36 D_1 - 36 D_2 + 18 D_3 \\
 & - 12 D_{-2}^2 + 54 D_0^2 - 71/2 D_1^2) + \mathbf{S}_{2,2} (24305/36 - 3 D_{-2} - 827/6 D_0 \\
 & + 1235/6 D_1 + 12 D_2 - 27 D_3 + 57 D_0^2 - 55/2 D_1^2) + \mathbf{S}_{3,1} (17689/18 + D_{-2} \\
 & - 6 D_{-1} - 6559/36 D_0 + 8071/36 D_1 + 84 D_2 - 126 D_3 + 12 D_{-2}^2 + 63 D_0^2 \\
 & - 19 D_1^2) + \mathbf{S}_{1,1,2} (-27307/72 + 1237/12 D_0 - 4073/24 D_1 + 24 D_2 - 12 D_3 \\
 & - 49 D_0^2 + 59/2 D_1^2) + \mathbf{S}_{1,2,1} (-10459/24 + 805/6 D_0 - 593/3 D_1 - 108 D_2 \\
 & + 135 D_3 - 111/2 D_0^2 + 51/2 D_1^2) + \mathbf{S}_{2,1,1} (-23191/36 + 613/4 D_0 - 1837/8 D_1 \\
 & + 84 D_2 - 123 D_3 - 64 D_0^2 + 47/2 D_1^2) + \mathbf{S}_{1,1,1,1} (25979/72 - 231/2 D_0 \\
 & + 357/2 D_1 + 52 D_0^2 - 23 D_1^2) + \mathbf{S}_3 (842039/648 - 3 D_{-2} - 6 D_{-1} - 18863/72 D_0 \\
 & + 11233/24 D_1 + 84 D_2 - 162 D_3 + 18 D_{-2}^2 + 3107/18 D_0^2 - 283/4 D_0^3 \\
 & - 421/4 D_1^2 + 91/4 D_1^3) + \mathbf{S}_{1,2} (-147071/324 - 5/2 D_{-2} + 2005/9 D_0 \\
 & - 34157/72 D_1 + 84 D_2 - 58 D_3 - 1969/12 D_0^2 + 143/2 D_0^3 + 134 D_1^2 - 24 D_1^3) \\
 & + \mathbf{S}_{2,1} (-1178369/1296 + 5/2 D_{-2} + 557/2 D_0 - 11939/24 D_1 - 163/2 D_3 \\
 & - 1127/6 D_0^2 + 81 D_0^3 + 323/3 D_1^2 - 49/2 D_1^3) + \mathbf{S}_{1,1,1} (46483/108 \\
 & - 8321/36 D_0 + 32905/72 D_1 + 2009/12 D_0^2 - 75 D_0^3 - 1331/12 D_1^2 + 21 D_1^3) \\
 & + \mathbf{S}_2 (-5764837/5184 - 15/2 D_{-2} + 1006649/2592 D_0 - 2225699/2592 D_1 - 24 D_2 \\
 & - 33/4 D_3 - 12665/36 D_0^2 + 16325/72 D_0^3 - 1025/12 D_0^4 + 875/3 D_1^2 \\
 & - 7073/72 D_1^3 + 263/12 D_1^4) + \mathbf{S}_{1,1} (2134163/5184 + 45/4 D_{-2} - 356983/864 D_0 \\
 & + 780301/864 D_1 + 24 D_2 - 15/2 D_3 + 1090/3 D_0^2 - 17063/72 D_0^3 + 1115/12 D_0^4 \\
 & - 7363/24 D_1^2 + 6887/72 D_1^3 - 239/12 D_1^4) + \mathbf{S}_1 (33182/81 + 27/2 D_{-2} + 6 D_{-1} \\
 & - 1115063/1728 D_0 + 243035/162 D_1 - 228 D_2 + 2431/8 D_3 - 27/2 D_{-2}^2 \\
 & + 275219/432 D_0^2 - 22763/48 D_0^3 + 19123/72 D_0^4 - 1069/12 D_0^5 \\
 & - 1669825/2592 D_1^2 + 34919/144 D_1^3 - 604/9 D_1^4 + 32/3 D_1^5) - 18199451/27648 \\
 & - 33/4 D_{-2} - 2362801/2304 D_0 + 5233867/2304 D_1 - 935/8 D_3 + 9/2 D_{-2}^2 \\
 & + 9889087/10368 D_0^2 - 1874987/2592 D_0^3 + 63839/144 D_0^4 - 14161/72 D_0^5
 \end{aligned}$$



$$\begin{aligned}
& + 1951/48 D_0^6 - 3790549/3456 D_1^2 + 367649/864 D_1^3 - 12191/144 D_1^4 \\
& - 41/3 D_1^5 + 149/16 D_1^6 \\
& + \zeta_3 \left[ - 331/6 \mathbf{S}_3 + 121/3 \mathbf{S}_{1,2} + 166/3 \mathbf{S}_{2,1} - 14 \mathbf{S}_{1,1,1} + \mathbf{S}_2 (215/2 + 28 D_{-2} \right. \\
& - 121/6 D_0 + 457/6 D_1 - 168 D_2 + 252 D_3) + \mathbf{S}_{1,1} (-111/2 - 20 D_{-2} + 7 D_0 \\
& - 312 D_2 + 180 D_3) + \mathbf{S}_1 (-274/3 + 26 D_{-2} - 12 D_{-1} - 29/3 D_0 - 497/4 D_1 \\
& + 73 D_1 + 552 D_2 - 600 D_3 + 24 D_{-2}^2 - 25 D_0^2 + 133/3 D_1^2) + 2083/32 - 9 D_{-2} \\
& + 12 D_{-1} - 101/24 D_0 - 6115/24 D_1 + 534 D_3 - 36 D_{-2}^2 - 122/3 D_0^2 \\
& \left. + 257/12 D_0^3 + 401/3 D_1^2 - 33/4 D_1^3 \right] \tag{3.4.11} \\
& + \zeta_5 \left[ - 191/2 \mathbf{S}_1 + 693/8 - 60 D_{-2} + 191/4 D_0 + 1729/4 D_1 - 1800 D_2 + 1260 D_3 \right] ,
\end{aligned}$$

$$\begin{aligned}
c_{2,\text{ns}}^{(4)\text{N}}(N) = & - 150 \mathbf{S}_{-6} - 1051/6 \mathbf{S}_6 + 6 \mathbf{S}_{-5,1} + 408 \mathbf{S}_{-4,-2} + 510 \mathbf{S}_{-3,-3} + 352 \mathbf{S}_{-2,-4} \\
& + 450 \mathbf{S}_{1,-5} + 446/3 \mathbf{S}_{1,5} + 538 \mathbf{S}_{2,-4} + 548/3 \mathbf{S}_{2,4} + 586 \mathbf{S}_{3,-3} + 273 \mathbf{S}_{3,3} \\
& + 434 \mathbf{S}_{4,-2} + 968/3 \mathbf{S}_{4,2} + 932/3 \mathbf{S}_{5,1} + 8 \mathbf{S}_{-4,1,1} - 264 \mathbf{S}_{-3,-2,1} + 4 \mathbf{S}_{-3,1,-2} \\
& - 216 \mathbf{S}_{-2,-3,1} - 136 \mathbf{S}_{-2,-2,2} - 4 \mathbf{S}_{1,-4,1} - 220 \mathbf{S}_{1,-3,-2} - 252 \mathbf{S}_{1,-2,-3} - 520 \mathbf{S}_{1,1,-4} \\
& - 770/3 \mathbf{S}_{1,1,4} - 496 \mathbf{S}_{1,2,-3} - 302 \mathbf{S}_{1,2,3} - 336 \mathbf{S}_{1,3,-2} - 160 \mathbf{S}_{1,3,2} + 4/3 \mathbf{S}_{1,4,1} \\
& - 4 \mathbf{S}_{2,-3,1} - 140 \mathbf{S}_{2,-2,-2} - 496 \mathbf{S}_{2,1,-3} - 326 \mathbf{S}_{2,1,3} - 320 \mathbf{S}_{2,2,-2} - 314 \mathbf{S}_{2,2,2} \\
& - 64 \mathbf{S}_{2,3,1} - 4 \mathbf{S}_{3,-2,1} - 344 \mathbf{S}_{3,1,-2} - 344 \mathbf{S}_{3,1,2} - 276 \mathbf{S}_{3,2,1} - 1016/3 \mathbf{S}_{4,1,1} \\
& + 8 \mathbf{S}_{-3,1,1,1} + 112 \mathbf{S}_{-2,-2,1,1} - 8 \mathbf{S}_{1,-3,1,1} + 144 \mathbf{S}_{1,-2,-2,1} - 8 \mathbf{S}_{1,-2,1,-2} + 112 \mathbf{S}_{1,1,-2,-2} \\
& + 448 \mathbf{S}_{1,1,1,-3} + 274 \mathbf{S}_{1,1,1,3} + 288 \mathbf{S}_{1,1,2,-2} + 252 \mathbf{S}_{1,1,2,2} + 58 \mathbf{S}_{1,1,3,1} + 288 \mathbf{S}_{1,2,1,-2} \\
& + 254 \mathbf{S}_{1,2,1,2} + 188 \mathbf{S}_{1,2,2,1} + 88 \mathbf{S}_{1,3,1,1} - 8 \mathbf{S}_{2,-2,1,1} + 288 \mathbf{S}_{2,1,1,-2} + 314 \mathbf{S}_{2,1,1,2} \\
& + 210 \mathbf{S}_{2,1,2,1} + 216 \mathbf{S}_{2,2,1,1} + 302 \mathbf{S}_{3,1,1,1} - 16 \mathbf{S}_{1,-2,1,1,1} - 256 \mathbf{S}_{1,1,1,1,-2} - 244 \mathbf{S}_{1,1,1,1,2} \\
& - 148 \mathbf{S}_{1,1,1,2,1} - 144 \mathbf{S}_{1,1,2,1,1} - 184 \mathbf{S}_{1,2,1,1,1} - 230 \mathbf{S}_{2,1,1,1,1} + 160 \mathbf{S}_{1,1,1,1,1,1} \\
& + \mathbf{S}_{-5} (310/3 - 297 D_0 + 585 D_1) + \mathbf{S}_5 (3463/9 - 7/3 D_0 - 857/3 D_1) \\
& + \mathbf{S}_{-4,1} (-40/3 + 2 D_0 - 2 D_1) + \mathbf{S}_{-3,-2} (-1192/3 + 174 D_0 - 430 D_1) \\
& + \mathbf{S}_{-2,-3} (-392 + 198 D_0 - 486 D_1) + \mathbf{S}_{1,-4} (-448 + 404 D_0 - 980 D_1) \\
& + \mathbf{S}_{1,4} (-6395/18 + 385/3 D_0 - 385/3 D_1) + \mathbf{S}_{2,-3} (-460 + 388 D_0 - 948 D_1) \\
& + \mathbf{S}_{2,3} (-6125/18 + 169 D_0 - 241 D_1) + \mathbf{S}_{3,-2} (-376 + 260 D_0 - 628 D_1) \\
& + \mathbf{S}_{3,2} (-5683/9 + 52 D_0 + 60 D_1) + \mathbf{S}_{4,1} (-7129/9 - 260/3 D_0 + 1292/3 D_1) \\
& + \mathbf{S}_{-3,1,1} (-40/3 + 4 D_0 - 4 D_1) + \mathbf{S}_{-2,-2,1} (160 - 120 D_0 + 312 D_1)
\end{aligned}$$

### 3.4. Results in N-space

---

$$\begin{aligned}
& + \mathbf{S}_{-2,1,-2} (4 D_0 - 4 D_1) + 40/3 \mathbf{S}_{1,-3,1} + \mathbf{S}_{1,-2,-2} (512/3 - 88 D_0 + 216 D_1) \\
& + \mathbf{S}_{1,1,-3} (1360/3 - 360 D_0 + 904 D_1) + \mathbf{S}_{1,1,3} (7679/18 - 159 D_0 + 247 D_1) \\
& + \mathbf{S}_{1,2,-2} (880/3 - 232 D_0 + 584 D_1) + \mathbf{S}_{1,2,2} (1417/3 - 142 D_0 + 206 D_1) \\
& + \mathbf{S}_{1,3,1} (5885/18 + 17 D_0 - 201 D_1) + 40/3 \mathbf{S}_{2,-2,1} + \mathbf{S}_{2,1,-2} (880/3 - 232 D_0 \\
& + 584 D_1) + \mathbf{S}_{2,1,2} (1027/2 - 141 D_0 + 197 D_1) + \mathbf{S}_{2,2,1} (1250/3 - 90 D_0 + 74 D_1) \\
& + \mathbf{S}_{3,1,1} (6313/9 - 2 D_0 - 166 D_1) + \mathbf{S}_{-2,1,1,1} (8 D_0 - 8 D_1) + 80/3 \mathbf{S}_{1,-2,1,1} \\
& + \mathbf{S}_{1,1,1,-2} (-800/3 + 208 D_0 - 528 D_1) + \mathbf{S}_{1,1,1,2} (-1163/3 + 140 D_0 - 212 D_1) \\
& + \mathbf{S}_{1,1,2,1} (-1015/3 + 66 D_0 - 34 D_1) + \mathbf{S}_{1,2,1,1} (-413 + 62 D_0 - 22 D_1) \\
& + \mathbf{S}_{2,1,1,1} (-1343/3 + 92 D_0 - 92 D_1) + \mathbf{S}_{1,1,1,1,1} (320 - 80 D_0 + 80 D_1) \\
& + \mathbf{S}_{-4} (-1270/9 + 144/5 D_{-2} + 1094 D_0 - 1182 D_1 + 1296/5 D_3 - 625 D_0^2 \\
& - 707 D_1^2) + \mathbf{S}_4 (-18371/72 + 1105/18 D_0 + 2344/9 D_1 - 133/3 D_0^2 - 206 D_1^2) \\
& + \mathbf{S}_{-3,1} (38/9 - 56/5 D_{-2} - 692/3 D_0 + 20/3 D_1 + 336 D_2 - 504/5 D_3 + 166 D_0^2 \\
& + 386 D_1^2) + \mathbf{S}_{-2,-2} (200 - 16/5 D_{-2} - 796/3 D_0 + 1612/3 D_1 - 96 D_2 - 144/5 D_3 \\
& + 110 D_0^2 - 54 D_1^2) + \mathbf{S}_{-2,2} (-36/5 D_{-2} - 140 D_0 - 4 D_1 + 216 D_2 - 324/5 D_3 \\
& + 104 D_0^2 + 248 D_1^2) + \mathbf{S}_{1,-3} (2338/9 - 68/5 D_{-2} - 2624/3 D_0 + 4928/3 D_1 \\
& - 408 D_2 - 612/5 D_3 + 388 D_0^2 - 44 D_1^2) + \mathbf{S}_{1,3} (4369/9 - 4/5 D_{-2} - 5005/18 D_0 \\
& + 3524/9 D_1 - 108 D_2 - 1086/5 D_3 + 156 D_0^2 + 53 D_1^2) + \mathbf{S}_{2,-2} (1522/9 \\
& - 44/5 D_{-2} - 1712/3 D_0 + 3248/3 D_1 - 264 D_2 - 396/5 D_3 + 252 D_0^2 - 36 D_1^2) \\
& + \mathbf{S}_{2,2} (12331/36 - 8/5 D_{-2} - 920/3 D_0 + 1541/3 D_1 - 48 D_2 - 72/5 D_3 + 160 D_0^2 \\
& - 32 D_1^2) + \mathbf{S}_{3,1} (23429/36 + 16/5 D_{-2} + 1067/18 D_0 - 2239/9 D_1 + 180 D_2 \\
& + 1194/5 D_3 - 25 D_0^2 - 14 D_1^2) + \mathbf{S}_{-2,1,1} (32/5 D_{-2} + 296/3 D_0 + 88/3 D_1 \\
& - 192 D_2 + 288/5 D_3 - 84 D_0^2 - 220 D_1^2) - 76/9 \mathbf{S}_{1,-2,1} + \mathbf{S}_{1,1,-2} (-496/3 + 8 D_{-2} \\
& + 1600/3 D_0 - 3136/3 D_1 + 240 D_2 + 72 D_3 - 232 D_0^2 + 56 D_1^2) \\
& + \mathbf{S}_{1,1,2} (-15511/36 + 4/5 D_{-2} + 799/3 D_0 - 1372/3 D_1 + 72 D_2 + 816/5 D_3 \\
& - 156 D_0^2 + 6 D_1^2) + \mathbf{S}_{1,2,1} (-1839/4 - 4/5 D_{-2} + 398/3 D_0 - 593/3 D_1 - 24 D_2 \\
& - 36/5 D_3 - 84 D_0^2 + 32 D_1^2) + \mathbf{S}_{2,1,1} (-3491/9 + 184 D_0 - 341 D_1 - 48 D_2 \\
& - 156 D_3 - 97 D_0^2 + 97 D_1^2) + \mathbf{S}_{1,1,1,1} (12119/36 - 165 D_0 + 291 D_1 + 104 D_0^2 \\
& - 46 D_1^2) + \mathbf{S}_{-3} (4346/27 - 214/25 D_{-2} - 16850/9 D_0 + 11870/9 D_1 + 408 D_2 \\
& - 4086/25 D_3 + 144/5 D_{-2}^2 + 1533 D_0^2 - 776 D_0^3 + 3839/3 D_1^2 - 408 D_1^3) \\
& + \mathbf{S}_3 (-103447/1296 + 6/5 D_{-2} - 3599/36 D_0 - 1963/12 D_1 + 108 D_2 + 1629/5 D_3 \\
& + 2131/18 D_0^2 - 197/2 D_0^3 + 530/3 D_1^2 - 171/2 D_1^3) + \mathbf{S}_{-2,1} (248/25 D_{-2}
\end{aligned}$$

$$\begin{aligned}
& + 24 D_{-1} + 4208/9 D_0 - 608/9 D_1 - 552 D_2 + 2952/25 D_3 - 48/5 D_{-2}^2 \\
& - 1220/3 D_0^2 + 206 D_0^3 - 1636/3 D_1^2 + 178 D_1^3) + \mathbf{S}_{1,-2} (-2428/27 - 52/25 D_{-2} \\
& - 24 D_{-1} + 2420/3 D_0 - 1108 D_1 + 312 D_2 + 252/25 D_3 - 48/5 D_{-2}^2 - 1766/3 D_0^2 \\
& + 266 D_0^3 + 106/3 D_1^2 - 10 D_1^3) + \mathbf{S}_{1,2} (-110893/324 - 6/5 D_{-2} + 4537/18 D_0 \\
& - 11255/36 D_1 + 150 D_2 - 4/5 D_3 - 237 D_0^2 + 146 D_0^3 + 475/6 D_1^2 + 5 D_1^3) \\
& + \mathbf{S}_{2,1} (-81845/648 + 6/5 D_{-2} + 146 D_0 - 3817/12 D_1 - 198 D_2 - 1166/5 D_3 \\
& - 935/6 D_0^2 + 112 D_0^3 + 1411/6 D_1^2 - 58 D_1^3) + \mathbf{S}_{1,1,1} (26339/108 - 2957/18 D_0 \\
& + 11089/36 D_1 + 1091/6 D_0^2 - 129 D_0^3 - 1061/6 D_1^2 + 43 D_1^3) + \mathbf{S}_{-2} (-232/3 \\
& + 23/375 D_{-2} + 24 D_{-1} + 88627/54 D_0 - 58711/54 D_1 - 480 D_2 + 5409/125 D_3 \\
& - 116/25 D_{-2}^2 + 96/5 D_{-2}^3 - 27859/18 D_0^2 + 3611/3 D_0^3 - 589 D_0^4 \\
& - 17027/18 D_1^2 + 1609/3 D_1^3 - 177 D_1^4) + \mathbf{S}_2 (162721/1296 - 3 D_{-2} \\
& - 66817/1296 D_0 + 566587/1296 D_1 - 414 D_2 - 147 D_3 - 4849/36 D_0^2 \\
& + 6167/36 D_0^3 - 707/6 D_0^4 - 1307/12 D_1^2 - 1355/36 D_1^3 - 61/6 D_1^4) \\
& + \mathbf{S}_{1,1} (239633/2592 + 24/5 D_{-2} + 26327/432 D_0 - 71081/432 D_1 + 144 D_2 \\
& - 759/5 D_3 + 385/3 D_0^2 - 5999/36 D_0^3 + 731/6 D_0^4 - 1475/12 D_1^2 \\
& + 5471/36 D_1^3 - 113/6 D_1^4) + \mathbf{S}_1 (161929/1728 + 186/25 D_{-2} - 24 D_{-1} \\
& + 33065/96 D_0 - 1073755/1296 D_1 + 366 D_2 - 21269/100 D_3 - 36/5 D_{-2}^2 \\
& - 1819/216 D_0^2 - 687/8 D_0^3 + 4237/36 D_0^4 - 287/3 D_0^5 + 493793/1296 D_1^2 \\
& + 2093/72 D_1^3 - 1285/18 D_1^4 - 43/6 D_1^5) - 61555/512 + 1807/125 D_{-2} \\
& - 269059/1296 D_0 - 810827/5184 D_1 + 153647/500 D_3 - 507/25 D_{-2}^2 \\
& + 72/5 D_{-2}^3 + 460601/2592 D_0^2 - 271195/2592 D_0^3 + 3533/72 D_0^4 - 595/9 D_0^5 \\
& + 1951/24 D_0^6 + 57113/96 D_1^2 - 380303/864 D_1^3 + 17011/72 D_1^4 - 1087/12 D_1^5 \\
& + 149/8 D_1^6 \\
& + \zeta_3 \left[ 436 \mathbf{S}_{-3} + 1061/3 \mathbf{S}_3 - 200 \mathbf{S}_{1,-2} - 496/3 \mathbf{S}_{1,2} - 100/3 \mathbf{S}_{2,1} + 44 \mathbf{S}_{1,1,1} \right. \\
& + \mathbf{S}_{-2} (-388 + 148 D_0 - 340 D_1) + \mathbf{S}_2 (-28 + 572/3 D_0 - 1868/3 D_1) \\
& + \mathbf{S}_{1,1} (35 - 94 D_0 + 382 D_1) + \mathbf{S}_1 (-397/6 - 12 D_{-2} - 1396/3 D_0 + 1005 D_1 \\
& - 96 D_2 + 624 D_3 + 142 D_0^2 - 688/3 D_1^2) - 15883/16 - 264/25 D_{-2} + 24 D_{-1} \\
& - 19655/12 D_0 + 22715/12 D_1 + 876 D_2 + 4614/25 D_3 + 144/5 D_{-2}^2 + 3947/3 D_0^2 \\
& - 3955/6 D_0^3 + 964/3 D_1^2 - 51/2 D_1^3 \\
& \left. + \zeta_5 \left[ 81 \mathbf{S}_1 - 513/4 - 171/2 D_0 + 531/2 D_1 \right] \right] \tag{3.4.12}
\end{aligned}$$

### 3.4. Results in N-space

and

$$c_{2,\text{ns}}^{(4)\text{Z}}(N) = 24 \mathbf{S}_2 - 80 \mathbf{S}_1 + 33 + 64 D_0 - 64 D_1 - 12 D_0^2 + 12 D_1^2 \quad (3.4.13)$$

Unlike the above expressions for  $\mathcal{C}_L$ , eqs. (3.4.11) and (3.4.12) include harmonic sums (up to  $w = 6$ ) without prefactors  $D_a$ ; these are the terms that do not vanish in the soft-gluon limit  $N \rightarrow \infty$ . As in eq. (3.4.5), only non-alternating sums occur in the large- $n_c$  result (3.4.11), and additional denominators (here in addition to  $D_0$  and  $D_1$ ) occur with  $w = 5$  sums in the form

$$D_{-2} - 6D_2 + 9D_3 \ .$$

Again as for  $\mathcal{C}_L$ , terms with  $D_a$ ,  $a \neq 0, 1$ , are not present with  $w = 5$  sums in the  $C_F^2 n_f^2$  coefficient (3.4.12). The situation at  $N = 2$  is the same as that for  $\mathcal{C}_L$  above, with

$$c_{2,\text{ns}}^{(4)\text{L}}(N=2) = \frac{1163533}{5832} - \frac{4613}{540} \zeta_3 - \frac{290}{3} \zeta_5 + 6 \zeta_3^2 \ , \quad (3.4.14)$$

$$c_{2,\text{ns}}^{(4)\text{N}}(N=2) = \frac{1720051}{29160} + \frac{247}{270} \zeta_3 + 30 \zeta_5 \ . \quad (3.4.15)$$

Finally the  $n_f^3$  coefficient in eq. (3.4.10) is given by

$$\begin{aligned} c_{2,\text{ns}}^{(4)\text{F}}(N) = & -119/2 \mathbf{S}_5 + 12 \mathbf{S}_{1,4} + 24 \mathbf{S}_{2,3} + 36 \mathbf{S}_{3,2} + 48 \mathbf{S}_{4,1} - 12 \mathbf{S}_{1,1,3} - 12 \mathbf{S}_{1,2,2} - 12 \mathbf{S}_{1,3,1} \\ & - 24 \mathbf{S}_{2,1,2} - 24 \mathbf{S}_{2,2,1} - 36 \mathbf{S}_{3,1,1} + 12 \mathbf{S}_{1,1,1,2} + 12 \mathbf{S}_{1,1,2,1} + 12 \mathbf{S}_{1,2,1,1} + 24 \mathbf{S}_{2,1,1,1} \\ & - 12 \mathbf{S}_{1,1,1,1,1} + \mathbf{S}_4 (853/6 - 6 D_0 + 6 D_1) + \mathbf{S}_{1,3} (-29 + 6 D_0 - 6 D_1) \\ & + \mathbf{S}_{2,2} (-67 + 6 D_0 - 6 D_1) + \mathbf{S}_{3,1} (-105 + 6 D_0 - 6 D_1) + \mathbf{S}_{1,1,2} (29 - 6 D_0 + 6 D_1) \\ & + \mathbf{S}_{1,2,1} (29 - 6 D_0 + 6 D_1) + \mathbf{S}_{2,1,1} (67 - 6 D_0 + 6 D_1) + \mathbf{S}_{1,1,1,1} (-29 + 6 D_0 \\ & - 6 D_1) + \mathbf{S}_3 (-524/3 + 13 D_0 - 34 D_1 - 12 D_0^2 + 6 D_1^2) + \mathbf{S}_{1,2} (235/6 - 13 D_0 \\ & + 34 D_1 + 12 D_0^2 - 6 D_1^2) + \mathbf{S}_{2,1} (641/6 - 13 D_0 + 34 D_1 + 12 D_0^2 - 6 D_1^2) \\ & + \mathbf{S}_{1,1,1} (-235/6 + 13 D_0 - 34 D_1 - 12 D_0^2 + 6 D_1^2) + \mathbf{S}_2 (14321/108 - 161/6 D_0 \\ & + 280/3 D_1 + 29 D_0^2 - 18 D_0^3 - 34 D_1^2 + 6 D_1^3) + \mathbf{S}_{1,1} (-4429/108 + 161/6 D_0 \\ & - 280/3 D_1 - 29 D_0^2 + 18 D_0^3 + 34 D_1^2 - 6 D_1^3) + \mathbf{S}_1 (-25279/648 + 5729/108 D_0 \\ & - 9259/54 D_1 - 325/6 D_0^2 + 45 D_0^3 - 24 D_0^4 + 280/3 D_1^2 - 34 D_1^3 + 6 D_1^4) \\ & + 281971/3456 + 55157/648 D_0 - 39803/162 D_1 - 9847/108 D_0^2 + 161/2 D_0^3 \\ & - 721/12 D_0^4 + 119/4 D_0^5 + 9241/54 D_1^2 - 277/3 D_1^3 + 397/12 D_1^4 - 23/4 D_1^5 \\ & + \zeta_3 \left[ \mathbf{S}_2 - 5/3 \mathbf{S}_1 + 1/8 + 11/6 D_0 - 11/6 D_1 - 1/2 D_0^2 + 1/2 D_1^2 \right] \\ & + \zeta_4 \left[ 3/2 \mathbf{S}_1 - 9/8 - 3/4 D_0 + 3/4 D_1 \right] \ . \end{aligned} \quad (3.4.16)$$

The numerical size of the above fourth-order results is shown in figs. 3.3 and 3.4 for QCD, i.e.,  $C_A = 3$  and  $C_F = 4/3$ , with  $n_f = 4$  light flavours, together with the corresponding third-order contributions for the physically very wide range  $2 \leq N \leq 50$ . The coefficient functions  $c_{L,ns}^{(n)}$  vanish for  $N \rightarrow \infty$ , yet only slowly: the size of the  $n_f^2$  parts of  $c_{L,ns}^{(4)}$  in the right part of fig. 3.3 decreases only by a factor of 2 from  $N=10$  to  $N=50$ . A further reduction by another factor of 2 and 4 is only reached at  $N = 175$  and  $N = 540$ , respectively.

The shape of the leading large- $n_f$  contributions ( $\sim n_f^{n-1}$  at order  $\alpha_s(n)$ ) in fig. 3.3 is similar to that of the subleading large- $n_f$  contributions ( $\sim n_f^{n-2}$  at order  $\alpha_s(n)$ ) in the  $N$ -range of the figure; its relative size is decreasing for  $n_f = 4$  from about 1/10 at  $n = 3$  to about 1/15 at  $n = 4$ . This pattern of a reduced numerical significance of the leading large- $n_f$  term at the fourth order is also seen for  $c_{2,ns}^{(n)}$  in fig. 3.4. Here the subleading large- $n_f$  contributions are larger by factors between 10 and 15 at  $4 \leq N \leq 50$  for  $n = 3$ ; the corresponding range for  $n = 4$  is 19 to 24.

Also shown in fig. 3.4 are the dominant contributions to  $\mathcal{C}_{2,ns}$  in the large- $N$  threshold limit, where our new contributions (3.4.11) – (3.4.13) to  $c_{2,ns}^{(4)}$  lead to the numerical expansion

$$\begin{aligned}
 c_{2,ns}^{(4)}(N) \Big|_{n_f^2} = & 0.7233196 \ln^6 \tilde{N} + 12.339095 \ln^5 \tilde{N} \\
 & + 87.721224 \ln^4 \tilde{N} + 293.04552 \ln^3 \tilde{N} \\
 & + 233.48456 \ln^2 \tilde{N} + 65.035706 \ln \tilde{N} - 12175.412 \\
 & + N^{-1} \left( 2.1069959 \ln^5 \tilde{N} + 67.193416 \ln^4 \tilde{N} \right. \\
 & + 691.16782 \ln^3 \tilde{N} + 3429.9787 \ln^2 \tilde{N} \\
 & \left. + 8755.5832 \ln \tilde{N} + 12282.167 \right) + \mathcal{O}(N^{-2}) \quad (3.4.17)
 \end{aligned}$$

with  $\ln \tilde{N} = \ln N + \gamma_e$ , where  $\gamma_e$  is the Euler-Mascheroni constant. Keeping only the  $\ln^\ell \tilde{N}$  terms in the first three lines, and the corresponding contributions at the third order, one arrives at the upper dotted curves in the figure. Adding to these the constant- $N$  contributions yields the lower dotted curves. Neither of these results can quantitatively replace the exact expressions at physically interesting moderate values of  $N$ .

An analytic  $x$ -space expression corresponding to eq. (3.4.17) and a further discussion of the threshold and high-energy limits can be found in section 3.5 below.

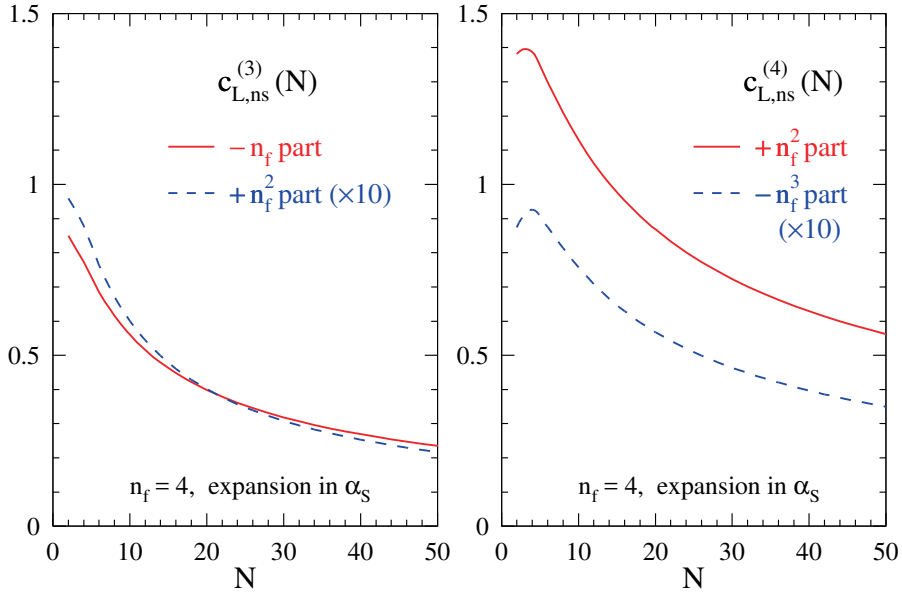


Figure 3.3: The leading (dashed) and sub-leading (solid) large- $n_f$  contributions to the three-loop (left panel) and four-loop (right panel) coefficient functions for the structure function  $F_{L,ns}$  for QCD with  $n_f = 4$  flavours. The results in eqs. (3.4.4) – (3.4.16) have been converted to an expansion in  $\alpha_s$ , and the leading large- $n_f$  curves have been scaled up by a factor of 10 for better visibility.

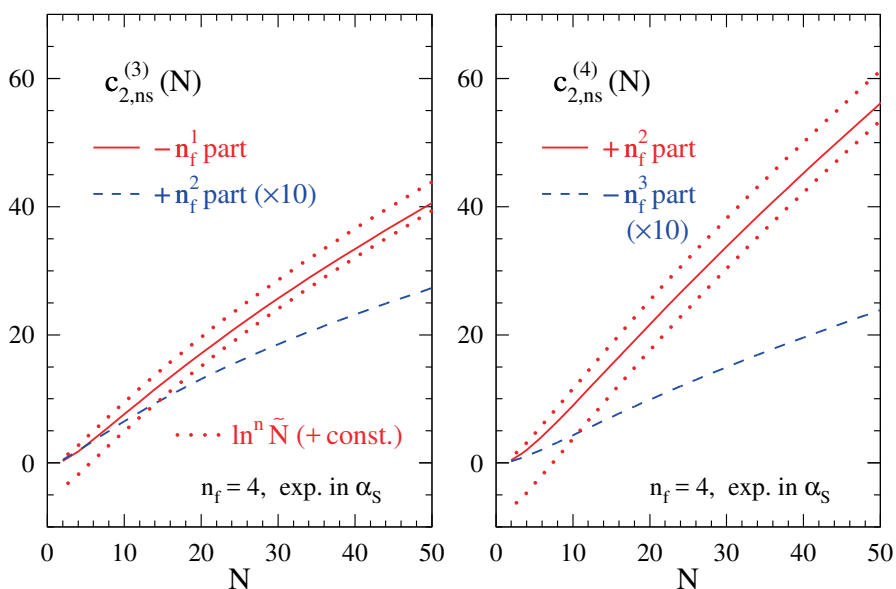


Figure 3.4: As fig. 3.3, but for the structure function  $F_{2,ns}$ . In addition the  $\ln^\ell \tilde{N}$  and  $\ln^\ell \tilde{N} + \text{const.}$  threshold contributions are shown here, respectively, by the upper and lower dotted curves.

### 3.4.1 A five-loop prediction

It is possible to predict a small part, the  $\zeta_4$  coefficients of  $n_f^3$  and  $n_f^4$ , of the  $n = 4$  five-loop non-singlet anomalous dimension in eq. (3.2.10), from our result (3.4.13) and eq. (3.4.16) for  $c_{2,\text{ns}}^{(4)}(N)$ . This possibility arises from the no- $\pi^2$  conjecture/theorem [216, 217] for Euclidean (space-like) physical quantities in a suitable renormalization scheme, which was investigated in the context of inclusive DIS in ref. [218]. For this one considers the physical evolution kernels which were expressed in terms of the splitting functions and coefficient functions for the non-singlet case to the fifth order in eqs. (2.7) – (2.9) of ref. [219].

Keeping only the terms with  $\zeta_4$  simplifies the fifth-order  $\overline{\text{MS}}$  kernel for  $F_{2,\text{ns}}$  to

$$\tilde{K}_{2,\text{ns}}^{(4)}(N) = -\tilde{\gamma}_{\text{ns}}^{(4)}(N) - 3\beta_1 \tilde{c}_a^{(3)}(N) - 4\beta_0 \left( \tilde{c}_{2,\text{ns}}^{(4)}(N) - c_{2,\text{ns}}^{(1)}(N) \tilde{c}_{2,\text{ns}}^{(3)}(N) \right), \quad (3.4.18)$$

where the tilde indicates the contribution with  $\zeta_4 = 1/90 \pi^4$ . At this order, a scheme transformation removing the  $\zeta_4$  term of the five-loop beta function [104, 106, 107] needs to be performed, and the prediction of the no- $\pi^2$  theorem becomes [218]

$$\beta_0 \tilde{K}_a^{(4)} + \frac{1}{3} \tilde{\beta}_4 K_a^{(0)} = 0. \quad (3.4.19)$$

Since  $\beta_0$  includes  $n_f$  and  $K_{2,\text{ns}}^{(0)} \sim C_F$ , only the  $\zeta_4 n_f^4$  terms in  $\beta_4$  can contribute, but there is no such term. Hence already the quantity (3.4.18) has to vanish for the  $n_f^3$  and  $n_f^4$  terms.

The three-loop coefficient function  $c_{2,\text{ns}}^{(3)}(N)$  does not include a  $\zeta_4$  term with  $n_f^2$ . Since the prefactors  $\beta_1$  and  $\beta_0 c_{2,\text{ns}}^{(1)}$  include no more than one power in  $n_f$ , the two terms with  $c_{2,\text{ns}}^{(3)}$  do not contribute to the  $n_f^3$  and  $n_f^4$  parts of eq. (3.4.18). So we end up with a simple relation for the  $\zeta_4 n_f^3$  and  $\zeta_4 n_f^4$  contributions,

$$\tilde{P}_{\text{ns}}^{(4)}(N) = -\tilde{\gamma}_{\text{ns}}^{(4)}(N) = 4\beta_0 \tilde{c}_{2,\text{ns}}^{(4)}(N), \quad (3.4.20)$$

which leads to

$$\begin{aligned} P_{\text{ns}}^{(4)}(N) \Big|_{\zeta_4} &= n_f^0, n_f^1 \text{ and } n_f^2 \text{ contributions} \\ &+ C_F C_A n_f^3 \left( \frac{64}{3} \mathbf{S}_2 - \frac{1568}{27} \mathbf{S}_1 + \frac{176}{9} + \frac{1360}{27} D_0 - \frac{1360}{27} D_1 - \frac{32}{3} D_0^2 + \frac{32}{3} D_1^2 \right) \\ &+ C_F^2 n_f^3 \left( -\frac{64}{3} \mathbf{S}_2 + \frac{640}{9} \mathbf{S}_1 - \frac{88}{3} - \frac{512}{9} D_0 + \frac{512}{9} D_1 + \frac{32}{3} D_0^2 - \frac{32}{3} D_1^2 \right) \end{aligned}$$



$$+ C_F n_f^4 \left( -\frac{64}{27} \mathbf{s}_1 + \frac{16}{9} + \frac{32}{27} D_0 - \frac{32}{27} D_1 \right). \quad (3.4.21)$$

At  $N = 2$  and  $N = 3$  this result agrees with those obtained by diagram calculations in ref. [220] using the program of ref. [221] for the  $R^*$  operation. Its last line was derived long ago as part of the complete leading large- $n_f$  result [222]. Due to eqs. (3.4.10) and (3.4.16), the whole of (3.4.21) is proportional to  $\beta_0$  and the lowest-order anomalous dimension  $\gamma_{qq}^{(0)}(N)$  for  $C_F = C_A$ .

### 3.5 The x-space coefficient functions

The coefficient functions  $c_{a,ns}^{(n)}(x)$  are obtained from the  $N$ -space results of the previous section by an inverse Mellin transformation, which expresses these functions in terms of harmonic polylogarithms (HPLs)  $H_{m_1, \dots, m_w}(x)$ ,  $m_j = 0, \pm 1$ . Following ref. [188], to which the reader is referred for a detailed discussion, the lowest-weight ( $w = 1$ ) functions  $H_m(x)$  are given by

$$H_0(x) = \ln x, \quad H_{\pm 1}(x) = \mp \ln(1 \mp x), \quad (3.5.1)$$

and the higher-weight ( $w \geq 2$ ) functions are recursively defined as

$$H_{m_1, \dots, m_w}(x) = \begin{cases} \frac{1}{w!} \ln^w x, & \text{if } m_1, \dots, m_w = 0, \dots, 0 \\ \int_0^x dz f_{m_1}(z) H_{m_2, \dots, m_w}(z), & \text{else} \end{cases} \quad (3.5.2)$$

with

$$f_0(x) = \frac{1}{x}, \quad f_{\pm 1}(x) = \frac{1}{1 \mp x}. \quad (3.5.3)$$

The inverse Mellin transformation exploits an isomorphism between the set of harmonic sums for even or odd  $N$  and the set of HPLs. Hence it can be performed by a completely algebraic procedure [111, 188], based on the fact that harmonic sums occur as coefficients of the Taylor expansion of harmonic polylogarithms. A FORTRAN program for the HPLs up to weight  $w = 4$  has been provided in ref. [223], later this was extended to  $w = 5$  and  $w = 6$ .

In our results below, the argument  $x$  of the HPLs is suppressed for brevity, and we use the abbreviations

$$x_m = 1 - x \quad \text{and} \quad x_p = 1 + x. \quad (3.5.4)$$

### 3.5. The x-space coefficient functions

Analogous to eq. (3.5.5) above, the  $x$ -space coefficient function for  $F_{L,\text{ns}}$  is decomposed as

$$c_{L,\text{ns}}^{(4)}(x) = n_f^0 \text{ and } n_f^1 \text{ contributions} \\ + C_F C_A n_f^2 \frac{16}{9} c_{L,\text{ns}}^{(4)\text{L}}(x) + C_F (C_F - \frac{1}{2} C_A) n_f^2 \frac{16}{9} c_{L,\text{ns}}^{(4)\text{N}}(x) + C_F n_f^3 \frac{16}{27} c_{L,\text{ns}}^{(4)\text{F}}(x) \quad (3.5.5)$$

The two  $n_f^2$  contributions in the second line are given by

$$c_{L,\text{ns}}^{(4)\text{L}}(x) = \\ + \text{H}_{0,0,0,0,1} (-40x + 80x^2 - 120x^3) + \text{H}_{0,0,0,1,0} (-16x + 32x^2 - 48x^3) \\ + \text{H}_{0,0,0,1,1} (-20x + 40x^2 - 60x^3) + \text{H}_{0,0,1,0,0} (16x - 32x^2 + 48x^3) + \text{H}_{0,0,1,0,1} (-4x \\ + 8x^2 - 12x^3) + \text{H}_{0,0,1,1,0} (4x - 8x^2 + 12x^3) + \text{H}_{0,1,0,0,0} (40x - 80x^2 + 120x^3) \\ + \text{H}_{0,1,0,0,1} (-48x^2 + 24x^3 - 4x + 8x^2 - 12x^3) + \text{H}_{0,1,0,1,0} (4x - 8x^2 + 12x^3) \\ + \text{H}_{0,1,0,1,1} (-18x + 72x^2 - 60x^3) + \text{H}_{0,1,1,0,0} (48x^2 - 24x^3 + 20x - 40x^2 + 60x^3) \\ + \text{H}_{0,1,1,0,1} (18x - 72x^2 + 60x^3) + \text{H}_{1,0,0,0,1} (-80x^2 + 40x^3 - 40x + 80x^2 \\ - 120x^3) + \text{H}_{1,0,0,1,0} (-32x^2 + 16x^3 - 16x + 32x^2 - 48x^3) + \text{H}_{1,0,0,1,1} (-40x^2 \\ + 20x^3 - 20x + 40x^2 - 60x^3) + \text{H}_{1,0,1,0,0} (32x^2 - 16x^3 + 16x - 32x^2 + 48x^3) \\ + \text{H}_{1,0,1,0,1} (-8x^2 + 4x^3 - 4x + 8x^2 - 12x^3) + \text{H}_{1,0,1,1,0} (8x^2 - 4x^3 + 4x - 8x^2 \\ + 12x^3) + \text{H}_{1,0,1,1,1} (80x^2 - 40x^3 + 40x - 80x^2 + 120x^3) + \text{H}_{1,1,0,0,1} (-8x^2 \\ + 4x^3 - 4x + 8x^2 - 12x^3) + \text{H}_{1,1,0,1,0} (8x^2 - 4x^3 + 4x - 8x^2 + 12x^3) \\ + \text{H}_{1,1,0,1,1} (-18x + 72x^2 - 60x^3) + \text{H}_{1,1,1,0,0} (40x^2 - 20x^3 + 20x - 40x^2 + 60x^3) \\ + \text{H}_{1,1,1,0,1} (18x - 72x^2 + 60x^3) + 188/3 x \text{H}_{0,0,0,0} + \text{H}_{0,0,0,1} (80x^{-1} + 115/2 x \\ + 184x^2 - 102x^3) + \text{H}_{0,0,1,0} (32x^{-1} + 86x + 48x^2) + \text{H}_{0,0,1,1} (40x^{-1} + 86x + 76x^2 \\ - 8x^3) + \text{H}_{0,1,0,0} (-32x^{-1} + 91x - 112x^2 + 102x^3) + \text{H}_{0,1,0,1} (8x^{-1} + 61x + 12x^2) \\ + \text{H}_{0,1,1,0} (-8x^{-1} + 65x - 28x^2 + 8x^3) + 61x \text{H}_{0,1,1,1} + \text{H}_{1,0,0,0} (-80x^{-1} + 115/3 x \\ - 120x^2) + \text{H}_{1,0,0,1} (16 - 20x^2 - 4x^3 + 7x + 76x^2 - 102x^3) + \text{H}_{1,0,1,0} (-8x^{-1} \\ + 40x - 12x^2) + \text{H}_{1,0,1,1} (4x + 76x^2 - 8x^3) + \text{H}_{1,1,0,0} (-16 + 20x^2 - 28x^3 + 75x \\ - 124x^2 + 102x^3) + \text{H}_{1,1,0,1} (80x - 60x^2) + \text{H}_{1,1,1,0} (34x - 16x^2 + 8x^3) \\ + 36x \text{H}_{1,1,1,1} + \text{H}_{0,0,0} (125/6 + 10969/36 x + 120x^2 + 40\zeta_2 x - 80\zeta_2 x^2 + 120\zeta_2 x^3) \\ + \text{H}_{0,0,1} (-23/2 - 12x^{-1} + 1613/6 x + 290x^2 - 197/3 x^3 + 4\zeta_2 x - 8\zeta_2 x^2 + 12\zeta_2 x^3) \\ + \text{H}_{0,1,0} (-23 - 32x^{-1} + 1307/6 x - 20x^2 + 197/3 x^3 + 48\zeta_2 x^2 - 24\zeta_2 x^3 + 4\zeta_2 x \\ - 8\zeta_2 x^2 + 12\zeta_2 x^3) + \text{H}_{0,1,1} (-29 - 40x^{-1} + 471/2 x + 8x^2 - 18\zeta_2 x + 72\zeta_2 x^2 \\ - 60\zeta_2 x^3) + \text{H}_{1,0,0} (-24 - 36x^{-1} + 1439/9 x - 90x^2 + 80\zeta_2 x^2 - 40\zeta_2 x^3)$$

$$\begin{aligned}
& + 40 \zeta_2 x - 80 \zeta_2 x^2 + 120 \zeta_2 x^3) + \mathbf{H}_{1,0,1} (-85/3 - 8 x^{-1} + 721/6 x + 152 x^2 \\
& - 197/3 x^3 + 8 \zeta_2 x^{-2} - 4 \zeta_2 x^{-1} + 4 \zeta_2 x - 8 \zeta_2 x^2 + 12 \zeta_2 x^3) + \mathbf{H}_{1,1,0} (-71/3 \\
& + 8 x^{-1} + 997/6 x - 100 x^2 + 197/3 x^3 + 8 \zeta_2 x^{-2} - 4 \zeta_2 x^{-1} + 4 \zeta_2 x - 8 \zeta_2 x^2 \\
& + 12 \zeta_2 x^3) + \mathbf{H}_{1,1,1} (-25 + 293/2 x - 18 \zeta_2 x + 72 \zeta_2 x^2 - 60 \zeta_2 x^3) \\
& + \mathbf{H}_{0,0} (-3301/36 + 2471/3 x + 210 x^2 - 80 \zeta_2 x^{-1} - 115/2 \zeta_2 x - 184 \zeta_2 x^2 \\
& + 102 \zeta_2 x^3 - 28 \zeta_3 x + 56 \zeta_3 x^2 - 84 \zeta_3 x^3) + \mathbf{H}_{0,1} (-941/6 - 36 x^{-1} + 10169/18 x \\
& + 611/3 x^2 - 8 \zeta_2 x^{-1} - 61 \zeta_2 x - 12 \zeta_2 x^2 - 48 \zeta_3 x^{-2} + 24 \zeta_3 x^{-1} + 62 \zeta_3 x \\
& - 304 \zeta_3 x^2 + 216 \zeta_3 x^3) + \mathbf{H}_{1,0} (-464/3 + 32 x^{-1} + 4565/12 x + 43/3 x^2 + 20 \zeta_2 x^{-2} \\
& + 4 \zeta_2 x^{-1} - 16 \zeta_2 - 7 \zeta_2 x - 76 \zeta_2 x^2 + 102 \zeta_2 x^3 - 56 \zeta_3 x^{-2} + 28 \zeta_3 x^{-1} - 28 \zeta_3 x \\
& + 56 \zeta_3 x^2 - 84 \zeta_3 x^3) + \mathbf{H}_{1,1} (-155 + 40 x^{-1} + 14459/36 x + 8 x^2 - 80 \zeta_2 x + 60 \zeta_2 x^2 \\
& - 56 \zeta_3 x^{-2} + 28 \zeta_3 x^{-1} + 62 \zeta_3 x - 304 \zeta_3 x^2 + 216 \zeta_3 x^3) + \mathbf{H}_0 (-3679/12 \\
& + 839905/648 x + 587/3 x^2 + 12 \zeta_2 x^{-1} + 23/2 \zeta_2 - 1613/6 \zeta_2 x - 290 \zeta_2 x^2 \\
& + 197/3 \zeta_2 x^3 + 56 \zeta_3 x^{-1} - 605/6 \zeta_3 x + 164 \zeta_3 x^2 - 110 \zeta_3 x^3 - 53 \zeta_4 x \\
& + 106 \zeta_4 x^2 - 159 \zeta_4 x^3) + \mathbf{H}_1 (-4483/12 + 84 x^{-1} + 842437/1296 x + 587/3 x^2 \\
& + 8 \zeta_2 x^{-1} + 85/3 \zeta_2 - 721/6 \zeta_2 x - 152 \zeta_2 x^2 + 197/3 \zeta_2 x^3 - 20 \zeta_3 x^{-2} + 44 \zeta_3 x^{-1} \\
& + 16 \zeta_3 + 397/3 \zeta_3 x - 136 \zeta_3 x^2 - 110 \zeta_3 x^3 - 106 \zeta_4 x^{-2} + 53 \zeta_4 x^{-1} - 53 \zeta_4 x \\
& + 106 \zeta_4 x^2 - 159 \zeta_4 x^3) - 763025/1296 + 3130309/2592 x + 36 \zeta_2 x^{-1} + 941/6 \zeta_2 \\
& - 10169/18 \zeta_2 x - 611/3 \zeta_2 x^2 + 12 \zeta_3 x^{-1} - 13/6 \zeta_3 - 391 \zeta_3 x + 650 \zeta_3 x^2 \\
& - 197 \zeta_3 x^3 + 22 \zeta_3 \zeta_2 x - 80 \zeta_3 \zeta_2 x^2 + 72 \zeta_3 \zeta_2 x^3 + 106 \zeta_4 x^{-1} + 33 \zeta_4 x \\
& + 263 \zeta_4 x^2 - 192 \zeta_4 x^3 + 140 \zeta_5 x - 640 \zeta_5 x^2 + 480 \zeta_5 x^3
\end{aligned} \tag{3.5.6}$$

and

$$\begin{aligned}
c_{L,\text{ns}}^{(4)\text{N}}(x) = & - 320 x \mathbf{H}_{-1,-1,-1,-1,0} + 544 x \mathbf{H}_{-1,-1,-1,0,0} + 352 x \mathbf{H}_{-1,-1,0,-1,0} - 576 x \mathbf{H}_{-1,-1,0,0,0} \\
& + 352 x \mathbf{H}_{-1,0,-1,-1,0} - 560 x \mathbf{H}_{-1,0,-1,0,0} - 368 x \mathbf{H}_{-1,0,0,-1,0} + 288 x \mathbf{H}_{-1,0,0,0,0} \\
& + 352 x \mathbf{H}_{0,-1,-1,-1,0} - 560 x \mathbf{H}_{0,-1,-1,0,0} - 368 x \mathbf{H}_{0,-1,0,-1,0} + 144 x \mathbf{H}_{0,-1,0,0,0} \\
& - 224 x \mathbf{H}_{0,-1,0,0,1} - 144 x \mathbf{H}_{0,-1,0,1,0} - 128 x \mathbf{H}_{0,-1,0,1,1} - 384 x \mathbf{H}_{0,0,-1,-1,0} \\
& + 48 x \mathbf{H}_{0,0,-1,0,0} - 288 x \mathbf{H}_{0,0,-1,0,1} - 48 x \mathbf{H}_{0,0,1,0,0} - 160 x \mathbf{H}_{0,1,0,-1,0} \\
& - 144 x \mathbf{H}_{0,1,0,0,0} - 184 x \mathbf{H}_{0,1,0,0,1} + 56 x \mathbf{H}_{0,1,0,1,0} + 16 x \mathbf{H}_{0,1,1,0,0} - 40 x \mathbf{H}_{0,1,1,0,1} \\
& + 40 x \mathbf{H}_{0,1,1,1,0} - 288 x \mathbf{H}_{1,0,-1,0,0} - 192 x \mathbf{H}_{1,0,-1,0,1} - 256 x \mathbf{H}_{1,0,0,-1,0} \\
& - 288 x \mathbf{H}_{1,0,0,0,0} - 344 x \mathbf{H}_{1,0,0,0,1} - 112 x \mathbf{H}_{1,0,0,1,0} - 168 x \mathbf{H}_{1,0,0,1,1} + 72 x \mathbf{H}_{1,0,1,0,0} \\
& - 16 x \mathbf{H}_{1,0,1,0,1} + 56 x \mathbf{H}_{1,0,1,1,0} - 128 x \mathbf{H}_{1,1,0,-1,0} - 184 x \mathbf{H}_{1,1,0,0,1} + 64 x \mathbf{H}_{1,1,0,1,0}
\end{aligned}$$

### 3.5. The x-space coefficient functions

---

$$\begin{aligned}
& -40x \mathbf{H}_{1,1,0,1,1} + 88x \mathbf{H}_{1,1,1,0,0} - 32x \mathbf{H}_{1,1,1,0,1} + 72x \mathbf{H}_{1,1,1,1,0} + \mathbf{H}_{-1,-1,-1,0} (160 \\
& + 32x^{-2} - 80x^{-1} + 672x + 160x^2 - 48x^3) + \mathbf{H}_{-1,-1,0,0} (-272 - 272/5x^{-2} + 136x^{-1} \\
& - 1040x - 272x^2 + 408/5x^3) + \mathbf{H}_{-1,0,-1,0} (-176 - 176/5x^{-2} + 88x^{-1} - 688x \\
& - 176x^2 + 264/5x^3) + \mathbf{H}_{-1,0,0,0} (576 + 576/5x^{-2} + 664x - 864/5x^3) + \mathbf{H}_{-1,0,0,1} (224 \\
& + 224/5x^{-2} + 112x^{-1} - 224x^2 - 336/5x^3) + \mathbf{H}_{-1,0,1,0} (144 + 144/5x^{-2} + 72x^{-1} \\
& - 144x^2 - 216/5x^3) + \mathbf{H}_{-1,0,1,1} (128 + 128/5x^{-2} + 64x^{-1} - 128x^2 - 192/5x^3) \\
& + \mathbf{H}_{0,-1,-1,0} (-192 - 192/5x^{-2} + 96x^{-1} - 688x - 160x^2 + 48x^3) + \mathbf{H}_{0,-1,0,0} (576 \\
& + 576/5x^{-2} + 216x + 272x^2 - 408/5x^3) + \mathbf{H}_{0,-1,0,1} (192 + 192/5x^{-2} + 96x^{-1} \\
& - 352x) + \mathbf{H}_{0,0,-1,0} (384 + 384/5x^{-2} + 24x + 240x^2 - 168/5x^3) + \mathbf{H}_{0,0,0,0} (-248/3x \\
& + 864/5x^3) + \mathbf{H}_{0,0,0,1} (127x + 344x^2 + 1132/5x^3) + \mathbf{H}_{0,0,1,0} (136x + 112x^2 \\
& + 168/5x^3) + \mathbf{H}_{0,0,1,1} (148x + 160x^2 + 712/5x^3) + \mathbf{H}_{0,1,0,0} (-34x - 72x^2 \\
& - 724/5x^3) + \mathbf{H}_{0,1,0,1} (98x + 16x^2 + 24/5x^3) + \mathbf{H}_{0,1,1,0} (154x - 48x^2 - 544/5x^3) \\
& + 122x \mathbf{H}_{0,1,1,1} + \mathbf{H}_{1,0,-1,0} (64 + 64/5x^{-2} + 32x^{-1} - 336x + 64x^2 + 96/5x^3) \\
& - 1138/3x \mathbf{H}_{1,0,0,0} + \mathbf{H}_{1,0,0,1} (64 + 64/5x^{-2} + 32x^{-1} - 370x + 120x^2 + 796/5x^3) \\
& + \mathbf{H}_{1,0,1,0} (-32 - 32/5x^{-2} - 16x^{-1} + 176x - 32x^2 - 48/5x^3) + \mathbf{H}_{1,0,1,1} (56x + 32x^2 \\
& + 104x^3) + \mathbf{H}_{1,1,0,0} (-16 - 16/5x^{-2} - 8x^{-1} + 126x - 72x^2 - 724/5x^3) + \mathbf{H}_{1,1,0,1} (16 \\
& + 16/5x^{-2} + 8x^{-1} - 8x + 16x^2 + 24/5x^3) + \mathbf{H}_{1,1,1,0} (-16 - 16/5x^{-2} - 8x^{-1} \\
& + 188x - 48x^2 - 544/5x^3) + 72x \mathbf{H}_{1,1,1,1} - 160\zeta_2 x \mathbf{H}_{-1,-1,-1} + \mathbf{H}_{-1,-1,0} (-336 \\
& - 1232/25x^{-2} + 128x^{-1} - 2752/3x - 320x^2 + 1968/25x^3 + 112\zeta_2 x) \\
& + 176\zeta_2 x \mathbf{H}_{-1,0,-1} + \mathbf{H}_{-1,0,0} (6104/5 + 3616/25x^{-2} + 272/5x^{-1} + 17152/15x \\
& - 408/5x^2 - 5784/25x^3 - 56\zeta_2 x) + \mathbf{H}_{-1,0,1} (448 + 1232/25x^{-2} + 160x^{-1} + 48x \\
& - 368x^2 - 1968/25x^3) + 176\zeta_2 x \mathbf{H}_{0,-1,-1} + \mathbf{H}_{0,-1,0} (784 + 2384/25x^{-2} + 112/5x^{-1} \\
& + 1264/5x + 296x^2 - 1968/25x^3 + 120\zeta_2 x) + 96\zeta_2 x \mathbf{H}_{0,0,-1} + \mathbf{H}_{0,0,0} (289/15 \\
& - 576/5x^{-1} - 73891/90x + 864/5x^2 + 5784/25x^3) + \mathbf{H}_{0,0,1} (-143 - 288/5x^{-1} \\
& - 143/15x + 424x^2 + 18104/75x^3 + 192\zeta_2 x) + \mathbf{H}_{0,1,0} (-342/5 - 112/5x^{-1} \\
& + 2383/15x - 476/5x^2 - 488/3x^3 + 288\zeta_2 x) + \mathbf{H}_{0,1,1} (216\zeta_2 x - 426/5 - 128/5x^{-1} \\
& + 659/5x - 328/5x^2) + 192\zeta_2 x \mathbf{H}_{1,0,-1} + \mathbf{H}_{1,0,0} (-192/5 + 16/5x^{-1} - 6862/45x \\
& + 724/5x^2 + 400\zeta_2 x) + \mathbf{H}_{1,0,1} (192\zeta_2 x - 814/15 - 16/5x^{-1} - 301/15x + 716/5x^2 \\
& + 488/3x^3) + \mathbf{H}_{1,1,0} (-746/15 + 16/5x^{-1} + 3131/15x - 196/5x^2 - 488/3x^3 \\
& + 296\zeta_2 x) + \mathbf{H}_{1,1,1} (-50 + 73x + 192\zeta_2 x) + \mathbf{H}_{-1,-1} (16\zeta_2 x^{-2} - 40\zeta_2 x^{-1} + 80\zeta_2 \\
& + 336\zeta_2 x + 80\zeta_2 x^2 - 24\zeta_2 x^3 + 160\zeta_3 x) + \mathbf{H}_{-1,0} (85732/75 + 32252/375x^{-2}
\end{aligned}$$

$$\begin{aligned}
& + 1632/25 x^{-1} + 79732/75 x - 2568/25 x^2 - 17916/125 x^3 - 56 \zeta_2 x^{-2} - 84 \zeta_2 x^{-1} \\
& - 280 \zeta_2 - 176 \zeta_2 x + 168 \zeta_2 x^2 + 84 \zeta_2 x^3 - 80 \zeta_3 x) + \mathbf{H}_{0,-1} (-288/5 \zeta_2 x^{-2} \\
& - 48 \zeta_2 x^{-1} - 288 \zeta_2 + 8 \zeta_2 x - 80 \zeta_2 x^2 + 24 \zeta_2 x^3 - 112 \zeta_3 x) + \mathbf{H}_{0,0} (-12541/450 \\
& - 3616/25 x^{-1} - 41282/25 x + 4444/25 x^2 + 17916/125 x^3 - 103 \zeta_2 x - 344 \zeta_2 x^2 \\
& - 260 \zeta_2 x^3 + 96 \zeta_3 x) + \mathbf{H}_{0,1} (-7937/75 - 752/25 x^{-1} - 67831/225 x - 12836/75 x^2 \\
& - 96/5 \zeta_2 x^{-2} - 48 \zeta_2 x^{-1} - 96 \zeta_2 + 246 \zeta_2 x - 96 \zeta_2 x^2 - 144/5 \zeta_2 x^3 + 160 \zeta_3 x) \\
& + \mathbf{H}_{1,0} (-536/15 + 112/5 x^{-1} - 799/6 x + 320/3 x^2 - 24 \zeta_2 x^{-2} - 60 \zeta_2 x^{-1} - 120 \zeta_2 \\
& + 546 \zeta_2 x - 176 \zeta_2 x^2 - 176 \zeta_2 x^3 + 56 \zeta_3 x) + \mathbf{H}_{1,1} (-122/5 + 128/5 x^{-1} \\
& - 13169/90 x - 328/5 x^2 - 96/5 \zeta_2 x^{-2} - 48 \zeta_2 x^{-1} - 96 \zeta_2 + 344 \zeta_2 x - 96 \zeta_2 x^2 \\
& - 144/5 \zeta_2 x^3 + 80 \zeta_3 x) + \mathbf{H}_{-1} (-1848/25 \zeta_2 x^{-2} - 96 \zeta_2 x^{-1} - 616 \zeta_2 \\
& - 1520/3 \zeta_2 x + 208 \zeta_2 x^2 + 2952/25 \zeta_2 x^3 - 144/5 \zeta_3 x^{-2} + 8 \zeta_3 x^{-1} - 144 \zeta_3 \\
& - 336 \zeta_3 x - 16 \zeta_3 x^2 + 216/5 \zeta_3 x^3 - 100 \zeta_4 x) + \mathbf{H}_0 (-16081/250 + 628/375 x^{-1} \\
& - 39052717/40500 x + 41888/375 x^2 + 80 \zeta_2 x^{-1} + 143 \zeta_2 + 787/3 \zeta_2 x - 424 \zeta_2 x^2 \\
& - 24008/75 \zeta_2 x^3 + 115/3 \zeta_3 x + 16 \zeta_3 x^2 + 872/5 \zeta_3 x^3 + 12 \zeta_4 x) \\
& + \mathbf{H}_1 (13997/150 + 1712/25 x^{-1} - 7089221/16200 x - 7916/75 x^2 - 616/25 \zeta_2 x^{-2} \\
& - 304/5 \zeta_2 x^{-1} - 1706/15 \zeta_2 + 7181/15 \zeta_2 x - 1516/5 \zeta_2 x^2 - 15152/75 \zeta_2 x^3 \\
& - 88/5 \zeta_3 x^{-2} - 44 \zeta_3 x^{-1} - 88 \zeta_3 + 362/3 \zeta_3 x + 1088/5 \zeta_3 x^3 - 190 \zeta_4 x) \\
& - 3918163/81000 + 49532/375 x^{-1} - 54681799/162000 x + 27156/125 x^2 \\
& + 2384/25 \zeta_2 x^{-1} + 7937/75 \zeta_2 + 307027/225 \zeta_2 x + 12836/75 \zeta_2 x^2 \\
& - 17916/125 \zeta_2 x^3 + 232/5 \zeta_3 x^{-1} + 1591/15 \zeta_3 + 1052/15 \zeta_3 x - 4/5 \zeta_3 x^2 \\
& + 1456/5 \zeta_3 x^3 - 136 \zeta_3 \zeta_2 x + 301 \zeta_4 x + 302 \zeta_4 x^2 + 677/5 \zeta_4 x^3 + 296 \zeta_5 x . \quad (3.5.7)
\end{aligned}$$

The  $n_f^3$  coefficient in the last line of eq. (3.5.5) reads

$$\begin{aligned}
c_{L,\text{ns}}^{(4)\text{F}}(x) = & - 48 x \mathbf{H}_{0,0,0} - 36 x \mathbf{H}_{0,0,1} - 24 x \mathbf{H}_{0,1,0} - 24 x \mathbf{H}_{0,1,1} - 12 x \mathbf{H}_{1,0,0} - 12 x \mathbf{H}_{1,0,1} \\
& - 12 x \mathbf{H}_{1,1,0} - 12 x \mathbf{H}_{1,1,1} + \mathbf{H}_{0,0} (12 - 150 x) + \mathbf{H}_{0,1} (12 - 100 x) + \mathbf{H}_{1,0} (12 - 50 x) \\
& + \mathbf{H}_{1,1} (12 - 50 x) + \mathbf{H}_0 (38 - 634/3 x + 36 \zeta_2 x) + \mathbf{H}_1 (38 - 317/3 x + 12 \zeta_2 x) \\
& + 203/3 - 8609/54 x - 12 \zeta_2 + 100 \zeta_2 x + 12 \zeta_3 x . \quad (3.5.8)
\end{aligned}$$

The corresponding results for  $F_{2,\text{ns}}$  are written in a very similar manner as

$$\begin{aligned}
c_{2,\text{ns}}^{(4)}(x) = & n_f^0 \text{ and } n_f^1 \text{ contributions} \\
& + C_F C_A n_f^2 \frac{4}{9} c_{2,\text{ns}}^{(4)\text{L}}(x) + C_F (C_F - \frac{1}{2} C_A) n_f^2 \frac{4}{9} c_{2,\text{ns}}^{(4)\text{N}}(x) + C_F n_f^3 \frac{4}{27} c_{2,\text{ns}}^{(4)\text{F}}(x) . \quad (3.5.9)
\end{aligned}$$

### 3.5. The x-space coefficient functions

---

with

$$\begin{aligned}
c_{2,\text{ns}}^{(4)\text{L}}(x) = & + \mathbf{H}_{0,0,0,0} (1951/4 - 1951/3 x_m^{-1} + 1951/4 x) + \mathbf{H}_{0,0,0,1} (607 - 2890/3 x_m^{-1} + 411 x \\
& + 480 x^2 - 720 x^3) + \mathbf{H}_{0,0,1,0} (1547/3 - 2572/3 x_m^{-1} + 1391/3 x + 192 x^2 - 288 x^3) \\
& + \mathbf{H}_{0,0,1,1} (1637/3 - 2752/3 x_m^{-1} + 1343/3 x + 240 x^2 - 360 x^3) + \mathbf{H}_{0,1,0,0} (387 \\
& - 670 x_m^{-1} + 475 x - 192 x^2 + 288 x^3) + \mathbf{H}_{0,1,0,1} (428 - 752 x_m^{-1} + 400 x + 48 x^2 \\
& - 72 x^3) + \mathbf{H}_{0,1,1,0} (390 - 676 x_m^{-1} + 436 x - 48 x^2 + 72 x^3) + \mathbf{H}_{0,1,1,1} (404 - 704 x_m^{-1} \\
& + 404 x) + \mathbf{H}_{1,0,0,0} (770/3 - 1408/3 x_m^{-1} + 1250/3 x - 480 x^2 + 720 x^3) \\
& + \mathbf{H}_{1,0,0,1} (296 - 48 x^{-2} - 548 x_m^{-1} + 256 x + 48 x^2 - 72 x^3) + \mathbf{H}_{1,0,1,0} (272 - 500 x_m^{-1} \\
& + 288 x - 48 x^2 + 72 x^3) + \mathbf{H}_{1,0,1,1} (300 - 556 x_m^{-1} + 162 x + 432 x^2 - 360 x^3) \\
& + \mathbf{H}_{1,1,0,0} (260 + 48 x^{-2} - 476 x_m^{-1} + 364 x - 240 x^2 + 360 x^3) + \mathbf{H}_{1,1,0,1} (266 \\
& - 488 x_m^{-1} + 386 x - 432 x^2 + 360 x^3) + \mathbf{H}_{1,1,1,0} (240 - 436 x_m^{-1} + 258 x) \\
& + \mathbf{H}_{1,1,1,1} (252 - 460 x_m^{-1} + 252 x) + \mathbf{H}_{1,0,0,0} (671/3 - 1342/3 x_m^{-1} + 671/3 x) \\
& + \mathbf{H}_{1,0,0,1} (824/3 - 80 x^{-2} - 1648/3 x_m^{-1} + 344/3 x + 480 x^2 - 720 x^3) + \mathbf{H}_{1,0,1,0} (234 \\
& - 32 x^{-2} - 468 x_m^{-1} + 170 x + 192 x^2 - 288 x^3) + \mathbf{H}_{1,0,1,1} (270 - 40 x^{-2} - 540 x_m^{-1} \\
& + 190 x + 240 x^2 - 360 x^3) + \mathbf{H}_{1,0,1,0} (178 + 32 x^{-2} - 356 x_m^{-1} + 242 x - 192 x^2 \\
& + 288 x^3) + \mathbf{H}_{1,0,1,1} (216 - 8 x^{-2} - 432 x_m^{-1} + 200 x + 48 x^2 - 72 x^3) + \mathbf{H}_{1,0,1,0} (206 \\
& + 8 x^{-2} - 412 x_m^{-1} + 222 x - 48 x^2 + 72 x^3) + \mathbf{H}_{1,0,1,1} (228 - 456 x_m^{-1} + 228 x) \\
& + \mathbf{H}_{1,1,0,0} (530/3 + 80 x^{-2} - 1060/3 x_m^{-1} + 1010/3 x - 480 x^2 + 720 x^3) \\
& + \mathbf{H}_{1,1,0,1} (196 - 8 x^{-2} - 392 x_m^{-1} + 180 x + 48 x^2 - 72 x^3) + \mathbf{H}_{1,1,0,1} (162 + 8 x^{-2} \\
& - 324 x_m^{-1} + 178 x - 48 x^2 + 72 x^3) + \mathbf{H}_{1,1,0,1} (188 - 376 x_m^{-1} + 68 x + 432 x^2 - 360 x^3) \\
& + \mathbf{H}_{1,1,1,0} (142 + 40 x^{-2} - 284 x_m^{-1} + 222 x - 240 x^2 + 360 x^3) + \mathbf{H}_{1,1,1,0} (164 \\
& - 328 x_m^{-1} + 284 x - 432 x^2 + 360 x^3) + \mathbf{H}_{1,1,1,0} (140 - 280 x_m^{-1} + 140 x) \\
& + \mathbf{H}_{1,1,1,1} (160 - 320 x_m^{-1} + 160 x) + \mathbf{H}_{0,0,0} (2997/2 - 20567/9 x_m^{-1} + 11249/6 x) \\
& + \mathbf{H}_{0,0,1} (3441/2 + 80 x^{-1} - 24686/9 x_m^{-1} + 3717/2 x + 1104 x^2 - 612 x^3) \\
& + \mathbf{H}_{0,0,1,0} (23231/18 + 32 x^{-1} - 19634/9 x_m^{-1} + 30677/18 x + 288 x^2) \\
& + \mathbf{H}_{0,0,1,1} (23231/18 + 40 x^{-1} - 19967/9 x_m^{-1} + 15163/9 x + 456 x^2 - 48 x^3) \\
& + \mathbf{H}_{0,1,0,0} (7015/9 - 32 x^{-1} - 13373/9 x_m^{-1} + 11956/9 x - 672 x^2 + 612 x^3) \\
& + \mathbf{H}_{0,1,0,1} (2593/3 + 8 x^{-1} - 4835/3 x_m^{-1} + 3628/3 x + 72 x^2) + \mathbf{H}_{0,1,1,0} (2302/3 \\
& - 8 x^{-1} - 4283/3 x_m^{-1} + 7361/6 x - 168 x^2 + 48 x^3) + \mathbf{H}_{0,1,1,1} (2261/3 - 4270/3 x_m^{-1} \\
& + 3473/3 x) + \mathbf{H}_{1,0,0} (3706/9 - 80 x^{-1} - 9995/9 x_m^{-1} + 8704/9 x - 720 x^2)
\end{aligned}$$

$$\begin{aligned}
& + \mathbf{H}_{1,0,0,1} (5740/9 - 8x^{-2} - 16x^{-1} - 12263/9x_m^{-1} + 7963/9x + 456x^2 - 612x^3) \\
& + \mathbf{H}_{1,0,1,0} (1546/3 - 8x^{-1} - 3212/3x_m^{-1} + 2506/3x - 72x^2) + \mathbf{H}_{1,0,1,1} (597 \\
& - 1210x_m^{-1} + 1333/2x + 456x^2 - 48x^3) + \mathbf{H}_{1,1,0,0} (3946/9 + 8x^{-2} - 16x^{-1} \\
& - 8495/9x_m^{-1} + 8275/9x - 744x^2 + 612x^3) + \mathbf{H}_{1,1,0,1} (1412/3 - 3022/3x_m^{-1} \\
& + 3128/3x - 360x^2) + \mathbf{H}_{1,1,1,0} (1321/3 - 2558/3x_m^{-1} + 4073/6x - 96x^2 + 48x^3) \\
& + \mathbf{H}_{1,1,1,1} (442 - 904x_m^{-1} + 714x) + \mathbf{H}_{0,0,0} (22496/9 - 152383/36x_m^{-1} + 39667/9x \\
& + 720x^2 + 2890/3\zeta_2x_m^{-1} - 607\zeta_2 - 411\zeta_2x - 480\zeta_2x^2 + 720\zeta_2x^3) \\
& + \mathbf{H}_{0,0,1} (73799/36 - 24x^{-1} - 35378/9x_m^{-1} + 136907/36x + 1740x^2 - 394x^3 \\
& + 752\zeta_2x_m^{-1} - 428\zeta_2 - 400\zeta_2x - 48\zeta_2x^2 + 72\zeta_2x^3) + \mathbf{H}_{0,1,0} (3868/3 - 32x^{-1} \\
& - 24305/9x_m^{-1} + 53105/18x - 120x^2 + 394x^3 + 48\zeta_2x^{-2} + 548\zeta_2x_m^{-1} - 296\zeta_2 \\
& - 256\zeta_2x - 48\zeta_2x^2 + 72\zeta_2x^3) + \mathbf{H}_{0,1,1} (10021/9 - 40x^{-1} - 23191/9x_m^{-1} \\
& + 26957/9x + 48x^2 + 488\zeta_2x_m^{-1} - 266\zeta_2 - 386\zeta_2x + 432\zeta_2x^2 - 360\zeta_2x^3) \\
& + \mathbf{H}_{1,0,0} (11321/18 - 24x^{-1} - 15200/9x_m^{-1} + 12601/6x - 540x^2 + 80\zeta_2x^{-2} \\
& + 1648/3\zeta_2x_m^{-1} - 824/3\zeta_2 - 344/3\zeta_2x - 480\zeta_2x^2 + 720\zeta_2x^3) + \mathbf{H}_{1,0,1} (3763/6 \\
& - 8x^{-1} - 10459/6x_m^{-1} + 10787/6x + 912x^2 - 394x^3 + 8\zeta_2x^{-2} + 432\zeta_2x_m^{-1} \\
& - 216\zeta_2 - 200\zeta_2x - 48\zeta_2x^2 + 72\zeta_2x^3) + \mathbf{H}_{1,1,0} (11303/18 + 8x^{-1} \\
& - 27307/18x_m^{-1} + 35993/18x - 600x^2 + 394x^3 + 8\zeta_2x^{-2} + 392\zeta_2x_m^{-1} - 196\zeta_2 \\
& - 180\zeta_2x - 48\zeta_2x^2 + 72\zeta_2x^3) + \mathbf{H}_{1,1,1} (9337/18 - 25979/18x_m^{-1} + 32905/18x \\
& + 328\zeta_2x_m^{-1} - 164\zeta_2 - 284\zeta_2x + 432\zeta_2x^2 - 360\zeta_2x^3) + \mathbf{H}_{0,0} (498587/216 \\
& - 842039/162x_m^{-1} + 1618205/216x + 1260x^2 - 80\zeta_2x^{-1} + 24686/9\zeta_2x_m^{-1} \\
& - 3441/2\zeta_2 - 3717/2\zeta_2x - 1104\zeta_2x^2 + 612\zeta_2x^3 + 1160/3\zeta_3x_m^{-1} - 769/3\zeta_3 \\
& - 1339/3\zeta_3x + 336\zeta_3x^2 - 504\zeta_3x^3) + \mathbf{H}_{0,1} (86396/81 - 24x^{-1} \\
& - 1178369/324x_m^{-1} + 439538/81x + 1222x^2 - 8\zeta_2x^{-1} + 4835/3\zeta_2x_m^{-1} \\
& - 2593/3\zeta_2 - 3628/3\zeta_2x - 72\zeta_2x^2 - 48\zeta_3x^{-2} + 976/3\zeta_3x_m^{-1} - 520/3\zeta_3 \\
& + 818/3\zeta_3x - 1824\zeta_3x^2 + 1296\zeta_3x^3) + \mathbf{H}_{1,0} (168623/648 + 32x^{-1} \\
& - 147071/81x_m^{-1} + 2253563/648x + 86x^2 + 8\zeta_2x^{-2} + 16\zeta_2x^{-1} + 12263/9\zeta_2x_m^{-1} \\
& - 5740/9\zeta_2 - 7963/9\zeta_2x - 456\zeta_2x^2 + 612\zeta_2x^3 - 56\zeta_3x^{-2} + 944/3\zeta_3x_m^{-1} \\
& - 472/3\zeta_3 - 808/3\zeta_3x + 336\zeta_3x^2 - 504\zeta_3x^3) + \mathbf{H}_{1,1} (15961/216 + 40x^{-1} \\
& - 46483/27x_m^{-1} + 784189/216x + 48x^2 + 3022/3\zeta_2x_m^{-1} - 1412/3\zeta_2 - 3128/3\zeta_2x \\
& + 360\zeta_2x^2 - 56\zeta_3x^{-2} + 176\zeta_3x_m^{-1} - 88\zeta_3 + 400\zeta_3x - 1824\zeta_3x^2 + 1296\zeta_3x^3) \\
& + \mathbf{H}_0 (1578379/2592 - 5764837/1296x_m^{-1} + 25289039/2592x + 1174x^2)
\end{aligned}$$

### 3.5. The x-space coefficient functions

$$\begin{aligned}
& + 24 \zeta_2 x^{-1} + 35378/9 \zeta_2 x_m^{-1} - 73799/36 \zeta_2 - 136907/36 \zeta_2 x - 1740 \zeta_2 x^2 \\
& + 394 \zeta_2 x^3 + 56 \zeta_3 x^{-1} + 3085/3 \zeta_3 x_m^{-1} - 5771/9 \zeta_3 - 24019/18 \zeta_3 x + 984 \zeta_3 x^2 \\
& - 660 \zeta_3 x^3 - 2506/3 \zeta_4 x_m^{-1} + 5755/12 \zeta_4 + 3463/12 \zeta_4 x + 636 \zeta_4 x^2 - 954 \zeta_4 x^3 \\
& + \textcolor{red}{H}_1 (-601625/648 + 72 x^{-1} - 2134163/1296 x_m^{-1} + 831119/162 x + 1174 x^2 \\
& + 8 \zeta_2 x^{-1} + 10459/6 \zeta_2 x_m^{-1} - 3763/6 \zeta_2 - 10787/6 \zeta_2 x - 912 \zeta_2 x^2 + 394 \zeta_2 x^3 \\
& - 8 \zeta_3 x^{-2} + 32 \zeta_3 x^{-1} + 5879/9 \zeta_3 x_m^{-1} - 3823/9 \zeta_3 + 9187/18 \zeta_3 x - 816 \zeta_3 x^2 \\
& - 660 \zeta_3 x^3 - 106 \zeta_4 x^{-2} - 1400/3 \zeta_4 x_m^{-1} + 700/3 \zeta_4 + 64/3 \zeta_4 x + 636 \zeta_4 x^2 \\
& - 954 \zeta_4 x^3) - 12941689/5184 - 132728/81 x_m^{-1} + 4964587/576 x + 24 \zeta_2 x^{-1} \\
& + 1178369/324 \zeta_2 x_m^{-1} - 86396/81 \zeta_2 - 439538/81 \zeta_2 x - 1222 \zeta_2 x^2 \\
& + 13247/9 \zeta_3 x_m^{-1} - 11459/12 \zeta_3 - 120413/36 \zeta_3 x + 3900 \zeta_3 x^2 - 1182 \zeta_3 x^3 \\
& - 980/3 \zeta_3 \zeta_2 x_m^{-1} + 209 \zeta_3 \zeta_2 + 405 \zeta_3 \zeta_2 x - 480 \zeta_3 \zeta_2 x^2 + 432 \zeta_3 \zeta_2 x^3 \\
& + 106 \zeta_4 x^{-1} - 72041/36 \zeta_4 x_m^{-1} + 87439/72 \zeta_4 + 98209/72 \zeta_4 x + 1578 \zeta_4 x^2 \\
& - 1152 \zeta_4 x^3 + 1036/3 \zeta_5 x_m^{-1} - 206 \zeta_5 + 834 \zeta_5 x - 3840 \zeta_5 x^2 + 2880 \zeta_5 x^3 \\
& + \delta(1-x) (-18199451/6912 - 5764837/1296 \zeta_2 - 29/648 \zeta_3 + 68705/72 \zeta_4 \\
& + 4300/9 \zeta_3 \zeta_2 + 3091/6 \zeta_5 + 35/3 \zeta_3^2 + 521/2 \zeta_6) , \tag{3.5.10}
\end{aligned}$$

$$\begin{aligned}
c_{2,\text{ns}}^{(4)\text{N}}(x) = & + \textcolor{red}{H}_{-1,-1,-1,-1,0} (192 - 1024 x_p^{-1} - 2112 x) + \textcolor{red}{H}_{-1,-1,-1,0,0} (-352 + 1792 x_p^{-1} + 3616 x) \\
& + \textcolor{red}{H}_{-1,-1,0,-1,0} (-224 + 1152 x_p^{-1} + 2336 x) + \textcolor{red}{H}_{-1,-1,0,0,0} (464 - 2080 x_p^{-1} - 3920 x) \\
& + \textcolor{red}{H}_{-1,0,-1,-1,0} (-224 + 1152 x_p^{-1} + 2336 x) + \textcolor{red}{H}_{-1,0,-1,0,0} (432 - 1984 x_p^{-1} - 3792 x) \\
& + \textcolor{red}{H}_{-1,0,0,-1,0} (304 - 1344 x_p^{-1} - 2512 x) + \textcolor{red}{H}_{-1,0,0,0,0} (-612 + 1800 x_p^{-1} + 2340 x) \\
& + \textcolor{red}{H}_{-1,0,0,0,1} (-8 + 16 x_p^{-1} + 8 x) + \textcolor{red}{H}_{-1,0,0,1,1} (16 - 32 x_p^{-1} - 16 x) + \textcolor{red}{H}_{-1,0,1,1,1} (-32 \\
& + 64 x_p^{-1} + 32 x) + \textcolor{red}{H}_{0,-1,-1,-1,0} (-224 + 1152 x_p^{-1} + 2336 x) + \textcolor{red}{H}_{0,-1,-1,0,0} (432 \\
& - 1984 x_p^{-1} - 3792 x) + \textcolor{red}{H}_{0,-1,0,-1,0} (272 - 1280 x_p^{-1} - 2480 x) + \textcolor{red}{H}_{0,-1,0,0,0} (-1060 \\
& + 1408 x_m^{-1} + 2152 x_p^{-1} + 1092 x) + \textcolor{red}{H}_{0,-1,0,0,1} (-216 + 864 x_m^{-1} + 16 x_p^{-1} - 1544 x) \\
& + \textcolor{red}{H}_{0,-1,0,1,0} (-128 + 544 x_m^{-1} - 992 x) + \textcolor{red}{H}_{0,-1,0,1,1} (-80 + 448 x_m^{-1} - 32 x_p^{-1} - 880 x) \\
& + \textcolor{red}{H}_{0,0,-1,-1,0} (296 + 16 x_m^{-1} - 1376 x_p^{-1} - 2616 x) + \textcolor{red}{H}_{0,0,-1,0,0} (-1280 + 2040 x_m^{-1} \\
& + 2344 x_p^{-1} + 392 x) + \textcolor{red}{H}_{0,0,-1,0,1} (-248 + 1056 x_m^{-1} + 16 x_p^{-1} - 1960 x) \\
& + \textcolor{red}{H}_{0,0,0,-1,0} (-1012 + 1632 x_m^{-1} + 1736 x_p^{-1} + 52 x) + \textcolor{red}{H}_{0,0,0,0,0} (1951/2 - 2102/3 x_m^{-1} \\
& - 600 x_p^{-1} + 751/2 x) + \textcolor{red}{H}_{0,0,0,0,1} (884 - 3728/3 x_m^{-1} - 24 x_p^{-1} + 860 x) \\
& + \textcolor{red}{H}_{0,0,0,1,0} (2458/3 - 3872/3 x_m^{-1} + 2458/3 x) + \textcolor{red}{H}_{0,0,0,1,1} (2506/3 - 4064/3 x_m^{-1}
\end{aligned}$$



$$\begin{aligned}
& + 32 x_p^{-1} + 2602/3 x) + \mathbf{H}_{0,0,1,0,0} (698 - 1092 x_m^{-1} + 410 x) + \mathbf{H}_{0,0,1,0,1} (656 \\
& - 1104 x_m^{-1} + 656 x) + \mathbf{H}_{0,0,1,1,0} (792 - 1376 x_m^{-1} + 792 x) + \mathbf{H}_{0,0,1,1,1} (724 - 1208 x_m^{-1} \\
& - 32 x_p^{-1} + 692 x) + \mathbf{H}_{0,1,0,-1,0} (-120 + 560 x_m^{-1} - 1080 x) + \mathbf{H}_{0,1,0,0,0} (1660/3 \\
& - 2192/3 x_m^{-1} - 932/3 x) + \mathbf{H}_{0,1,0,0,1} (356 - 256 x_m^{-1} - 748 x) + \mathbf{H}_{0,1,0,1,0} (616 \\
& - 1256 x_m^{-1} + 952 x) + \mathbf{H}_{0,1,0,1,1} (476 - 864 x_m^{-1} + 476 x) + \mathbf{H}_{0,1,1,0,0} (680 - 1304 x_m^{-1} \\
& + 776 x) + \mathbf{H}_{0,1,1,0,1} (504 - 840 x_m^{-1} + 264 x) + \mathbf{H}_{0,1,1,1,0} (632 - 1256 x_m^{-1} + 872 x) \\
& + \mathbf{H}_{0,1,1,1,1} (504 - 920 x_m^{-1} + 504 x) + \mathbf{H}_{1,0,-1,-1,0} (-16 + 32 x_m^{-1} - 16 x) \\
& + \mathbf{H}_{1,0,-1,0,0} (-216 + 1008 x_m^{-1} - 1944 x) + \mathbf{H}_{1,0,-1,0,1} (-96 + 576 x_m^{-1} - 1248 x) \\
& + \mathbf{H}_{1,0,0,-1,0} (-184 + 880 x_m^{-1} - 1720 x) + \mathbf{H}_{1,0,0,0,0} (1756/3 - 1784/3 x_m^{-1} - 3428/3 x) \\
& + \mathbf{H}_{1,0,0,0,1} (1024/3 + 16/3 x_m^{-1} - 5168/3 x) + \mathbf{H}_{1,0,0,1,0} (432 - 640 x_m^{-1} - 240 x) \\
& + \mathbf{H}_{1,0,0,1,1} (344 - 352 x_m^{-1} - 664 x) + \mathbf{H}_{1,0,1,0,0} (532 - 1208 x_m^{-1} + 964 x) \\
& + \mathbf{H}_{1,0,1,0,1} (392 - 752 x_m^{-1} + 296 x) + \mathbf{H}_{1,0,1,1,0} (452 - 1016 x_m^{-1} + 788 x) \\
& + \mathbf{H}_{1,0,1,1,1} (368 - 736 x_m^{-1} + 368 x) + \mathbf{H}_{1,1,0,-1,0} (-96 + 448 x_m^{-1} - 864 x) \\
& + \mathbf{H}_{1,1,0,0,0} (1540/3 - 3080/3 x_m^{-1} + 1540/3 x) + \mathbf{H}_{1,1,0,0,1} (300 - 232 x_m^{-1} - 804 x) \\
& + \mathbf{H}_{1,1,0,1,0} (440 - 1008 x_m^{-1} + 824 x) + \mathbf{H}_{1,1,0,1,1} (328 - 576 x_m^{-1} + 88 x) \\
& + \mathbf{H}_{1,1,1,0,0} (460 - 1096 x_m^{-1} + 988 x) + \mathbf{H}_{1,1,1,0,1} (328 - 592 x_m^{-1} + 136 x) \\
& + \mathbf{H}_{1,1,1,1,0} (416 - 976 x_m^{-1} + 848 x) + \mathbf{H}_{1,1,1,1,1} (320 - 640 x_m^{-1} + 320 x) \\
& + \mathbf{H}_{-1,-1,-1,0} (3200/3 + 32 x^{-2} + 3200/3 x_p^{-1} + 12544/3 x + 960 x^2 - 288 x^3) \\
& + \mathbf{H}_{-1,-1,0,0} (-5056/3 - 272/5 x^{-2} - 5440/3 x_p^{-1} - 19712/3 x - 1632 x^2 + 2448/5 x^3) \\
& + \mathbf{H}_{-1,0,-1,0} (-3328/3 - 176/5 x^{-2} - 3520/3 x_p^{-1} - 12992/3 x - 1056 x^2 + 1584/5 x^3) \\
& + \mathbf{H}_{-1,0,0,0} (2584 + 576/5 x^{-2} + 1792 x_p^{-1} + 4728 x - 5184/5 x^3) + \mathbf{H}_{-1,0,0,1} (2608/3 \\
& + 224/5 x^{-2} + 160/3 x_p^{-1} + 80/3 x - 1344 x^2 - 2016/5 x^3) + \mathbf{H}_{-1,0,1,0} (560 + 144/5 x^{-2} \\
& - 16 x - 864 x^2 - 1296/5 x^3) + \mathbf{H}_{-1,0,1,1} (1504/3 + 128/5 x^{-2} - 320/3 x_p^{-1} - 352/3 x \\
& - 768 x^2 - 1152/5 x^3) + \mathbf{H}_{0,-1,-1,0} (-3544/3 - 192/5 x^{-2} - 3520/3 x_p^{-1} - 12968/3 x \\
& - 960 x^2 + 288 x^3) + \mathbf{H}_{0,-1,0,0} (2724 + 576/5 x^{-2} + 1568 x_m^{-1} + 1840 x_p^{-1} + 1452 x \\
& + 1632 x^2 - 2448/5 x^3) + \mathbf{H}_{0,-1,0,1} (2800/3 + 192/5 x^{-2} + 640 x_m^{-1} + 160/3 x_p^{-1} \\
& - 6544/3 x) + \mathbf{H}_{0,0,-1,0} (5164/3 + 384/5 x^{-2} + 4768/3 x_m^{-1} + 1504 x_p^{-1} + 532/3 x \\
& + 1440 x^2 - 1008/5 x^3) + \mathbf{H}_{0,0,0,0} (1688 - 13852/9 x_m^{-1} - 1240/3 x_p^{-1} + 2584/3 x \\
& + 5184/5 x^3) + \mathbf{H}_{0,0,0,1} (2751 - 28516/9 x_m^{-1} - 160/3 x_p^{-1} + 8981/3 x + 2064 x^2 \\
& + 6792/5 x^3) + \mathbf{H}_{0,0,1,0} (16565/9 - 22732/9 x_m^{-1} + 22841/9 x + 672 x^2 + 1008/5 x^3)
\end{aligned}$$

### 3.5. The x-space coefficient functions

---

$$\begin{aligned}
& + \mathbf{H}_{0,0,1,1} (18773/9 - 25252/9 x_m^{-1} + 160/3 x_p^{-1} + 25169/9 x + 960 x^2 + 4272/5 x^3) \\
& + \mathbf{H}_{0,1,0,0} (7988/9 - 12250/9 x_m^{-1} + 7736/9 x - 432 x^2 - 4344/5 x^3) + \mathbf{H}_{0,1,0,1} (3130/3 \\
& - 5000/3 x_m^{-1} + 5194/3 x + 96 x^2 + 144/5 x^3) + \mathbf{H}_{0,1,1,0} (1106 - 2054 x_m^{-1} + 2146 x \\
& - 288 x^2 - 3264/5 x^3) + \mathbf{H}_{0,1,1,1} (3190/3 - 5372/3 x_m^{-1} + 5614/3 x) \\
& + \mathbf{H}_{1,0,-1,0} (1136/3 + 64/5 x^{-2} + 2048/3 x_m^{-1} - 6448/3 x + 384 x^2 + 576/5 x^3) \\
& + \mathbf{H}_{1,0,0,0} (10580/9 - 12790/9 x_m^{-1} - 9376/9 x) + \mathbf{H}_{1,0,0,1} (13904/9 + 64/5 x^{-2} \\
& - 11770/9 x_m^{-1} - 8956/9 x + 720 x^2 + 4776/5 x^3) + \mathbf{H}_{1,0,1,0} (1988/3 - 32/5 x^{-2} \\
& - 5668/3 x_m^{-1} + 6164/3 x - 192 x^2 - 288/5 x^3) + \mathbf{H}_{1,0,1,1} (916 - 1652 x_m^{-1} + 1364 x \\
& + 192 x^2 + 624 x^3) + \mathbf{H}_{1,1,0,0} (5348/9 - 16/5 x^{-2} - 15358/9 x_m^{-1} + 14096/9 x \\
& - 432 x^2 - 4344/5 x^3) + \mathbf{H}_{1,1,0,1} (2468/3 + 16/5 x^{-2} - 4060/3 x_m^{-1} + 2372/3 x \\
& + 96 x^2 + 144/5 x^3) + \mathbf{H}_{1,1,1,0} (1456/3 - 16/5 x^{-2} - 4652/3 x_m^{-1} + 5488/3 x - 288 x^2 \\
& - 3264/5 x^3) + \mathbf{H}_{1,1,1,1} (620 - 1280 x_m^{-1} + 1164 x) + \mathbf{H}_{-1,-1,-1} (-512 \zeta_2 x_p^{-1} + 96 \zeta_2 \\
& - 1056 \zeta_2 x) + \mathbf{H}_{-1,-1,0} (-7648/3 - 992/25 x^{-2} - 128 x^{-1} - 1984/3 x_p^{-1} - 5536 x \\
& - 1920 x^2 + 11808/25 x^3 + 352 \zeta_2 x_p^{-1} - 64 \zeta_2 + 736 \zeta_2 x) + \mathbf{H}_{-1,0,-1} (576 \zeta_2 x_p^{-1} \\
& - 112 \zeta_2 + 1168 \zeta_2 x) + \mathbf{H}_{-1,0,0} (289016/45 + 2896/25 x^{-2} + 272/5 x^{-1} + 9352/9 x_p^{-1} \\
& + 321856/45 x - 2448/5 x^2 - 34704/25 x^3 - 248 \zeta_2 x_p^{-1} + 68 \zeta_2 - 404 \zeta_2 x) \\
& + \mathbf{H}_{-1,0,1} (16528/9 + 992/25 x^{-2} - 96 x^{-1} + 304/9 x_p^{-1} + 2432/9 x - 2208 x^2 \\
& - 11808/25 x^3 - 16 \zeta_2 x_p^{-1} + 8 \zeta_2 - 8 \zeta_2 x) + \mathbf{H}_{0,-1,-1} (576 \zeta_2 x_p^{-1} - 112 \zeta_2 \\
& + 1168 \zeta_2 x) + \mathbf{H}_{0,-1,0} (42214/9 + 1904/25 x^{-2} + 112/5 x^{-1} + 800 x_m^{-1} \\
& + 6088/9 x_p^{-1} + 63946/45 x + 1776 x^2 - 11808/25 x^3 - 864 \zeta_2 x_m^{-1} - 376 \zeta_2 x_p^{-1} \\
& + 292 \zeta_2 + 844 \zeta_2 x) + \mathbf{H}_{0,0,-1} (-1048 \zeta_2 x_m^{-1} - 704 \zeta_2 x_p^{-1} + 396 \zeta_2 + 652 \zeta_2 x) \\
& + \mathbf{H}_{0,0,0} (65087/45 - 576/5 x^{-1} - 18371/18 x_m^{-1} - 5080/9 x_p^{-1} - 176803/45 x \\
& + 5184/5 x^2 + 34704/25 x^3 + 3572/3 \zeta_2 x_m^{-1} + 76 \zeta_2 x_p^{-1} - 884 \zeta_2 - 808 \zeta_2 x) \\
& + \mathbf{H}_{0,0,1} (41267/18 - 288/5 x^{-1} - 23429/9 x_m^{-1} - 152/9 x_p^{-1} + 139937/90 x + 2544 x^2 \\
& + 36208/25 x^3 + 416 \zeta_2 x_m^{-1} + 8 \zeta_2 x_p^{-1} - 508 \zeta_2 + 652 \zeta_2 x) + \mathbf{H}_{0,1,0} (12734/15 \\
& - 112/5 x^{-1} - 12331/9 x_m^{-1} + 79654/45 x - 2856/5 x^2 - 976 x^3 - 104 \zeta_2 x_m^{-1} \\
& - 280 \zeta_2 + 1448 \zeta_2 x) + \mathbf{H}_{0,1,1} (47296/45 - 128/5 x^{-1} - 13964/9 x_m^{-1} + 84266/45 x \\
& - 1968/5 x^2 + 264 \zeta_2 x_m^{-1} - 392 \zeta_2 + 904 \zeta_2 x) + \mathbf{H}_{1,0,-1} (-560 \zeta_2 x_m^{-1} + 88 \zeta_2 \\
& + 1240 \zeta_2 x) + \mathbf{H}_{1,0,0} (69457/45 + 16/5 x^{-1} - 17476/9 x_m^{-1} + 3181/15 x + 4344/5 x^2 \\
& - 712/3 \zeta_2 x_m^{-1} - 844/3 \zeta_2 + 6356/3 \zeta_2 x) + \mathbf{H}_{1,0,1} (6267/5 - 16/5 x^{-1} - 1839 x_m^{-1}
\end{aligned}$$

$$\begin{aligned}
& + 17429/15 x + 4296/5 x^2 + 976 x^3 + 176 \zeta_2 x_m^{-1} - 280 \zeta_2 + 872 \zeta_2 x) \\
& + \mathbf{H}_{1,1,0} (32257/45 + 16/5 x^{-1} - 15511/9 x_m^{-1} + 83923/45 x - 1176/5 x^2 - 976 x^3 \\
& - 120 \zeta_2 x_m^{-1} - 236 \zeta_2 + 1540 \zeta_2 x) + \mathbf{H}_{1,1,1} (6205/9 - 12119/9 x_m^{-1} + 11089/9 x \\
& + 80 \zeta_2 x_m^{-1} - 232 \zeta_2 + 920 \zeta_2 x) + \mathbf{H}_{-1,-1} (16 \zeta_2 x^{-2} + 1600/3 \zeta_2 x_p^{-1} \\
& + 1600/3 \zeta_2 + 6272/3 \zeta_2 x + 480 \zeta_2 x^2 - 144 \zeta_2 x^3 + 512 \zeta_3 x_p^{-1} - 96 \zeta_3 \\
& + 1056 \zeta_3 x) + \mathbf{H}_{-1,0} (4252378/675 + 21512/375 x^{-2} + 1392/25 x^{-1} + 9712/27 x_p^{-1} \\
& + 4279178/675 x - 15408/25 x^2 - 107496/125 x^3 - 56 \zeta_2 x^{-2} - 896/3 \zeta_2 x_p^{-1} \\
& - 3704/3 \zeta_2 - 3352/3 \zeta_2 x + 1008 \zeta_2 x^2 + 504 \zeta_2 x^3 - 256 \zeta_3 x_p^{-1} + 48 \zeta_3 \\
& - 528 \zeta_3 x) + \mathbf{H}_{0,-1} (-288/5 \zeta_2 x^{-2} - 640 \zeta_2 x_m^{-1} - 640 \zeta_2 x_p^{-1} - 1524 \zeta_2 \\
& + 20 \zeta_2 x - 480 \zeta_2 x^2 + 144 \zeta_2 x^3 - 224 \zeta_3 x_m^{-1} - 560 \zeta_3 x_p^{-1} + 152 \zeta_3 - 728 \zeta_3 x) \\
& + \mathbf{H}_{0,0} (-350027/5400 - 2896/25 x^{-1} + 103447/324 x_m^{-1} - 17384/27 x_p^{-1} \\
& - 16956149/1800 x + 26664/25 x^2 + 107496/125 x^3 + 28900/9 \zeta_2 x_m^{-1} \\
& + 32/3 \zeta_2 x_p^{-1} - 2751 \zeta_2 - 8449/3 \zeta_2 x - 2064 \zeta_2 x^2 - 1560 \zeta_2 x^3 + 5260/3 \zeta_3 x_m^{-1} \\
& + 148 \zeta_3 x_p^{-1} - 3230/3 \zeta_3 - 1346/3 \zeta_3 x) + \mathbf{H}_{0,1} (1332331/2025 - 512/25 x^{-1} \\
& - 81845/162 x_m^{-1} - 2398349/2025 x - 25672/25 x^2 - 96/5 \zeta_2 x^{-2} + 1080 \zeta_2 x_m^{-1} \\
& - 1634 \zeta_2 + 430 \zeta_2 x - 576 \zeta_2 x^2 - 864/5 \zeta_2 x^3 + 1976/3 \zeta_3 x_m^{-1} - 1532/3 \zeta_3 \\
& + 1348/3 \zeta_3 x) + \mathbf{H}_{1,0} (2535097/1620 + 112/5 x^{-1} - 110893/81 x_m^{-1} - 46891/324 x \\
& + 640 x^2 - 24 \zeta_2 x^{-2} + 9562/9 \zeta_2 x_m^{-1} - 17192/9 \zeta_2 + 18772/9 \zeta_2 x - 1056 \zeta_2 x^2 \\
& - 1056 \zeta_2 x^3 + 2008/3 \zeta_3 x_m^{-1} - 1172/3 \zeta_3 - 164/3 \zeta_3 x) + \mathbf{H}_{1,1} (654959/540 \\
& + 128/5 x^{-1} - 26339/27 x_m^{-1} - 159709/540 x - 1968/5 x^2 - 96/5 \zeta_2 x^{-2} \\
& + 820 \zeta_2 x_m^{-1} - 1356 \zeta_2 + 1300 \zeta_2 x - 576 \zeta_2 x^2 - 864/5 \zeta_2 x^3 + 504 \zeta_3 x_m^{-1} \\
& - 332 \zeta_3 + 148 \zeta_3 x) + \mathbf{H}_{-1} (-1488/25 \zeta_2 x^{-2} + 32 \zeta_2 x^{-1} - 3280/9 \zeta_2 x_p^{-1} \\
& - 28000/9 \zeta_2 - 27344/9 \zeta_2 x + 1248 \zeta_2 x^2 + 17712/25 \zeta_2 x^3 - 144/5 \zeta_3 x^{-2} \\
& - 480 \zeta_3 x_p^{-1} - 784 \zeta_3 - 2032 \zeta_3 x - 96 \zeta_3 x^2 + 1296/5 \zeta_3 x^3 - 516 \zeta_4 x_p^{-1} + 158 \zeta_4 \\
& - 758 \zeta_4 x) + \mathbf{H}_0 (-74841839/81000 + 7768/375 x^{-1} + 162721/324 x_m^{-1} \\
& - 928/3 x_p^{-1} - 423561229/81000 x + 83776/125 x^2 + 80 \zeta_2 x^{-1} + 2665 \zeta_2 x_m^{-1} \\
& - 404/9 \zeta_2 x_p^{-1} - 41267/18 \zeta_2 - 803/6 \zeta_2 x - 2544 \zeta_2 x^2 - 48016/25 \zeta_2 x^3 \\
& + 10856/3 \zeta_3 x_m^{-1} + 280 \zeta_3 x_p^{-1} - 19552/9 \zeta_3 - 13840/9 \zeta_3 x + 96 \zeta_3 x^2 \\
& + 5232/5 \zeta_3 x^3 - 3287/3 \zeta_4 x_m^{-1} + 300 \zeta_4 x_p^{-1} + 1961/3 \zeta_4 + 2645/3 \zeta_4 x) \\
& + \mathbf{H}_1 (6570689/4050 + 1472/25 x^{-1} - 239633/648 x_m^{-1} - 16747063/8100 x
\end{aligned}$$

### 3.5. The x-space coefficient functions

$$\begin{aligned}
& -15832/25 x^2 - 496/25 \zeta_2 x^{-2} + 336/5 \zeta_2 x^{-1} + 4525/3 \zeta_2 x_m^{-1} - 37921/15 \zeta_2 \\
& + 24091/15 \zeta_2 x - 9096/5 \zeta_2 x^2 - 30304/25 \zeta_2 x^3 - 88/5 \zeta_3 x^{-2} + 11626/9 \zeta_3 x_m^{-1} \\
& - 10424/9 \zeta_3 + 1180/9 \zeta_3 x + 6528/5 \zeta_3 x^3 - 484/3 \zeta_4 x_m^{-1} + 812/3 \zeta_4 \\
& - 2608/3 \zeta_4 x - 79641581/162000 + 35192/375 x^{-1} - 161929/432 x_m^{-1} \\
& - 113391919/162000 x + 162936/125 x^2 + 1904/25 \zeta_2 x^{-1} + 52709/162 \zeta_2 x_m^{-1} \\
& + 4856/27 \zeta_2 x_p^{-1} - 1332331/2025 \zeta_2 + 15235883/2025 \zeta_2 x + 25672/25 \zeta_2 x^2 \\
& - 107496/125 \zeta_2 x^3 + 232/5 \zeta_3 x^{-1} + 31993/9 \zeta_3 x_m^{-1} + 356 \zeta_3 x_p^{-1} - 42073/30 \zeta_3 \\
& - 4933/90 \zeta_3 x - 24/5 \zeta_3 x^2 + 8736/5 \zeta_3 x^3 - 3628/3 \zeta_3 \zeta_2 x_m^{-1} - 52 \zeta_3 \zeta_2 x_p^{-1} \\
& + 842 \zeta_3 \zeta_2 - 10 \zeta_3 \zeta_2 x - 47453/18 \zeta_4 x_m^{-1} + 3488/3 \zeta_4 x_p^{-1} + 69301/36 \zeta_4 \\
& + 144733/36 \zeta_4 x + 1812 \zeta_4 x^2 + 4062/5 \zeta_4 x^3 + 44/3 \zeta_5 x_m^{-1} + 508 \zeta_5 x_p^{-1} \\
& - 448 \zeta_5 + 1660 \zeta_5 x + \delta(1-x) (-61555/128 + 212833/324 \zeta_2 - 707833/162 \zeta_3 \\
& + 123449/36 \zeta_4 + 7322/9 \zeta_3 \zeta_2 + 1394/3 \zeta_5 + 976/3 \zeta_3^2 + 1124/3 \zeta_6) \quad (3.5.11)
\end{aligned}$$

and

$$\begin{aligned}
c_{2,\text{ns}}^{(4)F}(x) = & + \mathbf{H}_{0,0,0,0} (-119 + 238 x_m^{-1} - 119 x) + \mathbf{H}_{0,0,0,1} (-96 + 192 x_m^{-1} - 96 x) + \mathbf{H}_{0,0,1,0} (-72 \\
& + 144 x_m^{-1} - 72 x) + \mathbf{H}_{0,0,1,1} (-72 + 144 x_m^{-1} - 72 x) + \mathbf{H}_{0,1,0,0} (-48 + 96 x_m^{-1} - 48 x) \\
& + \mathbf{H}_{0,1,0,1} (-48 + 96 x_m^{-1} - 48 x) + \mathbf{H}_{0,1,1,0} (-48 + 96 x_m^{-1} - 48 x) + \mathbf{H}_{0,1,1,1} (-48 \\
& + 96 x_m^{-1} - 48 x) + \mathbf{H}_{1,0,0,0} (-24 + 48 x_m^{-1} - 24 x) + \mathbf{H}_{1,0,0,1} (-24 + 48 x_m^{-1} - 24 x) \\
& + \mathbf{H}_{1,0,1,0} (-24 + 48 x_m^{-1} - 24 x) + \mathbf{H}_{1,0,1,1} (-24 + 48 x_m^{-1} - 24 x) + \mathbf{H}_{1,1,0,0} (-24 \\
& + 48 x_m^{-1} - 24 x) + \mathbf{H}_{1,1,0,1} (-24 + 48 x_m^{-1} - 24 x) + \mathbf{H}_{1,1,1,0} (-24 + 48 x_m^{-1} - 24 x) \\
& + \mathbf{H}_{1,1,1,1} (-24 + 48 x_m^{-1} - 24 x) + \mathbf{H}_{0,0,0} (-985/3 + 1706/3 x_m^{-1} - 1621/3 x) \\
& + \mathbf{H}_{0,0,1} (-240 + 420 x_m^{-1} - 408 x) + \mathbf{H}_{0,1,0} (-152 + 268 x_m^{-1} - 272 x) + \mathbf{H}_{0,1,1} (-152 \\
& + 268 x_m^{-1} - 272 x) + \mathbf{H}_{1,0,0} (-64 + 116 x_m^{-1} - 136 x) + \mathbf{H}_{1,0,1} (-64 + 116 x_m^{-1} - 136 x) \\
& + \mathbf{H}_{1,1,0} (-64 + 116 x_m^{-1} - 136 x) + \mathbf{H}_{1,1,1} (-64 + 116 x_m^{-1} - 136 x) + \mathbf{H}_{0,0} (-1130/3 \\
& + 2096/3 x_m^{-1} - 1116 x - 192 \zeta_2 x_m^{-1} + 96 \zeta_2 + 96 \zeta_2 x) + \mathbf{H}_{0,1} (-632/3 \\
& + 1282/3 x_m^{-1} - 2240/3 x - 96 \zeta_2 x_m^{-1} + 48 \zeta_2 + 48 \zeta_2 x) + \mathbf{H}_{1,0} (-148/3 \\
& + 470/3 x_m^{-1} - 1120/3 x - 48 \zeta_2 x_m^{-1} + 24 \zeta_2 + 24 \zeta_2 x) + \mathbf{H}_{1,1} (-148/3 + 470/3 x_m^{-1} \\
& - 1120/3 x - 48 \zeta_2 x_m^{-1} + 24 \zeta_2 + 24 \zeta_2 x) + \mathbf{H}_0 (-4474/27 + 14321/27 x_m^{-1} \\
& - 37000/27 x - 420 \zeta_2 x_m^{-1} + 240 \zeta_2 + 408 \zeta_2 x - 44 \zeta_3 x_m^{-1} + 22 \zeta_3 + 22 \zeta_3 x) \\
& + \mathbf{H}_1 (1300/27 + 4429/27 x_m^{-1} - 18518/27 x - 116 \zeta_2 x_m^{-1} + 64 \zeta_2 + 136 \zeta_2 x) \\
& + 14939/81 + 25279/162 x_m^{-1} - 79606/81 x - 1282/3 \zeta_2 x_m^{-1} + 632/3 \zeta_2
\end{aligned}$$

$$+ 2240/3 \zeta_2 x - 436/3 \zeta_3 x_m^{-1} + 266/3 \zeta_3 + 386/3 \zeta_3 x + 102 \zeta_4 x_m^{-1} - 51 \zeta_4 (1+x) \\ + \delta(1-x) (281971/864 + 14321/27 \zeta_2 - 1/6 \zeta_3 + 4 \zeta_3 \zeta_2 + 1027/6 \zeta_4 + 2 \zeta_5) . \quad (3.5.12)$$

The structure of these expressions reflects the  $N$ -space results presented above. The large- $n_c$  coefficients (3.5.6), (3.5.8), (3.5.10) and (3.5.12) include only HPLs with non-negative indices corresponding to the non-alternating harmonic sums in eqs. (3.4.5), (3.4.9), (3.4.11) and (3.4.16). At the highest weight,  $w = 5$ , the  $n_f^2$  coefficients (3.5.6) and (3.5.10) do not only appear with factors  $x$  for  $\mathcal{C}_L$  and  $x_m^{-1} = 1/(1-x)$ , 1 and  $x$  for  $\mathcal{C}_2$ , but also include additional fixed combinations of  $x^a$  with  $a = -2, -1, 2, 3$ . These do not occur with  $w = 5$  HPLs in the  $C_F^2 n_f^2$  coefficients (3.5.7) and (3.5.11) corresponding to eqs. (3.4.6) and (3.4.12), which however include HPLs with negative indices and terms with  $x_p^{-1} = 1/(1+x)$ .

Up to terms that vanish in the corresponding limit, the large- $x$  and small- $x$  behaviour of the coefficient functions is given by plus-distributions,

$$\mathcal{D}_n = \left[ \frac{\ln^n(1-x)}{1-x} \right]_+ , \quad (3.5.13)$$

the  $\delta$ -function  $\delta(1-x)$  and powers of the logarithms

$$L_1 = \ln(1-x) , \quad L_0 = \ln x . \quad (3.5.14)$$

The  $n_f^2$  and  $n_f^3$  coefficients of  $\mathcal{D}_n$  and  $\delta(1-x)$  for  $\mathcal{C}_2$  are

$$c_{2,\text{ns}}^{(4)}(x) \Big|_{\mathcal{D}_5} = \frac{64}{27} C_F^2 n_f^2 , \quad (3.5.15)$$

$$c_{2,\text{ns}}^{(4)}(x) \Big|_{\mathcal{D}_4} = -\frac{44}{9} C_F C_A n_f^2 - \frac{640}{27} C_F^2 n_f^2 + \frac{8}{27} C_F n_f^3 , \quad (3.5.16)$$

$$c_{2,\text{ns}}^{(4)}(x) \Big|_{\mathcal{D}_3} = C_F C_A n_f^2 \left( \frac{1540}{27} - \frac{32}{9} \zeta_2 \right) + C_F^2 n_f^2 \left( \frac{24238}{243} - \frac{928}{27} \zeta_2 \right) \\ - \frac{232}{81} C_F n_f^3 , \quad (3.5.17)$$

$$c_{2,\text{ns}}^{(4)}(x) \Big|_{\mathcal{D}_2} = C_F C_A n_f^2 \left( -\frac{7403}{27} + \frac{688}{9} \zeta_2 + 16 \zeta_3 \right) \\ + C_F^2 n_f^2 \left( -\frac{52678}{243} + \frac{6104}{27} \zeta_2 + \frac{304}{9} \zeta_3 \right) + C_F n_f^3 \left( \frac{940}{81} - \frac{32}{9} \zeta_2 \right)$$

$$c_{2,\text{ns}}^{(4)}(x) \Big|_{\mathcal{D}_1} = C_F C_A n_f^2 \left( \frac{315755}{486} - \frac{9848}{27} \zeta_2 + \frac{64}{5} \zeta_2^2 - \frac{688}{9} \zeta_3 \right) \\ + C_F^2 n_f^2 \left( \frac{239633}{1458} - \frac{50140}{81} \zeta_2 + \frac{1312}{27} \zeta_2^2 - \frac{19304}{81} \zeta_3 \right)$$

### 3.5. The x-space coefficient functions

$$+ C_F n_f^3 \left( -\frac{17716}{729} + \frac{464}{27} \zeta_2 \right), \quad (3.5.18)$$

$$\begin{aligned} c_{2,\text{ns}}^{(4)}(x) \Big|_{D_0} = & C_F C_A n_f^2 \left( -\frac{3761509}{5832} + \frac{131878}{243} \zeta_2 - \frac{616}{9} \zeta_2^2 + \frac{6092}{81} \zeta_3 - \frac{400}{9} \zeta_3 \zeta_2 \right. \\ & + \left. \frac{1192}{9} \zeta_5 \right) + C_F^2 n_f^2 \left( -\frac{161929}{972} + \frac{385300}{729} \zeta_2 - \frac{19904}{135} \zeta_2^2 + \frac{3812}{9} \zeta_3 \right. \\ & - \left. \frac{1376}{27} \zeta_3 \zeta_2 - \frac{64}{9} \zeta_5 \right) + C_F n_f^3 \left( \frac{50558}{2187} - \frac{1880}{81} \zeta_2 + \frac{16}{9} \zeta_2^2 + \frac{80}{81} \zeta_3 \right), \end{aligned} \quad (3.5.19)$$

$$\begin{aligned} c_{2,\text{ns}}^{(4)}(x) \Big|_{\delta} = & C_F C_A n_f^2 \left( -\frac{8268733}{7776} - \frac{2063501}{972} \zeta_2 - \frac{18248}{135} \zeta_2^2 \right. \\ & + \frac{17477}{18} \zeta_3 + \frac{284}{9} \zeta_3 \zeta_2 - \frac{604}{9} \zeta_3^2 + \frac{3394}{27} \zeta_5 + \frac{878}{27} \zeta_6 \Big) \\ & + C_F^2 n_f^2 \left( -\frac{61555}{288} + \frac{212833}{729} \zeta_2 + \frac{246898}{405} \zeta_2^2 - \frac{1415666}{729} \zeta_3 \right. \\ & + \frac{29288}{81} \zeta_3 \zeta_2 + \frac{3904}{27} \zeta_3^2 + \frac{5576}{27} \zeta_5 + \frac{4496}{27} \zeta_6 \Big) \\ & + C_F n_f^3 \left( \frac{281971}{5832} + \frac{57284}{729} \zeta_2 + \frac{4108}{405} \zeta_2^2 - \frac{2}{81} \zeta_3 + \frac{16}{27} \zeta_3 \zeta_2 + \frac{8}{27} \zeta_3^2 \right). \end{aligned} \quad (3.5.20)$$

The coefficients of  $\mathcal{D}_n$  have been obtained from the soft-gluon exponentiation in eqs. (5.6) - (5.9) of ref. [224] for  $n = 2, \dots, 5$ , and in eq. (A.4) of ref. [225] for  $n = 1$  and  $n = 0$ ; our results in eqs. (3.5.15) - (3.5.19) agree with these predictions. On the other hand, the coefficient of  $\delta(1-x)$  in eq. (3.5.20) is a new result of the present chapter.

The corresponding terms with powers of  $\ln(1-x)$ , which are subleading for  $\mathcal{C}_2$  but leading for  $\mathcal{C}_L$  in the threshold limit, are given by

$$c_{2,\text{ns}}^{(4)}(x) \Big|_{L_1^5} = -\frac{64}{27} C_F^2 n_f^2, \quad (3.5.21)$$

$$c_{2,\text{ns}}^{(4)}(x) \Big|_{L_1^4} = \frac{44}{9} C_F C_A n_f^2 + \frac{1352}{27} C_F^2 n_f^2 - \frac{8}{27} C_F n_f^3, \quad (3.5.22)$$

$$\begin{aligned} c_{2,\text{ns}}^{(4)}(x) \Big|_{L_1^3} = & C_F C_A n_f^2 \left( -\frac{3652}{27} + \frac{448}{27} \zeta_2 \right) + C_F^2 n_f^2 \left( -\frac{70132}{243} + \frac{224}{27} \zeta_2 \right) \\ & + \frac{592}{81} C_F n_f^3, \end{aligned} \quad (3.5.23)$$

$$\begin{aligned} c_{2,\text{ns}}^{(4)}(x) \Big|_{L_1^2} = & C_F C_A n_f^2 \left( \frac{32249}{27} - 209 \zeta_2 - 112 \zeta_3 \right) + C_F^2 n_f^2 \left( \frac{122221}{243} \right. \\ & - \left. \frac{6800}{27} \zeta_2 + \frac{848}{9} \zeta_3 \right) + C_F n_f^3 \left( -\frac{4432}{81} + \frac{32}{9} \zeta_2 \right), \end{aligned} \quad (3.5.24)$$

Chapter 3. Four-loop large- $n_f$  contributions to the non-singlet structure functions  $F_2$  and  $F_L$

$$\begin{aligned} c_{2,\text{ns}}^{(4)}(x) \Big|_{L_1^1} = & C_F C_A n_f^2 \left( -\frac{1120828}{243} + \frac{30136}{27} \zeta_2 - \frac{512}{45} \zeta_2^2 + \frac{6734}{9} \zeta_3 \right) \\ & + C_F^2 n_f^2 \left( \frac{360863}{729} + \frac{98632}{81} \zeta_2 + \frac{800}{27} \zeta_2^2 - \frac{35056}{81} \zeta_3 \right) \\ & + C_F n_f^3 \left( \frac{136624}{729} - \frac{1184}{27} \zeta_2 \right), \end{aligned} \quad (3.5.25)$$

$$\begin{aligned} c_{2,\text{ns}}^{(4)}(x) \Big|_{L_1^0} = & C_F C_A n_f^2 \left( \frac{36059503}{5832} - \frac{544594}{243} \zeta_2 + \frac{572}{9} \zeta_2^2 - \frac{37004}{81} \zeta_3 \right. \\ & \left. + \frac{2704}{9} \zeta_3 \zeta_2 - \frac{1912}{9} \zeta_5 \right) + C_F^2 n_f^2 \left( -\frac{706090}{729} - \frac{1170910}{729} \zeta_2 \right. \\ & \left. + \frac{6496}{45} \zeta_2^2 - \frac{19336}{81} \zeta_3 - \frac{6688}{27} \zeta_3 \zeta_2 + \frac{1504}{9} \zeta_5 \right) \\ & + C_F n_f^3 \left( -\frac{583016}{2187} + \frac{8864}{81} \zeta_2 - \frac{16}{9} \zeta_2^2 - \frac{128}{81} \zeta_3 \right) \end{aligned} \quad (3.5.26)$$

and

$$c_{L,\text{ns}}^{(4)}(x) \Big|_{L_1^4} = \frac{16}{3} C_F^2 n_f^2, \quad (3.5.27)$$

$$\begin{aligned} c_{L,\text{ns}}^{(4)}(x) \Big|_{L_1^3} = & C_F C_A n_f^2 \left( -\frac{880}{27} + \frac{352}{27} \zeta_2 \right) + C_F^2 n_f^2 \left( -\frac{184}{27} - \frac{704}{27} \zeta_2 \right) \\ & + \frac{32}{27} C_F n_f^3, \end{aligned} \quad (3.5.28)$$

$$\begin{aligned} c_{L,\text{ns}}^{(4)}(x) \Big|_{L_1^2} = & C_F C_A n_f^2 \left( \frac{3200}{9} - 64 \zeta_2 - \frac{320}{3} \zeta_3 \right) \\ & + C_F^2 n_f^2 \left( -\frac{15172}{81} + \frac{736}{9} \zeta_2 + 128 \zeta_3 \right) - \frac{304}{27} C_F n_f^3, \end{aligned} \quad (3.5.29)$$

$$\begin{aligned} c_{L,\text{ns}}^{(4)}(x) \Big|_{L_1^1} = & C_F C_A n_f^2 \left( -\frac{35846}{27} + \frac{6592}{27} \zeta_2 + \frac{1216}{45} \zeta_2^2 + \frac{2944}{9} \zeta_3 \right) \\ & + C_F^2 n_f^2 \left( \frac{494242}{729} - \frac{2032}{27} \zeta_2 + \frac{704}{9} \zeta_2^2 - \frac{12512}{27} \zeta_3 \right) \\ & + C_F n_f^3 \left( \frac{3248}{81} - \frac{64}{9} \zeta_2 \right), \end{aligned} \quad (3.5.30)$$

$$\begin{aligned} c_{L,\text{ns}}^{(4)}(x) \Big|_{L_1^0} = & C_F C_A n_f^2 \left( \frac{275278}{243} - \frac{12320}{27} \zeta_2 + \frac{704}{15} \zeta_2^2 + \frac{304}{3} \zeta_3 + 256 \zeta_3 \zeta_2 \right. \\ & \left. - \frac{560}{3} \zeta_5 \right) + C_F^2 n_f^2 \left( -\frac{15803}{243} - \frac{1480}{27} \zeta_2 - \frac{17728}{135} \zeta_2^2 + \frac{7984}{81} \zeta_3 \right. \\ & \left. - \frac{896}{3} \zeta_3 \zeta_2 + 160 \zeta_5 \right) + C_F n_f^3 \left( -\frac{39640}{729} + \frac{608}{27} \zeta_2 \right). \end{aligned} \quad (3.5.31)$$

The coefficients (3.5.21) and (3.5.22) have been predicted in ref. [226] up to

### 3.5. The x-space coefficient functions

one number that was determined as  $\xi_{\text{DIS}_4} = 100/3$  a little later [227, 228]; eq. (3.5.22) provides the first check of this result by a four-loop diagram calculation. Also the coefficient (3.5.27) has been predicted before [226, 229]; all other results in eqs. (3.5.21) – (3.5.31) are new.

The small- $x$  limit of the non-singlet splitting functions and coefficient function is given by the terms with  $x^0 \ln^\ell x = x^0 L_0^\ell$ . Their  $n_f^2$  and  $n_f^3$  contributions read

$$c_{2,\text{ns}}^{(4)}(x) \Big|_{L_0^5} = -\frac{1951}{1620} C_F^2 n_f^2, \quad (3.5.32)$$

$$c_{2,\text{ns}}^{(4)}(x) \Big|_{L_0^4} = -\frac{1309}{108} C_F C_A n_f^2 - \frac{1190}{243} C_F^2 n_f^2 + \frac{119}{162} C_F n_f^3, \quad (3.5.33)$$

$$\begin{aligned} c_{2,\text{ns}}^{(4)}(x) \Big|_{L_0^3} &= C_F C_A n_f^2 \left( -\frac{10051}{81} + \frac{110}{9} \zeta_2 \right) \\ &+ C_F^2 n_f^2 \left( -\frac{3533}{243} + \frac{2296}{81} \zeta_2 \right) + \frac{1442}{243} C_F n_f^3, \end{aligned} \quad (3.5.34)$$

$$\begin{aligned} c_{2,\text{ns}}^{(4)}(x) \Big|_{L_0^2} &= C_F C_A n_f^2 \left( -\frac{386531}{648} + \frac{1654}{9} \zeta_2 - \frac{188}{3} \zeta_3 \right) \\ &+ C_F^2 n_f^2 \left( -\frac{271195}{2916} + \frac{8474}{81} \zeta_2 + \frac{4948}{27} \zeta_3 \right) \\ &+ C_F n_f^3 \left( \frac{644}{27} - \frac{64}{9} \zeta_2 \right), \end{aligned} \quad (3.5.35)$$

$$\begin{aligned} c_{2,\text{ns}}^{(4)}(x) \Big|_{L_0^1} &= C_F C_A n_f^2 \left( -\frac{2989295}{1944} + \frac{20702}{27} \zeta_2 - 224 \zeta_3 - \frac{1139}{9} \zeta_4 \right) \\ &+ C_F^2 n_f^2 \left( -\frac{460601}{1458} + \frac{458}{3} \zeta_2 + \frac{62144}{81} \zeta_3 - \frac{568}{9} \zeta_4 \right) \\ &+ C_F n_f^3 \left( \frac{39388}{729} - \frac{80}{3} \zeta_2 - \frac{88}{27} \zeta_3 \right), \end{aligned} \quad (3.5.36)$$

$$\begin{aligned} c_{2,\text{ns}}^{(4)}(x) \Big|_{L_0^0} &= C_F C_A n_f^2 \left( -\frac{19112737}{11664} + \frac{30782}{27} \zeta_2 - 328 \zeta_3 + \frac{368}{9} \zeta_3 \zeta_2 \right. \\ &\quad \left. - \frac{12785}{27} \zeta_4 + \frac{136}{3} \zeta_5 \right) + C_F^2 n_f^2 \left( -\frac{269059}{729} - \frac{3638}{243} \zeta_2 \right. \\ &\quad \left. + \frac{90502}{81} \zeta_3 - \frac{5032}{27} \zeta_3 \zeta_2 + \frac{5417}{27} \zeta_4 + \frac{896}{27} \zeta_5 \right) \\ &+ C_F n_f^3 \left( \frac{110314}{2187} - \frac{2600}{81} \zeta_2 - \frac{680}{81} \zeta_3 + \frac{68}{9} \zeta_4 \right) \end{aligned} \quad (3.5.37)$$

and

$$c_{L,\text{ns}}^{(4)}(x) \Big|_{L_0^3} = -\frac{920}{81} C_F^2 n_f^2, \quad (3.5.38)$$



$$c_{L,ns}^{(4)}(x)\Big|_{L_0^2} = -\frac{176}{3} C_F C_A n_f^2 - \frac{5140}{81} C_F^2 n_f^2 + \frac{32}{9} C_F n_f^3, \quad (3.5.39)$$

$$c_{L,ns}^{(4)}(x)\Big|_{L_0^1} = C_F C_A n_f^2 \left( -\frac{4064}{9} + \frac{160}{3} \zeta_2 \right) + C_F^2 n_f^2 \left( -\frac{2456}{27} + \frac{80}{3} \zeta_2 \right) + \frac{608}{27} C_F n_f^3, \quad (3.5.40)$$

$$c_{L,ns}^{(4)}(x)\Big|_{L_0^0} = C_F C_A n_f^2 \left( -\frac{26422}{27} + \frac{752}{3} \zeta_2 - 64 \zeta_3 \right) + C_F^2 n_f^2 \left( -\frac{2062}{729} + \frac{1040}{27} \zeta_2 + \frac{3632}{27} \zeta_3 \right) + C_F n_f^3 \left( \frac{3248}{81} - \frac{64}{9} \zeta_2 \right). \quad (3.5.41)$$

Eqs. (3.5.32) and (3.5.38) agree with the resummation predictions (4.5) and (4.6) of ref. [230] after using that  $\ln^\ell x$  transforms to  $(-1)^\ell \ell! N^{-\ell-1}$ . All other small- $x$  coefficients are new.

In the case of QCD, eqs. (3.5.32) – (3.5.41) lead to the numerical small- $x$  expansions

$$c_{2,ns}^{(4)}(x)\Big|_{n_f^2} = -2.1410151 \ln^5 x - 57.187471 \ln^4 x - 358.88192 \ln^3 x - 945.87933 \ln^2 x - 1327.8897 \ln x - 688.88341 + \mathcal{O}(x) \quad (3.5.42)$$

and

$$c_{L,ns}^{(4)}(x)\Big|_{n_f^2} = -20.192044 \ln^3 x - 347.47874 \ln^2 x - 1539.0328 \ln x - 2177.6994 + \mathcal{O}(x) \quad (3.5.43)$$

which yield the successive approximations shown in fig. 3.5. The pattern seen in this figure is the same seen for the complete third-order non-singlet coefficient functions in the right parts of fig. 2 and fig. 7 in ref. [43] and for the four- and five-loop resummation predictions in figs. 1 – 3 of ref. [230]: the leading, next-to-leading and next-to-next-to-leading logarithmic small- $x$  approximations wildly oscillate and thus, in general, cannot be used to obtain any reliable prediction for even the rough shape of high-order coefficient functions at any physically relevant small values of  $x$ .

## 3.6 Summary and outlook

As a step towards the determination of the fourth-order QCD coefficient functions  $c_a^{(4)}(x)$  in inclusive deep-inelastic scattering (DIS), we have computed

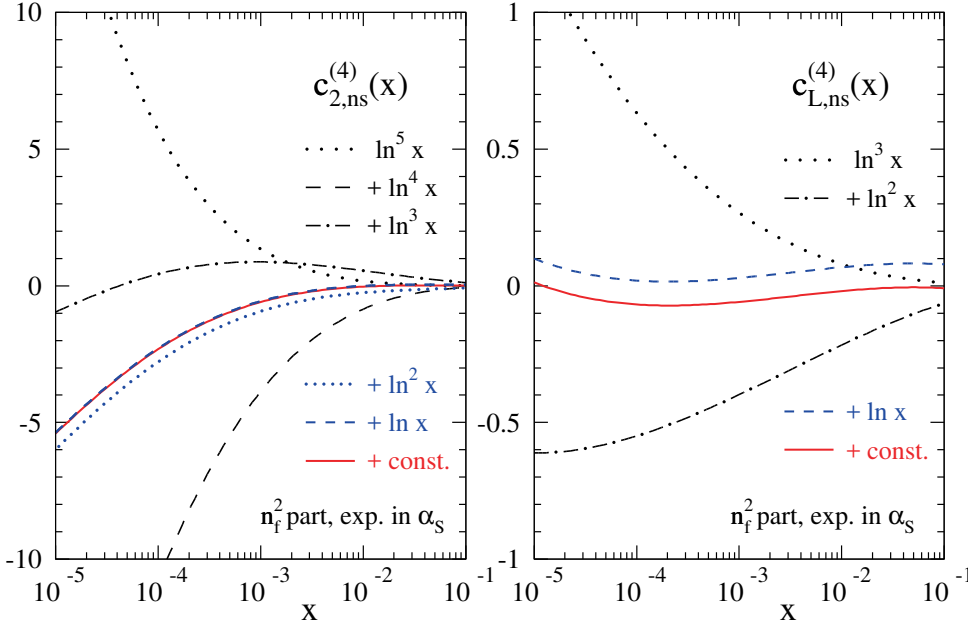


Figure 3.5: Successive small- $x$  approximations for the  $n_f^2$  contributions to the fourth-order coefficient functions for  $F_{2,\text{ns}}$  (left panel) and  $\bar{F}_{L,\text{ns}}$  (right panel). The coefficients in eqs. (3.5.42) and (3.5.43) have been converted to an expansion in  $\alpha_s$ .

the double-fermionic ( $n_f^2$ ) non-singlet contributions to the structure functions  $F_2$  and  $F_L$ . Our results are applicable to electromagnetic DIS (where we have ignored the very small [43, 56] contributions in which the photon couples to different quark lines) and to charged-current ( $W^+ + W^-$ ) exchange. The analytic dependence of these coefficient functions on Mellin- $N$ , and hence Bjorken- $x$ , has been reconstructed from a very large number of even values of  $N$ , up to  $N \simeq 1200$ .

Our calculations verify the corresponding contributions to the next-to-next-to-leading order splitting function  $P_{\text{ns}}^{+(3)}(x)$  obtained in ref. [14], and the much simpler (and much smaller)  $C_F n_f^3$  leading large- $n_f$  contributions to  $c_L^{(4)}(x)$  and  $c_2^{(4)}(x)$  [185, 186]. The coefficients of all large- $x$  plus-distributions in  $C_2$  at this order,  $[(1-x)^{-1} \ln^\ell(1-x)]_+$  with  $0 \leq \ell \leq 5$ , have been predicted by the soft-gluon exponentiation [224, 225]; we agree with these predictions. Our results for both structure functions make contact, just, with the resummations of  $\ln(1-x)$  and  $\ln x$  double logarithms in refs. [226–230], as the

leading terms of the  $n_f^2$  parts contribute to the overall next-to-next-to-leading logarithms; also here we find full agreement. Finally we have predicted the analytic form of the  $\zeta_4 n_f^3$  contributions to the Mellin- $N$  moments of the five-loop splitting function  $P_{ns}^{+(4)}(x)$ , and verified the corresponding  $\zeta_4 n_f^4$  parts of ref. [222].

To compute the large number of moments required for the reconstruction of the all- $N$  coefficient functions, we have developed a new approach based on the method of integration by parts, differential equations and the optical theorem. By employing the knowledge that the Mellin moments of the forward scattering amplitude correspond to the coefficients of the Taylor series around  $\omega = 1/x = 0$ , we derive a system of recurrence relations which holds for any linear system of differential equations, whose matrix contains no higher-order poles in  $\omega$ . While such higher poles are generically present, we find a simple algorithm which allows to change the basis of master integrals into a form where only simple poles appear in the differential matrix. The thereby obtained recurrence relations for the master integrals allow to obtain the Mellin moments at, in principle, arbitrary high  $N$  from the knowledge of the boundary conditions, which we compute using the FORCER program [184].

In practice, we find that the algorithm starts to become computationally demanding for the problem under consideration at values of  $N$  around about 1000. One element which allowed us to speed up the calculation considerably was to convert the basis of master integrals into one where the  $\varepsilon$ -dependence of the reduction coefficients factorizes from the dependence on  $x$ . An important feature of the method is the simplicity with which the recurrences can be solved - a procedure which we have implemented in FORM [52, 53, 195].

In spirit the method is not dissimilar from the ‘method of arbitrary high moments’ [199], which was used recently to recompute the 3-loop DIS coefficient functions [181]. Their method also derives recurrence relations from differential equations, but differs from our method in several ways, e.g., it relies on more advanced combinatorial algorithms to construct and recursively solve to high  $N$  the differential equations, and is implemented largely in MATHEMATICA. While it is possible that their approach leads to a faster algorithm at very large  $N$ , it is difficult at this stage to comment on timings without explicit performance benchmarks.

We plan to present the  $n_f^2$  fourth-order contributions to the structure function  $F_3$  in  $(W^+ + W^-)$  charged-current DIS in a forthcoming publication. The computation of its ‘standard’  $C_F C_A n_f^2$  and  $C_F^2 n_f^2$  parts is not much more difficult than that presented in this chapter, but some additional contributions with the group invariant  $d^{abc} d_{abc}$ , for the third-order results see

### 3.6. Summary and outlook

---

refs. [44, 181, 231], prove to be more challenging. We have also started to work on a first set of  $n_f^1$  contributions, the  $C_F^3 n_f$  terms, where we hope to be able to provide the first exact results of  $n_f^1$  parts of  $P_{\text{ns}}^{+(3)}(x)$  beyond the large- $n_c$  limit of ref. [15].

FORM files with our results can be obtained from the preprint server <https://arXiv.org> by downloading the source of the article on which this chapter is based. They are also available from the authors upon request. These files include also the analytic  $N$ -dependence of the third-order quantities  $a_{2,\text{ns}}^{(n)}(N)$  and  $a_{L,\text{ns}}^{(n)}(N)$  in eq. (3.2.8) which we have not included in section 3.4 above.



# Chapter 4

## Overall Conclusions

This thesis consists of two different studies in the field of precision calculations for elementary particle interactions in QCD. In the first study in chapter 2 we developed an automated algorithm to calculate one-loop jet functions. The algorithm has been implemented in the MATHEMATICA package GOJET [1]. By using the geometric subtraction scheme, we regulate the soft and collinear singularities in order to render jet functions finite. The package allows one to calculate jet functions for generic IR-safe observables at one-loop order in QCD. While the collinear counterterm (which is not always required) does not depend on the specifics of the chosen observable, the soft counterterm does. The power-law behaviour of the observable in the soft limit should be extracted by the user and provided to the program. This has been demonstrated in a systematic manner in the non-trivial example of the jet function for angularities with recoil. Up to an integration over the azimuthal angle, one can analytically obtain the IR poles in the dimensional regulator. The finite term is given as an expression to be integrated over numerically. We have verified our algorithm by recalculating the jet functions for the jet shape, angularities and jet functions for the  $k_T$  and cone algorithm. The previously mentioned jet function for angularities with recoil accounts for the formally power-suppressed but potentially large effect of recoil in  $e^+e^-$  collision measurements and has never been calculated before. While performing the numerical integration of the finite term, we encountered convergence issues due to an integrable divergence. We presented an approach to improve the convergence of the numerical integral by remapping the counterterm.

Even though one might consider analytic approaches to calculate jet functions preferable, we have shown that our program is capable to compute one-loop jet functions for highly non-trivial observables for which analytic results are too difficult to obtain. Efforts to calculate resummed cross sections at

next-to-leading logarithmic accuracy should therefore benefit from our algorithm. Moreover, in the case that one obtains analytic results for a one-loop jet function for any given IR finite observable, our algorithm should allow one to crosscheck the obtained results.

A possible next step would be an automated implementation of the geometric subtraction scheme at NNLO. However, at this order the collinear and soft singularities are no longer factorized in our framework. Due to the non-commutativity of the collinear and soft limits, one has to keep track of the specific ordering of the subtractions. Furthermore, the soft limit of the observables will no longer be described by a power-law. We expect the mathematical behaviour of the soft limit of the observables to be more involved. This complicates the construction of the counterterms.

In the second study in chapter 3 we calculated, for the first time ever, the doubly fermionic  $n_f^2$  non-singlet coefficient functions  $C_2$  and  $C_L$  for inclusive Deep Inelastic Scattering (DIS) at order  $N^4\text{LO}$  in the strong coupling constant  $\alpha_s$ . By using the optical theorem, the integration-by-parts technique and the method of differential equations we were able to recursively compute a sufficiently large number of Mellin moments ( $N = 1500$ ), which allowed us to reconstruct full analytic expressions in both Mellin- $N$  space and Bjorken- $x$  space, in terms of harmonic sums and harmonic polylogarithms respectively. We verified the  $C_F n_f^3$  leading large- $n_f$  contributions to  $c_L^{(4)}(x)$  and  $c_2^{(4)}(x)$  [185, 186]. On top of what we agree with the coefficients of the large- $x$  plus-distribution in  $C_2$  of [224, 225] and with the resummations of  $\log(x)$  and  $\log(1-x)$  in [226–230]. As a byproduct we obtained the  $N^3\text{LO}$   $n_f^2$  non-singlet splitting function  $P_{\text{ns}}^{(3)+}(x)$ . Therefore we are also the first ones to verify the results of [14]. Furthermore, the no- $\pi^2$  theorem of [218] allowed us to predict the  $\zeta_4$ -terms of the 5-loop non-singlet splitting function at order  $C_F C_A n_f^3$  and order  $C_F^2 n_f^3$ .

The main bottleneck in our algorithm is the reduction of the scalar Feynman integrals to master integrals. We found that FIRE [61] was the most effective reduction program for the type of integrals that we encountered, which depend on the variables of dimension  $d$  and inverse Bjorken- $x$   $\omega$ . The program FIRE was complemented by the program LITERED [116] to exhaust all the internal- and external symmetries for each topology in order to speed up the reduction procedure. Another bottleneck is the expansion of the differential matrix. Unfactorized expressions in the differential matrix result in spurious poles in  $\epsilon$  when performing expansions of the differential matrix. These expressions result from coefficients in the reduction table in which the kinematical invariants mix with the dimension. To solve this problem we employed an algorithm [118] which searches for an improved basis of master

---

integrals, such that the kinematical variables do not anymore mix with the dimension in the reduction table, resulting in a factorized differential matrix.

The resulting differential matrix could however still contain higher order poles in  $\omega$ . We constructed an approach to scale away these poles by changing the basis of master integrals. Consequently the differential matrix contains only simple poles, allowing one to obtain recurrence relations for the master integrals. These recurrence relations have been implemented in FORM [52, 53, 195] to compute the Mellin moments  $N$ , using the FORCER program [184] to provide the boundary conditions.

The study in chapter 3 serves a proof of concept for our algorithm. The strength of our algorithm lies in the modularity of our approach and in the recursive algorithm. In particular, the differential equations are solved by using a power-series ansatz for the master integrals. This bypasses the necessity to fully solve the differential systems, which we expect to be a much harder problem. As mentioned before, the main bottleneck of our algorithm is the reduction of scalar Feynman integrals to master integrals. Therefore, as reduction programs improve, we expect our algorithm to become more powerful. In the next section we will give a preview of our approach to calculate the N<sup>4</sup>LO DIS non-singlet splitting function at order  $C_F^3 n_f$  in which we replaced FIRE by a new reduction algorithm which is fine tuned to the specific problem.





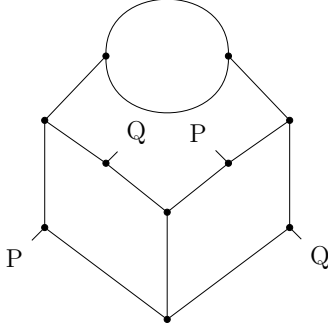
# Chapter 5

## Outlook

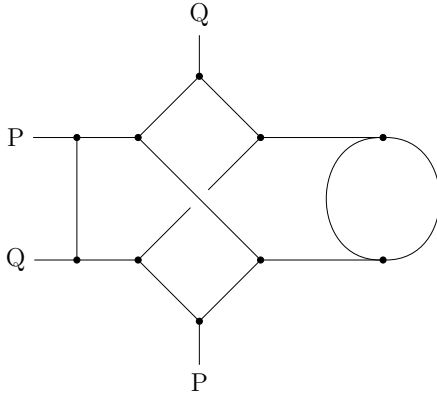
In chapter 3 the non-singlet N<sup>4</sup>LO DIS coefficient functions at order  $n_f^2$  have been calculated using our new algorithm. This algorithm combined the optical theorem, integration by parts technique and the method of differential equations to calculate 1500 Mellin moments. Subsequently we were able to reconstruct an all- $N$  expression for the coefficient functions by Gaussian elimination. Lastly these coefficient functions were transformed to momentum-fraction  $x$  space. The N<sup>4</sup>LO non-singlet quark-quark splitting functions at order  $n_f^2$  have already been calculated in [14].

As a next step we would like to calculate the non-singlet N<sup>4</sup>LO splitting functions at order  $n_f$ . At this order, the diagrams are more numerous and complex, since one has to replace a quark self-energy loop by a more complicated loop which results from the different vertices such as the gluon vertices. Due to the complexity we have to split up the diagrams in subsections. The simplest subsection is a set of diagrams at order  $C_F^3 n_f$ . Using our same topologisation routine as before, we obtain 91 new topologies. Including the 13 topologies at order  $n_f^2$ , our library contains 104 topologies. In table 5.1 a subset of characteristic topologies is illustrated.

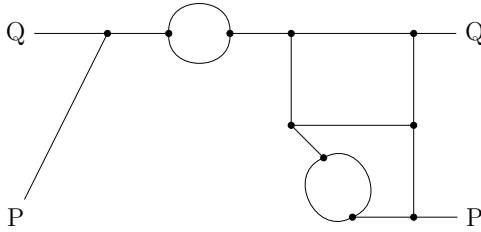
Topo 66 has been used as a benchmark to test reduction algorithms, because we a priori expected it to be the most difficult topology due to its planarity. It took FIRE (including LITERED) two weeks to reduce the integrals required for the  $g_{\mu\nu}$  polarization. Of this, one day was spent to produce the LITERED symmetry files. Even though we do not expect all of the topologies to be of the same complexity (we count approximately 20 topologies of a similar complexity), it would be unrealistic to pursue the splitting functions and DIS coefficient functions at  $O(n_f)$  using FIRE. Therefore our collaborator Andrea Pelloni has written his own reduction routine, which uses finite field methods. Using this new reduction routine, called LACHIAVE, he has been able to reduce the integrals required for topo 66 to masters integrals in a cou-



Topo 20



Topo 66



Topo 104

Table 5.1: Depicted are three out of 104 topologies which are required to calculate the DIS Mellin moments for the contributions to the non-singlet splitting functions at order  $n_f C_F^3$  at N<sup>4</sup>LO. Note that propagators which do not include a loop momentum term, are not present in our actual topology definitions.

---

ple of days. With LACHIAVE one has to run multiple reductions for a fixed set of parameters (i.e. assigning a numerical value to each parameter, the finite field). This allows one to parallelise the reduction process in a highly efficient manner, since each of the finite fields can be run on a different CPU core. For a sufficient number of finite fields, one is able to reconstruct full algebraic expressions for the reduction tables. The upside of this routine is the speed at which it reduces the integrals. The downside is that it does not allow the user to submit a basis of preferred masters. Therefore one might end up with unfactorised expressions in the differential matrix.

The recursive calculation of the coefficients of the master integrals relies on the factorisation of the differential matrix. Without a factorised differential matrix, the recursive algorithm slows down by a significant factor. We would not have been able to calculate 1500 moments at order  $n_f^2$  with an unfactorised differential matrix. In fact, using unfactorised expressions, we could only calculate moments up till  $O(\sim \omega^{200})$  at that order. We therefore choose to process the master integrals resulting from LACHIAVE with FIRE and LITERED (and the improved masters routine if necessary). So far this has always resulted in factorised expressions for the differential matrix. The first and the second reductions (to close the differential system) have been performed for all topologies with LACHIAVE, except for topo 20 (see table 5.1). Topo 20 truly turns out to be the most complicated topology. We do not yet know which topologies require additional factorisation.

This calculation should result in the first (non-leading- $N_c$ ) full all- $x$  expressions that contribute to the non-singlet quark-quark splitting function which is not  $n_f^2$  or  $n_f^3$ . The next subsection of diagrams are of order  $C_F^2 C_A n_f$ . After that one should tackle diagrams at order  $d_{RR}^4 n_f$ . This is a quartic Casimir invariant which is defined as [232]

$$d_{xy}^{(4)} \equiv d_x^{abcd} d_y^{abcd}. \quad (5.0.1)$$

Here  $x$  and  $y$  denote the representations. The totally symmetric tensors  $d_y^{abcd}$  can be expressed in terms of the group generators  $T_r^a$  as

$$d_r^{abcd} = \frac{1}{6} \text{tr}(T_r^a T_r^b T_r^c T_r^d + \text{five } bcd \text{ permutations}). \quad (5.0.2)$$

This would be sufficient to obtain the complete  $n_f$  part of the splitting function, because the expressions at order  $C_F C_A^2 n_f$  can already be inferred from the leading- $N_c$  results [15].



# Appendices



# Appendix A

## $G_2$ Subtraction Term for Rapidity Divergences

When the soft limit of the observable scales as  $1/z$ , we need a rapidity regulator to control the singularities. The resulting expressions for  $G_2$  with rapidity regulator are given by

$$\begin{aligned}
 G_{q,2} &= \frac{2C_F}{\epsilon} \frac{e^{\gamma_E \epsilon}}{\sqrt{\pi} \Gamma(\frac{1}{2} - \epsilon)} \left( \frac{\nu}{\omega} \right)^\eta \int_0^\pi d\phi \Theta(\Phi) (\sin \phi)^{-2\epsilon} \\
 &\quad \left[ \frac{(c_1^+)^{-\epsilon}}{\eta + \epsilon(1 - \alpha_1^+)} A^{-\eta - \epsilon(1 - \alpha_1^+)} - \frac{(c_1^-)^{-\epsilon}}{\eta + \epsilon(1 - \alpha_1^-)} A^{-\eta - \epsilon(1 - \alpha_1^-)} \right], \\
 G_{g,2} &= \frac{C_A}{\epsilon} \frac{e^{\gamma_E \epsilon}}{\sqrt{\pi} \Gamma(\frac{1}{2} - \epsilon)} \left( \frac{\nu}{\omega} \right)^\eta \int_0^\pi d\phi \Theta(\Phi) (\sin \phi)^{-2\epsilon} \\
 &\quad \left[ \frac{(c_0^+)^{-\epsilon}}{\eta + \epsilon(1 - \alpha_0^+)} A^{-\eta - \epsilon(1 - \alpha_0^+)} - \frac{(c_0^-)^{-\epsilon}}{\eta + \epsilon(1 - \alpha_0^-)} A^{-\eta - \epsilon(1 - \alpha_0^-)} \right. \\
 &\quad \left. + \frac{(c_1^+)^{-\epsilon}}{\eta + \epsilon(1 - \alpha_1^+)} A^{-\eta - \epsilon(1 - \alpha_1^+)} - \frac{(c_1^-)^{-\epsilon}}{\eta + \epsilon(1 - \alpha_1^-)} A^{-\eta - \epsilon(1 - \alpha_1^-)} \right].
 \end{aligned}
 \tag{A.0.1}$$





# Appendix B

## Counterterm Mapping

In this appendix we discuss how to improve the convergence of the soft subtraction through a mapping. For simplicity, we consider only the soft singularity at  $z = 0$ , for which the finite term generated by the geometric subtraction is of the form:

$$\int_0^1 dz \left[ \frac{f(z)\Theta(O(z)) - f(0)\Theta(O_0(z))}{z} \right]. \quad (\text{B.0.1})$$

Here we suppressed the dependence (and integrals) over  $s$  and  $\phi$ , extracting the  $1/z$  singularity from the integrand  $Q$ , i.e.  $f = zQ$ . While this integrand is by construction integrable, poor numerical convergence may be caused by mismatch of the observable  $O$  and its soft limit  $O_0$ . This problem can become particularly severe if  $O(z)$  has a fractional power series in  $z$ , as we illustrate below.

To improve the convergence of the integral, we apply the following mapping (to the counterterm only):

$$G: z \rightarrow \frac{z + g(z)}{1 + g(z)}. \quad (\text{B.0.2})$$

This maps the interval  $0 \leq z \leq 1$  onto itself, as long as  $z + g(z) > 0$ , and the subtracted integral will remain the same as long as the function  $g(z)$  decreases faster near  $z = 0$  than  $z$  itself, i.e., it satisfies

$$\lim_{z \rightarrow 0} \frac{g(z)}{z} = 0. \quad (\text{B.0.3})$$

Applying this map, we can replace eq. (B.0.1) with:

$$\int_0^1 dz \left[ \frac{f(z)\Theta(O(z))}{z} - \frac{f(0)\Theta(O_0(G(z)))}{G(z)} \left| \frac{\partial G(z)}{\partial z} \right| \right]. \quad (\text{B.0.4})$$

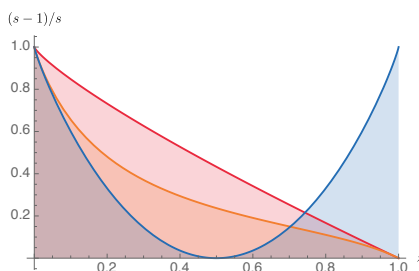


Figure B.1: The plot shows the observable (blue), its soft approximation in eq. (B.0.7) (red) and the remapped soft approximation in eq. (B.0.8) (orange).

One can now construct the function  $g(z)$  to map  $O_0(G(z))$  closer to  $O(z)$  in the region  $z \rightarrow 0$ .

For the angularities with recoil in section 2.4.2, we encounter the following instructive example

$$O(z) = 1/s - \frac{(z(1-z))^{\frac{b-1}{b+1}}}{(z^b + (1-z)^b)^{\frac{2}{1+b}}}, \quad (\text{B.0.5})$$

which has poor convergence for small positive values of  $b$ . Already  $b = 1/10$  yields a sufficiently challenging scenario, for which the power series around  $z = 0$  is given by:

$$\begin{aligned} O(z) = 1/s - z^{\frac{9}{11}} &+ \frac{20}{11} z^{\frac{101}{110}} + \frac{90}{121} z^{\frac{56}{55}} - \frac{60}{1331} z^{\frac{123}{110}} + \frac{195}{14641} z^{\frac{67}{55}} - \frac{936}{161051} z^{\frac{29}{22}} \\ &+ \frac{5460}{1771561} z^{\frac{78}{55}} - \frac{35880}{19487171} z^{\frac{167}{110}} + \frac{255645}{214358881} z^{\frac{89}{55}} - \frac{1931540}{2357947691} z^{\frac{189}{110}} \\ &- \frac{25922165435}{25937424601} z^{\frac{20}{11}} - \frac{5136983395938}{3138428376721} z^{\frac{211}{110}} + \mathcal{O}(z^2). \end{aligned} \quad (\text{B.0.6})$$

It is thus apparent that the leading term approximation

$$O_0(s, z, \phi) = 1/s - z^{\frac{9}{11}} \quad (\text{B.0.7})$$

gives only a poor approximation of the full result. Substituting  $z = G(z)$  with

$$g(z) = z \sum_{i=1}^{11} c_i z^{\frac{i}{10}} \quad (\text{B.0.8})$$

---

into eq. (B.0.7) we can match eq. (B.0.6) by iteratively solving for the constants  $c_i$ . This procedure yields:

$$\begin{aligned}
c_1 &= \frac{20}{9}, & c_2 &= \frac{110}{81}, & c_3 &= \frac{220}{2187}, & c_4 &= -\frac{385}{19683}, & c_5 &= \frac{1232}{177147}, & c_6 &= -\frac{15400}{4782969}, \\
c_7 &= \frac{74800}{43046721}, & c_8 &= -\frac{402050}{387420489}, & c_9 &= \frac{20906600}{31381059609}, & c_{10} &= -\frac{345319185959}{282429536481}, \\
c_{11} &= -\frac{6338162484818}{2541865828329}.
\end{aligned} \tag{B.0.9}$$

The resulting curves are plotted in figure B.1, highlighting the improvement due to the remapping. A VEGAS run using  $5 \cdot 10^9$  points for the finite part of the quark jet function of this observable yields  $-48.63(2)$  without the mapping, while we obtain  $-48.745(9)$  after the mapping. The true value is  $-48.7731$ , indicating that the remapped counterterm yields a result significantly closer to the true value. In both cases it becomes clear that the offset is not completely covered by the uncertainty. While the remapping may thus improve convergence, it may not completely solve the issue.



# Appendix C

## Azimuthal Integral

In this appendix we evaluate the integral

$$I(a, b; \epsilon) = \int_a^b d\phi (\sin \phi)^{-2\epsilon}. \quad (\text{C.0.1})$$

One can convert this integral into a Gauss-type hypergeometric integral using the transformation  $\cos \phi = 1 - 2x$ . However this leads to square roots in the denominator which do not naively lead to a polylogarithmic expression. Instead, one can rewrite the integral as a contour integral in the complex plane using the transformation  $z = e^{i\phi}$ , such that

$$\sin \phi = \frac{z^2 - 1}{2iz}, \quad (\text{C.0.2})$$

leading to the following representation

$$I(a, b; \epsilon) = -i \int_{e^{ia}}^{e^{ib}} \frac{dz}{z} \left( \frac{z^2 - 1}{2iz} \right)^{-2\epsilon}. \quad (\text{C.0.3})$$

The integrand can be chosen to have branch cuts on the real axis for  $z < 0$  and for  $z > 1$ . For  $0 < a, b < \pi$ , which is the range of physical interest, no branch cuts are ever crossed.

It is convenient to perform the integral on a contour along the real axis from  $0 < z < A$  with  $0 < A < 1$ , i.e.,

$$F(A; \epsilon) = -i 2^{2\epsilon} e^{-i\pi\epsilon} \int_0^A \frac{dz}{z} \left( \frac{1 - z^2}{z} \right)^{-2\epsilon}. \quad (\text{C.0.4})$$

The result can be analytically continued to the case of interest with  $A = e^{ia}$ . We then obtain (in essence via the residue theorem)

$$I(a, b; \epsilon) = F(e^{ia}; \epsilon) - F(e^{ib}; \epsilon). \quad (\text{C.0.5})$$

While the divergence at  $z = 0$  requires careful treatment, this drops out in the difference of the two terms in eq. (C.0.5). We performed the integral using the Maple package Hyperint [233], finding that the integral can be performed order by order in  $\epsilon$  in terms of harmonic polylogarithms. This is to be expected, given that its singularities are located at  $z = 0, -1, 1$ . Up to order  $\epsilon^2$  we can express the result in terms of the classical polylogarithms:

$$I(a, b; \epsilon) = \sum_{n=0}^{\infty} I^{(n)}(a, b) \epsilon^n \quad (\text{C.0.6})$$

with

$$\begin{aligned} I^{(0)}(a, b) &= b - a, \\ I^{(1)}(a, b) &= 2i \operatorname{Li}_2(e^{ia}) - 2i \operatorname{Li}_2(e^{ib}) + 2i \operatorname{Li}_2(-e^{ia}) - 2i \operatorname{Li}_2(-e^{ib}) + i(a-b)(-a+\pi-b) \\ &\quad + (-2a+2b) \ln 2, \\ I^{(2)}(a, b) &= -\frac{2}{3}i \ln^3(e^{ib}+1) - 2i \ln^2(e^{ib}+1) \ln(1-e^{ib}) - 4b \ln(e^{ib}+1) \ln(1-e^{ib}) \\ &\quad + 2i \ln^2(e^{ia}+1) \ln(1-e^{ia}) + 4a \ln(e^{ia}+1) \ln(1-e^{ia}) - 2i \ln(e^{ib}+1) \ln^2 2 \\ &\quad - 2i \ln(1-e^{ib}) \ln^2 2 + 2i \ln(e^{ia}+1) \ln^2 2 + 2i \ln(1-e^{ia}) \ln^2 2 - 4i \operatorname{Li}_3(e^{ia}) \\ &\quad + 4i \operatorname{Li}_3[-(-1+e^{ia})/(e^{ia}+1)] - 4i \operatorname{Li}_3[-(-1+e^{ib})/(e^{ib}+1)] \\ &\quad + 2a \ln^2(e^{ia}+1) \\ &\quad - 2b \ln^2(1-e^{ib}) - 2b \ln^2(e^{ib}+1) + 4i \operatorname{Li}_3(\tfrac{1}{2} + \tfrac{1}{2}e^{ia}) - 8i \operatorname{Li}_3[1/(e^{ia}+1)] \\ &\quad + 4i \operatorname{Li}_3(\tfrac{1}{2} - \tfrac{1}{2}e^{ia}) - 8i \operatorname{Li}_3(1-e^{ia}) + 4i \operatorname{Li}_3(e^{ib}) - 4i \operatorname{Li}_3(\tfrac{1}{2} - \tfrac{1}{2}e^{ib}) \\ &\quad + 8i \operatorname{Li}_3(1-e^{ib}) + 4i \operatorname{Li}_3(-e^{ib}) + 8i \operatorname{Li}_3(1/(e^{ib}+1)) - 4i \operatorname{Li}_3(\tfrac{1}{2} + \tfrac{1}{2}e^{ib}) \\ &\quad + 2(b-a) \ln^2 2 + 2i(a-b)(-a+\pi-b) \ln 2 - 4i \ln(e^{ia}+1) \ln(1-e^{ia}) \ln 2 \\ &\quad + (2\pi-4a) \operatorname{Li}_2(-e^{ia}) + \tfrac{1}{3}i\pi^2 \ln(1-e^{ia}) + 4i \ln 2 \operatorname{Li}_2(-e^{ia}) \\ &\quad - 4i \ln 2 \operatorname{Li}_2(e^{ib}) + 4i \ln(e^{ib}+1) \operatorname{Li}_2(e^{ib}) + 4i \ln(1-e^{ib}) \operatorname{Li}_2(e^{ib}) \\ &\quad - 4i \ln(e^{ia}+1) \operatorname{Li}_2(e^{ia}) - 4i \ln(1-e^{ia}) \operatorname{Li}_2(e^{ia}) + 4i \ln 2 \operatorname{Li}_2(e^{ia}) \\ &\quad + \tfrac{1}{6}(a-b)(3\pi^2-6\pi a-6\pi b+4a^2+4ab+4b^2) + \tfrac{2}{3}i \ln^3(e^{ia}+1) \\ &\quad + (-2\pi+4b) \operatorname{Li}_2(e^{ib}) + (2\pi-4a) \operatorname{Li}_2(e^{ia}) - \tfrac{1}{3}i\pi^2 \ln(1-e^{ib}) \\ &\quad + 4i \ln(e^{ib}+1) \ln(1-e^{ib}) \ln 2 + 4i \ln(e^{ib}+1) \operatorname{Li}_2(-e^{ib}) \\ &\quad + 4i \ln(1-e^{ib}) \operatorname{Li}_2(-e^{ib}) - 4i \ln 2 \operatorname{Li}_2(-e^{ib}) + i\pi^2 \ln(e^{ib}+1) \\ &\quad - i\pi^2 \ln(e^{ia}+1) - 4i \ln(e^{ia}+1) \operatorname{Li}_2(-e^{ia}) - 4i \ln(1-e^{ia}) \operatorname{Li}_2(-e^{ia}) \\ &\quad + 2a \ln^2(1-e^{ia}) - 4i \operatorname{Li}_3(-e^{ia}) + (-2\pi+4b) \operatorname{Li}_2(-e^{ib}). \quad (\text{C.0.7}) \end{aligned}$$

After this article was posted, we were informed that the azimuthal integral in app. C was evaluated before in terms of so-called Log-sine functions, which

---

were introduced and studied in [234, 235] and have been implemented in a C++ library in [236]. Relations can also be found in these references to convert them into Nielsen polylogarithms, although not directly into classical polylogarithms (which is only possible up to order  $\epsilon^2$ ).





# Appendix D

## Harmonic Sums

The results in Mellin space for DIS involve so-called *harmonic sums* [187]. The simplest harmonic sum one can define is

$$S_m(n) = \sum_{i=1}^n \frac{1}{i^m}, \quad (\text{D.0.1})$$

in which the index  $m$  is a positive integer. For a negative index one obtains an alternating sum

$$S_{-m}(n) = \sum_{i=1}^n \frac{(-1)^i}{i^m}, \quad (\text{D.0.2})$$

with  $m > 0$ . Notice that eq. (D.0.1) generalises to the Riemann zeta function for  $n \rightarrow \infty$ ,

$$\zeta(m) = \sum_{k=1}^{\infty} \frac{1}{k^m}. \quad (\text{D.0.3})$$

In general harmonic sums depend on a vector of integer indices  $\vec{m} = \{m_1, m_2, \dots, m_p\}$ . These are defined recursively as

$$S_{m_1, m_2, \dots, m_p}(n) = \sum_{i=1}^n \frac{1}{i^{m_1}} S_{m_2, \dots, m_p}(i) \quad (\text{D.0.4})$$

and

$$S_{-m_1, m_2, \dots, m_p}(n) = \sum_{i=1}^n \frac{(-1)^i}{i^{m_1}} S_{m_2, \dots, m_p}(i), \quad (\text{D.0.5})$$

with again  $m_1 > 0$  and  $S(n) = 1$ . By summing the absolute values of all the indices in a harmonic series, one obtains the weight of the series,

$$W(S_{m_1, m_2, \dots, m_p}(n)) = \sum_{i=1}^p |m_i|. \quad (\text{D.0.6})$$

# Appendix E

## Harmonic Polylogarithms

To describe the results of DIS in  $x$ -space, one requires the *harmonic polylogarithms* (hpl's) [188]. The Mellin transforms of the hpl's are related to the harmonic sums, described in app. D. Let us first define the hpl's.

Just like the harmonic sums, the harmonic polylogarithms depend on a vector of integer indices  $\vec{m} = \{m_1, m_2, \dots, m_w\}$  (and of course its argument  $x$ ). The weight  $w$  is defined as the dimension of the vector. In the case that  $w = 1$ , the hpl's are

$$\begin{aligned} H_0(x) &= \log(x), \\ H_1(x) &= \int_0^x \frac{dx'}{1-x'} = -\log(1-x), \\ H_{-1}(x) &= \int_0^x \frac{dx'}{1+x'} = \log(1+x). \end{aligned} \tag{E.0.1}$$

By taking the derivatives of the hpl's in eq. (E.0.1) as

$$\frac{d}{dx} H_a(x) = f_a(x), \tag{E.0.2}$$

one obtains the three rational fractions

$$\begin{aligned} f_0(x) &= \frac{1}{x}, \\ f_1(x) &= \frac{1}{1-x}, \\ f_{-1}(x) &= \frac{1}{1+x}. \end{aligned} \tag{E.0.3}$$

An hpl with a null vector of weight  $w$  is defined as

$$H_{\vec{0}_w} = \frac{1}{w!} \log^w(x). \tag{E.0.4}$$

Using this as a boundary condition, one can define arbitrary hpl's recursively as

$$H_{\{m_1, m_2, \dots, m_w\}}(x) = \int_0^x dx' f_{m_1}(x') H_{\{m_2, m_3, \dots, m_w\}}(x'). \quad (\text{E.0.5})$$

For example, this allows us to calculate the hpl's for unit vectors of weight  $w$  and  $(-1)_w$ ,

$$\begin{aligned} H_{\vec{1}_w}(x) &= \frac{1}{w!} (-\log(1-x))^w, \\ H_{(-1)_w}(x) &= \frac{1}{w!} \log^w(1+x). \end{aligned} \quad (\text{E.0.6})$$

The method also applies to more general hpl's.

Lastly, by applying the Mellin transform to the hpl's, one obtains harmonic sums. At  $w = 1$  they are related to each other as

$$\begin{aligned} \int_0^1 dx x^n H_0(x) &= -\frac{1}{(n+1)^2}, \\ \int_0^1 dx x^n H_1(x) &= \frac{S_1(n+1)}{(n+1)}, \\ \int_0^1 dx x^n H_{-1}(x) &= (-1)^n \frac{S_{-1}(n+1)}{(n+1)} + \frac{\log(2)}{(n+1)} (1 + (-1)^n). \end{aligned} \quad (\text{E.0.7})$$

The Mellin transforms of more complicated hpl's can be calculated in a recursive manner.

# Appendix F

## One-loop Example Recursive Algorithm

In this appendix we will explicitly show a one-loop example of our recursive algorithm, which we used to calculate the bare Mellin moments in DIS.

### F.1 Master integrals

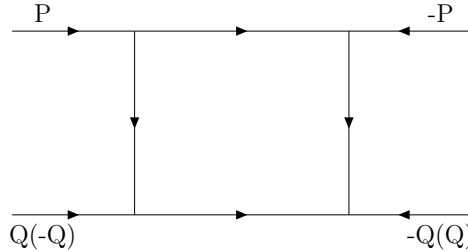


Figure F.1: The topology of the master integral topo1 (topo3) is illustrated.

Using IBP relations, we find that the following master integrals are present at one loop for DIS: topo1(1,0,1), topo1(0,1,1) and topo3(1,0,1). Here the topologies are defined as

$$\begin{aligned} \text{topo1}(A1, A2, A3) &= \int d^D K \left( \frac{1}{(K^2)^{A1}} \right) \left( \frac{1}{((P-K)^2)^{A2}} \right) \left( \frac{1}{((Q+K)^2)^{A3}} \right) \\ \text{topo3}(A1, A2, A3) &= \int d^D K \left( \frac{1}{((P-K)^2)^{A1}} \right) \left( \frac{1}{(K^2)^{A2}} \right) \left( \frac{1}{((K-Q)^2)^{A3}} \right). \end{aligned} \quad (\text{F.1.1})$$

The diagrams corresponding to the topologies are illustrated in figure F.1. In the following we only focus on topo1, because one can relate topo3 to topo1 by exploiting the symmetry  $\omega \rightarrow -\omega$ .

## F.2 Derivation of the differential equation

Say that  $M_i(x)$  is a master integral that depends on the variable  $x$ , then in general it should obey an equation of the form

$$\frac{\partial}{\partial x} M_i(x) = A_{ij}(x) M_j(x), \quad (\text{F.2.1})$$

where  $A_{ij}(x)$  is a  $N \times N$  matrix, given that there are  $N$  master integrals for a given topology. In our case  $x = \frac{1}{2P \cdot Q}$ . Before constructing a system of differential equations, one has to choose (obtain) suitable differential operators. We will discuss the construction of the differential operator in section F.3. We choose the operator  $p \cdot \frac{\partial}{\partial p}$ , which can be rewritten as

$$\begin{aligned} P \cdot \frac{\partial}{\partial P} M(x) &= \frac{\partial M}{\partial x} P \cdot \frac{\partial x}{\partial P} \\ &= \frac{\partial M}{\partial x} P \cdot \frac{\partial}{\partial P} \left( \frac{1}{2P \cdot Q} \right) \\ &= \frac{\partial M}{\partial x} P_\mu \left( \frac{(-1)}{(2P \cdot Q)^2} \right) (2Q^\mu) \\ &= -x \frac{\partial M}{\partial x}. \end{aligned} \quad (\text{F.2.2})$$

Now,  $M_1 = \text{topo1}(1,0,1)$ , which has no  $P$  or  $x$  dependance, therefore  $\partial_x M_1 = 0$ . Thus the first master is not part of the system of differential equations. For the second master  $\text{topo1}(0,1,1) = M_2$  we obtain

$$\frac{\partial M_2}{\partial x} = -\frac{1}{x} P \cdot \frac{\partial}{\partial P} \int d^D K \left( \frac{1}{(P-K)^2} \right) \left( \frac{1}{(Q+K)^2} \right). \quad (\text{F.2.3})$$

Here we use that

$$\begin{aligned} \frac{\partial}{\partial P} \left( \frac{1}{(P-K)^2} \right) &= \frac{-\frac{\partial}{\partial P} (P-K)^2}{((P-K)^2)^2} \\ &= \frac{-2(P-K)}{((P-K)^2)^2}, \end{aligned} \quad (\text{F.2.4})$$

thus

$$\begin{aligned}\frac{\partial M_2}{\partial x} &= \frac{1}{x} P \cdot \int d^D K \frac{2(P-K)}{((P-K)^2)^2} \left( \frac{1}{(Q+K)^2} \right) \\ &= \frac{1}{x} \int d^D K \frac{(-2P \cdot K)}{((P-K)^2)^2} \left( \frac{1}{(Q+K)^2} \right),\end{aligned}\tag{F.2.5}$$

since  $P^2 = 0$ . Notice that  $-2P \cdot K = (P-K)^2 - K^2$ , therefore

$$\frac{\partial M_2}{\partial x} = \int \frac{d^D K}{x} \left[ \left( \frac{1}{(P-K)^2} \right) \left( \frac{1}{(Q+K)^2} \right) - \left( \frac{K^2}{((P-K)^2)^2} \right) \left( \frac{1}{(Q+K)^2} \right) \right].\tag{F.2.6}$$

We recognize the first term on the right hand side as  $\text{topo1}(0,1,1)$ , however we need to reduce the second term  $\text{topo1}(-1,2,1)$  to a master integral. According to KIRA we have the following relation

$$\text{topo1}(-1,2,1) = \text{topo1}(0,1,1) \left( \frac{2x+D-2}{2x+2} \right).\tag{F.2.7}$$

Then eq. (F.2.6) becomes

$$\frac{\partial M_2}{\partial x} = \frac{\epsilon}{x(1+x)} M_2,\tag{F.2.8}$$

with  $D = 4 - 2\epsilon$ . As a boundary condition one could take  $M_2(x \rightarrow \infty) = M_1$ , given that the solution to  $M_1$  is known.

### F.3 Construction of the differential operators

We would like to construct differential operators (DOs) from the kinematic invariants in our calculation. A suitable choice of kinematic invariants is the orthogonal basis  $P \cdot P$ ,  $Q \cdot Q$  and  $\frac{2P \cdot Q}{Q^2} = \omega$ . However, since  $P^2 = 0$  we are confined to the  $Q^2 - \omega$  plane.

Let us start with the ansatz  $\partial_{Q^2} = (\alpha P + \beta Q) \cdot \partial_Q$ , which has to fulfil the following conditions:

1.  $\partial_{Q^2} (Q^2) = 1$ ,
2.  $\partial_{Q^2} (\omega) = 0$ ,
3.  $P^2 = 0$  or  $\partial_{Q^2} (P^2) = 0$ .



The first condition fixes the normalisation, the second condition corresponds to the orthogonality of the basis and the third is the on-shell condition. It is convenient to begin with the second condition:

$$\begin{aligned}
 \partial_{Q^2}(\omega) &= \alpha P \cdot (\partial_Q \omega) + \beta Q \cdot (\partial_Q \omega) \\
 &= \alpha \frac{2}{Q^2} P^2 + \beta \omega = 0 \\
 &\Rightarrow \beta = 0,
 \end{aligned} \tag{F.3.1}$$

since  $P^2 = 0$ . Thus we are left with  $\partial_{Q^2} = \alpha P \cdot \partial_Q$ . Notice that this operator satisfies the third condition  $\partial_{Q^2}(P^2) = 0$ . For the normalisation we obtain

$$\begin{aligned}
 \partial_{Q^2}(Q^2) &= \alpha P \cdot (\partial_Q Q^2) \\
 &= 2\alpha P \cdot Q = 1 \\
 &\Rightarrow \alpha = \frac{1}{2P \cdot Q} = \frac{1}{\omega Q^2},
 \end{aligned} \tag{F.3.2}$$

resulting in  $\partial_{Q^2} = \frac{1}{\omega Q^2} P \cdot \partial_Q$ .

Likewise one can make an ansatz for the differential operator in the  $\omega$  direction,  $\partial_\omega = (\alpha P + \beta Q) \cdot \partial_P$ . The corresponding conditions are

1.  $\partial_\omega(\omega) = 1$ ,
2.  $\partial_\omega(Q^2) = 0$ ,
3.  $\partial_\omega(P^2) = 0$ .

Starting with the third condition,

$$\begin{aligned}
 \partial_\omega(P^2) &= \alpha P \cdot (\partial_P P^2) + \beta Q \cdot (\partial_P P^2) \\
 &= 2\beta Q \cdot P = 0 \\
 &\Rightarrow \beta = 0.
 \end{aligned} \tag{F.3.3}$$

The first condition then becomes

$$\begin{aligned}
 \partial_\omega(\omega) &= \alpha P \cdot (\partial_P \omega) \\
 &= \alpha P \cdot \left( \frac{2Q}{Q^2} \right) \\
 &= \alpha \omega = 1 \\
 &\Rightarrow \alpha = \frac{1}{\omega}.
 \end{aligned} \tag{F.3.4}$$

Thus  $\partial_\omega = \frac{1}{\omega} P \cdot \partial_P$ . In our setup we choose to continue with this second operator.

## F.4 Series solution

Let us now solve eq. (F.2.8) using a series solution. We make the ansatz

$$\begin{aligned} M(x) &= \sum_{r=0}^{\infty} x^{r\epsilon} \sum_{n=0}^{\infty} x^{-n} a_{n,r} \\ r &\rightarrow 0 \\ &= \sum_{n=0}^{\infty} x^{-n} a_{n,0}. \end{aligned} \tag{F.4.1}$$

From now on we will omit the  $r = 0$  label on the coefficients. It will be convenient to expand in  $\omega = \frac{1}{x}$ , with  $\frac{\partial}{\partial x} = -\omega^2 \frac{\partial}{\partial \omega}$ , such that eq. (F.2.8) becomes

$$\frac{\partial M_2}{\partial \omega} = -\frac{\epsilon}{1 + \omega} M_2. \tag{F.4.2}$$

In terms of  $\omega$  the series of  $M_2$  and its derivative are

$$\begin{aligned} M_2(\omega, \epsilon) &= \sum_{n=0}^{\infty} \omega^n a_n(\epsilon) \\ \frac{\partial M_2(\omega, \epsilon)}{\partial \omega} &= \sum_{n=0}^{\infty} n \omega^{n-1} a_n(\epsilon). \end{aligned} \tag{F.4.3}$$

Notice that the left hand side of eq. (F.4.2) always is of a higher order in  $n$  for fixed  $\omega$  than the right hand side. This allows us to derive a recursive relation for the coefficients. Expanding both sides of the differential equation,

$$\begin{aligned} (1 + \omega) \sum_{n=0}^{\infty} n \omega^{n-1} a_n &= -\epsilon \sum_{n=0}^{\infty} \omega^n a_n \\ \Rightarrow \sum_{n=0}^{\infty} \omega^n ((n+1)a_{n+1} + n a_n) &= -\epsilon \sum_{n=0}^{\infty} \omega^n a_n. \end{aligned} \tag{F.4.4}$$

This results in

$$a_n = -\frac{(\epsilon + n - 1) a_{n-1}}{n}. \tag{F.4.5}$$

Thus by knowing  $a_{n=0}$ , one can recursively obtain all the coefficients. In other words,  $a_{n=0}$  is our boundary condition. And indeed, at  $M_2(x \rightarrow \infty) = M_2(\omega \rightarrow 0) = a_{n=0}$ , thus  $a_{n=0}$  has to be  $M_1$ .

## F.5 Full solution

By dimensional analysis one finds that

$$\begin{aligned}
 M_1 &= F(Q^2) = (Q^2)^{-\epsilon} A(\epsilon) \\
 M_2 &= F((P+Q)^2) = ((P+Q)^2)^{-\epsilon} A(\epsilon) \\
 &= (Q^2)^{-\epsilon} \left( \frac{2P \cdot Q}{Q^2} + 1 \right)^{-\epsilon} A(\epsilon) \\
 &= (Q^2)^{-\epsilon} (\omega + 1)^{-\epsilon} A(\epsilon),
 \end{aligned} \tag{F.5.1}$$

in which  $A(\epsilon)$  is dimensionless. By taking the derivative, we obtain

$$\begin{aligned}
 \frac{\partial M_2}{\partial \omega} &= -\epsilon (Q^2)^{-\epsilon} (\omega + 1)^{-\epsilon-1} A(\epsilon) \\
 &= -\frac{\epsilon}{1 + \omega} M_2,
 \end{aligned} \tag{F.5.2}$$

which is equal to eq. (F.4.2). After rewriting this as

$$\frac{\partial M_2}{M_2} = -\epsilon \frac{\partial \omega}{1 + \omega} \tag{F.5.3}$$

it becomes obvious that one can obtain the full solution by integrating both sides,

$$\int_{M_2(0)}^{M_2(\omega)} d \log(M_2) = -\epsilon \int_0^\omega \frac{d \omega'}{1 + \omega'} + \text{constant}. \tag{F.5.4}$$

Thus

$$\begin{aligned}
 \log \left( \frac{M_2(\omega)}{M_2(0)} \right) &= -\epsilon \log(1 + \omega) \\
 \Rightarrow M_2(\omega) &= M_2(0) (1 + \omega)^{-\epsilon}.
 \end{aligned} \tag{F.5.5}$$

Of course, we want to compare this with the solution found in eq. (F.4.3) and eq. (F.4.5). Let us choose the boundary condition to be  $M_2(0) = 1$ , which corresponds to  $a_{n=0} = 1$ . We then find that eq. (F.5.5) and eqs. (F.4.3) and (F.4.5) result in the same expression for small  $\omega$ , e.g. up to  $\mathcal{O}(\omega^3)$  we obtain

$$M_2(\omega) = 1 - \omega\epsilon + \frac{w^2\epsilon}{2} - \frac{w^3\epsilon}{3} + \frac{w^2\epsilon^2}{2} - \frac{w^3\epsilon^2}{2} - \frac{w^3\epsilon^3}{6}. \tag{F.5.6}$$

# Appendix G

## The Larin Scheme for the Non-Singlet Axial Current

In this appendix we will describe the Larin scheme for the non-singlet axial current [237, 238]. It provides a prescription to deal with the  $\gamma_5$ -matrix in dimensional regularization.

Let us recall the four spinor gamma matrices  $\gamma^\mu$  with  $\mu = \{0, 1, 2, 3\}$  obeying the Clifford algebra

$$\{\gamma^\mu, \gamma^\nu\} = 2g^{\mu\nu}. \quad (\text{G.0.1})$$

It is convenient to define a fifth gamma matrix as

$$\gamma^5 = \frac{1}{4!} \epsilon_{\mu\nu\rho\sigma} \gamma^\mu \gamma^\nu \gamma^\rho \gamma^\sigma \quad (\text{G.0.2})$$

which anti-commutes with the four gamma matrices. The Levi-Civita tensor  $\epsilon_{\mu\nu\rho\sigma} \gamma^\mu \gamma^\nu \gamma^\rho \gamma^\sigma$  is completely anti-symmetric in four dimensions. However, this tensor cannot be generalised to arbitrary non-integer dimensions without losing its properties. Therefore we require a prescription to resolve this issue. We will do this in the context of a non-singlet axial current, which occurs in the expressions for the deep inelastic scattering non-singlet coefficient function  $C_3$ .

The non-singlet axial current is defined as

$$A_\mu^a(x) = \bar{\psi}(x) \gamma_\mu \gamma_5 t^a \psi(x), \quad (\text{G.0.3})$$

in which  $\psi$  is a quark and  $t^a$  a flavour group generator. We will employ the  $R$ -operation in dimensional regularization to renormalize the theory<sup>1</sup>.

---

<sup>1</sup>The  $R$ -operation is a procedure to renormalize Feynman graphs by summing over all the UV-divergent 1PI subgraphs and multiplying each subgraph by its corresponding counterterm. For further reading see [239–241] or [114].

Whenever we use this operation, we take the Levi-Civita tensor outside of the operation, keeping the four-dimensional structure intact. All the indices inside of the operation are  $d$ -dimensional. Note that the  $\gamma_5$  matrix does not anticommute with  $\gamma_\mu$  in  $d$  dimensions. To correct for this, we will use the symmetric form of the axial current

$$A_\mu^a(x) = \frac{1}{2} \bar{\psi}(x) (\gamma_\mu \gamma_5 - \gamma_5 \gamma_\mu) t^a \psi(x), \quad (\text{G.0.4})$$

which is equivalent to [242]

$$A_\mu^a(x) = i \frac{1}{3!} \epsilon_{\mu\nu\rho\sigma} \bar{\psi} \gamma_\nu \gamma_\rho \gamma_\sigma t^a \psi. \quad (\text{G.0.5})$$

The axial Ward identity is violated if one uses eq. (G.0.2). In MS the renormalization constant for the axial current is not equal to one and receives higher order corrections in  $\alpha_s$  [114]<sup>2</sup>. At two-loop order it is

$$Z_A(a) = 1 + a^2 \frac{1}{\epsilon} \left( \frac{22}{3} C_F C_A - \frac{4}{3} C_F n_f \right), \quad (\text{G.0.6})$$

with  $a \equiv \frac{\alpha_s}{4\pi}$ . To obtain the expected value (from the axial Ward identity) of zero for the anomalous dimension of the axial current, we introduce an extra renormalization constant  $Z_5(a)$ , such that the expression of the renormalized axial current becomes

$$(A_\mu^a)_R = Z_5 Z_A (A_\mu^a)_B = Z_5 Z_A i \frac{1}{3!} \epsilon_{\mu\nu\rho\sigma} \bar{\psi}_B \gamma_\nu \gamma_\rho \gamma_\sigma t^a \psi_B, \quad (\text{G.0.7})$$

in which  $\psi_B$  are the bare quark fields. The anomalous dimension  $\gamma_A$  then becomes

$$\gamma_A = \mu^2 \frac{d}{d\mu^2} \log(Z_5 Z_A) = \beta(a) \frac{\partial \log Z_5}{\partial a} + \mu^2 \frac{\partial \log Z_A}{\partial \mu^2} = 0, \quad (\text{G.0.8})$$

where  $\beta$  is the QCD beta function. This equation can be solved to find an expression for  $Z_5$ . However, recall that the beta function (eq. (1.1.30)) starts at  $O(a^2)$ . This renders it impossible to perturbatively obtain  $Z_5(a)$  at the same order in  $a$  as the known approximation for  $Z_A(a)$ . Alternatively one can require that the renormalized vector and axial vertices coincide as

$$(R_{MS} V_\mu^a) \gamma_5 = Z_5 R_{MS} A_\mu^a, \quad (\text{G.0.9})$$

---

<sup>2</sup>Recall that renormalized operators  $(O)_R$  are related to the bare operators  $(O)_B$  as  $(O)_R = Z(O)_B$ .

---

which effectively restores the anticommutativity of  $\gamma_5$ . Here  $V_\mu^a = \bar{\psi}\gamma_\mu t^a\psi$  is the vector non-singlet quark current. Note that eq. (G.0.9) satisfies eq. (G.0.8), since the anomalous dimension for the vector current vanishes. Finally one obtains a result for  $Z_5$ , which at two-loop order becomes

$$Z_5 = 1 + a(-4C_F) + a^2\left(22C_F^2 - \frac{107}{9}C_FC_A + \frac{2}{9}C_Fn_f\right). \quad (\text{G.0.10})$$



# Appendix H

## $N = 100$ 3-loop DIS

The calculation of the 4-loop coefficient functions in chapter 3 required around 1500 Mellin moments. We were able to achieve such a high number, by using our new sophisticated and efficient algorithm. In principle we would be able to provide all the 1500 moments to the reader in this thesis, however the expressions become increasingly complex and lengthy at each succeeding moment. To demonstrate this, as a proof of concept, we will print the 100<sup>th</sup> Mellin moment for the non-singlet splitting functions  $p_{qq,ns}^{(2)}(N = 100)$  and coefficient functions  $c_{2,ns}^{(3)}(N = 100)$ ,  $c_{L,ns}^{(3)}(N = 100)$  and  $c_{3,ns}^{(3)}(N = 101)$  at 3-loop order (order  $\alpha_s^3$ ), calculated using our new algorithm as explained earlier in the thesis, and in agreement with [12], [43] and [44]. Higher moments would be too lengthy to print in a thesis. On top of that, we also provide for the first time ever the  $O(\epsilon)$  contributions to the 100<sup>th</sup> Mellin moment of the coefficient functions at 3-loop order<sup>1</sup>. The higher  $O(\epsilon)$  terms are required for the renormalization of 4-loop coefficient functions.

The following results will include the  $G$ -scheme constant  $G_{00}$  for generality. The constant represents the fundamental one-loop integral. In general the  $G$ -functions are defined by the integral [243]

$$\int \frac{d^{4-2\epsilon} p \, p^{(\mu_q, \dots, \mu_n)}}{(2\pi)^{4-2\epsilon} p^{2\alpha} (p-k)^{2\beta}} \equiv \frac{1}{(4\pi)^2} \frac{k^{(\mu_q, \dots, \mu_n)}}{(k^2)^{\alpha+\beta-2+\epsilon}} G^{(n)}(\alpha, \beta), \quad (\text{H.0.1})$$

$$G^{(0)}(\alpha, \beta) \equiv G(\alpha, \beta) = G(\beta, \alpha),$$

in which the tensors  $p^{(\mu_q, \dots, \mu_n)}$  and  $k^{(\mu_q, \dots, \mu_n)}$  are traceless and symmetric. Explicitly they can be calculated as

$$G^{(n)}(\alpha, \beta) = (4\pi)^\epsilon B(n+2-\alpha-\epsilon, 2-\beta-\epsilon) \times \frac{\Gamma(\alpha+\beta-2+\epsilon)}{\Gamma(\alpha)\Gamma(\beta)}, \quad (\text{H.0.2})$$

---

<sup>1</sup>For  $c_3$  we provide the 101<sup>th</sup> moment.



in which  $B(a, b)$  is the Euler beta-function

$$B(a, b) = \frac{\Gamma(a)\Gamma(b)}{\Gamma(a+b)} = \int_0^1 dx (1-x)^{a-1} x^{b-1}. \quad (\text{H.0.3})$$

We define  $G(0, 0) \equiv G_{00}$ . One normally neglects this constant, however if it is consistently provided a different value, QCD observables should remain unaffected. Note that the splitting functions at  $O(\epsilon^{-1})$  and coefficient functions at order  $O(\epsilon^0)$  remain invariant. Higher order terms in  $\epsilon$  will differ.

As explained in app. G the operator renormalization in  $c_{3,ns}$  requires special attention due to the  $\gamma_5$  originating from the axial-vector coupling of the  $W$ -boson. The value of the constant  $Z_A$  has been inserted and the  $O(\epsilon^0)$  parts of  $Z_5$  have been substituted. The  $Z_5$  terms are kept open for generality at higher orders in  $\epsilon$ . By using the fact that  $c_2$  and  $c_3$  become identical in the soft limit, one can fix the coefficients of  $Z_5$  at the different order in  $\alpha_s$ ,  $\epsilon$  and colour factors.

$$\begin{aligned} p_{qq,ns}^{(2)}(N=100) = & \\ & + C_F^3( \\ & - 526157017682052035590161402948771842527011902371885529774307793272 \\ & 754614469166157721484922616589287061198171235024111571174221185902585 \\ & 798824663457638702069600464965593792193564457223262524795684778161147 \\ & 592947701/33817031875127029884959496403553805613265624055141577497830 \\ & 811768723291267948893586740559857791759102311644513845587164006559058 \\ & 516556895775995223986476571289883372231100987417334849887008991286197 \\ & 104640000000000 \\ & + 137330585797559864276651550142241940646269342400477431535195411889 \\ & 13671016888438479/362219161238280186895347600369529741321744716147316 \\ & 481578188199010598884440440000\zeta_3) \\ & + C_A C_F^2( \\ & - 241630725825751820705309081659119993968258084196022976517388641907 \\ & 733459856884710363458093255372053088080780343352180612500969960997532 \\ & 046786276639733399710424742978789880652678860978742410433/ \\ & 440969379132504164520403558950536682762329164189068145117525908125882 \\ & 535569107434279831384412811018409365417452479541710548004530868840184 \\ & 1550520975574864671795788113860538588282880000000000 \\ & - 137330585797559864276651550142241940646269342400477431535195411889 \end{aligned}$$

---


$$\begin{aligned}
& 13671016888438479/241479440825520124596898400246353160881163144098210 \\
& 987718792132673732589626960000\zeta_3) \\
& + C_A^2 C_F ( \\
& + 272780668692195751322772300410694974556378106121932738420200243492 \\
& 252526860404042108174954425024500263988267682414129042639539518554944 \\
& 838797842296080658285650962030380661/ \\
& 635133429943650364046684529279031204879806738017704337654648071602877 \\
& 869794936464640201328888151201665642422726621909000366129507254586561 \\
& 134197701174803021824000000000 \\
& + 137330585797559864276651550142241940646269342400477431535195411889 \\
& 13671016888438479/724438322476560373790695200739059482643489432294632 \\
& 963156376398021197768880880000\zeta_3) \\
& + n_f C_F^2 ( \\
& - 106241733900341856546875447724257436114237282755084703240194251891 \\
& 444021253291419685352651336355981658071878278316015842037599758488440 \\
& 81625136526293922681818766438561595757/ \\
& 768377041392273038152634280639497558307903474214316017414895709373438 \\
& 641418046131963440658560775973997685901064332296001586308660235882785 \\
& 07840928849877503148236800000000 \\
& + 31246589580262017971960074362943348349524891/220054934318780006050 \\
& 559834452079458101150\zeta_3) \\
& + n_f C_A C_F ( \\
& - 438521882246775353997206828340983512413978350138506237837272291138 \\
& 846823892881081287505882991924272713948147944974879757301955788379050 \\
& 088505111704781/11271970634510094912738512768470280323186780497162251 \\
& 470746860733028698432094848046182461798257207407885368969700579311114 \\
& 350237221663077068800000000 \\
& - 31246589580262017971960074362943348349524891/220054934318780006050 \\
& 559834452079458101150\zeta_3) \\
& + n_f^2 C_F ( \\
& - 764618759589378287499209497078589053101005916220431936837453063605 \\
& 405600559548229173590037846685142292168942246311704296890440881/ \\
& 196410994882320885652593227825077464195129304709686687203387624005411 \\
& 615381328825645590814639586733066928129849222388608768000000)
\end{aligned}$$

$$\begin{aligned}
 c_{2,ns}^{(3)}(N = 100) = & \\
 & + C_F^3( \\
 & + 870428654015078951219549159187643535972390571435951269203263593935 \\
 & 872331253377371593947103501969436715490097410037252333195666622569451 \\
 & 041601298911346339386347118469802350808327821898912359697587007774565 \\
 & 854103115351210107335151399211249579680767393582059393369/ \\
 & 245275291839401071410471414811179938261687300226513560910473469829069 \\
 & 600389414494475101922509624464688562660187924654688640412708134256642 \\
 & 693306237664864089591239334204993419175374652490709504012411054424103 \\
 & 73161669767074025344482182086150291456000000000000 \\
 & + 184369585650133256712391915159670412705885379706018826366059758558 \\
 & 579179949053391348181697690501517443380781579405299720150499370981/ \\
 & 403316038135547273170197417583392719539440159192538452590688302881925 \\
 & 7652367796858352442964090397429404624675931001998944000000\zeta_3 \\
 & + 137330585797559864276651550142241940646269342400477431535195411889 \\
 & 13671016888438479/724438322476560373790695200739059482643489432294632 \\
 & 963156376398021197768880880000\zeta_4 \\
 & - 346874762066880121174840575440619118191578563/62872838376794287443 \\
 & 01709555773698802890\zeta_5) \\
 & + C_A C_F^2( \\
 & + 184963427523969443529482964892942507804125085617542270519609481446 \\
 & 215585735580980914145014548925032599058419827693449731400113184530755 \\
 & 068664506777193488810956927105251014227424271900766954929211681764075 \\
 & 1416886846466355369967066063421659/ \\
 & 606004218307367512534358014743108840408447017829916354150296319210687 \\
 & 903284102024724126661710854052213806550255875245482118459644013398473 \\
 & 923134768630351429835144944828696238021894775708440838207338227451859 \\
 & 96724286788730880000000000 \\
 & - 761043391539873536313304149868107970495471878545818189634863429722 \\
 & 0506640036681560700872682766594900335522801457524146833016321393989/ \\
 & 187317893267398622427936133944286840852762207269423414647675234005161 \\
 & 077632193231865702350998865125054570346059906537284288000000\zeta_3
 \end{aligned}$$

---


$$\begin{aligned}
& -137330585797559864276651550142241940646269342400477431535195411889 \\
& 13671016888438479/482958881651040249193796800492706321762326288196421 \\
& 975437584265347465179253920000\zeta_4 \\
& +133235190664280708268868528314805257456559559/25149135350717714977 \\
& 20683822309479521156\zeta_5) \\
& + C_A^2 C_F ( \\
& +449074584527462040871619510713548644006286422897639358376542298934 \\
& 027034702784774296021434943024443916291745819800842971302776432877498 \\
& 341555998487148268245624786868748192784546325273292898908581228304429 \\
& 46968136572263/230331476105934058426096616670085718853102720920839965 \\
& 295012186518496850363500837680394791193382348271421621648164422146923 \\
& 290070279989623808201910469051404989357566299987945699549876630993663 \\
& 2975720448000000000000 \\
& +221109924013392596255251083727874142559332602131016082669260665169 \\
& 93029784300298822890767457371202410948932661/ \\
& 137396205149658873624931721030054644306896799889380841754946493350293 \\
& 05426021624490092551147132666704000000\zeta_3 \\
& +137330585797559864276651550142241940646269342400477431535195411889 \\
& 13671016888438479/144887664495312074758139040147811896528697886458926 \\
& 5926312752796042395537761760000\zeta_4 \\
& -341271466883348638892459002792698348923564213/29340657909170667473 \\
& 407977926943927746820\zeta_5) \\
& + n_f C_F^2 ( \\
& -899455605932450077972769975103318789650427467769349233841126285331 \\
& 194058043066379378855879148522289229320708167821421449038879108159586 \\
& 854144052280994565238279245843584460565054853960712128958719324037289 \\
& 203553017877501/10031484335437682145074385013150200897119114719717197 \\
& 548956532003074077121724359793570719676215347420109726228587154976330 \\
& 905679118351437562991223243348410107431003538633796907478209870482347 \\
& 17513750912040960000000000 \\
& -602711952525646156276193861435952249612166646718265821947926644040 \\
& 937995614735511867751/13680520962263001589066679532105202974648485250 \\
& 41628433231914676138596247255961476800\zeta_3 \\
& +31246589580262017971960074362943348349524891/440109868637560012101
\end{aligned}$$

$$\begin{aligned}
 & 119668904158916202300\zeta_4) \\
 & + n_f C_A C_F ( \\
 & - 184846395882508945799614704766413599807115671888479287131198761776 \\
 & 308047899884147373458058666100881050869824340997792398199966265446663 \\
 & 062429106038022559977454625360823913604222544367371444123311 / \\
 & 348390864593038091344102925409500714421033353866420031696545326846045 \\
 & 264607297663276196329560235068805808302822541365198021022897825637656 \\
 & 85659087593959371171204791888199311971632640000000000 \\
 & + 676893868303290299338435730994050933226724454418799500664571165717 \\
 & 35610986290368120173/929563645271219288715460655452692883154138970616 \\
 & 52096996926836856631467004384880000\zeta_3 \\
 & - 31246589580262017971960074362943348349524891/440109868637560012101 \\
 & 119668904158916202300\zeta_4) \\
 & + n_f^2 C_F ( \\
 & + 163836931859299757843369748314125627789658498579759920696563294411 \\
 & 669073841376990463402888166944160087167095337083211497093819283692576 \\
 & 6580001222051703656009852212244111514343 / \\
 & 414923602351827440602422511545328681486267876075730649404043683061656 \\
 & 866365744911260257955622819025958750386574739439840856606676527376703 \\
 & 9423410157893385170004787200000000 \\
 & + 31246589580262017971960074362943348349524891/594148322660706016336 \\
 & 5115530206145368731050\zeta_3 \\
 & )
 \end{aligned}$$

$$\begin{aligned}
 & c_{L,ns}^{(3)}(N = 100) = \\
 & + C_F^3 ( \\
 & - 609147246477604304735828772177608286630890539376845633557523807837 \\
 & 285530381441714615068256964240195545893143492519005615846711118339774 \\
 & 23336350032240816791127312237245283854234713102579308228313 / \\
 & 157198599071120040403410843793260348754906307704576162134170721139590 \\
 & 329567959266483847749879752730812571032363018969127830787466538443877 \\
 & 25359831989801547922107228668002613707171840000000000
 \end{aligned}$$

---


$$\begin{aligned}
& -417857672263426965859578123849997518788437655902957148713940259053 \\
& 658222848661480013485989/39901519473267087968111148635306842009391415 \\
& 313714162635930844720709057211632209740000\zeta_3 \\
& + 1611840/101\zeta_5) \\
& + C_A C_F^2 ( \\
& + 839468122107342915036345592465981392184443815576200211465096917852 \\
& 841644485554583897078224975261839919429896136578927158602420637362955 \\
& 752942654339938289675744872532832163474721218353113239281659/ \\
& 215146639187279663426533736393235528905620597475403247644182377280364 \\
& 794985559258724949312289829375823937758936025544824041052736902849921 \\
& 427228049703047344776562925344669435333591040000000000 \\
& + 844932546645814524259903166054625220595354629341177245757281066618 \\
& 413644597785645181161299/79803038946534175936222297270613684018782830 \\
& 627428325271861689441418114423264419480000\zeta_3 \\
& - 1612640/101\zeta_5) \\
& + C_A^2 C_F ( \\
& - 503156465077490075738228952028313758566317562511990184670404330584 \\
& 889056033104052898962666661971732804626942088033327455631120882331043 \\
& 49940987832117946743403728912157125739/ \\
& 56073208529310846425835862727773263736743662992773258100817868929397 \\
& 890761815335925206316075539203756238596064360485374608954336404763563 \\
& 97276311332289752498176000000000 \\
& - 428650304918601725427852769025821526852573191556741285397720941021 \\
& 57354094587298850497851/159606077893068351872444594541227368037565661 \\
& 25485665054372337888283622884652883896000\zeta_3 \\
& + 403360/101\zeta_5) \\
& + n_f C_F^2 ( \\
& - 112435762527684201020219516279162646688123949839725354388315718259 \\
& 070152828782838714426758018154915081465757797972269808891745503371065 \\
& 775969367653996971/21986683220776597008228515311949311162896014533496 \\
& 044134408673538568290585453007042081778141363074124543405010961586232 \\
& 535484784590680185765011200000000 \\
& - 480414539333753162588447359213502070946197002/33998487352251510934 \\
& 811494422846276276627675\zeta_3)
\end{aligned}$$

$$\begin{aligned}
 & + n_f C_A C_F ( \\
 & - 130650414750560699441140177157865385281663576102077801882497537866 \\
 & 536550233184000909652712173633118997533551048769069884099991943776372 \\
 & 461093934629950584971/65280857071747385255718486848983756747814424141 \\
 & 631620940856168522236227532333146057222610188435234341268082125615450 \\
 & 29121525918022824924858625305600000000 \\
 & + 25625220434926117896969311985587217964141754764642/280375325647812 \\
 & 5352261099510568863865704654474225\zeta_3) \\
 & + n_f^2 C_F ( \\
 & + 6343491175726639348317210396092737889290669826143838095068728975161/ \\
 & 5217505736497266095375656610116722484070574294596562374874093270000 \\
 & )
 \end{aligned}$$

$$\begin{aligned}
 & c_{3,ns}^{(3)}(N = 101) = \\
 & + 164349012000605756828319589219300768183683853181886882447709026000223 \\
 & 082488763426293884062907458598660988306324292098711378285807972780409157 \\
 & 8244026218259605507336590319841959/ \\
 & 414923602351827440602422511545328681486267876075730649404043683061656866 \\
 & 365744911260257955622819025958750386574739439840856606676527376703942341 \\
 & 0157893385170004787200000000 C_F n_f^2 \\
 & + 1252652671632905412915875168184201074406811/2376593290642824065346046 \\
 & 21208245814749242 C_F n_f^2 \zeta_3 \\
 & - 221990991508168332828611396538998332873874437159924082114317589812228 \\
 & 735529948782364632482797714428850257752548821827766931169343756209246701 \\
 & 40967013073441165728353049096995500644128547131373407/ \\
 & 417547103632105577640872419966442803800489412873612023007095522811739642 \\
 & 975038397934018072881180606808459389150611374020100102349453947753535989 \\
 & 0647965168080444020001581940011581440000000000 C_F C_A n_f \\
 & - 1252652671632905412915875168184201074406811/1760439474550240048404478 \\
 & 6756166356648092 C_F C_A n_f \zeta_4 \\
 & + 329143061282214192204789868345316503322239245121721054356080734363497 \\
 & 8424357731144490379/4560173654087667196355559844035067658216161750138761
 \end{aligned}$$

---


$$\begin{aligned}
& 444106382253795320824186538256000C_FC_An_f\zeta_3 \\
& + 473196313669475993618073546280433315011649390704025953677894889313372 \\
& 256822929661572994203520080346861297400434670538578915790022452144826747 \\
& 208350200164766181157653072120090389804335301942973983525964674906296162 \\
& 493/39039233238293908207812985876285715059847918800142366999154607884490 \\
& 991587034040284812676473454635300240952821722783414732761028861015190475 \\
& 966425503229051693111451915252194186364385869659942931791872000000000000 \\
& C_FC_A^2 + 107860021987265044581147076645670301017955815/ \\
& 5868131581834133494681595585388785549364C_FC_A^2\zeta_5 \\
& + 274661144856911747872874079174626414568313258512994270880938896437968 \\
& 0723812190531/2897753289906241495162780802956237930573957729178531852625 \\
& 50559208479107552352000C_FC_A^2\zeta_4 \\
& - 248744536445185265419936402276245613579046867703816688519139243601036 \\
& 790590557374257844552730495625074258263783/13739620514965887362493172103 \\
& 005464430689679988938084175494649335029305426021624490092551147132666704 \\
& 000000C_FC_A^2\zeta_3 \\
& - 906899749313008454709967346282514409302542989956880352479542575835231 \\
& 477252349861826809875785991769127059963698080167982531722021050976670696 \\
& 606104676032148702096351784149560266321679851869203907508834280477741304 \\
& 816561/10031484335437682145074385013150200897119114719717197548956532003 \\
& 074077121724359793570719676215347420109726228587154976330905679118351437 \\
& 562991223243348410107431003538633796907478209870482347175137509120409600 \\
& 0000000C_F^2n_f \\
& + 1252652671632905412915875168184201074406811/1760439474550240048404478 \\
& 6756166356648092C_F^2n_f\zeta_4 \\
& - 293273222480185581303677425511394028384110578189896589729016148846979 \\
& 7146070698653835983/6840260481131500794533339766052601487324242625208142 \\
& 166159573380692981236279807384000C_F^2n_f\zeta_3 \\
& + 916241283215449798644071034343109524977845924941517183614407687003488 \\
& 518753372146150458914014233376233844154374199196857118200609483305318688 \\
& 627317532769289182970625353749642621380190236465553304929748229239471262 \\
& 49521658572190981431076941/ \\
& 151501054576841878133589503685777210102111754457479088537574079802671975 \\
& 821025506181031665427713513053451637563968811370529614911003349618480783
\end{aligned}$$





---

316251831708808542513531545278381782709752335212573729607382419954022  
 192075067759518259499990247123278425584420451311108065980151503896620  
 336762451592482824329707681838986227574731892046842273109563090758037  
 2508319031412460399646008921733/  
 426956232059989788648491574767419479659653824816286102114980381318917  
 559520918116953494621466978605491675014768075509569185169727604285140  
 013589400078546144575858228987765190936225665288882087727996980699006  
 672932885640725196961567703101941886871708035418970240991507093454142  
 81320737013760000000000000  
 – 458377465019485018519314525228127315819264819351916452765271070815  
 299296639041152379636459089655387804432666368662744738067911086452588  
 879459196019611524768423717868130236932810948871994180128378607608726  
 38597017043/361921411372596975357426048466127685493143802596832936431  
 634105886001779456309229021972546973022170994639673726775514798732404  
 639642080489910316778450585378353266859998405216506593711165313619116  
 4907520000000000 $\zeta_2 G_{00}\zeta_2$   
 + 346568908967995659673448589198898994027013445189368416313790881216  
 312000338393334853405578211883409634275641282152914854310362632104266  
 77988124876538910503103517719977447920697/  
 812570976089575823540799151047092264362893536477240692658954204619498  
 658971695715111656892610772757988581511602023657125282012417906945820  
 06547489450593145025881600000000 $\zeta_3$   
 – 793715381941185551259339682590756392327407545797804820533306808697  
 1680255779721204441/4966581960824880254930439212759128953123153511789  
 166372408618959510711627039110000 $\zeta_3\zeta_2 G_{00}\zeta_2$   
 – 3693783881329131225217122819443657390685906479/3143641918839714372  
 1508547778868494014450 $\zeta_3^2$   
 + 184369585650133256712391915159670412705885379706018826366059758558  
 579179949053391348181697690501517443380781579405299720150499370981/  
 268877358757031515446798278388928479692960106128358968393792201921283  
 8434911864572234961976060264952936416450620667999296000000 $\zeta_4$   
 – 241706963938392401712738811060020987998492732152011998750392289794  
 628257190123933534585131/21000799722772151562163762439635180004942850  
 16511271717680570774774160905875379460000 $\zeta_5$

$$\begin{aligned}
 & - 346874762066880121174840575440619118191578563/25149135350717714977 \\
 & 20683822309479521156\zeta_6) \\
 & + C_A C_F^2 ( \\
 & + 326587820993512134162148070806082496467093915063166310815981761006210 \\
 & 795349958040266136874038958419826577202705732728838855425639674666888 \\
 & 765895311675236365001779161290500024090327353602370408155573917996387 \\
 & 0505565227138831081718697892786472957535628291921755288287949541719147 \\
 & 059513/ \\
 & 823587236353236786965341917431539789736262961494823279294156395245249 \\
 & 420185358901564505450502920819211433592698629570196698167532311927056 \\
 & 079917421522958584997481488502273733035608552970784238798745189960012 \\
 & 714230128154028609031645968445353101225349647809634107392000000000000 \\
 & - 337493304005820001163564665983490112838048044445919101042540232436 \\
 & 167378142596986042347898477451474470227115555548670230851398710460185 \\
 & 30564343952198939459365184689562016443450848177149701793861/ \\
 & 225175853174044679755099689676869795453104254053992244315332378617471 \\
 & 933056565498355658579274626903017548298273606574490492598058316003498 \\
 & 2919414966250994726023381164524530342952960000000000\zeta_2 G_{00}\zeta_2 \\
 & - 519717940228509558736016006342619100007475620408559466945409915107 \\
 & 791413612629219837742448767151501988017234739685698878173284364732718 \\
 & 2235346718349685967226725736216225822096071/ \\
 & 135861867202177077696021618055073826601475799298994643812577143012380 \\
 & 175780067523566669032444521205135690828739858355471347152476274041341 \\
 & 114947402361391738483274035200000000\zeta_3 \\
 & + 114738780871741279952440638561833973596417205150023231649274169411 \\
 & 9645446748561997723599/1033049047851575093025531356253898822249615930 \\
 & 452146605460992743578228018424134880000\zeta_3\zeta_2 G_{00}\zeta_2 \\
 & + 49119930846562868839692236356427334379662546293/440109868637560012 \\
 & 101119668904158916202300\zeta_3^2 \\
 & - 761043391539873536313304149868107970495471878545818189634863429722 \\
 & 0506640036681560700872682766594900335522801457524146833016321393989/ \\
 & 124878595511599081618624089296191227235174804846282276431783489336774 \\
 & 051754795487910468233999243416703046897373271024856192000000\zeta_4 \\
 & + 379389505092015732409930272967649624945952195901979545919955339568
 \end{aligned}$$

---


$$\begin{aligned}
& 410729800745535349506229/44335021636963431075679054039229824454879350 \\
& 34857129181770093857856561912403578860000\zeta_5 \\
& + 666175953321403541344342641574026287282797795/50298270701435429954 \\
& 41367644618959042312\zeta_6) \\
& + C_A^2 C_F( \\
& + 745655913615671305688627992642311910100829097844807824160784460432 \\
& 102401519586703405814889124291012784490129062422221042194112341791605 \\
& 481207507966603138306506988651079267000426047797594207963208616360054 \\
& 2623139692104643401073234096382723777107931262613855944251087/ \\
& 551296893115796620842198315924100684543323242991570696416315524876317 \\
& 162600046358950757326029214860219871772200006431872130404857114155058 \\
& 65785570303658343010253928406368882108384395966605522694985626661212 \\
& 99578758028388317031830002482994059673600000000000000 \\
& - 464793346419649005405603001230484153892505014947085122769786776946 \\
& 471701210533694086687722890950528889449789142438760689820034137306544 \\
& 7264213695042409694092691035810734221/ \\
& 127026685988730072809336905855806240975961347603540867530929614320575 \\
& 573958987292928040265777630240333128484545324381800073225901450917312 \\
& 2268395402349606043648000000000\zeta_2 G_{00}\zeta_2 \\
& + 410046832828924984220215717813947202613653941505729067201904400232 \\
& 997897965205377461805284799979166640730785135248722654888530974693591 \\
& 444151379855347574500991233288460309278617/ \\
& 203792800803265616544032427082610739902213698948491965718865714518570 \\
& 263670101285350003548666781807703536243109787533207020728714411062011 \\
& 672421103542087607724911052800000000\zeta_3 \\
& + 102468834860950679194956367583005501847755469992228040424105966772 \\
& 8686989121987518321/1448876644953120747581390401478118965286978864589 \\
& 265926312752796042395537761760000\zeta_3\zeta_2 G_{00}\zeta_2 \\
& - 215206734459685740277941700951746196217462309/86296052674031374921 \\
& 78817037336449337300\zeta_3^2 \\
& + 221109924013392596255251083727874142559332602131016082669260665169 \\
& 93029784300298822890767457371202410948932661/ \\
& 915974700997725824166211473533697628712645332595872278366309955668620 \\
& 361734774966006170076475511136000000\zeta_4
\end{aligned}$$

$$\begin{aligned}
 & - 827012477494238165373895271836641391466787003845648212726446021537 \\
 & 554192323139430309649969/79803038946534175936222297270613684018782830 \\
 & 627428325271861689441418114423264419480000\zeta_5 \\
 & - 341271466883348638892459002792698348923564213/11736263163668266989 \\
 & 363191170777571098728\zeta_6) \\
 & + n_f C_F^2 ( \\
 & - 934281362335128697167069347589103478775865996165765477078944325352 \\
 & 701897103228223566256341038827308872830918316677640405771185807115545 \\
 & 362361105905740232451305911244054724922980694951897183938113942612575 \\
 & 776103757272614123755571230492941246027210885880700143417/ \\
 & 141879143893061764017008385963083376010972506413932730214271771947457 \\
 & 599663655699155832912704759957110126803787188427843762513212708057194 \\
 & 509852116416881719777592987985198018533175650159596090773061922671436 \\
 & 62678284231708667521132550395919859712000000000000 \\
 & + 343296322815534833344838482178221968692278668744258198936846963171 \\
 & 832056906343438076242278355646086725810964597120422910975172354513485 \\
 & 54042313666855387444602910714221687429/ \\
 & 113833635761818227874464337872518156786356070253972743320725290277546 \\
 & 465395266093624213430897892736888546059416938117926160934616331241894 \\
 & 08569026496278148614553600000000\zeta_2 G_{00}\zeta_2 \\
 & - 815579930203428150552086016694561792599960064794825010503152068950 \\
 & 2360743711006663670166709240134860371318008716757763126234566989521/ \\
 & 572451715578720405463835591757210664188496371886007160588115193152036 \\
 & 2163682740415588112506899383656887473982336264617446208000000\zeta_3 \\
 & + 20962137030127130465419692206895430451861323/440109868637560012101 \\
 & 119668904158916202300\zeta_3\zeta_2 G_{00}\zeta_2 \\
 & - 602711952525646156276193861435952249612166646718265821947926644040 \\
 & 937995614735511867751/91203473081753343927111196880701353164323235002 \\
 & 7752288821276450759064164837307651200\zeta_4 \\
 & - 25013588034725722513450751844126428411546971/200049940289800005500 \\
 & 50894041098132554650\zeta_5) \\
 & + n_f C_A C_F ( \\
 & - 309196222879269299242865283584434808497126416991060391730486262273 \\
 & 735608954657450215941713327116343759733124859267247329504165901789820
 \end{aligned}$$

---


$$\begin{aligned}
& 211321911117214011839049305335869057001808821311020705515633159152050 \\
& 702959927440686208677475872880961499/ \\
& 626382177056787793325566180379716901767252190436520935777533396141892 \\
& 373271296300555518949102891574040010256435254148983365752917253989866 \\
& 268085251167041064183474642797407678420166237356383126956915974184836 \\
& 2443103657335193600000000000 \\
& + 178911840106831547483822093910838565732721993484267797706823863569 \\
& 841352848503885222478455614429179243370046566823463520051845679178133 \\
& 76417740879/142345102969183567669045671826504208494531569764369767002 \\
& 695948174082736186302443673269173033756314927810613965257567847430078 \\
& 08633815040000000\zeta_2 G_{00}\zeta_2 \\
& + 939693063615950237645918963405019060118093967113912695191726811761 \\
& 25562815795658296629506417865638546443392886473449989250838514575821/ \\
& 913914142415150121003667348243967902476371400730292133570499694330443 \\
& 7840265427681026635756628840575030879515659650529607104000000\zeta_3 \\
& - 26104363305194574218689883284919389400693107/440109868637560012101 \\
& 119668904158916202300\zeta_3\zeta_2 G_{00}\zeta_2 \\
& + 676893868303290299338435730994050933226724454418799500664571165717 \\
& 35610986290368120173/619709096847479525810307103635128588769425980411 \\
& 01397997951224571087644669589920000\zeta_4 \\
& + 2874138474437166555136855589884227914766160693/1789394071171132154 \\
& 463762864360330330348825\zeta_5) \\
& + n_f^2 C_F ( \\
& + 106963724894313924921874355943219881515242841943658856349558775320 \\
& 875709909849949268514872651017203988963730752353177984003113893125239 \\
& 017309193324900391603735696679441223657176568204025858270872044107508 \\
& 502142436746983/29217915540109753820605004892670488049861499183642322 \\
& 958125821368176923655507844058943843717132079864397260859962587309701 \\
& 667026558305157950459873524315757594459233607671253128577310302375768 \\
& 471274298408960000000000 \\
& - 287786247463969247791895796868267956487550934146995062036732124116 \\
& 1664945196314692745567984973334981046162770240487748179833016647/ \\
& 280587135546172693789418896892967805993041863870980981719125177150588 \\
& 02197332689377941544948512390438132589978460341229824000000\zeta_2 G_{00}\zeta_2
\end{aligned}$$

$$\begin{aligned}
 & - 664290151329703350323468266536427350656378918121233501680805955635 \\
 & 1362152441807905406481/4183848643798879126753401992828290230110944518 \\
 & 3311937521170206114918234746177462640000\zeta_3 \\
 & + 31246589580262017971960074362943348349524891/396098881773804010891 \\
 & 0077020137430245820700\zeta_4 \\
 & )
 \end{aligned}$$

$$\begin{aligned}
 & c_{L,ns}^{(3),\epsilon}(N = 100) = \\
 & + C_F^3( \\
 & + 500487761292753334114233383802143431708507147913862899182721171441 \\
 & 757052303416383099594829242643515137841940427058024497682391478635348 \\
 & 258622173347169897959054192960343157721395697564505908711553378470026 \\
 & 407884264264600440802324698884109837/ \\
 & 469067104393716088757062978227125094253651363577724689897733081008094 \\
 & 215614919149047997742691816570325909936183918912109410590452133287524 \\
 & 123688318308150738435640837875961827689119892239204616061825861620662 \\
 & 14577585971961856000000000000 \\
 & - 163595957208195871092440097174303013487885580455587303351273609587 \\
 & 605813387605080057824412929135207536459779839027079635256428015422300 \\
 & 01131058821/131726084913918056416003076540374919023206270056045841987 \\
 & 507715648570301137558824518313564236173643444342886590967927895512903 \\
 & 8332220221440000000\zeta_2 G_{00}\zeta_2 \\
 & - 184168122206759900817311979250100213078055253578395971521636443024 \\
 & 7101855089309929756369859794704392689582018310683576128215319022380063/ \\
 & 14470307254906543582558066347196158455875880511562958781532911826898 \\
 & 693247086927161625506614662330910465559233127780005211248000000\zeta_3 \\
 & - 31246589580262017971960074362943348349524891/370425806103279676851 \\
 & 7757213276670878036025\zeta_3\zeta_2 G_{00}\zeta_2 \\
 & + 3553344/101\zeta_3^2 \\
 & - 417857672263426965859578123849997518788437655902957148713940259053 \\
 & 658222848661480013485989/26601012982178058645407432423537894672927610 \\
 & 209142775090620563147139371474421473160000\zeta_4
 \end{aligned}$$

---


$$\begin{aligned}
& + 1170185496411019789411783636743494688278465565427/1760947293629437 \\
& 2330338261213884481558663565\zeta_5 \\
& + 4029600/101\zeta_6) \\
& + C_A C_F^2 ( \\
& - 115372227747727795945204361546191576324805002175376679112196759537 \\
& 999372675310807639090730310868942247964649169416880052445648842503582 \\
& 992734078302934566804623566884685306185538721966886444992063768857849 \\
& 24585204490783343559357476428173074699/ \\
& 988291879356265185024782195710220000566109011577621920893441580579430 \\
& 188939156385320929897473451150152016182375623212840421521269445184011 \\
& 222978951841331456822815547524798781507373396717848933643134092602741 \\
& 629911910379552768000000000000 \\
& - 402504975612677290660108575159883546720128616191755215731507450991 \\
& 680951934821676243685462467348421356854769823232807632838727768779997 \\
& 565679995047/22771657847495141237855581350445010753912687873055053476 \\
& 256284309148885721403733426631235956075166480576502969092079416392626 \\
& 741861945610240000000\zeta_2 G_{00}\zeta_2 \\
& + 843987913669747393518919474178965527773904893309075425356768277801 \\
& 2528572298582725530073272533546844534164154584882265573590339464383/ \\
& 654765034158667130432491689918378210673116765229093157535425874520302 \\
& 86185913697563916319523358963395771761235872307715888000000\zeta_3 \\
& + 5426810620191830595361053787232691932323291/7408516122065593537035 \\
& 514426553341756072050\zeta_3\zeta_2 G_{00}\zeta_2 \\
& - 3555680/101\zeta_3^2 \\
& + 844932546645814524259903166054625220595354629341177245757281066618 \\
& 413644597785645181161299/53202025964356117290814864847075789345855220 \\
& 418285550181241126294278742948842946320000\zeta_4 \\
& - 10032148020914268992268473355024802636577261037731/152615432114551 \\
& 226862931597186998840175084230\zeta_5 \\
& - 4031600/101\zeta_6) \\
& + C_A^2 C_F ( \\
& + 219057553691923746368605843525237973487904944974415779498540461292 \\
& 776556628234696253675589973998664816659378647900035209007227796035174 \\
& 617645104953258709429979481871758387381267401813056094841774198129567
\end{aligned}$$



$$\begin{aligned}
 & 79177047043513253/ \\
 & 521931124856046576393534933374414238921130765606623361358497614650913 \\
 & 862923692898183774596844204401183041394654740580584928175299254456487 \\
 & 549385529122870483705884245235772684955180020445831641032298253516800 \\
 & 0000000000 \\
 & - 841366492535199718616261517624185342899927452285389593384233752696 \\
 & 8979494305745476413456417866356499717/1763892547857291164245292093782 \\
 & 295040448005133780063763202394201720844795124335969200680561294412800 \\
 & 000\zeta_2 G_{00}\zeta_2 \\
 & - 170613047881502811357927978155845505846527348863419865032536742693 \\
 & 5868135265129110806541155293543947237466169307611485577102578216593/ \\
 & 520983159492584827454835872086270331444676166032869803115496375405893 \\
 & 54624975435325384362249009292206896702909550963115072000000\zeta_3 \\
 & + 176/101\zeta_3\zeta_2 G_{00}\zeta_2 \\
 & + 889504/101\zeta_3^2 \\
 & - 428650304918601725427852769025821526852573191556741285397720941021 \\
 & 57354094587298850497851/106404051928712234581629729694151578691710440 \\
 & 83657110036248225258855748589768589264000\zeta_4 \\
 & + 270490998090486344796371857632073152728862443/1666713856365685040 \\
 & 36692679854749370413270\zeta_5 \\
 & + 1008400/101\zeta_6) \\
 & + n_f C_F^2 ( \\
 & + 415208170565796152245134836312345360926076736320674905865973582155 \\
 & 156454334228900759603648197455690168385640258730846779714496837931178 \\
 & 809329180319237445456089294317157811170160398758670946628813/ \\
 & 480330262746688288033490723655245725943880840758988475748563510686427 \\
 & 683913336066285361139524896140104277849601106940285604092930926279445 \\
 & 6273525747758497254499371024267845622710648064000000000 \\
 & + 161854380442164559523522298334246994700094282970547988582824706001 \\
 & 4365869882910776917695670801652708721863/4899211551673626208691298790 \\
 & 480324474844334259074127102294649895279646418457843154454890258995231 \\
 & 55200000\zeta_2 G_{00}\zeta_2 \\
 & - 581311251820564381993604963763630026922060637528322667455449448410 \\
 & 08170376255848403906109/205492825287325503035772415471830236348365788
 \end{aligned}$$

---


$$\begin{aligned}
& 865627937575043850311651644639905880161000\zeta_3 \\
& + 64/101\zeta_3\zeta_2G_{00}\zeta_2 \\
& - 240207269666876581294223679606751035473098501/11332829117417170311 \\
& 603831474282092092209225\zeta_4 \\
& - 2560/303\zeta_5) \\
& + n_f C_A C_F ( \\
& - 723950060047084242187518140023320151841505909602638181936675759546 \\
& 036438976832154190153430588710537772023690940279643309082558171301904 \\
& 75288760027526174878002940978391383696810728737937818955255923129/ \\
& 206678978442136405663266006546421712422276521607690379899620513843755 \\
& 677521315737004774779112718379936275150596481052440435753998678603892 \\
& 78841574333353446023601252940050939948769813944320000000000 \\
& + 164855114252203169642517991134726180675778785675331814079188281612 \\
& 38881405983685204977723912516373971717/970140901321510140334910651580 \\
& 262272246402823579035069761316810946464637318384783060374308711927040 \\
& 0000\zeta_2G_{00}\zeta_2 \\
& + 341451691786563802135561527663027069498217933220688411693853350287 \\
& 87838685478365829015163659897/203356521875638467106212525440585089211 \\
& 288178124580869536013694443811714142229418630846244000\zeta_3 \\
& - 32/101\zeta_3\zeta_2G_{00}\zeta_2 \\
& + 12812610217463058948484655992793608982070877382321/934584418826041 \\
& 784087033170189621288568218158075\zeta_4 \\
& + 9274848640/857904201\zeta_5) \\
& + n_f^2 C_F ( \\
& + 236665397969543567357345350624116892335552308368764291766511155184 \\
& 35036414191375061/127892542730903165122911982752509044399889266247219 \\
& 1992619481322262743922576000000 \\
& - 58687018662546871880248683327355339262904307/400059870591542050999 \\
& 917779033880454827890700\zeta_2G_{00}\zeta_2 \\
& - 64/909\zeta_3 \\
& )
\end{aligned}$$

$$\begin{aligned}
& c_{3,ns}^{(3),\epsilon}(N = 101) = \\
& + 108075187249611511296999010985480277909153865812614897208924140437517
\end{aligned}$$

$$\begin{aligned}
 & 265402927002939297174132559062808772438166849146787541938428576587147751 \\
 & 325014161484420239957221534701396692580794793710811439827417206217596480 \\
 & 889063/29217915540109753820605004892670488049861499183642322958125821368 \\
 & 176923655507844058943843717132079864397260859962587309701667026558305157 \\
 & 950459873524315757594459233607671253128577310302375768471274298408960000 \\
 & 000000C_F n_f^2 + C_F n_f^2 Z_5(\alpha_s^3, \epsilon, C_F, n_f^2) \\
 & + 1252652671632905412915875168184201074406811/1584395527095216043564030 \\
 & 80805497209832828C_F n_f^2 \zeta_4 \\
 & - 26454075341529980382333754280933226817554585474528697567337668077495 \\
 & 130577052978995273/16735394575195516507013607971313160920443778073324775 \\
 & 00846808244596729389847098505600C_F n_f^2 \zeta_3 \\
 & - 288770646567628421501990854242285887014743282883953055386292794645324 \\
 & 1913453021600637799407341968306436556826722275123324344276231/ \\
 & 280587135546172693789418896892967805993041863870980981719125177150588021 \\
 & 97332689377941544948512390438132589978460341229824000000C_F n_f^2 \zeta_2 \\
 & G_{00}\zeta_2 - 91840176843530526967749362430455697567342226903242448681747 \\
 & 4000010576393120461408587992944354771935405782295069633315815161036788 \\
 & 500531415891366727668780460686491290067457088678408095476189322771570901 \\
 & 535245648473323318152276137987985965349/ \\
 & 183394369365080137427279170337978969177216105241208191505999468561131375 \\
 & 267059947791512764479609491780786508069703276609562756524226941362907356 \\
 & 918898391404358872988200478124403430114854858565005942408936591230292931 \\
 & 82300979200000000000C_F C_A n_f + C_F C_A n_f Z_5(\alpha_s^3, \epsilon, C_F, C_A, n_f) \\
 & + 572437335263108034455464653357837364325724641/35787881423422643089275 \\
 & 2572872066066069765C_F C_A n_f \zeta_5 \\
 & + 324278876051187347195343937845012431153475339254906375482367259959449 \\
 & 5002233074736426379/3040115769391778130903706562690045105477441166759174 \\
 & 296070921502530213882791025504000C_F C_A n_f \zeta_4 \\
 & + 188934091281480698132219020481372053118790009949984508346567676601372 \\
 & 06558788214034701953829258796975022595873412729296625551539657553/ \\
 & 182782828483030024200733469648793580495274280146058426714099938866088756 \\
 & 8053085536205327151325768115006175903131930105921420800000C_F C_A \\
 & n_f \zeta_3 + 1033728975849098658623066274158929536095892560582317010282398
 \end{aligned}$$

---


$$\begin{aligned}
& 604057132257752305431697269383053637433790990769053938578605489939933157 \\
& 813131361180471437/819779682509825084562800928616020387140856763429981925 \\
& 1452262351293598859705344033587244944187059933007541068873148589901345627 \\
& 07030041968640000000C_FC_{An_f\zeta_2}G_{00}\zeta_2 \\
& - 1041413605348686354651879792562937208806875/1760439474550240048404478 \\
& 6756166356648092C_FC_{An_f\zeta_2\zeta_3}G_{00}\zeta_2 \\
& + 186733564218751537353830912491683032584337391931269078516938265273602 \\
& 135572527252162582838801715203042744785249794555707307598436895532931704 \\
& 970743437379883694705121487357871575386087835741657847896039599884666714 \\
& 8242738805527450991906851156510783636041996484018823/ \\
& 110259378623159324168439663184820136908664648598314139283263104975263432 \\
& 520009271790151465205842972043974354440001286374426080971422831011731571 \\
& 14060731668602050785681273776421676879193321104538997125332242599157516 \\
& 05677663406366000496598811934720000000000000C_FC_A^2 + C_FC_A^2 \\
& Z_5(\alpha_s^3, \epsilon, C_F, C_A^2) + 53930010993632522905735383228351505089779075/ \\
& 11736263163668266989363191170777571098728C_FC_A^2\zeta_6 \\
& + 11306795243829412507222495039521664474507226150221208563199867662971 \\
& 20320123729377014529/158025819696107279081628311426957790136203625004808 \\
& 564894775622656273493907454296000C_FC_A^2\zeta_5 \\
& - 249513955194023355112236019914013919587165489783197221232966943963798 \\
& 431694414585229289735594735054409682263783/91597470099772582416621147353 \\
& 369762871264533259587227836630995566862036173477496600617007647551111360 \\
& 00000C_FC_A^2\zeta_4 \\
& - 863671568863672652898090183658918100990416028122291796645450144793187 \\
& 018476080018010058448251707717418536214054578955994567920980071913355167 \\
& 5972790640016452426795165945930335793/ \\
& 407585601606531233088064854165221479804427397896983931437731429037140527 \\
& 340202570700007097333563615407072486219575066414041457428822124023344842 \\
& 207084175215449822105600000000C_FC_A^2\zeta_3 \\
& + 241005879939253543467979575915640837731979499/58681315818341334946815 \\
& 95585388785549364C_FC_A^2\zeta_3^2 \\
& - 466242464854445107513371245114931681893904214176724792698718305999241 \\
& 942328341764191126123665879675810335798419434221806497428799893487573633 \\
& 4411532307083805276753560645497/
\end{aligned}$$

$$\begin{aligned}
 & 127026685988730072809336905855806240975961347603540867530929614320575573 \\
 & 958987292928040265777630240333128484545324381800073225901450917312226839 \\
 & 5402349606043648000000000C_FC_A^2\zeta_2G_{00}\zeta_2 \\
 & + 204940219517124605947921855065053472299911291932528588557401366193503 \\
 & 357200517897469/28977532899062414951627808029562379305739577291785318526 \\
 & 2550559208479107552352000C_FC_A^2\zeta_2\zeta_3G_{00}\zeta_2 \\
 & - 976544922855672645496274385872067986997718329861983761831416899145215 \\
 & 247520801727647623022468792735788041506379390402600095699843031091637468 \\
 & 692042186044047750179144280831478996347773299094717107616983132474071789 \\
 & 202709975153441237633960706382578713832071156341/ \\
 & 141879143893061764017008385963083376010972506413932730214271771947457599 \\
 & 663655699155832912704759957110126803787188427843762513212708057194509852 \\
 & 116416881719777592987985198018533175650159596090773061922671436626782842 \\
 & 31708667521132550395919859712000000000000C_F^2n_fC_F^2n_f \\
 & Z_5(\alpha_s^3, \epsilon, C_F^2, n_f) + 5580594929677923726111563990204608995868175429 \\
 & 637688908974347723/909280046443771934407416546981968649534677305204772930 \\
 & 73648000C_F^2n_fZ_5(\alpha_s^2, \epsilon, n_f) + 412519129136857029517897181494817557 \\
 & 428289459019301732295650779945800339017222932281460422387272009578690 \\
 & 82501402354492366832577299/26188132650976118087012430376676995226017 \\
 & 240627958224960451683200721548717510510086078775285278231075590417313 \\
 & 2296518145024000000C_F^2n_fZ_5(\alpha_s, \epsilon) - 996605318561124736232244409 \\
 & 855396388831131/800199761159200022002035761643925302186C_F^2n_f\zeta_5 \\
 & - 285976944633645313789508529760937920130964719389674571418445937240907 \\
 & 2012883714041739983/4560173654087667196355559844035067658216161750138761 \\
 & 444106382253795320824186538256000C_F^2n_f\zeta_4 \\
 & - 762308757518537441510463195580869214648065827425197696690283317492808 \\
 & 1527741750176769243863181435112567815251265269669330337061620933/ \\
 & 572451715578720405463835591757210664188496371886007160588115193152036216 \\
 & 3682740415588112506899383656887473982336264617446208000000C_F^2n_f\zeta_3 \\
 & + 207269862279344349452260916006403105070452060675115966839001636341152 \\
 & 494405054949471706622006303820108790041973934307307342375765791455073027 \\
 & 64413781791393789495857092071947/ \\
 & 683001814570909367246786027235108940718136421523836459924351741665278792 \\
 & 371596561745280585387356421331276356501628707556965607697987451364514141
 \end{aligned}$$

---


$$\begin{aligned}
& 5897766889168732160000000C_F^2n_f\zeta_2G_{00}\zeta_2 \\
& + 830174539064467296387884416941673343206939/17604394745502400484044786 \\
& 756166356648092C_F^2n_f\zeta_2\zeta_3G_{00}\zeta_2 \\
& + 969311353780260373868031223678798656408172014301087738855432440262166 \\
& 664841726968186058588050361577043302980523890571896621060521002086538168 \\
& 224086072382795632537158913261868966441082451255658635611249427583283194 \\
& 8769586663944481828501960658006843905917187470653492357381724769576201/ \\
& 334582314768502444704670153956563039580356828107271957213251035568382576 \\
& 950302053760580339266811582804644897033818262892408630560001720366532466 \\
& 452493701925155226854704048704045715974644381097011990233421255165155989 \\
& 56257412241910617468092469737279829442266385612800000000000000C_F^2C_A \\
& + C_F^2C_AZ_5(\alpha_s^3, \epsilon, C_F^2, C_A) \\
& + 5580594929677923726111563990204608995868175429637688908974347723/C_F^2C_A \\
& 90928004644377193440741654698196864953467730520477293073648000 \\
& Z_5(\alpha_s^2, \epsilon, C_A) - 6121694372007177576427122664114012770085858607523529506 \\
& 216274208078804286433805394241400139184815764286097044899977061286457454 \\
& 1232123294918779313669/707260902557496151387514526649115628121523482174886 \\
& 366791959889131212450641245367603605446165158111867317268687095172462076 \\
& 877629594546012160000000C_F^2C_AZ_5(\alpha_s, \epsilon) \\
& - 843285169070828569430969045115054361990586525/50298270701435429954413 \\
& 67644618959042312C_F^2C_A\zeta_6 \\
& - 212094585892002323816018025666355793684614335050575075823666303910261 \\
& 402027259307655154679/88670043273926862151358108078459648909758700697142 \\
& 5836354018771571312382480715772000C_F^2C_A\zeta_5 \\
& + 719024696765840091789575556419473464082295351769057302569174308219703 \\
& 8412144821340045997461067713670727533984867226036047339128468403/ \\
& 124878595511599081618624089296191227235174804846282276431783489336774051 \\
& 754795487910468233999243416703046897373271024856192000000C_F^2C_A\zeta_4 \\
& + 184908423151534778120127104336765089319635990067121505410689596269410 \\
& 160124364540407005143434933647011155728650821234495536034961762376416507 \\
& 5807114514985250075601803410044004493/ \\
& 399593727065226699105945935456099490004340586173513658272285714742294634 \\
& 647257422254908918954474132752031849234877516092197507283158945120926315 \\
& 8892982109955390412800000000C_F^2C_A\zeta_3
\end{aligned}$$

$$\begin{aligned}
 & + 1147033138490795883783877480373569141606843/5868131581834133494681595 \\
 & 585388785549364C_F^2C_A\zeta_3Z_5(\alpha_s, \epsilon) \\
 & - 2683266182887500443957084918303070322653730147/1760439474550240048404 \\
 & 4786756166356648092C_F^2C_A\zeta_3^2 \\
 & - 754726398273427521622547441079539712540969129560494528383071945035888 \\
 & 614844058941027335010600771057986602074157527785458385442992499918115777 \\
 & 737497846937799174987476218646640760111677011426009/ \\
 & 500390784831210399455777088170821767673565009008871654034071952483270962 \\
 & 347923329679241287276948673372329551719125721089983551240702229996204314 \\
 & 43694466549467186248100545118732288000000000C_F^2C_A\zeta_2G_{00}\zeta_2 \\
 & + 230638187753418058545629773449909859970721417299260298470156705847634 \\
 & 348803323422464059/20660980957031501860510627125077976444992318609042932 \\
 & 1092198548715645603684826976000C_F^2C_A\zeta_2\zeta_3G_{00}\zeta_2 \\
 & + 454607869683324156043387232347467108084898696857863819627647740205893263 \\
 & 552817674758506127943000816054349602076895407549224036913899076691306908 \\
 & 787861562313354800983891279029986830276606112779711873081425301983478196 \\
 & 500474224363310098303152544975271749937354436594214162913165789101834850 \\
 & 178526782782730173/ \\
 & 207260306825237761479850279013310427019249429522468981609213777339280368 \\
 & 699474814055094476440280876452269424644696849305429694042526352009715334 \\
 & 660232303953677601082032895723755449352081981595984464553737381880064507 \\
 & 592585047068722185971816449937722347290762252908498589055409132624936960 \\
 & 000000000000C_F^3 + C_F^3Z_5(\alpha_s^3, \epsilon, C_F^3) + 558059492967792372611156399 \\
 & 0204608995868175429637688908974347723/9092800464437719344074165469819 \\
 & 6864953467730520477293073648000C_F^3Z_5(\alpha_s^2, \epsilon, C_F) \\
 & - 875508195220574605779594755355467993785495861096011823227622989787476 \\
 & 368511127233254602476486975673616664436942431415410249228899229330948450 \\
 & 092566454116762296196603462921/51655599421329279875807346597613281230783 \\
 & 426837937211254782904831827807826423269375693489651144603293962077382476 \\
 & 12073960244091833518539731619558242008571640217600000000C_F^3Z_5(\alpha_s, \epsilon) \\
 & + 407870489231826351502821755951843094936636125/25149135350717714977206 \\
 & 83822309479521156C_F^3\zeta_6 \\
 & + 874810439852611313976685979953926019068033277269135859466426278117043 \\
 & 63813029376789349841/420015994455443031243275248792703600098857003302254
 \end{aligned}$$

---


$$\begin{aligned}
& 343536114154954832181175075892000C_F^3\zeta_5 \\
& - 624452595449582300261817368399396706003705227999364647521862692317291 \\
& 5952734846657272455961075467617866184925515162839806214213/ \\
& 124902382476439594670320192497295712218590656444631842984991964473119265 \\
& 801638155443627164772623447435147324319258048000000C_F^3\zeta_4 \\
& - 411912661612280960366814965610863344274270666155830419832019999445050 \\
& 872809591602615878204753342838213278388459773910865583364061442355165964 \\
& 94252671688583069964807914494619/ \\
& 986129825351426970316503824086277019857880505433544529925915296868323615 \\
& 256912275620942830838316453869637756798572399423885937400372507063186255 \\
& 93993438282798400000000C_F^3\zeta_3 \\
& - 1041413605348686354651879792562937208806875/5868131581834133494681595 \\
& 585388785549364C_F^3\zeta_3Z_5(\alpha_s, \epsilon) \\
& + 184263187922937315784524888553280248769562745/12574567675358857488603 \\
& 41911154739760578C_F^3\zeta_3^2 \\
& - 92617808070457423416715692191092250189852997854167338840850174178367 \\
& 486549430879097619152728529544744961478577239900823986822921435983512367 \\
& 0482117599941674213941663605260170045809249695872925249571918533266713527/ \\
& 72384282274519395071485209693225537098628760519366587286326821177200355 \\
& 891261845804394509394604434198927934745355102959746480927928416097982063 \\
& 3556901170756706533719996810433013187422330627238232981504000000000C_F^3 \\
& \zeta_2G_{00}\zeta_2 - 466698319682383485048083935484579799294368728082459809 \\
& 36767272044044519983183977673/2921518800485223679370846595740664090072 \\
& 4432422289213955344817408886538982583000C_F^3\zeta_2\zeta_3G_{00}\zeta_2
\end{aligned}$$





# Appendix I

## $C_3$ at N<sup>4</sup>LO order $n_f^2$

$$\begin{aligned}
c_{3,\text{ns}}^{(4)}(N) &= n_f^0 \text{ and } n_f^1 \text{ contributions} \\
&+ C_F C_A n_f^2 \frac{16}{9} c_{3,\text{ns}}^{(4)\text{L}}(N) + C_F (C_F - \frac{1}{2} C_A) n_f^2 \frac{16}{9} c_{3,\text{ns}}^{(4)\text{N}}(N) \\
&+ C_F (C_F - C_A) n_f^2 \frac{1}{3} \zeta_4 c_{3,\text{ns}}^{(4)\text{Z}}(N) + C_F n_f^3 \frac{16}{27} c_{3,\text{ns}}^{(4)\text{F}}(N) . \quad (\text{I.0.1})
\end{aligned}$$

$$\begin{aligned}
c_{3,\text{ns}}^{(4)\text{L}}(N) &= \\
&- 1951/12 \mathbf{S}_6 + 671/6 \mathbf{S}_{1,5} + 352/3 \mathbf{S}_{2,4} + 335/2 \mathbf{S}_{3,3} + 643/3 \mathbf{S}_{4,2} \\
&+ 1445/6 \mathbf{S}_{5,1} - 265/3 \mathbf{S}_{1,1,4} - 89 \mathbf{S}_{1,2,3} - 117 \mathbf{S}_{1,3,2} - 412/3 \mathbf{S}_{1,4,1} \\
&- 119 \mathbf{S}_{2,1,3} - 125 \mathbf{S}_{2,2,2} - 137 \mathbf{S}_{2,3,1} - 169 \mathbf{S}_{3,1,2} - 188 \mathbf{S}_{3,2,1} - 688/3 \mathbf{S}_{4,1,1} \\
&+ 71 \mathbf{S}_{1,1,1,3} + 81 \mathbf{S}_{1,1,2,2} + 98 \mathbf{S}_{1,1,3,1} + 103 \mathbf{S}_{1,2,1,2} + 108 \mathbf{S}_{1,2,2,1} + 135 \mathbf{S}_{1,3,1,1} \\
&+ 109 \mathbf{S}_{2,1,1,2} + 122 \mathbf{S}_{2,1,2,1} + 139 \mathbf{S}_{2,2,1,1} + 176 \mathbf{S}_{3,1,1,1} - 70 \mathbf{S}_{1,1,1,1,2} \\
&- 82 \mathbf{S}_{1,1,1,2,1} - 94 \mathbf{S}_{1,1,2,1,1} - 114 \mathbf{S}_{1,2,1,1,1} - 115 \mathbf{S}_{2,1,1,1,1} + 80 \mathbf{S}_{1,1,1,1,1,1} \\
&+ \mathbf{S}_5 (20567/36 - 671/12 D_0 + 671/12 D_1) + \mathbf{S}_{1,4} (-9995/36 + 20 D_{-1} + 265/6 D_0 \\
&- 265/6 D_1 - 20 D_2) + \mathbf{S}_{2,3} (-13373/36 + 8 D_{-1} + 89/2 D_0 - 89/2 D_1 - 8 D_2) \\
&+ \mathbf{S}_{3,2} (-9817/18 - 8 D_{-1} + 117/2 D_0 - 117/2 D_1 + 8 D_2) \\
&+ \mathbf{S}_{4,1} (-12343/18 - 20 D_{-1} + 206/3 D_0 - 206/3 D_1 + 20 D_2) \\
&+ \mathbf{S}_{1,1,3} (8495/36 - 10 D_{-1} - 71/2 D_0 + 71/2 D_1 + 10 D_2) + \mathbf{S}_{1,2,2} (803/3 - 2 D_{-1} \\
&- 81/2 D_0 + 81/2 D_1 + 2 D_2) + \mathbf{S}_{1,3,1} (12263/36 + 2 D_{-1} - 49 D_0 + 49 D_1 - 2 D_2) \\
&+ \mathbf{S}_{2,1,2} (4283/12 - 2 D_{-1} - 103/2 D_0 + 103/2 D_1 + 2 D_2) \\
&+ \mathbf{S}_{2,2,1} (4835/12 + 2 D_{-1} - 54 D_0 + 54 D_1 - 2 D_2) + \mathbf{S}_{3,1,1} (19967/36 + 10 D_{-1} \\
&- 135/2 D_0 + 135/2 D_1 - 10 D_2) + \mathbf{S}_{1,1,1,2} (-1279/6 + 35 D_0 - 35 D_1)
\end{aligned}$$

$$\begin{aligned}
 & + \mathbf{S}_{1,1,2,1} (-1511/6 + 41 D_0 - 29 D_1 - 18 D_2) + \mathbf{S}_{1,2,1,1} (-605/2 + 47 D_0 - 59 D_1 \\
 & + 18 D_2) + \mathbf{S}_{2,1,1,1} (-2135/6 + 57 D_0 - 57 D_1) + \mathbf{S}_{1,1,1,1,1} (226 - 40 D_0 + 40 D_1) \\
 & + \mathbf{S}_4 (-152383/144 - 20 D_{-1} + 6259/36 D_0 - 3647/18 D_1 + 20 D_2 - 319/6 D_0^2 \\
 & + 20 D_1^2) + \mathbf{S}_{1,3} (3800/9 + 6 D_{-1} - 5035/36 D_0 + 6277/36 D_1 - D_2 + 12 D_{-1}^2 \\
 & + 54 D_0^2 - 71/2 D_1^2) + \mathbf{S}_{2,2} (24305/36 + 2 D_{-1} - 941/6 D_0 + 1121/6 D_1 - 2 D_2 \\
 & + 57 D_0^2 - 55/2 D_1^2) + \mathbf{S}_{3,1} (17689/18 + 2 D_{-1} - 7225/36 D_0 + 8197/36 D_1 \\
 & - 7 D_2 - 12 D_{-1}^2 + 63 D_0^2 - 19 D_1^2) + \mathbf{S}_{1,1,2} (-27307/72 + 1441/12 D_0 \\
 & - 3665/24 D_1 + 4 D_2 - 49 D_0^2 + 59/2 D_1^2) + \mathbf{S}_{1,2,1} (-10459/24 + 865/6 D_0 \\
 & - 536/3 D_1 + 18 D_2 - 111/2 D_0^2 + 51/2 D_1^2) + \mathbf{S}_{2,1,1} (-23191/36 + 741/4 D_0 \\
 & - 1653/8 D_1 - 22 D_2 - 64 D_0^2 + 47/2 D_1^2) + \mathbf{S}_{1,1,1,1} (25979/72 - 267/2 D_0 \\
 & + 321/2 D_1 + 52 D_0^2 - 23 D_1^2) + \mathbf{S}_3 (842039/648 + 8 D_{-1} - 21523/72 D_0 \\
 & + 29311/72 D_1 - 7 D_2 - 12 D_{-1}^2 + 1801/9 D_0^2 - 283/4 D_0^3 - 385/4 D_1^2 \\
 & + 91/4 D_1^3) + \mathbf{S}_{1,2} (-147071/324 + 2 D_{-1} + 9607/36 D_0 - 27887/72 D_1 + 13/2 D_2 \\
 & - 2311/12 D_0^2 + 143/2 D_0^3 + 239/2 D_1^2 - 24 D_1^3) \\
 & + \mathbf{S}_{2,1} (-1178369/1296 - 2 D_{-1} + 3877/12 D_0 - 3363/8 D_1 - 57/2 D_2 - 667/3 D_0^2 \\
 & + 81 D_0^3 + 571/6 D_1^2 - 49/2 D_1^3) + \mathbf{S}_{1,1,1} (46483/108 - 4903/18 D_0 \\
 & + 27127/72 D_1 + 2375/12 D_0^2 - 75 D_0^3 - 1181/12 D_1^2 + 21 D_1^3) \\
 & + \mathbf{S}_2 (-5764837/5184 + 8 D_{-1} + 1108709/2592 D_0 - 1703519/2592 D_1 - 33/2 D_2 \\
 & - 3953/9 D_0^2 + 19493/72 D_0^3 - 1025/12 D_0^4 + 721/3 D_1^2 - 6101/72 D_1^3 \\
 & + 263/12 D_1^4) + \mathbf{S}_{1,1} (2134163/5184 - 10 D_{-1} - 373243/864 D_0 + 584977/864 D_1 \\
 & - 12 D_2 + 5377/12 D_0^2 - 20519/72 D_0^3 + 1115/12 D_0^4 - 5983/24 D_1^2 \\
 & + 5987/72 D_1^3 - 239/12 D_1^4) + \mathbf{S}_1 (33182/81 - 20 D_{-1} - 3116159/5184 D_0 \\
 & + 2604439/2592 D_1 + 21/2 D_2 + 12 D_{-1}^2 + 327839/432 D_0^2 - 29179/48 D_0^3 \\
 & + 23137/72 D_0^4 - 1069/12 D_0^5 - 1220581/2592 D_1^2 + 28139/144 D_1^3 \\
 & - 2083/36 D_1^4 + 32/3 D_1^5) - 18199451/27648 - 682319/768 D_0 + 1067909/768 D_1 \\
 & + 3772493/3456 D_0^2 - 2437127/2592 D_0^3 + 83797/144 D_0^4 - 16417/72 D_0^5 \\
 & + 1951/48 D_0^6 - 7326779/10368 D_1^2 + 283373/864 D_1^3 - 13321/144 D_1^4 \\
 & - 49/12 D_1^5 + 149/16 D_1^6 \\
 & + \zeta_3 \left[ -331/6 \mathbf{S}_3 + 121/3 \mathbf{S}_{1,2} + 166/3 \mathbf{S}_{2,1} - 14 \mathbf{S}_{1,1,1} + \mathbf{S}_2 (215/2 - 28 D_{-1} \right. \\
 & - 121/6 D_0 + 121/6 D_1 + 28 D_2) + \mathbf{S}_{1,1} (-111/2 + 20 D_{-1} + 7 D_0 - 55 D_1 + 52 D_2) \\
 & \left. + \mathbf{S}_1 (-274/3 - 12 D_{-1} + 122/3 D_0 - 791/12 D_1 - 62 D_2 - 24 D_{-1}^2 - 25 D_0^2 \right.
 \end{aligned}$$

---


$$\begin{aligned}
& + 133/3 D_1^2) + 2083/32 - 4 D_{-1} + 535/24 D_0 - 4327/24 D_1 + 141 D_2 + 24 D_{-1}^2 \\
& - 136/3 D_0^2 + 257/12 D_0^3 + 376/3 D_1^2 - 33/4 D_1^3 \Big] \\
& + \zeta_5 \left[ - 191/2 \mathbf{S}_1 + 693/8 + 60 D_{-1} + 191/4 D_0 - 1151/4 D_1 + 300 D_2 \right] \\
c_{3,\text{ns}}^{(4)\text{N}}(N) = & \\
& - 150 \mathbf{S}_{-6} - 1051/6 \mathbf{S}_6 + 6 \mathbf{S}_{-5,1} + 408 \mathbf{S}_{-4,-2} + 510 \mathbf{S}_{-3,-3} + 352 \mathbf{S}_{-2,-4} \\
& + 450 \mathbf{S}_{1,-5} + 446/3 \mathbf{S}_{1,5} + 538 \mathbf{S}_{2,-4} + 548/3 \mathbf{S}_{2,4} + 586 \mathbf{S}_{3,-3} + 273 \mathbf{S}_{3,3} \\
& + 434 \mathbf{S}_{4,-2} + 968/3 \mathbf{S}_{4,2} + 932/3 \mathbf{S}_{5,1} + 8 \mathbf{S}_{-4,1,1} - 264 \mathbf{S}_{-3,-2,1} + 4 \mathbf{S}_{-3,1,-2} \\
& - 216 \mathbf{S}_{-2,-3,1} - 136 \mathbf{S}_{-2,-2,2} - 4 \mathbf{S}_{1,-4,1} - 220 \mathbf{S}_{1,-3,-2} - 252 \mathbf{S}_{1,-2,-3} \\
& - 520 \mathbf{S}_{1,1,-4} - 770/3 \mathbf{S}_{1,1,4} - 496 \mathbf{S}_{1,2,-3} - 302 \mathbf{S}_{1,2,3} - 336 \mathbf{S}_{1,3,-2} \\
& - 160 \mathbf{S}_{1,3,2} + 4/3 \mathbf{S}_{1,4,1} - 4 \mathbf{S}_{2,-3,1} - 140 \mathbf{S}_{2,-2,-2} - 496 \mathbf{S}_{2,1,-3} - 326 \mathbf{S}_{2,1,3} \\
& - 320 \mathbf{S}_{2,2,-2} - 314 \mathbf{S}_{2,2,2} - 64 \mathbf{S}_{2,3,1} - 4 \mathbf{S}_{3,-2,1} - 344 \mathbf{S}_{3,1,-2} - 344 \mathbf{S}_{3,1,2} \\
& - 276 \mathbf{S}_{3,2,1} - 1016/3 \mathbf{S}_{4,1,1} + 8 \mathbf{S}_{-3,1,1,1} + 112 \mathbf{S}_{-2,-2,1,1} - 8 \mathbf{S}_{1,-3,1,1} \\
& + 144 \mathbf{S}_{1,-2,-2,1} - 8 \mathbf{S}_{1,-2,1,-2} + 112 \mathbf{S}_{1,1,-2,-2} + 448 \mathbf{S}_{1,1,1,-3} + 274 \mathbf{S}_{1,1,1,3} \\
& + 288 \mathbf{S}_{1,1,2,-2} + 252 \mathbf{S}_{1,1,2,2} + 58 \mathbf{S}_{1,1,3,1} + 288 \mathbf{S}_{1,2,1,-2} + 254 \mathbf{S}_{1,2,1,2} \\
& + 188 \mathbf{S}_{1,2,2,1} + 88 \mathbf{S}_{1,3,1,1} - 8 \mathbf{S}_{2,-2,1,1} + 288 \mathbf{S}_{2,1,1,-2} + 314 \mathbf{S}_{2,1,1,2} \\
& + 210 \mathbf{S}_{2,1,2,1} + 216 \mathbf{S}_{2,2,1,1} + 302 \mathbf{S}_{3,1,1,1} - 16 \mathbf{S}_{1,-2,1,1,1} - 256 \mathbf{S}_{1,1,1,1,-2} \\
& - 244 \mathbf{S}_{1,1,1,1,2} - 148 \mathbf{S}_{1,1,1,2,1} - 144 \mathbf{S}_{1,1,2,1,1} - 184 \mathbf{S}_{1,2,1,1,1} - 230 \mathbf{S}_{2,1,1,1,1} \\
& + 160 \mathbf{S}_{1,1,1,1,1,1} + \mathbf{S}_{-5} (310/3 - 153 D_0 + 153 D_1) + \mathbf{S}_5 (3463/9 - 439/3 D_0 \\
& + 439/3 D_1) + \mathbf{S}_{-4,1} (-40/3 + 2 D_0 - 2 D_1) + \mathbf{S}_{-3,-2} (-1192/3 + 46 D_0 - 46 D_1) \\
& + \mathbf{S}_{-2,-3} (-392 + 54 D_0 - 54 D_1) + \mathbf{S}_{1,-4} (-448 + 116 D_0 - 116 D_1) \\
& + \mathbf{S}_{1,4} (-6395/18 + 385/3 D_0 - 385/3 D_1) + \mathbf{S}_{2,-3} (-460 + 108 D_0 - 108 D_1) \\
& + \mathbf{S}_{2,3} (-6125/18 + 133 D_0 - 133 D_1) + \mathbf{S}_{3,-2} (-376 + 76 D_0 - 76 D_1) \\
& + \mathbf{S}_{3,2} (-5683/9 + 108 D_0 - 108 D_1) + \mathbf{S}_{4,1} (-7129/9 + 256/3 D_0 - 256/3 D_1) \\
& + \mathbf{S}_{-3,1,1} (-40/3 + 4 D_0 - 4 D_1) + \mathbf{S}_{-2,-2,1} (160 - 24 D_0 + 24 D_1) \\
& + \mathbf{S}_{-2,1,-2} (4 D_0 - 4 D_1 - 4 D_1) + 40/3 \mathbf{S}_{1,-3,1} + \mathbf{S}_{1,-2,-2} (512/3 - 24 D_0 \\
& + 24 D_1) + \mathbf{S}_{1,1,-3} (1360/3 - 88 D_0 + 88 D_1) + \mathbf{S}_{1,1,3} (7679/18 - 115 D_0 + 115 D_1) \\
& + \mathbf{S}_{1,2,-2} (880/3 - 56 D_0 + 56 D_1) + \mathbf{S}_{1,2,2} (1417/3 - 110 D_0 + 110 D_1) \\
& + \mathbf{S}_{1,3,1} (5885/18 - 75 D_0 + 75 D_1) + 40/3 \mathbf{S}_{2,-2,1} + \mathbf{S}_{2,1,-2} (880/3 - 56 D_0 \\
& + 56 D_1) + \mathbf{S}_{2,1,2} (1027/2 - 113 D_0 + 113 D_1) + \mathbf{S}_{2,2,1} (1250/3 - 98 D_0 + 98 D_1) \\
& + \mathbf{S}_{3,1,1} (6313/9 - 86 D_0 + 86 D_1) + \mathbf{S}_{-2,1,1,1} (8 D_0 - 8 D_1 - 8 D_1)
\end{aligned}$$

$$\begin{aligned}
 & + 80/3 \mathbf{S}_{1,-2,1,1} + \mathbf{S}_{1,1,1,-2} (-800/3 + 48 D_0 - 48 D_1) + \mathbf{S}_{1,1,1,2} (-1163/3 + 104 D_0 \\
 & - 104 D_1) + \mathbf{S}_{1,1,2,1} (-1015/3 + 82 D_0 - 82 D_1) + \mathbf{S}_{1,2,1,1} (-413 + 82 D_0 - 82 D_1) \\
 & + \mathbf{S}_{2,1,1,1} (-1343/3 + 92 D_0 - 92 D_1) + \mathbf{S}_{1,1,1,1,1} (320 - 80 D_0 + 80 D_1) \\
 & + \mathbf{S}_{-4} (-1270/9 - 144 D_{-1} + 330 D_0 - 330 D_1 + 144 D_2 - 57 D_0^2 + 149 D_1^2) \\
 & + \mathbf{S}_4 (-18371/72 + 5899/18 D_0 - 3467/9 D_1 - 349/3 D_0^2 + 10 D_1^2) \\
 & + \mathbf{S}_{-3,1} (38/9 + 56 D_{-1} - 380/3 D_0 + 380/3 D_1 - 56 D_2 - 50 D_0^2 - 54 D_1^2) \\
 & + \mathbf{S}_{-2,-2} (200 + 16 D_{-1} - 100/3 D_0 + 100/3 D_1 - 16 D_2 + 30 D_0^2 - 6 D_1^2) \\
 & + \mathbf{S}_{-2,2} (36 D_{-1} - 76 D_0 + 76 D_1 - 36 D_2 - 32 D_0^2 - 32 D_1^2) \\
 & + \mathbf{S}_{1,-3} (2338/9 + 68 D_{-1} - 224/3 D_0 + 224/3 D_1 - 68 D_2 + 108 D_0^2 - 20 D_1^2) \\
 & + \mathbf{S}_{1,3} (4369/9 + 4 D_{-1} - 5707/18 D_0 + 2885/9 D_1 - 102 D_2 + 148 D_0^2 - 55 D_1^2) \\
 & + \mathbf{S}_{2,-2} (1522/9 + 44 D_{-1} - 128/3 D_0 + 128/3 D_1 - 44 D_2 + 68 D_0^2 - 12 D_1^2) \\
 & + \mathbf{S}_{2,2} (12331/36 + 8 D_{-1} - 812/3 D_0 + 1001/3 D_1 - 8 D_2 + 132 D_0^2 - 44 D_1^2) \\
 & + \mathbf{S}_{3,1} (23429/36 - 16 D_{-1} - 4171/18 D_0 + 3134/9 D_1 + 114 D_2 + 67 D_0^2 \\
 & - 14 D_1^2) + \mathbf{S}_{-2,1,1} (-32 D_{-1} + 152/3 D_0 - 152/3 D_1 + 32 D_2 + 28 D_0^2 + 20 D_1^2) \\
 & - 76/9 \mathbf{S}_{1,-2,1} + \mathbf{S}_{1,1,-2} (-496/3 - 40 D_{-1} + 64/3 D_0 - 64/3 D_1 + 40 D_2 - 56 D_0^2 \\
 & + 8 D_1^2) + \mathbf{S}_{1,1,2} (-15511/36 - 4 D_{-1} + 781/3 D_0 - 838/3 D_1 + 72 D_2 - 136 D_0^2 \\
 & + 54 D_1^2) + \mathbf{S}_{1,2,1} (-1839/4 + 4 D_{-1} + 686/3 D_0 - 857/3 D_1 - 4 D_2 - 104 D_0^2 \\
 & + 44 D_1^2) + \mathbf{S}_{2,1,1} (-3491/9 + 212 D_0 - 313 D_1 - 68 D_2 - 97 D_0^2 + 37 D_1^2) \\
 & + \mathbf{S}_{1,1,1,1} (12119/36 - 201 D_0 + 255 D_1 + 104 D_0^2 - 46 D_1^2) \\
 & + \mathbf{S}_{-3} (4346/27 + 200 D_{-1} - 3536/9 D_0 + 3536/9 D_1 - 200 D_2 - 144 D_{-1}^2 \\
 & + 107 D_0^2 - 26 D_0^3 - 799/3 D_1^2 + 138 D_1^3) + \mathbf{S}_3 (-103447/1296 - 4 D_{-1} \\
 & - 14155/36 D_0 + 18343/36 D_1 + 102 D_2 + 4561/18 D_0^2 - 245/2 D_0^3 - 166/3 D_1^2 \\
 & - 27/2 D_1^3) + \mathbf{S}_{-2,1} (-80 D_{-1} + 1760/9 D_0 - 1760/9 D_1 + 80 D_2 + 48 D_{-1}^2 \\
 & - 92/3 D_0^2 - 58 D_0^3 + 260/3 D_1^2 - 38 D_1^3) + \mathbf{S}_{1,-2} (-2428/27 - 40 D_{-1} - 8 D_0 \\
 & + 8 D_1 + 40 D_2 + 48 D_{-1}^2 - 122/3 D_0^2 + 78 D_0^3 + 70/3 D_1^2 - 14 D_1^3) \\
 & + \mathbf{S}_{1,2} (-110893/324 + 4 D_{-1} + 3818/9 D_0 - 15857/36 D_1 + 60 D_2 - 314 D_0^2 \\
 & + 146 D_0^3 + 1033/6 D_1^2 - 31 D_1^3) + \mathbf{S}_{2,1} (-81845/648 - 4 D_{-1} + 1699/6 D_0 \\
 & - 6299/12 D_1 - 128 D_2 - 1229/6 D_0^2 + 112 D_0^3 + 637/6 D_1^2 - 22 D_1^3) \\
 & + \mathbf{S}_{1,1,1} (26339/108 - 2671/9 D_0 + 15031/36 D_1 + 1409/6 D_0^2 - 121 D_0^3 \\
 & - 959/6 D_1^2 + 35 D_1^3) + \mathbf{S}_{-2} (-232/3 - 460/3 D_{-1} + 13351/54 D_0 - 13351/54 D_1 \\
 & + 460/3 D_2 + 140 D_{-1}^2 - 96 D_{-1}^3 - 1297/18 D_0^2 + 109/3 D_0^3 - 13 D_0^4)
 \end{aligned}$$

---


$$\begin{aligned}
& + 4231/18 D_1^2 - 505/3 D_1^3 + 99 D_1^4) + \mathbf{S}_2 (162721/1296 + 28 D_{-1} \\
& + 518651/1296 D_0 - 702953/1296 D_1 - 104 D_2 - 12079/36 D_0^2 + 8615/36 D_0^3 \\
& - 707/6 D_0^4 + 1385/12 D_1^2 - 1463/36 D_1^3 - 61/6 D_1^4) \\
& + \mathbf{S}_{1,1} (239633/2592 - 32 D_{-1} - 183109/432 D_0 + 257467/432 D_1 - 36 D_2 \\
& + 2137/6 D_0^2 - 9575/36 D_0^3 + 779/6 D_0^4 - 2623/12 D_1^2 + 5051/36 D_1^3 \\
& - 209/6 D_1^4) + \mathbf{S}_1 (161929/1728 - 104 D_{-1} - 1091171/2592 D_0 + 407591/648 D_1 \\
& - 70 D_2 + 48 D_{-1}^2 + 87833/216 D_0^2 - 16559/72 D_0^3 + 5683/36 D_0^4 - 269/3 D_0^5 \\
& - 211555/1296 D_1^2 + 7369/72 D_1^3 - 398/9 D_1^4 - 175/6 D_1^5) - 61555/512 \\
& - 1084/3 D_{-1} - 840065/2592 D_0 + 1650655/5184 D_1 + 1084/3 D_2 + 236 D_{-1}^2 \\
& - 96 D_{-1}^3 + 400535/864 D_0^2 + 273677/2592 D_0^3 - 28801/72 D_0^4 + 2570/9 D_0^5 \\
& - 1649/24 D_0^6 + 1486625/2592 D_1^2 - 67615/96 D_1^3 + 5589/8 D_1^4 - 6661/12 D_1^5 \\
& + 3189/8 D_1^6 \\
& + \zeta_3 \left[ 436 \mathbf{S}_{-3} + 1061/3 \mathbf{S}_3 - 200 \mathbf{S}_{1,-2} - 496/3 \mathbf{S}_{1,2} - 100/3 \mathbf{S}_{2,1} + 44 \mathbf{S}_{1,1,1} \right. \\
& + \mathbf{S}_{-2} (-388 + 52 D_0 - 52 D_1) + \mathbf{S}_2 (-28 - 76/3 D_0 + 76/3 D_1) + \mathbf{S}_{1,1} (35 + 50 D_0 \\
& - 50 D_1) + \mathbf{S}_1 (-397/6 + 60 D_{-1} + 982/3 D_0 - 607/3 D_1 + 272 D_2 - 98 D_0^2 \\
& + 176/3 D_1^2) - 15883/16 + 222 D_{-1} + 5977/12 D_0 + 179/12 D_1 + 238 D_2 \\
& \left. - 144 D_{-1}^2 - 1553/3 D_0^2 + 821/6 D_0^3 - 238/3 D_1^2 + 325/2 D_1^3 \right] \\
& + \zeta_5 \left[ 81 \mathbf{S}_1 - 513/4 + 9/2 D_0 - 9/2 D_1 \right] \\
c_{3,\text{ns}}^{(4)\text{Z}}(N) = & \\
& 24 \mathbf{S}_2 - 80 \mathbf{S}_1 + 33 + 64 D_0 - 64 D_1 - 12 D_0^2 + 12 D_1^2 \\
c_{3,\text{ns}}^{(4)\text{F}}(N) = & \\
& - 119/2 \mathbf{S}_5 + 12 \mathbf{S}_{1,4} + 24 \mathbf{S}_{2,3} + 36 \mathbf{S}_{3,2} + 48 \mathbf{S}_{4,1} - 12 \mathbf{S}_{1,1,3} - 12 \mathbf{S}_{1,2,2} \\
& - 12 \mathbf{S}_{1,3,1} - 24 \mathbf{S}_{2,1,2} - 24 \mathbf{S}_{2,2,1} - 36 \mathbf{S}_{3,1,1} + 12 \mathbf{S}_{1,1,1,2} + 12 \mathbf{S}_{1,1,2,1} \\
& + 12 \mathbf{S}_{1,2,1,1} + 24 \mathbf{S}_{2,1,1,1} - 12 \mathbf{S}_{1,1,1,1,1} + \mathbf{S}_4 (853/6 - 6 D_0 + 6 D_1) \\
& + \mathbf{S}_{1,3} (-29 + 6 D_0 - 6 D_1) + \mathbf{S}_{2,2} (-67 + 6 D_0 - 6 D_1) + \mathbf{S}_{3,1} (-105 + 6 D_0 - 6 D_1) \\
& + \mathbf{S}_{1,1,2} (29 - 6 D_0 + 6 D_1) + \mathbf{S}_{1,2,1} (29 - 6 D_0 + 6 D_1) + \mathbf{S}_{2,1,1} (67 - 6 D_0 + 6 D_1) \\
& + \mathbf{S}_{1,1,1,1} (-29 + 6 D_0 - 6 D_1) + \mathbf{S}_3 (-524/3 + 19 D_0 - 28 D_1 - 12 D_0^2 + 6 D_1^2) \\
& + \mathbf{S}_{1,2} (235/6 - 19 D_0 + 28 D_1 + 12 D_0^2 - 6 D_1^2) + \mathbf{S}_{2,1} (641/6 - 19 D_0 + 28 D_1 \\
& + 12 D_0^2 - 6 D_1^2) + \mathbf{S}_{1,1,1} (-235/6 + 19 D_0 - 28 D_1 - 12 D_0^2 + 6 D_1^2) \\
& + \mathbf{S}_2 (14321/108 - 203/6 D_0 + 187/3 D_1 + 41 D_0^2 - 18 D_0^3 - 28 D_1^2 + 6 D_1^3)
\end{aligned}$$

$$\begin{aligned}
 & + \mathbf{S}_{1,1} (-4429/108 + 203/6 D_0 - 187/3 D_1 - 41 D_0^2 + 18 D_0^3 + 28 D_1^2 - 6 D_1^3) \\
 & + \mathbf{S}_1 (-25279/648 + 4631/108 D_0 - 2528/27 D_1 - 445/6 D_0^2 + 63 D_0^3 - 24 D_0^4 \\
 & + 187/3 D_1^2 - 28 D_1^3 + 6 D_1^4) + 281971/3456 + 28727/648 D_0 - 36661/324 D_1 \\
 & - 10351/108 D_0^2 + 227/2 D_0^3 - 1009/12 D_0^4 + 119/4 D_0^5 + 2519/27 D_1^2 \\
 & - 184/3 D_1^3 + 325/12 D_1^4 - 23/4 D_1^5 \\
 & + \zeta_3 \left[ \mathbf{S}_2 - 5/3 \mathbf{S}_1 + 1/8 + 11/6 D_0 - 11/6 D_1 - 1/2 D_0^2 + 1/2 D_1^2 \right] \\
 & + \zeta_4 \left[ 3/2 \mathbf{S}_1 - 9/8 - 3/4 D_0 + 3/4 D_1 \right]
 \end{aligned} \tag{I.0.2}$$

The  $x$ -space results are:

$$\begin{aligned}
 c_{3,\text{ns}}^{(4)}(x) &= n_f^0 \text{ and } n_f^1 \text{ contributions} \\
 &+ C_F C_A n_f^2 \frac{4}{9} c_{3,\text{ns}}^{(4)\text{L}}(x) + C_F (C_F - \frac{1}{2} C_A) n_f^2 \frac{4}{9} c_{3,\text{ns}}^{(4)\text{N}}(x) + C_F n_f^3 \frac{4}{27} c_{3,\text{ns}}^{(4)\text{F}}(x)
 \end{aligned}$$

$$\begin{aligned}
 c_{3,\text{ns}}^{(4)\text{L}}(x) &= \\
 & \mathbf{H}_{0,0,0,0} (1951/4 - 1951/3 x_m^{-1} + 1951/4 x) + \mathbf{H}_{0,0,0,1} (607 - 2890/3 x_m^{-1} + 571 x \\
 & - 80 x^2) + \mathbf{H}_{0,0,0,1,0} (1547/3 - 2572/3 x_m^{-1} + 1583/3 x - 32 x^2) + \mathbf{H}_{0,0,0,1,1} (1637/3 \\
 & - 2752/3 x_m^{-1} + 1583/3 x - 40 x^2) + \mathbf{H}_{0,0,1,0,0} (387 - 670 x_m^{-1} + 411 x + 32 x^2) \\
 & + \mathbf{H}_{0,0,1,0,1} (428 - 752 x_m^{-1} + 416 x - 8 x^2) + \mathbf{H}_{0,0,1,1,0} (390 - 676 x_m^{-1} + 420 x + 8 x^2) \\
 & + \mathbf{H}_{0,0,1,1,1} (404 - 704 x_m^{-1} + 404 x) + \mathbf{H}_{0,1,0,0,0} (770/3 - 1408/3 x_m^{-1} + 770/3 x \\
 & + 80 x^2) + \mathbf{H}_{0,1,0,0,1} (296 + 48 x^{-1} - 548 x_m^{-1} + 272 x - 8 x^2) + \mathbf{H}_{0,1,0,1,0} (272 - 500 x_m^{-1} \\
 & + 272 x + 8 x^2) + \mathbf{H}_{0,1,0,1,1} (300 - 556 x_m^{-1} + 330 x - 72 x^2) + \mathbf{H}_{0,1,1,0,0} (260 - 48 x^{-1} \\
 & - 476 x_m^{-1} + 284 x + 40 x^2) + \mathbf{H}_{0,1,1,0,1} (266 - 488 x_m^{-1} + 218 x + 72 x^2) + \mathbf{H}_{0,1,1,1,0} (240 \\
 & - 436 x_m^{-1} + 258 x) + \mathbf{H}_{0,1,1,1,1} (252 - 460 x_m^{-1} + 252 x) + \mathbf{H}_{1,0,0,0,0} (671/3 \\
 & - 1342/3 x_m^{-1} + 671/3 x) + \mathbf{H}_{1,0,0,0,1} (824/3 + 80 x^{-1} - 1648/3 x_m^{-1} + 824/3 x - 80 x^2) \\
 & + \mathbf{H}_{1,0,0,1,0} (234 + 32 x^{-1} - 468 x_m^{-1} + 234 x - 32 x^2) + \mathbf{H}_{1,0,0,1,1} (270 + 40 x^{-1} \\
 & - 540 x_m^{-1} + 270 x - 40 x^2) + \mathbf{H}_{1,0,1,0,0} (178 - 32 x^{-1} - 356 x_m^{-1} + 178 x + 32 x^2) \\
 & + \mathbf{H}_{1,0,1,0,1} (216 + 8 x^{-1} - 432 x_m^{-1} + 216 x - 8 x^2) + \mathbf{H}_{1,0,1,1,0} (206 - 8 x^{-1} - 412 x_m^{-1} \\
 & + 206 x + 8 x^2) + \mathbf{H}_{1,0,1,1,1} (228 - 456 x_m^{-1} + 228 x) + \mathbf{H}_{1,1,0,0,0} (530/3 - 80 x^{-1} \\
 & - 1060/3 x_m^{-1} + 530/3 x + 80 x^2) + \mathbf{H}_{1,1,0,0,1} (196 + 8 x^{-1} - 392 x_m^{-1} + 196 x - 8 x^2) \\
 & + \mathbf{H}_{1,1,0,1,0} (162 - 8 x^{-1} - 324 x_m^{-1} + 162 x + 8 x^2) + \mathbf{H}_{1,1,0,1,1} (188 - 376 x_m^{-1} + 236 x
 \end{aligned}$$

---


$$\begin{aligned}
& -72x^2) + \mathbf{H}_{1,1,1,0,0}(142 - 40x^{-1} - 284x_m^{-1} + 142x + 40x^2) + \mathbf{H}_{1,1,1,0,1}(164 \\
& - 328x_m^{-1} + 116x + 72x^2) + \mathbf{H}_{1,1,1,1,0}(140 - 280x_m^{-1} + 140x) + \mathbf{H}_{1,1,1,1,1}(160 \\
& - 320x_m^{-1} + 160x) + \mathbf{H}_{0,0,0,0}(8239/6 - 20567/9x_m^{-1} + 3499/2x) + \mathbf{H}_{0,0,0,1}(2755/2 \\
& - 24686/9x_m^{-1} + 3871/2x - 36x^2) + \mathbf{H}_{0,0,1,0}(19199/18 - 19634/9x_m^{-1} \\
& + 28733/18x) + \mathbf{H}_{0,0,1,1}(18695/18 - 19967/9x_m^{-1} + 14335/9x + 16x^2) \\
& + \mathbf{H}_{0,1,0,0}(6457/9 - 13373/9x_m^{-1} + 9454/9x + 36x^2) + \mathbf{H}_{0,1,0,1}(2143/3 \\
& - 4835/3x_m^{-1} + 3310/3x) + \mathbf{H}_{0,1,1,0}(1996/3 - 4283/3x_m^{-1} + 6485/6x - 16x^2) \\
& + \mathbf{H}_{0,1,1,1}(1895/3 - 4270/3x_m^{-1} + 3107/3x) + \mathbf{H}_{1,0,0,0}(4456/9 - 9995/9x_m^{-1} \\
& + 6574/9x) + \mathbf{H}_{1,0,0,1}(4966/9 + 16x^{-1} - 12263/9x_m^{-1} + 8269/9x - 36x^2) \\
& + \mathbf{H}_{1,0,1,0}(1354/3 - 3212/3x_m^{-1} + 2218/3x) + \mathbf{H}_{1,0,1,1}(469 - 1210x_m^{-1} + 1797/2x \\
& + 16x^2) + \mathbf{H}_{1,1,0,0}(3820/9 - 16x^{-1} - 8495/9x_m^{-1} + 5917/9x + 36x^2) \\
& + \mathbf{H}_{1,1,0,1}(1292/3 - 3022/3x_m^{-1} + 1928/3x) + \mathbf{H}_{1,1,1,0}(1117/3 - 2558/3x_m^{-1} \\
& + 3665/6x - 16x^2) + \mathbf{H}_{1,1,1,1}(370 - 904x_m^{-1} + 642x) + \mathbf{H}_{0,0,0}(11431/6 \\
& - 152383/36x_m^{-1} + 68785/18x + 2890/3\zeta_2x_m^{-1} - 607\zeta_2 - 571\zeta_2x + 80\zeta_2x^2) \\
& + \mathbf{H}_{0,0,1}(54551/36 - 35378/9x_m^{-1} + 128459/36x + 34x^2 + 752\zeta_2x_m^{-1} - 428\zeta_2 \\
& - 416\zeta_2x + 8\zeta_2x^2) + \mathbf{H}_{0,1,0}(2927/3 - 24305/9x_m^{-1} + 45911/18x - 34x^2 \\
& - 48\zeta_2x^{-1} + 548\zeta_2x_m^{-1} - 296\zeta_2 - 272\zeta_2x + 8\zeta_2x^2) + \mathbf{H}_{0,1,1}(7420/9 \\
& - 23191/9x_m^{-1} + 22106/9x + 488\zeta_2x_m^{-1} - 266\zeta_2 - 218\zeta_2x - 72\zeta_2x^2) \\
& + \mathbf{H}_{1,0,0}(3151/6 - 15200/9x_m^{-1} + 28807/18x - 80\zeta_2x^{-1} + 1648/3\zeta_2x_m^{-1} \\
& - 824/3\zeta_2 - 824/3\zeta_2x + 80\zeta_2x^2) + \mathbf{H}_{1,0,1}(2753/6 - 10459/6x_m^{-1} + 3523/2x \\
& + 34x^2 - 8\zeta_2x^{-1} + 432\zeta_2x_m^{-1} - 216\zeta_2 - 216\zeta_2x + 8\zeta_2x^2) + \mathbf{H}_{1,1,0}(7949/18 \\
& - 27307/18x_m^{-1} + 28031/18x - 34x^2 - 8\zeta_2x^{-1} + 392\zeta_2x_m^{-1} - 196\zeta_2 - 196\zeta_2x \\
& + 8\zeta_2x^2) + \mathbf{H}_{1,1,1}(6367/18 - 25979/18x_m^{-1} + 27127/18x + 328\zeta_2x_m^{-1} - 164\zeta_2 \\
& - 116\zeta_2x - 72\zeta_2x^2) + \mathbf{H}_{0,0}(310343/216 - 842039/162x_m^{-1} + 1281401/216x \\
& + 24686/9\zeta_2x_m^{-1} - 2755/2\zeta_2 - 3871/2\zeta_2x + 36\zeta_2x^2 + 1160/3\zeta_3x_m^{-1} \\
& - 769/3\zeta_3 - 1003/3\zeta_3x - 56\zeta_3x^2) + \mathbf{H}_{0,1}(51305/81 - 1178369/324x_m^{-1} \\
& + 371453/81x + 4835/3\zeta_2x_m^{-1} - 2143/3\zeta_2 - 3310/3\zeta_2x + 48\zeta_3x^{-1} \\
& + 976/3\zeta_3x_m^{-1} - 520/3\zeta_3 - 1366/3\zeta_3x + 304\zeta_3x^2) + \mathbf{H}_{1,0}(47123/648 \\
& - 147071/81x_m^{-1} + 1746287/648x - 16\zeta_2x^{-1} + 12263/9\zeta_2x_m^{-1} - 4966/9\zeta_2 \\
& - 8269/9\zeta_2x + 36\zeta_2x^2 + 56\zeta_3x^{-1} + 944/3\zeta_3x_m^{-1} - 472/3\zeta_3 - 472/3\zeta_3x \\
& - 56\zeta_3x^2) + \mathbf{H}_{1,1}(-10019/216 - 46483/27x_m^{-1} + 574609/216x + 3022/3\zeta_2x_m^{-1}
\end{aligned}$$



$$\begin{aligned}
 & -1292/3 \zeta_2 - 1928/3 \zeta_2 x + 56 \zeta_3 x^{-1} + 176 \zeta_3 x_m^{-1} - 88 \zeta_3 - 328 \zeta_3 x + 304 \zeta_3 x^2 \\
 & + \mathbf{H}_0 (212195/2592 - 5764837/1296 x_m^{-1} + 661237/96 x + 35378/9 \zeta_2 x_m^{-1} \\
 & - 54551/36 \zeta_2 - 128459/36 \zeta_2 x - 34 \zeta_2 x^2 + 3085/3 \zeta_3 x_m^{-1} - 5792/9 \zeta_3 \\
 & - 17797/18 \zeta_3 x - 20 \zeta_3 x^2 - 2506/3 \zeta_4 x_m^{-1} + 5755/12 \zeta_4 + 6007/12 \zeta_4 x \\
 & - 106 \zeta_4 x^2) + \mathbf{H}_1 (-90473/108 - 2134163/1296 x_m^{-1} + 2631655/648 x \\
 & + 10459/6 \zeta_2 x_m^{-1} - 2753/6 \zeta_2 - 3523/2 \zeta_2 x - 34 \zeta_2 x^2 + 16 \zeta_3 x^{-1} \\
 & + 5879/9 \zeta_3 x_m^{-1} - 2317/9 \zeta_3 - 14585/18 \zeta_3 x - 20 \zeta_3 x^2 + 106 \zeta_4 x^{-1} \\
 & - 1400/3 \zeta_4 x_m^{-1} + 700/3 \zeta_4 + 700/3 \zeta_4 x - 106 \zeta_4 x^2) + \delta(1-x) (-18199451/6912 \\
 & - 5764837/1296 \zeta_2 - 29/648 \zeta_3 + 4300/9 \zeta_3 \zeta_2 + 35/3 \zeta_3^2 + 68705/72 \zeta_4 + 3091/6 \zeta_5 \\
 & + 521/2 \zeta_6) - 9928021/5184 - 132728/81 x_m^{-1} + 1067909/192 x \\
 & + 1178369/324 \zeta_2 x_m^{-1} - 51305/81 \zeta_2 - 371453/81 \zeta_2 x + 13247/9 \zeta_3 x_m^{-1} \\
 & - 8167/12 \zeta_3 - 46241/36 \zeta_3 x + 102 \zeta_3 x^2 - 980/3 \zeta_3 \zeta_2 x_m^{-1} + 209 \zeta_3 \zeta_2 \\
 & + 221 \zeta_3 \zeta_2 x + 80 \zeta_3 \zeta_2 x^2 - 72041/36 \zeta_4 x_m^{-1} + 62383/72 \zeta_4 + 113329/72 \zeta_4 x \\
 & - 96 \zeta_4 x^2 + 1036/3 \zeta_5 x_m^{-1} - 206 \zeta_5 - 686 \zeta_5 x + 640 \zeta_5 x^2 \\
 c_{3,\text{ns}}^{(4)\text{N}}(x) = & \\
 & + \mathbf{H}_{-1,-1,-1,-1,0} (-832 + 1024 x_p^{-1} + 192 x) + \mathbf{H}_{-1,-1,-1,0,0} (1440 - 1792 x_p^{-1} - 352 x) \\
 & + \mathbf{H}_{-1,-1,0,-1,0} (928 - 1152 x_p^{-1} - 224 x) + \mathbf{H}_{-1,-1,0,0,0} (-1616 + 2080 x_p^{-1} + 464 x) \\
 & + \mathbf{H}_{-1,0,-1,-1,0} (928 - 1152 x_p^{-1} - 224 x) + \mathbf{H}_{-1,0,-1,0,0} (-1552 + 1984 x_p^{-1} + 432 x) \\
 & + \mathbf{H}_{-1,0,0,-1,0} (-1040 + 1344 x_p^{-1} + 304 x) + \mathbf{H}_{-1,0,0,0,0} (1188 - 1800 x_p^{-1} - 612 x) \\
 & + \mathbf{H}_{-1,0,0,0,1} (8 - 16 x_p^{-1} - 8 x) + \mathbf{H}_{-1,0,0,1,1} (-16 + 32 x_p^{-1} + 16 x) + \mathbf{H}_{-1,0,1,1,1} (32 \\
 & - 64 x_p^{-1} - 32 x) + \mathbf{H}_{0,-1,-1,-1,0} (928 - 1152 x_p^{-1} - 224 x) + \mathbf{H}_{0,-1,-1,0,0} (-1552 \\
 & + 1984 x_p^{-1} + 432 x) + \mathbf{H}_{0,-1,0,-1,0} (-1008 + 1280 x_p^{-1} + 272 x) + \mathbf{H}_{0,-1,0,0,0} (516 \\
 & + 1408 x_m^{-1} - 2152 x_p^{-1} - 1060 x) + \mathbf{H}_{0,-1,0,0,1} (-648 + 864 x_m^{-1} - 16 x_p^{-1} - 216 x) \\
 & + \mathbf{H}_{0,-1,0,1,0} (-416 + 544 x_m^{-1} - 128 x) + \mathbf{H}_{0,-1,0,1,1} (-368 + 448 x_m^{-1} + 32 x_p^{-1} - 80 x) \\
 & + \mathbf{H}_{0,0,-1,-1,0} (-1080 + 16 x_m^{-1} + 1376 x_p^{-1} + 296 x) + \mathbf{H}_{0,0,-1,0,0} (200 + 2040 x_m^{-1} \\
 & - 2344 x_p^{-1} - 1280 x) + \mathbf{H}_{0,0,-1,0,1} (-808 + 1056 x_m^{-1} - 16 x_p^{-1} - 248 x) \\
 & + \mathbf{H}_{0,0,0,-1,0} (52 + 1632 x_m^{-1} - 1736 x_p^{-1} - 1012 x) + \mathbf{H}_{0,0,0,0,0} (751/2 - 2102/3 x_m^{-1} \\
 & + 600 x_p^{-1} + 1951/2 x) + \mathbf{H}_{0,0,0,0,1} (860 - 3728/3 x_m^{-1} + 24 x_p^{-1} + 884 x) \\
 & + \mathbf{H}_{0,0,0,1,0} (2458/3 - 3872/3 x_m^{-1} + 2458/3 x) + \mathbf{H}_{0,0,0,1,1} (2602/3 - 4064/3 x_m^{-1} \\
 & - 32 x_p^{-1} + 2506/3 x) + \mathbf{H}_{0,0,1,0,0} (602 - 1092 x_m^{-1} + 698 x) + \mathbf{H}_{0,0,1,0,1} (656
 \end{aligned}$$

---


$$\begin{aligned}
& -1104x_m^{-1} + 656x) + \mathbf{H}_{0,0,1,1,0}(792 - 1376x_m^{-1} + 792x) + \mathbf{H}_{0,0,1,1,1}(692 - 1208x_m^{-1} \\
& + 32x_p^{-1} + 724x) + \mathbf{H}_{0,1,0,-1,0}(-440 + 560x_m^{-1} - 120x) + \mathbf{H}_{0,1,0,0,0}(796/3 \\
& - 2192/3x_m^{-1} + 1660/3x) + \mathbf{H}_{0,1,0,0,1}(-12 - 256x_m^{-1} + 356x) + \mathbf{H}_{0,1,0,1,0}(728 \\
& - 1256x_m^{-1} + 616x) + \mathbf{H}_{0,1,0,1,1}(476 - 864x_m^{-1} + 476x) + \mathbf{H}_{0,1,1,0,0}(712 - 1304x_m^{-1} \\
& + 680x) + \mathbf{H}_{0,1,1,0,1}(424 - 840x_m^{-1} + 504x) + \mathbf{H}_{0,1,1,1,0}(712 - 1256x_m^{-1} + 632x) \\
& + \mathbf{H}_{0,1,1,1,1}(504 - 920x_m^{-1} + 504x) + \mathbf{H}_{1,0,-1,-1,0}(-16 + 32x_m^{-1} - 16x) \\
& + \mathbf{H}_{1,0,-1,0,0}(-792 + 1008x_m^{-1} - 216x) + \mathbf{H}_{1,0,-1,0,1}(-480 + 576x_m^{-1} - 96x) \\
& + \mathbf{H}_{1,0,0,-1,0}(-696 + 880x_m^{-1} - 184x) + \mathbf{H}_{1,0,0,0,0}(28/3 - 1784/3x_m^{-1} + 1756/3x) \\
& + \mathbf{H}_{1,0,0,0,1}(-1040/3 + 16/3x_m^{-1} + 1024/3x) + \mathbf{H}_{1,0,0,1,0}(208 - 640x_m^{-1} + 432x) \\
& + \mathbf{H}_{1,0,0,1,1}(8 - 352x_m^{-1} + 344x) + \mathbf{H}_{1,0,1,0,0}(676 - 1208x_m^{-1} + 532x) + \mathbf{H}_{1,0,1,0,1}(360 \\
& - 752x_m^{-1} + 392x) + \mathbf{H}_{1,0,1,1,0}(564 - 1016x_m^{-1} + 452x) + \mathbf{H}_{1,0,1,1,1}(368 - 736x_m^{-1} \\
& + 368x) + \mathbf{H}_{1,1,0,-1,0}(-352 + 448x_m^{-1} - 96x) + \mathbf{H}_{1,1,0,0,0}(1540/3 - 3080/3x_m^{-1} \\
& + 1540/3x) + \mathbf{H}_{1,1,0,0,1}(-68 - 232x_m^{-1} + 300x) + \mathbf{H}_{1,1,0,1,0}(568 - 1008x_m^{-1} + 440x) \\
& + \mathbf{H}_{1,1,0,1,1}(248 - 576x_m^{-1} + 328x) + \mathbf{H}_{1,1,1,0,0}(636 - 1096x_m^{-1} + 460x) \\
& + \mathbf{H}_{1,1,1,0,1}(264 - 592x_m^{-1} + 328x) + \mathbf{H}_{1,1,1,1,0}(560 - 976x_m^{-1} + 416x) \\
& + \mathbf{H}_{1,1,1,1,1}(320 - 640x_m^{-1} + 320x) + \mathbf{H}_{-1,-1,-1,0}(2944/3 - 160x^{-1} - 3200/3x_p^{-1} \\
& - 256/3x - 160x^2) + \mathbf{H}_{-1,-1,0,0}(-4544/3 + 272x^{-1} + 5440/3x_p^{-1} + 896/3x + 272x^2) \\
& + \mathbf{H}_{-1,0,-1,0}(-3008/3 + 176x^{-1} + 3520/3x_p^{-1} + 512/3x + 176x^2) + \mathbf{H}_{-1,0,0,0}(472 \\
& - 576x^{-1} - 1792x_p^{-1} - 1320x - 576x^2) + \mathbf{H}_{-1,0,0,1}(-1360/3 - 224x^{-1} - 160/3x_p^{-1} \\
& - 1520/3x - 224x^2) + \mathbf{H}_{-1,0,1,0}(-304 - 144x^{-1} - 304x - 144x^2) + \mathbf{H}_{-1,0,1,1}(-928/3 \\
& - 128x^{-1} + 320/3x_p^{-1} - 608/3x - 128x^2) + \mathbf{H}_{0,-1,-1,0}(-3032/3 + 192x^{-1} \\
& + 3520/3x_p^{-1} + 536/3x + 160x^2) + \mathbf{H}_{0,-1,0,0}(-156 - 576x^{-1} + 1568x_m^{-1} - 1840x_p^{-1} \\
& - 1364x - 272x^2) + \mathbf{H}_{0,-1,0,1}(-2128/3 - 192x^{-1} + 640x_m^{-1} - 160/3x_p^{-1} - 1040/3x) \\
& + \mathbf{H}_{0,0,-1,0}(-692/3 - 384x^{-1} + 4768/3x_m^{-1} - 1504x_p^{-1} - 3212/3x - 112x^2) \\
& + \mathbf{H}_{0,0,0,0}(2268 - 13852/9x_m^{-1} + 1240/3x_p^{-1} + 2940x + 576x^2) + \mathbf{H}_{0,0,0,1}(7451/3 \\
& - 28516/9x_m^{-1} + 160/3x_p^{-1} + 3409x + 680x^2) + \mathbf{H}_{0,0,1,0}(14117/9 - 22732/9x_m^{-1} \\
& + 22409/9x + 112x^2) + \mathbf{H}_{0,0,1,1}(16157/9 - 25252/9x_m^{-1} - 160/3x_p^{-1} + 23897/9x \\
& + 400x^2) + \mathbf{H}_{0,1,0,0}(3128/9 - 12250/9x_m^{-1} + 13532/9x - 408x^2) + \mathbf{H}_{0,1,0,1}(2542/3 \\
& - 5000/3x_m^{-1} + 4702/3x + 16x^2) + \mathbf{H}_{0,1,1,0}(798 - 2054x_m^{-1} + 1806x - 288x^2) \\
& + \mathbf{H}_{0,1,1,1}(2554/3 - 5372/3x_m^{-1} + 4978/3x) + \mathbf{H}_{1,0,-1,0}(-1648/3 - 64x^{-1}
\end{aligned}$$

$$\begin{aligned}
 & + 2048/3 x_m^{-1} - 400/3 x + 64 x^2) + \mathbf{H}_{1,0,0,0} (992/9 - 12790/9 x_m^{-1} + 13868/9 x) \\
 & + \mathbf{H}_{1,0,0,1} (3428/9 - 64 x^{-1} - 11770/9 x_m^{-1} + 12536/9 x + 456 x^2) + \mathbf{H}_{1,0,1,0} (2420/3 \\
 & + 32 x^{-1} - 5668/3 x_m^{-1} + 4004/3 x - 32 x^2) + \mathbf{H}_{1,0,1,1} (804 - 1652 x_m^{-1} + 1252 x \\
 & + 272 x^2) + \mathbf{H}_{1,1,0,0} (3944/9 + 16 x^{-1} - 15358/9 x_m^{-1} + 11540/9 x - 408 x^2) \\
 & + \mathbf{H}_{1,1,0,1} (1316/3 - 16 x^{-1} - 4060/3 x_m^{-1} + 3428/3 x + 16 x^2) + \mathbf{H}_{1,1,1,0} (1528/3 \\
 & + 16 x^{-1} - 4652/3 x_m^{-1} + 3352/3 x - 288 x^2) + \mathbf{H}_{1,1,1,1} (476 - 1280 x_m^{-1} + 1020 x) \\
 & + \mathbf{H}_{-1,-1,-1} (512 \zeta_2 x_p^{-1} - 416 \zeta_2 + 96 \zeta_2 x) + \mathbf{H}_{-1,-1,0} (-1600/3 + 320 x^{-1} \\
 & + 1984/3 x_p^{-1} + 128 x + 320 x^2 - 352 \zeta_2 x_p^{-1} + 288 \zeta_2 - 64 \zeta_2 x) \\
 & + \mathbf{H}_{-1,0,-1} (-576 \zeta_2 x_p^{-1} + 464 \zeta_2 - 112 \zeta_2 x) + \mathbf{H}_{-1,0,0} (-7240/9 - 1072 x^{-1} \\
 & - 9352/9 x_p^{-1} - 16592/9 x - 1072 x^2 + 248 \zeta_2 x_p^{-1} - 180 \zeta_2 + 68 \zeta_2 x) \\
 & + \mathbf{H}_{-1,0,1} (-6736/9 - 320 x^{-1} - 304/9 x_p^{-1} - 7040/9 x - 320 x^2 + 16 \zeta_2 x_p^{-1} - 8 \zeta_2 \\
 & + 8 \zeta_2 x) + \mathbf{H}_{0,-1,-1} (-576 \zeta_2 x_p^{-1} + 464 \zeta_2 - 112 \zeta_2 x) + \mathbf{H}_{0,-1,0} (-4714/9 \\
 & - 752 x^{-1} + 800 x_m^{-1} - 6088/9 x_p^{-1} - 10334/9 x - 320 x^2 - 864 \zeta_2 x_m^{-1} + 376 \zeta_2 x_p^{-1} \\
 & + 364 \zeta_2 + 292 \zeta_2 x) + \mathbf{H}_{0,0,-1} (-1048 \zeta_2 x_m^{-1} + 704 \zeta_2 x_p^{-1} + 268 \zeta_2 + 396 \zeta_2 x) \\
 & + \mathbf{H}_{0,0,0} (23690/9 - 18371/18 x_m^{-1} + 5080/9 x_p^{-1} + 28822/9 x + 1072 x^2 \\
 & + 3572/3 \zeta_2 x_m^{-1} - 76 \zeta_2 x_p^{-1} - 808 \zeta_2 - 884 \zeta_2 x) + \mathbf{H}_{0,0,1} (35179/18 \\
 & - 23429/9 x_m^{-1} + 152/9 x_p^{-1} + 70805/18 x + 848 x^2 + 416 \zeta_2 x_m^{-1} - 8 \zeta_2 x_p^{-1} \\
 & - 116 \zeta_2 - 508 \zeta_2 x) + \mathbf{H}_{0,1,0} (140 - 12331/9 x_m^{-1} + 21596/9 x - 528 x^2 - 104 \zeta_2 x_m^{-1} \\
 & + 296 \zeta_2 - 280 \zeta_2 x) + \mathbf{H}_{0,1,1} (2294/9 - 13964/9 x_m^{-1} + 21604/9 x + 264 \zeta_2 x_m^{-1} \\
 & + 40 \zeta_2 - 392 \zeta_2 x) + \mathbf{H}_{1,0,-1} (-560 \zeta_2 x_m^{-1} + 472 \zeta_2 + 88 \zeta_2 x) + \mathbf{H}_{1,0,0} (353 \\
 & - 17476/9 x_m^{-1} + 22015/9 x - 712/3 \zeta_2 x_m^{-1} + 1556/3 \zeta_2 - 844/3 \zeta_2 x) \\
 & + \mathbf{H}_{1,0,1} (2167/3 - 1839 x_m^{-1} + 6251/3 x + 528 x^2 + 176 \zeta_2 x_m^{-1} + 104 \zeta_2 - 280 \zeta_2 x) \\
 & + \mathbf{H}_{1,1,0} (95/9 - 15511/9 x_m^{-1} + 18449/9 x - 528 x^2 - 120 \zeta_2 x_m^{-1} + 356 \zeta_2 \\
 & - 236 \zeta_2 x) + \mathbf{H}_{1,1,1} (1435/9 - 12119/9 x_m^{-1} + 15031/9 x + 80 \zeta_2 x_m^{-1} + 152 \zeta_2 \\
 & - 232 \zeta_2 x) + \mathbf{H}_{-1,-1} (-80 \zeta_2 x^{-1} - 1600/3 \zeta_2 x_p^{-1} + 1472/3 \zeta_2 - 128/3 \zeta_2 x \\
 & - 80 \zeta_2 x^2 - 512 \zeta_3 x_p^{-1} + 416 \zeta_3 - 96 \zeta_3 x) + \mathbf{H}_{-1,0} (-27790/27 - 3040/3 x^{-1} \\
 & - 9712/27 x_p^{-1} - 37502/27 x - 3040/3 x^2 + 280 \zeta_2 x^{-1} + 896/3 \zeta_2 x_p^{-1} + 680/3 \zeta_2 \\
 & + 1576/3 \zeta_2 x + 280 \zeta_2 x^2 + 256 \zeta_3 x_p^{-1} - 208 \zeta_3 + 48 \zeta_3 x) + \mathbf{H}_{0,-1} (288 \zeta_2 x^{-1} \\
 & - 640 \zeta_2 x_m^{-1} + 640 \zeta_2 x_p^{-1} + 204 \zeta_2 + 436 \zeta_2 x + 80 \zeta_2 x^2 - 224 \zeta_3 x_m^{-1} \\
 & + 560 \zeta_3 x_p^{-1} - 280 \zeta_3 + 152 \zeta_3 x) + \mathbf{H}_{0,0} (12749/24 + 103447/324 x_m^{-1}
 \end{aligned}$$

---


$$\begin{aligned}
& + 17384/27 x_p^{-1} + 423841/216 x + 3040/3 x^2 + 28900/9 \zeta_2 x_m^{-1} - 32/3 \zeta_2 x_p^{-1} \\
& - 8143/3 \zeta_2 - 3409 \zeta_2 x - 792 \zeta_2 x^2 + 5260/3 \zeta_3 x_m^{-1} - 148 \zeta_3 x_p^{-1} - 2498/3 \zeta_3 \\
& - 3230/3 \zeta_3 x) + \mathbf{H}_{0,1} (-72683/81 - 81845/162 x_m^{-1} + 211645/81 x + 96 \zeta_2 x^{-1} \\
& + 1080 \zeta_2 x_m^{-1} - 342 \zeta_2 - 1478 \zeta_2 x - 96 \zeta_2 x^2 + 1976/3 \zeta_3 x_m^{-1} - 572/3 \zeta_3 \\
& - 1532/3 \zeta_3 x) + \mathbf{H}_{1,0} (-111367/324 - 110893/81 x_m^{-1} + 837737/324 x + 120 \zeta_2 x^{-1} \\
& + 9562/9 \zeta_2 x_m^{-1} - 1388/9 \zeta_2 - 12368/9 \zeta_2 x - 512 \zeta_2 x^2 + 2008/3 \zeta_3 x_m^{-1} \\
& - 836/3 \zeta_3 - 1172/3 \zeta_3 x) + \mathbf{H}_{1,1} (-91577/108 - 26339/27 x_m^{-1} + 241915/108 x \\
& + 96 \zeta_2 x^{-1} + 820 \zeta_2 x_m^{-1} + 52 \zeta_2 - 1100 \zeta_2 x - 96 \zeta_2 x^2 + 504 \zeta_3 x_m^{-1} - 172 \zeta_3 \\
& - 332 \zeta_3 x) + \mathbf{H}_{-1} (480 \zeta_2 x^{-1} + 3280/9 \zeta_2 x_p^{-1} + 4336/9 \zeta_2 + 7616/9 \zeta_2 x \\
& + 480 \zeta_2 x^2 + 144 \zeta_3 x^{-1} + 480 \zeta_3 x_p^{-1} - 336 \zeta_3 + 144 \zeta_3 x + 144 \zeta_3 x^2 \\
& + 516 \zeta_4 x_p^{-1} - 358 \zeta_4 + 158 \zeta_4 x) + \mathbf{H}_0 (-1402631/648 + 162721/324 x_m^{-1} \\
& + 928/3 x_p^{-1} + 99875/72 x + 2665 \zeta_2 x_m^{-1} + 404/9 \zeta_2 x_p^{-1} - 14869/6 \zeta_2 \\
& - 70805/18 \zeta_2 x - 1168 \zeta_2 x^2 + 10856/3 \zeta_3 x_m^{-1} - 280 \zeta_3 x_p^{-1} - 11314/9 \zeta_3 \\
& - 28642/9 \zeta_3 x + 432 \zeta_3 x^2 - 3287/3 \zeta_4 x_m^{-1} - 300 \zeta_4 x_p^{-1} + 2501/3 \zeta_4 \\
& + 1961/3 \zeta_4 x) + \mathbf{H}_1 (-186851/108 - 239633/648 x_m^{-1} + 362231/162 x + 160 \zeta_2 x^{-1} \\
& + 4525/3 \zeta_2 x_m^{-1} - 1367/3 \zeta_2 - 6059/3 \zeta_2 x - 688 \zeta_2 x^2 + 88 \zeta_3 x^{-1} \\
& + 11626/9 \zeta_3 x_m^{-1} + 364/9 \zeta_3 - 10784/9 \zeta_3 x + 576 \zeta_3 x^2 - 484/3 \zeta_4 x_m^{-1} \\
& - 328/3 \zeta_4 + 812/3 \zeta_4 x) + \delta(1-x) (-61555/128 + 212833/324 \zeta_2 - 707833/162 \zeta_3 \\
& + 7322/9 \zeta_3 \zeta_2 + 976/3 \zeta_3^2 + 123449/36 \zeta_4 + 1394/3 \zeta_5 + 1124/3 \zeta_6) - 3067495/1296 \\
& - 161929/432 x_m^{-1} + 3523807/1296 x + 52709/162 \zeta_2 x_m^{-1} - 4856/27 \zeta_2 x_p^{-1} \\
& - 10687/81 \zeta_2 - 211645/81 \zeta_2 x - 3040/3 \zeta_2 x^2 + 31993/9 \zeta_3 x_m^{-1} - 356 \zeta_3 x_p^{-1} \\
& - 4937/6 \zeta_3 - 77141/18 \zeta_3 x + 784 \zeta_3 x^2 - 3628/3 \zeta_3 \zeta_2 x_m^{-1} + 52 \zeta_3 \zeta_2 x_p^{-1} \\
& + 534 \zeta_3 \zeta_2 + 842 \zeta_3 \zeta_2 x - 47453/18 \zeta_4 x_m^{-1} - 3488/3 \zeta_4 x_p^{-1} + 79477/36 \zeta_4 \\
& + 82861/36 \zeta_4 x + 414 \zeta_4 x^2 + 44/3 \zeta_5 x_m^{-1} - 508 \zeta_5 x_p^{-1} + 476 \zeta_5 - 448 \zeta_5 x \\
c_{3,\text{ns}}^{(4)\text{F}}(x) = & \\
& + \mathbf{H}_{0,0,0} (-119 + 238 x_m^{-1} - 119 x) + \mathbf{H}_{0,0,1} (-96 + 192 x_m^{-1} - 96 x) \\
& + \mathbf{H}_{0,0,1,0} (-72 + 144 x_m^{-1} - 72 x) + \mathbf{H}_{0,0,1,1} (-72 + 144 x_m^{-1} - 72 x) \\
& + \mathbf{H}_{0,1,0,0} (-48 + 96 x_m^{-1} - 48 x) + \mathbf{H}_{0,1,0,1} (-48 + 96 x_m^{-1} - 48 x) \\
& + \mathbf{H}_{0,1,1,0} (-48 + 96 x_m^{-1} - 48 x) + \mathbf{H}_{0,1,1,1} (-48 + 96 x_m^{-1} - 48 x) \\
& + \mathbf{H}_{1,0,0,0} (-24 + 48 x_m^{-1} - 24 x) + \mathbf{H}_{1,0,0,1} (-24 + 48 x_m^{-1} - 24 x)
\end{aligned}$$

$$\begin{aligned}
 & + \mathbf{H}_{1,0,1,0}(-24 + 48 x_m^{-1} - 24 x) + \mathbf{H}_{1,0,1,1}(-24 + 48 x_m^{-1} - 24 x) \\
 & + \mathbf{H}_{1,1,0,0}(-24 + 48 x_m^{-1} - 24 x) + \mathbf{H}_{1,1,0,1}(-24 + 48 x_m^{-1} - 24 x) \\
 & + \mathbf{H}_{1,1,1,0}(-24 + 48 x_m^{-1} - 24 x) + \mathbf{H}_{1,1,1,1}(-24 + 48 x_m^{-1} - 24 x) \\
 & + \mathbf{H}_{0,0,0}(-697/3 + 1706/3 x_m^{-1} - 1333/3 x) + \mathbf{H}_{0,0,1}(-168 + 420 x_m^{-1} - 336 x) \\
 & + \mathbf{H}_{0,1,0}(-104 + 268 x_m^{-1} - 224 x) + \mathbf{H}_{0,1,1}(-104 + 268 x_m^{-1} - 224 x) \\
 & + \mathbf{H}_{1,0,0}(-40 + 116 x_m^{-1} - 112 x) + \mathbf{H}_{1,0,1}(-40 + 116 x_m^{-1} - 112 x) \\
 & + \mathbf{H}_{1,1,0}(-40 + 116 x_m^{-1} - 112 x) + \mathbf{H}_{1,1,1}(-40 + 116 x_m^{-1} - 112 x) \\
 & + \mathbf{H}_{0,0}(-734/3 + 2096/3 x_m^{-1} - 744 x - 192 \zeta_2 x_m^{-1} + 96 \zeta_2 + 96 \zeta_2 x) \\
 & + \mathbf{H}_{0,1}(-392/3 + 1282/3 x_m^{-1} - 1496/3 x - 96 \zeta_2 x_m^{-1} + 48 \zeta_2 + 48 \zeta_2 x) \\
 & + \mathbf{H}_{1,0}(-64/3 + 470/3 x_m^{-1} - 748/3 x - 48 \zeta_2 x_m^{-1} + 24 \zeta_2 + 24 \zeta_2 x) \\
 & + \mathbf{H}_{1,1}(-64/3 + 470/3 x_m^{-1} - 748/3 x - 48 \zeta_2 x_m^{-1} + 24 \zeta_2 + 24 \zeta_2 x) \\
 & + \mathbf{H}_0(-3970/27 + 14321/27 x_m^{-1} - 20188/27 x - 420 \zeta_2 x_m^{-1} + 168 \zeta_2 + 336 \zeta_2 x \\
 & - 44 \zeta_3 x_m^{-1} + 22 \zeta_3 + 22 \zeta_3 x) + \mathbf{H}_1(202/27 + 4429/27 x_m^{-1} - 10112/27 x \\
 & - 116 \zeta_2 x_m^{-1} + 40 \zeta_2 + 112 \zeta_2 x) + 1724/81 + 25279/162 x_m^{-1} - 36661/81 x \\
 & - 1282/3 \zeta_2 x_m^{-1} + 392/3 \zeta_2 + 1496/3 \zeta_2 x - 436/3 \zeta_3 x_m^{-1} + 194/3 \zeta_3 + 314/3 \zeta_3 x \\
 & + 102 \zeta_4 x_m^{-1} - 51 \zeta_4 - 51 \zeta_4 x + \delta(1-x)(281971/864 + 14321/27 \zeta_2 - 1/6 \zeta_3 \\
 & + 4 \zeta_3 \zeta_2 + 1027/6 \zeta_4 + 2 \zeta_5)
 \end{aligned}
 \tag{I.0.4}$$

# Appendix J

## Order $\epsilon$ coefficient functions at N<sup>3</sup>LO

The following are the (non-physical) order  $\epsilon$  DIS coefficient functions at N<sup>3</sup>LO. These are required for the renormalization of the 4-loop coefficient functions. I would like to stress that this is a new result. Note that the order  $n_f^0$  is not included (yet), as the reconstruction for this part will require more Mellin moments.

To abbreviate the formulas, we have defined the  $Z_5$  factors as

$$\begin{aligned} Z_{5,1} &\equiv Z_5(\alpha_s, \epsilon), \\ Z_{5,2} &\equiv Z_5(\alpha_s^2, \epsilon, n_f), \\ Z_{5,3a} &\equiv Z_5(\alpha_s^3, \epsilon, C_F C_A n_f), \\ Z_{5,3b} &\equiv Z_5(\alpha_s^3, \epsilon, C_F^2 n_f), \\ Z_{5,3c} &\equiv Z_5(\alpha_s^3, \epsilon, C_F n_f^2). \end{aligned} \tag{J.0.1}$$

The following is the  $a_2$ :

$$\begin{aligned} a_{2,\text{ns}}^{(3)}(N) &= n_f^0 \text{ contributions} \\ &+ C_F C_A n_f \frac{16}{9} a_{2,\text{ns}}^{(3)\text{L}}(N) + C_F (C_F - \frac{1}{2} C_A) n_f \frac{16}{9} a_{2,\text{ns}}^{(3)\text{N}}(N) + C_F n_f^2 \frac{16}{27} a_{2,\text{ns}}^{(3)\text{F}}(N) \\ a_{2,\text{ns}}^{(3)\text{L}}(N) &= \\ &+ 225 \mathbf{S}_6 - 229 \mathbf{S}_{1,5} - 209 \mathbf{S}_{2,4} - 281 \mathbf{S}_{3,3} - 338 \mathbf{S}_{4,2} - 363 \mathbf{S}_{5,1} + 186 \mathbf{S}_{1,1,4} \\ &+ 401/2 \mathbf{S}_{1,2,3} + 529/2 \mathbf{S}_{1,3,2} + 300 \mathbf{S}_{1,4,1} + 481/2 \mathbf{S}_{2,1,3} + 249 \mathbf{S}_{2,2,2} + 519/2 \mathbf{S}_{2,3,1} \\ &+ 637/2 \mathbf{S}_{3,1,2} + 675/2 \mathbf{S}_{3,2,1} + 389 \mathbf{S}_{4,1,1} - 343/2 \mathbf{S}_{1,1,1,3} - 191 \mathbf{S}_{1,1,2,2} \\ &- 459/2 \mathbf{S}_{1,1,3,1} - 235 \mathbf{S}_{1,2,1,2} - 246 \mathbf{S}_{1,2,2,1} - 607/2 \mathbf{S}_{1,3,1,1} - 238 \mathbf{S}_{2,1,1,2} - 256 \mathbf{S}_{2,1,2,1} \end{aligned}$$

$$\begin{aligned}
 & -276 \mathbf{S}_{2,2,1,1} - 681/2 \mathbf{S}_{3,1,1,1} + 171 \mathbf{S}_{1,1,1,1,2} + 202 \mathbf{S}_{1,1,1,2,1} + 225 \mathbf{S}_{1,1,2,1,1} \\
 & + 258 \mathbf{S}_{1,2,1,1,1} + 249 \mathbf{S}_{2,1,1,1,1} - 195 \mathbf{S}_{1,1,1,1,1,1} + \mathbf{S}_5 (-1387/2 + 229/2 D_0 \\
 & - 229/2 D_1) + \mathbf{S}_{1,4} (1387/3 + 18 D_{-2} - 93 D_0 + 129 D_1 - 108 D_2 + 162 D_3) \\
 & + \mathbf{S}_{2,3} (12923/24 + 9 D_{-2} - 401/4 D_0 + 473/4 D_1 - 54 D_2 + 81 D_3) \\
 & + \mathbf{S}_{3,2} (17861/24 - 9 D_{-2} - 529/4 D_0 + 457/4 D_1 + 54 D_2 - 81 D_3) + \mathbf{S}_{4,1} (2669/3 \\
 & - 24 D_{-2} - 150 D_0 + 102 D_1 + 144 D_2 - 216 D_3) + \mathbf{S}_{1,1,3} (-9793/24 - 15 D_{-2} \\
 & + 343/4 D_0 - 463/4 D_1 + 90 D_2 - 135 D_3) + \mathbf{S}_{1,2,2} (-5555/12 - 3 D_{-2} + 191/2 D_0 \\
 & - 203/2 D_1 + 18 D_2 - 27 D_3) + \mathbf{S}_{1,3,1} (-14011/24 + 9 D_{-2} + 459/4 D_0 - 387/4 D_1 \\
 & - 54 D_2 + 81 D_3) + \mathbf{S}_{2,1,2} (-6937/12 - 3 D_{-2} + 235/2 D_0 - 247/2 D_1 + 18 D_2 \\
 & - 27 D_3) + \mathbf{S}_{2,2,1} (-1235/2 + 3 D_{-2} + 123 D_0 - 117 D_1 - 18 D_2 + 27 D_3) \\
 & + \mathbf{S}_{3,1,1} (-6519/8 + 15 D_{-2} + 607/4 D_0 - 487/4 D_1 - 90 D_2 + 135 D_3) \\
 & + \mathbf{S}_{1,1,1,2} (1609/4 - 171/2 D_0 + 171/2 D_1) + \mathbf{S}_{1,1,2,1} (5551/12 - 101 D_0 + 146 D_1 \\
 & - 162 D_2 + 135 D_3) + \mathbf{S}_{1,2,1,1} (6317/12 - 225/2 D_0 + 135/2 D_1 + 162 D_2 - 135 D_3) \\
 & + \mathbf{S}_{2,1,1,1} (1780/3 - 129 D_0 + 129 D_1) + \mathbf{S}_{1,1,1,1,1} (-1713/4 + 195/2 D_0 - 195/2 D_1) \\
 & + \mathbf{S}_4 (92111/72 - 69/4 \zeta_2 - 27 D_{-2} - 1375/6 D_0 + 2023/6 D_1 + 108 D_2 - 243 D_3 \\
 & + 91 D_0^2 - 25 D_1^2) + \mathbf{S}_{1,3} (-11867/18 + 75/4 \zeta_2 + 313/10 D_{-2} - 9 D_{-1} \\
 & + 4295/24 D_0 - 1033/3 D_1 + 9 D_2 + 477/10 D_3 + 18 D_{-2}^2 - 427/4 D_0^2 + 42 D_1^2 \\
 & + 36 D_2^2 - 54 D_3^2) + \mathbf{S}_{2,2} (-34529/36 + 39/2 \zeta_2 + 9/2 D_{-2} + 610/3 D_0 \\
 & - 1081/3 D_1 - 9 D_2 + 36 D_3 - 111 D_0^2 + 44 D_1^2) + \mathbf{S}_{3,1} (-10457/8 + 99/4 \zeta_2 \\
 & - 223/10 D_{-2} + 9 D_{-1} + 6461/24 D_0 - 2447/6 D_1 - 63 D_2 + 423/10 D_3 - 18 D_{-2}^2 \\
 & - 465/4 D_0^2 + 63/2 D_1^2 - 36 D_2^2 + 54 D_3^2) + \mathbf{S}_{1,1,2} (5005/8 - 15 \zeta_2 - 167 D_0 \\
 & + 1311/4 D_1 - 63 D_2 + 63/2 D_3 + 211/2 D_0^2 - 109/2 D_1^2) + \mathbf{S}_{1,2,1} (8489/12 \\
 & - 39/2 \zeta_2 - 647/3 D_0 + 2197/6 D_1 + 171 D_2 - 207 D_3 + 229/2 D_0^2 - 39 D_1^2) \\
 & + \mathbf{S}_{2,1,1} (3889/4 - 39/2 \zeta_2 - 700/3 D_0 + 4831/12 D_1 - 99 D_2 + 171 D_3 + 249/2 D_0^2 \\
 & - 63/2 D_1^2) + \mathbf{S}_{1,1,1,1} (-4969/8 + 15 \zeta_2 + 765/4 D_0 - 687/2 D_1 - 111 D_0^2 \\
 & + 81/2 D_1^2) + \mathbf{S}_3 (-369797/216 + 717/16 \zeta_2 + 182 \zeta_3 - 189/20 D_{-2} + 9 D_{-1} \\
 & + 44417/144 D_0 - 75/8 D_0 \zeta_2 - 95951/144 D_1 + 75/8 D_1 \zeta_2 - 99 D_2 \\
 & + 1647/10 D_3 - 27 D_{-2}^2 - 1195/6 D_0^2 + 451/4 D_0^3 + 2801/24 D_1^2 - 20 D_1^3 \\
 & - 36 D_2^2 + 81 D_3^2) + \mathbf{S}_{1,2} (162311/216 - 77/2 \zeta_2 - 161 \zeta_3 + 15/4 D_{-2} \\
 & - 4335/16 D_0 + 15/2 D_0 \zeta_2 + 34973/48 D_1 - 15/2 D_1 \zeta_2 - 102 D_2 + 219/4 D_3 \\
 & + 5203/24 D_0^2 - 263/2 D_0^3 - 4285/24 D_1^2 + 45/2 D_1^3 - 18 D_2^2 + 9 D_3^2)
 \end{aligned}$$

---


$$\begin{aligned}
& + \mathbf{S}_{2,1} (290789/216 - 369/8 \zeta_2 - 209 \zeta_3 - 15/4 D_{-2} - 16145/48 D_0 + 39/4 D_0 \zeta_2 \\
& + 12101/16 D_1 - 39/4 D_1 \zeta_2 - 6 D_2 + 141 D_3 + 1847/8 D_0^2 - 141 D_0^3 \\
& - 3281/24 D_1^2 + 33 D_1^3 + 18 D_2^2 - 9 D_3^2) + \mathbf{S}_{1,1,1} (-105325/144 + 35 \zeta_2 + 90 \zeta_3 \\
& + 4817/16 D_0 - 15/2 D_0 \zeta_2 - 11849/16 D_1 + 15/2 D_1 \zeta_2 - 5527/24 D_0^2 \\
& + 285/2 D_0^3 + 3901/24 D_1^2 - 57/2 D_1^3) + \mathbf{S}_2 (17298037/10368 - 1937/32 \zeta_2 \\
& - 4405/12 \zeta_3 - 63/2 \zeta_4 + 63/8 D_{-2} - 36 D_{-2} \zeta_3 - 656285/1728 D_0 + 37/2 D_0 \zeta_2 \\
& + 161/2 D_0 \zeta_3 + 2019479/1728 D_1 - 29 D_1 \zeta_2 - 305/2 D_1 \zeta_3 + 57 D_2 \\
& + 216 D_2 \zeta_3 + 27/4 D_3 - 324 D_3 \zeta_3 + 12673/36 D_0^2 - 69/8 D_0^2 \zeta_2 \\
& - 11765/48 D_0^3 + 1031/8 D_0^4 - 50035/144 D_1^2 + 27/8 D_1^2 \zeta_2 + 4403/48 D_1^3 \\
& - 95/8 D_1^4 + 18 D_2^2 - 27/2 D_3^2) + \mathbf{S}_{1,1} (-2425003/3456 + 1265/32 \zeta_2 + 451/2 \zeta_3 \\
& + 27/2 \zeta_4 - 135/8 D_{-2} + 30 D_{-2} \zeta_3 + 247847/576 D_0 - 35/2 D_0 \zeta_2 - 45 D_0 \zeta_3 \\
& - 746681/576 D_1 + 28 D_1 \zeta_2 - 75 D_1 \zeta_3 - 9 D_2 + 468 D_2 \zeta_3 - 45/8 D_3 \\
& - 270 D_3 \zeta_3 - 1569/4 D_0^2 + 69/8 D_0^2 \zeta_2 + 4447/16 D_0^3 - 1235/8 D_0^4 \\
& + 19507/48 D_1^2 - 27/8 D_1^2 \zeta_2 - 1769/16 D_1^3 + 123/8 D_1^4) \\
& + \mathbf{S}_1 (-49108273/62208 + 21169/576 \zeta_2 + 57143/144 \zeta_3 - 9/2 \zeta_3 \zeta_2 + 503/8 \zeta_4 \\
& + 129 \zeta_5 - 63/5 D_{-2} - 313/5 D_{-2} \zeta_3 + 9 D_{-2} \zeta_4 - 9 D_{-1} + 18 D_{-1} \zeta_3 \\
& + 117017/216 D_0 - 773/32 D_0 \zeta_2 - 5/2 D_0 \zeta_3 - 27/4 D_0 \zeta_4 - 6892781/3456 D_1 \\
& + 875/16 D_1 \zeta_2 + 567/2 D_1 \zeta_3 + 99/4 D_1 \zeta_4 + 354 D_2 - 846 D_2 \zeta_3 - 54 D_2 \zeta_4 \\
& - 8193/20 D_3 + 4023/5 D_3 \zeta_3 + 81 D_3 \zeta_4 + 81/4 D_{-2}^2 - 36 D_{-2}^2 \zeta_3 \\
& - 1003709/1728 D_0^2 + 41/2 D_0^2 \zeta_2 + 373/4 D_0^2 \zeta_3 + 10727/24 D_0^3 \\
& - 39/4 D_0^3 \zeta_2 - 832/3 D_0^4 + 132 D_0^5 + 332543/432 D_1^2 - 89/8 D_1^2 \zeta_2 \\
& - 331/4 D_1^2 \zeta_3 - 4131/16 D_1^3 + 15/8 D_1^3 \zeta_2 + 2471/48 D_1^4 - 33/8 D_1^5 \\
& + 54 D_2^2 - 72 D_2^2 \zeta_3 - 72 D_3^2 + 108 D_3^2 \zeta_3) + 28828057/20736 - 38161/768 \zeta_2 \\
& - 17885/48 \zeta_3 + 27/8 \zeta_3 \zeta_2 - 651/16 \zeta_4 - 477/4 \zeta_5 + 423/40 D_{-2} + 207/5 D_{-2} \zeta_3 \\
& - 27/2 D_{-2} \zeta_4 + 90 D_{-2} \zeta_5 - 18 D_{-1} \zeta_3 + 59624393/62208 D_0 \\
& - 50581/1152 D_0 \zeta_2 - 7879/144 D_0 \zeta_3 + 9/4 D_0 \zeta_3 \zeta_2 - 211/8 D_0 \zeta_4 \\
& - 129/2 D_0 \zeta_5 - 93923935/31104 D_1 + 111229/1152 D_1 \zeta_2 + 45569/72 D_1 \zeta_3 \\
& - 9/4 D_1 \zeta_3 \zeta_2 + 127/2 D_1 \zeta_4 - 1311/2 D_1 \zeta_5 + 36 D_2 \zeta_3 - 27 D_2 \zeta_4 \\
& + 2700 D_2 \zeta_5 + 6807/40 D_3 - 3987/5 D_3 \zeta_3 - 81 D_3 \zeta_4 - 1890 D_3 \zeta_5 \\
& - 27/4 D_{-2}^2 + 54 D_{-2}^2 \zeta_3 - 537971/648 D_0^2 + 799/24 D_0^2 \zeta_2 + 1343/12 D_0^2 \zeta_3 \\
& + 27/2 D_0^2 \zeta_4 + 1058389/1728 D_0^3 - 531/32 D_0^3 \zeta_2 - 269/4 D_0^3 \zeta_3
\end{aligned}$$



$$\begin{aligned}
 & -57155/144 D_0^4 + 69/16 D_0^4 \zeta_2 + 617/3 D_0^5 - 225/4 D_0^6 + 3091853/2592 D_1^2 \\
 & - 2087/96 D_1^2 \zeta_2 - 1117/6 D_1^2 \zeta_3 - 99/4 D_1^2 \zeta_4 - 167153/432 D_1^3 \\
 & - 33/32 D_1^3 \zeta_2 - 73/2 D_1^3 \zeta_3 + 5197/72 D_1^4 + 27/16 D_1^4 \zeta_2 + 31/4 D_1^5 \\
 & - 27/4 D_1^6 - 36 D_2^2 \zeta_3 + 45/2 D_3^2 - 108 D_3^2 \zeta_3 \\
 a_{2,\text{ns}}^{(3)\text{N}}(N) = & \\
 & + 220 \mathbf{S}_{-6} + 230 \mathbf{S}_6 - 92 \mathbf{S}_{-5,1} - 984 \mathbf{S}_{-4,-2} - 60 \mathbf{S}_{-4,2} - 1104 \mathbf{S}_{-3,-3} + 72 \mathbf{S}_{-3,3} \\
 & - 672 \mathbf{S}_{-2,-4} + 96 \mathbf{S}_{-2,4} - 748 \mathbf{S}_{1,-5} - 200 \mathbf{S}_{1,5} - 940 \mathbf{S}_{2,-4} - 166 \mathbf{S}_{2,4} - 1192 \mathbf{S}_{3,-3} \\
 & - 326 \mathbf{S}_{3,3} - 988 \mathbf{S}_{4,-2} - 508 \mathbf{S}_{4,2} - 484 \mathbf{S}_{5,1} + 16 \mathbf{S}_{-4,1,1} + 576 \mathbf{S}_{-3,-2,1} \\
 & + 192 \mathbf{S}_{-3,1,-2} + 456 \mathbf{S}_{-2,-3,1} + 24 \mathbf{S}_{-2,-2,-2} + 264 \mathbf{S}_{-2,-2,2} + 192 \mathbf{S}_{-2,1,-3} \\
 & + 72 \mathbf{S}_{-2,2,-2} + 272 \mathbf{S}_{1,-4,1} + 672 \mathbf{S}_{1,-3,-2} + 144 \mathbf{S}_{1,-3,2} + 672 \mathbf{S}_{1,-2,-3} + 1024 \mathbf{S}_{1,1,-4} \\
 & + 320 \mathbf{S}_{1,1,4} + 976 \mathbf{S}_{1,2,-3} + 495 \mathbf{S}_{1,2,3} + 712 \mathbf{S}_{1,3,-2} + 311 \mathbf{S}_{1,3,2} + 4 \mathbf{S}_{1,4,1} \\
 & + 272 \mathbf{S}_{2,-3,1} + 408 \mathbf{S}_{2,-2,-2} + 96 \mathbf{S}_{2,-2,2} + 976 \mathbf{S}_{2,1,-3} + 511 \mathbf{S}_{2,1,3} + 592 \mathbf{S}_{2,2,-2} \\
 & + 612 \mathbf{S}_{2,2,2} + 61 \mathbf{S}_{2,3,1} + 200 \mathbf{S}_{3,-2,1} + 712 \mathbf{S}_{3,1,-2} + 639 \mathbf{S}_{3,1,2} + 493 \mathbf{S}_{3,2,1} \\
 & + 582 \mathbf{S}_{4,1,1} + 16 \mathbf{S}_{-3,1,1,1} - 240 \mathbf{S}_{-2,-2,1,1} - 96 \mathbf{S}_{-2,1,-2,1} - 16 \mathbf{S}_{1,-3,1,1} - 384 \mathbf{S}_{1,-2,-2,1} \\
 & - 96 \mathbf{S}_{1,-2,1,-2} - 272 \mathbf{S}_{1,1,-3,1} - 384 \mathbf{S}_{1,1,-2,-2} - 96 \mathbf{S}_{1,1,-2,2} - 976 \mathbf{S}_{1,1,1,-3} \\
 & - 497 \mathbf{S}_{1,1,1,3} - 592 \mathbf{S}_{1,1,2,-2} - 560 \mathbf{S}_{1,1,2,2} - 73 \mathbf{S}_{1,1,3,1} - 176 \mathbf{S}_{1,2,-2,1} - 592 \mathbf{S}_{1,2,1,-2} \\
 & - 524 \mathbf{S}_{1,2,1,2} - 432 \mathbf{S}_{1,2,2,1} - 157 \mathbf{S}_{1,3,1,1} - 16 \mathbf{S}_{2,-2,1,1} - 176 \mathbf{S}_{2,1,-2,1} - 592 \mathbf{S}_{2,1,1,-2} \\
 & - 664 \mathbf{S}_{2,1,1,2} - 434 \mathbf{S}_{2,1,2,1} - 422 \mathbf{S}_{2,2,1,1} - 583 \mathbf{S}_{3,1,1,1} - 32 \mathbf{S}_{1,-2,1,1,1} + 160 \mathbf{S}_{1,1,1,-2,1} \\
 & + 576 \mathbf{S}_{1,1,1,1,-2} + 570 \mathbf{S}_{1,1,1,1,2} + 354 \mathbf{S}_{1,1,1,2,1} + 334 \mathbf{S}_{1,1,2,1,1} + 408 \mathbf{S}_{1,2,1,1,1} \\
 & + 498 \mathbf{S}_{2,1,1,1,1} - 390 \mathbf{S}_{1,1,1,1,1,1} + \mathbf{S}_{-5} (-278/3 + 482 D_0 - 914 D_1) + \mathbf{S}_5 (-407 \\
 & - 8 D_0 + 440 D_1) + \mathbf{S}_{-4,1} (166/3 - 172 D_0 + 316 D_1) + \mathbf{S}_{-3,-2} (548 - 528 D_0 \\
 & + 1296 D_1) + \mathbf{S}_{-3,2} (40 - 84 D_0 + 132 D_1) + \mathbf{S}_{-2,-3} (472 - 528 D_0 + 1296 D_1) \\
 & + \mathbf{S}_{-2,3} (-78 + 12 D_0 - 60 D_1) + \mathbf{S}_{1,-4} (1406/3 - 800 D_0 + 1952 D_1) \\
 & + \mathbf{S}_{1,4} (1516/3 - 88 D_0 - 200 D_1) + \mathbf{S}_{2,-3} (1520/3 - 776 D_0 + 1928 D_1) \\
 & + \mathbf{S}_{2,3} (3187/12 - 483/2 D_0 + 435/2 D_1) + \mathbf{S}_{3,-2} (1610/3 - 560 D_0 + 1376 D_1) \\
 & + \mathbf{S}_{3,2} (9335/12 - 209/2 D_0 - 199/2 D_1) + \mathbf{S}_{4,1} (1040 + 136 D_0 - 688 D_1) \\
 & + \mathbf{S}_{-3,1,1} (-80/3 + 8 D_0 - 8 D_1) + \mathbf{S}_{-2,-2,1} (-164 + 312 D_0 - 792 D_1) \\
 & + \mathbf{S}_{-2,1,-2} (-156 + 72 D_0 - 168 D_1) + \mathbf{S}_{1,-3,1} (-640/3 + 208 D_0 - 496 D_1) \\
 & + \mathbf{S}_{1,-2,-2} (-316 + 312 D_0 - 792 D_1) + \mathbf{S}_{1,-2,2} (-80 + 72 D_0 - 168 D_1) \\
 & + \mathbf{S}_{1,1,-3} (-1760/3 + 800 D_0 - 2048 D_1) + \mathbf{S}_{1,1,3} (-6425/12 + 509/2 D_0 \\
 & - 557/2 D_1) + \mathbf{S}_{1,2,-2} (-1040/3 + 488 D_0 - 1256 D_1) + \mathbf{S}_{1,2,2} (-2236/3 + 313 D_0
 \end{aligned}$$

---


$$\begin{aligned}
& -445 D_1) + \mathbf{S}_{1,3,1} (-6961/12 - 179/2 D_0 + 1187/2 D_1) + \mathbf{S}_{2,-2,1} (-400/3 + 136 D_0 \\
& - 328 D_1) + \mathbf{S}_{2,1,-2} (-1040/3 + 488 D_0 - 1256 D_1) + \mathbf{S}_{2,1,2} (-759 + 286 D_0 \\
& - 382 D_1) + \mathbf{S}_{2,2,1} (-1610/3 + 213 D_0 - 201 D_1) + \mathbf{S}_{3,1,1} (-12481/12 - 11/2 D_0 \\
& + 683/2 D_1) + \mathbf{S}_{-2,1,1,1} (16 D_0 - 16 D_1) + 160/3 \mathbf{S}_{1,-2,1,1} + \mathbf{S}_{1,1,-2,1} (160 - 128 D_0 \\
& + 320 D_1) + \mathbf{S}_{1,1,1,-2} (1120/3 - 480 D_0 + 1248 D_1) + \mathbf{S}_{1,1,1,2} (4003/6 - 327 D_0 \\
& + 495 D_1) + \mathbf{S}_{1,1,2,1} (1209/2 - 156 D_0 + 72 D_1) + \mathbf{S}_{1,2,1,1} (4193/6 - 143 D_0 \\
& + 47 D_1) + \mathbf{S}_{2,1,1,1} (2108/3 - 204 D_0 + 204 D_1) + \mathbf{S}_{1,1,1,1,1} (-1185/2 + 195 D_0 \\
& - 195 D_1) + \mathbf{S}_{-4} (4175/18 - 15 \zeta_2 - 252/5 D_{-2} - 4798/3 D_0 + 4402/3 D_1 \\
& - 2268/5 D_3 + 1130 D_0^2 + 1458 D_1^2) + \mathbf{S}_4 (6785/36 - 39/2 \zeta_2 + 36/5 D_{-2} \\
& + 313/3 D_0 - 673/3 D_1 + 324/5 D_3 - 100 D_0^2 + 2 D_1^2) + \mathbf{S}_{-3,1} (-764/9 \\
& + 138/5 D_{-2} + 2360/3 D_0 - 1520/3 D_1 - 396 D_2 + 1242/5 D_3 - 514 D_0^2 \\
& - 858 D_1^2) + \mathbf{S}_{-2,-2} (-265 + 18 \zeta_2 + 48/5 D_{-2} + 592 D_0 - 1128 D_1 + 288 D_2 \\
& + 432/5 D_3 - 336 D_0^2) + \mathbf{S}_{-2,2} (-24 + 72/5 D_{-2} + 364 D_0 - 124 D_1 - 288 D_2 \\
& + 648/5 D_3 - 252 D_0^2 - 492 D_1^2) + \mathbf{S}_{1,-3} (-3088/9 + 36 \zeta_2 + 156/5 D_{-2} \\
& + 4312/3 D_0 - 6952/3 D_1 + 504 D_2 + 1404/5 D_3 - 908 D_0^2 - 396 D_1^2) \\
& + \mathbf{S}_{1,3} (-12355/18 + 69/2 \zeta_2 - 12/5 D_{-2} + 1363/12 D_0 - 412/3 D_1 + 108 D_2 \\
& + 2142/5 D_3 - 385/2 D_0^2 - 176 D_1^2) + \mathbf{S}_{2,-2} (-1876/9 + 24 \zeta_2 + 84/5 D_{-2} \\
& + 2476/3 D_0 - 4252/3 D_1 + 360 D_2 + 756/5 D_3 - 524 D_0^2 - 156 D_1^2) \\
& + \mathbf{S}_{2,2} (-2329/9 + 39 \zeta_2 + 12/5 D_{-2} + 1226/3 D_0 - 2477/3 D_1 + 90 D_2 + 333/5 D_3 \\
& - 306 D_0^2 + 23 D_1^2) + \mathbf{S}_{3,1} (-29203/36 + 81/2 \zeta_2 - 6 D_{-2} - 1381/12 D_0 \\
& + 481/3 D_1 - 396 D_2 - 594 D_3 + 179/2 D_0^2 + 186 D_1^2) + \mathbf{S}_{-2,1,1} (-12 D_{-2} \\
& - 848/3 D_0 + 128/3 D_1 + 360 D_2 - 108 D_3 + 188 D_0^2 + 412 D_1^2) + \mathbf{S}_{1,-2,1} (664/9 \\
& - 48/5 D_{-2} - 400 D_0 + 560 D_1 - 432/5 D_3 + 208 D_0^2 + 160 D_1^2) + \mathbf{S}_{1,1,-2} (664/3 \\
& - 24 \zeta_2 - 72/5 D_{-2} - 2480/3 D_0 + 4784/3 D_1 - 432 D_2 - 648/5 D_3 + 488 D_0^2 \\
& - 8 D_1^2) + \mathbf{S}_{1,1,2} (8135/12 - 36 \zeta_2 - 6/5 D_{-2} - 1171/3 D_0 + 4781/6 D_1 - 162 D_2 \\
& - 1899/5 D_3 + 326 D_0^2 + 31 D_1^2) + \mathbf{S}_{1,2,1} (2167/3 - 33 \zeta_2 + 6/5 D_{-2} - 369/2 D_0 \\
& + 396 D_1 + 54 D_2 + 279/5 D_3 + 169 D_0^2 - 67 D_1^2) + \mathbf{S}_{2,1,1} (997/2 - 39 \zeta_2 \\
& - 719/3 D_0 + 3517/6 D_1 + 126 D_2 + 369 D_3 + 184 D_0^2 - 191 D_1^2) \\
& + \mathbf{S}_{1,1,1,1} (-6931/12 + 30 \zeta_2 + 501/2 D_0 - 555 D_1 - 222 D_0^2 + 81 D_1^2) \\
& + \mathbf{S}_{-3} (-8054/27 + 10 \zeta_2 - 1124 \zeta_3 - 266/25 D_{-2} + 26552/9 D_0 - 21 D_0 \zeta_2 \\
& - 19340/9 D_1 + 33 D_1 \zeta_2 - 504 D_2 + 3366/25 D_3 - 312/5 D_{-2}^2 - 7324/3 D_0^2
\end{aligned}$$

$$\begin{aligned}
 & + 1646 D_0^3 - 1868 D_1^2 + 42 D_1^3 + 648/5 D_3^2) + \mathbf{S}_3 (12853/36 + 109/8 \zeta_2 - 948 \zeta_3 \\
 & - 29/25 D_{-2} - 19171/72 D_0 - 57/4 D_0 \zeta_2 + 37453/72 D_1 + 9/4 D_1 \zeta_2 - 108 D_2 \\
 & - 17496/25 D_3 + 24/5 D_{-2}^2 + 703/3 D_0^2 + 11/2 D_0^3 + 1141/12 D_1^2 - 3 D_1^3) \\
 & + \mathbf{S}_{-2,1} (58 + 168 \zeta_3 - 44/25 D_{-2} - 36 D_{-1} - 9434/9 D_0 + 4502/9 D_1 + 528 D_2 \\
 & - 2556/25 D_3 + 24 D_{-2}^2 + 2660/3 D_0^2 - 568 D_0^3 + 2548/3 D_1^2 - 104 D_1^3 \\
 & + 144 D_2^2 - 216/5 D_3^2) + \mathbf{S}_{1,-2} (4390/27 - 20 \zeta_2 + 544 \zeta_3 + 136/25 D_{-2} + 36 D_{-1} \\
 & - 4018/3 D_0 + 18 D_0 \zeta_2 + 4166/3 D_1 - 42 D_1 \zeta_2 - 96 D_2 - 936/25 D_3 + 24 D_{-2}^2 \\
 & + 3364/3 D_0^2 - 692 D_0^3 + 1588/3 D_1^2 + 4 D_1^3 - 144 D_2^2 - 216/5 D_3^2) \\
 & + \mathbf{S}_{1,2} (60533/108 - 55 \zeta_2 + 410 \zeta_3 + 9/5 D_{-2} - 1239/8 D_0 + 18 D_0 \zeta_2 + 1151/8 D_1 \\
 & - 18 D_1 \zeta_2 - 339 D_2 + 1617/10 D_3 + 895/4 D_0^2 - 264 D_0^3 - 1073/12 D_1^2 \\
 & + 24 D_1^3 - 36 D_2^2 - 90 D_3^2) + \mathbf{S}_{2,1} (3905/108 - 193/4 \zeta_2 + 50 \zeta_3 - 9/5 D_{-2} \\
 & - 1/24 D_0 + 33/2 D_0 \zeta_2 + 6871/24 D_1 - 33/2 D_1 \zeta_2 + 447 D_2 + 3243/10 D_3 \\
 & + 1171/12 D_0^2 - 191 D_0^3 - 3217/12 D_1^2 + 34 D_1^3 + 36 D_2^2 + 90 D_3^2) \\
 & + \mathbf{S}_{1,1,1} (-10099/24 + 48 \zeta_2 - 72 \zeta_3 + 907/24 D_0 - 15 D_0 \zeta_2 - 6379/24 D_1 \\
 & + 15 D_1 \zeta_2 - 1939/12 D_0^2 + 228 D_0^3 + 3265/12 D_1^2 - 54 D_1^3) + \mathbf{S}_{-2} (989/6 \\
 & - 6 \zeta_2 + 698 \zeta_3 + 126 \zeta_4 + 1233/250 D_{-2} + 6/5 D_{-2} \zeta_2 - 36 D_{-1} - 85259/27 D_0 \\
 & + 43 D_0 \zeta_2 - 440 D_0 \zeta_3 + 73856/27 D_1 - 31 D_1 \zeta_2 + 1112 D_1 \zeta_3 + 312 D_2 \\
 & - 4983/250 D_3 + 54/5 D_3 \zeta_2 - 162/25 D_{-2}^2 - 48 D_{-2}^3 + 23603/9 D_0^2 \\
 & - 27 D_0^2 \zeta_2 - 6514/3 D_0^3 + 1406 D_0^4 + 10237/9 D_1^2 - 39 D_1^2 \zeta_2 + 766/3 D_1^3 \\
 & - 74 D_1^4 + 144 D_2^2 - 1242/25 D_3^2) + \mathbf{S}_2 (-395315/576 + 1261/48 \zeta_2 + 47/2 \zeta_3 \\
 & + 63 \zeta_4 + 36/5 D_{-2} + 276499/864 D_0 + 26 D_0 \zeta_2 - 499 D_0 \zeta_3 - 935425/864 D_1 \\
 & - 47 D_1 \zeta_2 + 1675 D_1 \zeta_3 + 753 D_2 + 2403/10 D_3 - 544/9 D_0^2 - 69/4 D_0^2 \zeta_2 \\
 & - 2405/24 D_0^3 + 815/4 D_0^4 + 23573/72 D_1^2 + 15/4 D_1^2 \zeta_2 + 41/8 D_1^3 \\
 & + 13/4 D_1^4 + 36 D_2^2 + 135 D_3^2) + \mathbf{S}_{1,1} (-4915/192 + 691/48 \zeta_2 - 96 \zeta_3 - 27 \zeta_4 \\
 & - 9 D_{-2} - 39971/96 D_0 - 24 D_0 \zeta_2 + 234 D_0 \zeta_3 + 20503/32 D_1 + 45 D_1 \zeta_2 \\
 & - 1026 D_1 \zeta_3 - 234 D_2 + 1521/4 D_3 + 115/2 D_0^2 + 69/4 D_0^2 \zeta_2 + 1007/8 D_0^3 \\
 & - 875/4 D_0^4 + 701/8 D_1^2 - 27/4 D_1^2 \zeta_2 - 1873/8 D_1^3 + 223/4 D_1^4) \\
 & + \mathbf{S}_1 (116597/1152 - 995/32 \zeta_2 + 1891/24 \zeta_3 + 9 \zeta_3 \zeta_2 - 219/4 \zeta_4 - 198 \zeta_5 \\
 & - 483/25 D_{-2} + 156/5 D_{-2} \zeta_3 + 36 D_{-1} - 22999/24 D_0 + 109/48 D_0 \zeta_2 \\
 & + 2161/2 D_0 \zeta_3 + 117/2 D_0 \zeta_4 + 885769/576 D_1 + 235/24 D_1 \zeta_2 - 3587/2 D_1 \zeta_3 \\
 & - 477/2 D_1 \zeta_4 - 63 D_2 - 72 D_2 \zeta_3 + 44007/100 D_3 - 8136/5 D_3 \zeta_3 + 18 D_{-2}^2
 \end{aligned}$$

---


$$\begin{aligned}
& + 284155/864 D_0^2 + 29/2 D_0^2 \zeta_2 - 899/2 D_0^2 \zeta_3 - 1049/12 D_0^3 - 15 D_0^3 \zeta_2 \\
& - 215/3 D_0^4 + 189 D_0^5 - 60553/216 D_1^2 - 63/4 D_1^2 \zeta_2 + 485/2 D_1^2 \zeta_3 \\
& - 4817/24 D_1^3 + 9/4 D_1^3 \zeta_2 + 4735/24 D_1^4 - 245/4 D_1^5 - 108 D_2^2 \\
& + 801/10 D_3^2) - 30137/384 + 1989/128 \zeta_2 + 19787/8 \zeta_3 - 81/4 \zeta_3 \zeta_2 + 1251/4 \zeta_4 \\
& + 657/2 \zeta_5 - 6839/250 D_{-2} + 9/10 D_{-2} \zeta_2 - 63/25 D_{-2} \zeta_3 + 54/5 D_{-2} \zeta_4 \\
& - 36 D_{-1} \zeta_3 - 978511/3456 D_0 - 919/192 D_0 \zeta_2 + 73849/24 D_0 \zeta_3 \\
& - 27/2 D_0 \zeta_3 \zeta_2 + 366 D_0 \zeta_4 + 219 D_0 \zeta_5 + 2579933/1728 D_1 - 6857/192 D_1 \zeta_2 \\
& - 42197/12 D_1 \zeta_3 + 99/2 D_1 \zeta_3 \zeta_2 - 2229/4 D_1 \zeta_4 - 699 D_1 \zeta_5 - 2406 D_2 \zeta_3 \\
& - 54 D_2 \zeta_4 - 340197/500 D_3 + 81/10 D_3 \zeta_2 + 16263/25 D_3 \zeta_3 - 1539/5 D_3 \zeta_4 \\
& + 2007/50 D_{-2}^2 - 72 D_{-2}^2 \zeta_3 - 36 D_{-2}^3 + 44497/216 D_0^2 - 49/12 D_0^2 \zeta_2 \\
& - 2754 D_0^2 \zeta_3 - 180 D_0^2 \zeta_4 - 116099/864 D_0^3 - 3/16 D_0^3 \zeta_2 + 3427/2 D_0^3 \zeta_3 \\
& + 849/8 D_0^4 + 69/8 D_0^4 \zeta_2 - 97/3 D_0^5 - 225/2 D_0^6 - 17031/16 D_1^2 \\
& + 1325/48 D_1^2 \zeta_2 - 1336 D_1^2 \zeta_3 - 99/2 D_1^2 \zeta_4 + 108055/216 D_1^3 \\
& - 209/16 D_1^3 \zeta_2 - 49 D_1^3 \zeta_3 - 2329/12 D_1^4 + 27/8 D_1^4 \zeta_2 + 379/6 D_1^5 \\
& - 27/2 D_1^6 - 72 D_2^2 \zeta_3 - 3384/25 D_3^2 - 2052/5 D_3^2 \zeta_3 \\
a_{2,\text{ns}}^{(3)\text{F}}(N) = & \\
& + 121 \mathbf{S}_5 - 36 \mathbf{S}_{1,4} - 66 \mathbf{S}_{2,3} - 90 \mathbf{S}_{3,2} - 108 \mathbf{S}_{4,1} + 36 \mathbf{S}_{1,1,3} + 36 \mathbf{S}_{1,2,2} + 36 \mathbf{S}_{1,3,1} \\
& + 66 \mathbf{S}_{2,1,2} + 66 \mathbf{S}_{2,2,1} + 90 \mathbf{S}_{3,1,1} - 36 \mathbf{S}_{1,1,1,2} - 36 \mathbf{S}_{1,1,2,1} - 36 \mathbf{S}_{1,2,1,1} - 66 \mathbf{S}_{2,1,1,1} \\
& + 36 \mathbf{S}_{1,1,1,1,1} + \mathbf{S}_4 (-830/3 + 18 D_0 - 18 D_1) + \mathbf{S}_{1,3} (77 - 18 D_0 + 18 D_1) \\
& + \mathbf{S}_{2,2} (162 - 18 D_0 + 18 D_1) + \mathbf{S}_{3,1} (228 - 18 D_0 + 18 D_1) + \mathbf{S}_{1,1,2} (-77 + 18 D_0 \\
& - 18 D_1) + \mathbf{S}_{1,2,1} (-77 + 18 D_0 - 18 D_1) + \mathbf{S}_{2,1,1} (-162 + 18 D_0 - 18 D_1) \\
& + \mathbf{S}_{1,1,1,1} (77 - 18 D_0 + 18 D_1) + \mathbf{S}_3 (4787/12 - 9 \zeta_2 - 28 D_0 + 91 D_1 + 33 D_0^2 \\
& - 15 D_1^2) + \mathbf{S}_{1,2} (-1325/12 + 3 \zeta_2 + 28 D_0 - 91 D_1 - 33 D_0^2 + 15 D_1^2) \\
& + \mathbf{S}_{2,1} (-1087/4 + 6 \zeta_2 + 28 D_0 - 91 D_1 - 33 D_0^2 + 15 D_1^2) + \mathbf{S}_{1,1,1} (1325/12 - 3 \zeta_2 \\
& - 28 D_0 + 91 D_1 + 33 D_0^2 - 15 D_1^2) + \mathbf{S}_2 (-21083/54 + 67/4 \zeta_2 + 26 \zeta_3 \\
& + 571/12 D_0 - 3/2 D_0 \zeta_2 - 700/3 D_1 + 3/2 D_1 \zeta_2 - 57 D_0^2 + 45 D_0^3 + 74 D_1^2 \\
& - 12 D_1^3) + \mathbf{S}_{1,1} (4963/36 - 29/4 \zeta_2 - 12 \zeta_3 - 571/12 D_0 + 3/2 D_0 \zeta_2 + 700/3 D_1 \\
& - 3/2 D_1 \zeta_2 + 57 D_0^2 - 45 D_0^3 - 74 D_1^2 + 12 D_1^3) + \mathbf{S}_1 (205661/1296 \\
& - 235/24 \zeta_2 - 97/3 \zeta_3 + 3 \zeta_4 - 3209/36 D_0 + 13/4 D_0 \zeta_2 + 6 D_0 \zeta_3 + 7723/18 D_1 \\
& - 17/2 D_1 \zeta_2 - 6 D_1 \zeta_3 + 361/4 D_0^2 - 3 D_0^2 \zeta_2 - 78 D_0^3 + 54 D_0^4 - 560/3 D_1^2 \\
& + 3/2 D_1^2 \zeta_2 + 57 D_1^3 - 9 D_1^4) - 542837/1728 + 203/16 \zeta_2 + 115/4 \zeta_3 - 9/4 \zeta_4
\end{aligned}$$

$$\begin{aligned}
 & -198913/1296 D_0 + 161/24 D_0 \zeta_2 + 50/3 D_0 \zeta_3 - 3/2 D_0 \zeta_4 + 426917/648 D_1 \\
 & - 70/3 D_1 \zeta_2 - 113/3 D_1 \zeta_3 + 3/2 D_1 \zeta_4 + 4013/27 D_0^2 - 29/4 D_0^2 \zeta_2 \\
 & - 13 D_0^2 \zeta_3 - 485/4 D_0^3 + 9/2 D_0^3 \zeta_2 + 557/6 D_0^4 - 121/2 D_0^5 \\
 & - 37151/108 D_1^2 + 17/2 D_1^2 \zeta_2 + 7 D_1^2 \zeta_3 + 142 D_1^3 - 3/2 D_1^3 \zeta_2 - 251/6 D_1^4 \\
 & + 13/2 D_1^5
 \end{aligned} \tag{J.0.3}$$

The following is the  $a_L$ :

$$\begin{aligned}
 a_{L,\text{ns}}^{(3)}(N) &= n_f^0 \text{ contributions} \\
 &+ C_F C_A n_f \frac{16}{9} a_{L,\text{ns}}^{(3)\text{L}}(N) + C_F (C_F - \frac{1}{2} C_A) n_f \frac{16}{9} a_{L,\text{ns}}^{(3)\text{N}}(N) + C_F n_f^2 \frac{16}{27} a_{L,\text{ns}}^{(3)\text{F}}(N)
 \end{aligned}$$

$$\begin{aligned}
 a_{L,\text{ns}}^{(3)\text{L}}(N) &= \\
 &+ \mathbf{S}_{1,4} (72 D_{-2} - 36 D_{-1} + 36 D_1 - 72 D_2 + 108 D_3) + \mathbf{S}_{2,3} (36 D_{-2} - 18 D_{-1} \\
 &+ 18 D_1 - 36 D_2 + 54 D_3) + \mathbf{S}_{3,2} (-36 D_{-2} + 18 D_{-1} - 18 D_1 + 36 D_2 - 54 D_3) \\
 &+ \mathbf{S}_{4,1} (-96 D_{-2} + 48 D_{-1} - 48 D_1 + 96 D_2 - 144 D_3) + \mathbf{S}_{1,1,3} (-60 D_{-2} + 30 D_{-1} \\
 &- 30 D_1 + 60 D_2 - 90 D_3) + \mathbf{S}_{1,2,2} (-12 D_{-2} + 6 D_{-1} - 6 D_1 + 12 D_2 - 18 D_3) \\
 &+ \mathbf{S}_{1,3,1} (36 D_{-2} - 18 D_{-1} + 18 D_1 - 36 D_2 + 54 D_3) + \mathbf{S}_{2,1,2} (-12 D_{-2} + 6 D_{-1} \\
 &- 6 D_1 + 12 D_2 - 18 D_3) + \mathbf{S}_{2,2,1} (12 D_{-2} - 6 D_{-1} + 6 D_1 - 12 D_2 + 18 D_3) \\
 &+ \mathbf{S}_{3,1,1} (60 D_{-2} - 30 D_{-1} + 30 D_1 - 60 D_2 + 90 D_3) + \mathbf{S}_{1,1,2,1} (27 D_1 - 108 D_2 \\
 &+ 90 D_3) + \mathbf{S}_{1,2,1,1} (-27 D_1 + 108 D_2 - 90 D_3) + \mathbf{S}_4 (-108 D_{-2} + 36 D_{-1} + 54 D_1 \\
 &+ 72 D_2 - 162 D_3) + \mathbf{S}_{1,3} (476/5 D_{-2} - 68 D_{-1} + 24 D_0 - 203/2 D_1 + 2 D_2 \\
 &+ 189/5 D_3 + 72 D_{-2}^2 - 36 D_{-1}^2 - 12 D_1^2 + 24 D_2^2 - 36 D_3^2) + \mathbf{S}_{2,2} (18 D_{-2} \\
 &- 6 D_{-1} - 87 D_1 - 6 D_2 + 24 D_3) + \mathbf{S}_{3,1} (-296/5 D_{-2} + 56 D_{-1} - 24 D_0 \\
 &- 145/2 D_1 - 38 D_2 + 111/5 D_3 - 72 D_{-2}^2 + 36 D_{-1}^2 + 12 D_1^2 - 24 D_2^2 + 36 D_3^2) \\
 &+ \mathbf{S}_{1,1,2} (84 D_1 - 42 D_2 + 21 D_3) + \mathbf{S}_{1,2,1} (90 D_1 + 114 D_2 - 138 D_3) \\
 &+ \mathbf{S}_{2,1,1} (102 D_1 - 66 D_2 + 114 D_3) - 87 D_1 \mathbf{S}_{1,1,1,1} + \mathbf{S}_3 (36/5 D_{-2} + 20 D_{-1} \\
 &+ 48 D_0 - 409/2 D_1 - 62 D_2 + 504/5 D_3 - 108 D_{-2}^2 + 36 D_{-1}^2 + 24 D_1^2 - 24 D_2^2 \\
 &+ 54 D_3^2) + \mathbf{S}_{1,2} (15 D_{-2} - 6 D_{-1} - 43 D_0 + 527/2 D_1 - 66 D_2 + 71/2 D_3 \\
 &- 51 D_1^2 - 12 D_2^2 + 6 D_3^2) + \mathbf{S}_{2,1} (-15 D_{-2} + 6 D_{-1} - 53 D_0 + 531/2 D_1 - 6 D_2 \\
 &+ 95 D_3 - 42 D_1^2 + 12 D_2^2 - 6 D_3^2) + \mathbf{S}_{1,1,1} (48 D_0 - 270 D_1 + 48 D_1^2)
 \end{aligned}$$

---


$$\begin{aligned}
& + \mathbf{S}_2 (63/2 D_{-2} - 144 D_{-2} \zeta_3 - 18 D_{-1} + 72 D_{-1} \zeta_3 - 187 D_0 + 12755/24 D_1 \\
& - 6 D_1 \zeta_2 - 72 D_1 \zeta_3 + 36 D_2 + 144 D_2 \zeta_3 + 6 D_3 - 216 D_3 \zeta_3 + 99/2 D_0^2 \\
& - 123 D_1^2 + 57/2 D_1^3 + 12 D_2^2 - 9 D_3^2) + \mathbf{S}_{1,1} (-135/2 D_{-2} + 120 D_{-2} \zeta_3 \\
& + 30 D_{-1} - 60 D_{-1} \zeta_3 + 205 D_0 - 14687/24 D_1 + 6 D_1 \zeta_2 - 48 D_1 \zeta_3 - 6 D_2 \\
& + 312 D_2 \zeta_3 - 15/4 D_3 - 180 D_3 \zeta_3 - 123/2 D_0^2 + 160 D_1^2 - 75/2 D_1^3) \\
& + \mathbf{S}_1 (-1683/20 D_{-2} - 952/5 D_{-2} \zeta_3 + 36 D_{-2} \zeta_4 + 22 D_{-1} + 136 D_{-1} \zeta_3 \\
& - 18 D_{-1} \zeta_4 + 2357/6 D_0 - 15/4 D_0 \zeta_2 - 48 D_0 \zeta_3 - 309073/288 D_1 \\
& + 161/8 D_1 \zeta_2 + 140 D_1 \zeta_3 + 18 D_1 \zeta_4 + 230 D_2 - 556 D_2 \zeta_3 - 36 D_2 \zeta_4 \\
& - 2651/10 D_3 + 2622/5 D_3 \zeta_3 + 54 D_3 \zeta_4 + 81 D_{-2}^2 - 144 D_{-2}^2 \zeta_3 - 36 D_{-1}^2 \\
& + 72 D_{-1}^2 \zeta_3 - 327/2 D_0^2 + 171/4 D_0^3 + 4781/12 D_1^2 - 9/4 D_1^2 \zeta_2 + 24 D_1^2 \zeta_3 \\
& - 435/4 D_1^3 + 45/4 D_1^4 + 36 D_2^2 - 48 D_2^2 \zeta_3 - 48 D_3^2 + 72 D_3^2 \zeta_3) \\
& + 1071/20 D_{-2} + 378/5 D_{-2} \zeta_3 - 54 D_{-2} \zeta_4 + 360 D_{-2} \zeta_5 - 76 D_{-1} \zeta_3 \\
& + 18 D_{-1} \zeta_4 - 180 D_{-1} \zeta_5 + 21667/36 D_0 - 57/4 D_0 \zeta_2 - 45/2 D_0 \zeta_3 \\
& - 2937455/1728 D_1 + 133/3 D_1 \zeta_2 + 1111/4 D_1 \zeta_3 + 9/2 D_1 \zeta_4 - 360 D_1 \zeta_5 \\
& + 28 D_2 \zeta_3 - 18 D_2 \zeta_4 + 1800 D_2 \zeta_5 + 2219/20 D_3 - 2598/5 D_3 \zeta_3 - 54 D_3 \zeta_4 \\
& - 1260 D_3 \zeta_5 - 27 D_{-2}^2 + 216 D_{-2}^2 \zeta_3 - 72 D_{-1}^2 \zeta_3 - 3065/12 D_0^2 + 3 D_0^2 \zeta_2 \\
& + 347/4 D_0^3 - 75/4 D_0^4 + 2731/4 D_1^2 - 4 D_1^2 \zeta_2 - 51/2 D_1^2 \zeta_3 - 2443/12 D_1^3 \\
& - 3 D_1^3 \zeta_2 + 29/2 D_1^4 + 75/4 D_1^5 - 24 D_2^2 \zeta_3 + 15 D_3^2 - 72 D_3^2 \zeta_3 \\
& a_{L,\text{ns}}^{(3)\text{N}}(N) = \\
& - 432 D_1 \mathbf{S}_{-5} + 432 D_1 \mathbf{S}_5 + 144 D_1 \mathbf{S}_{-4,1} + 768 D_1 \mathbf{S}_{-3,-2} + 48 D_1 \mathbf{S}_{-3,2} \\
& + 768 D_1 \mathbf{S}_{-2,-3} - 48 D_1 \mathbf{S}_{-2,3} + 1152 D_1 \mathbf{S}_{1,-4} - 288 D_1 \mathbf{S}_{1,4} \\
& + 1152 D_1 \mathbf{S}_{2,-3} - 24 D_1 \mathbf{S}_{2,3} + 816 D_1 \mathbf{S}_{3,-2} - 204 D_1 \mathbf{S}_{3,2} - 552 D_1 \mathbf{S}_{4,1} \\
& - 480 D_1 \mathbf{S}_{-2,-2,1} - 96 D_1 \mathbf{S}_{-2,1,-2} - 288 D_1 \mathbf{S}_{1,-3,1} - 480 D_1 \mathbf{S}_{1,-2,-2} \\
& - 96 D_1 \mathbf{S}_{1,-2,2} - 1248 D_1 \mathbf{S}_{1,1,-3} - 24 D_1 \mathbf{S}_{1,1,3} - 768 D_1 \mathbf{S}_{1,2,-2} \\
& - 132 D_1 \mathbf{S}_{1,2,2} + 504 D_1 \mathbf{S}_{1,3,1} - 192 D_1 \mathbf{S}_{2,-2,1} - 768 D_1 \mathbf{S}_{2,1,-2} \\
& - 96 D_1 \mathbf{S}_{2,1,2} + 12 D_1 \mathbf{S}_{2,2,1} + 336 D_1 \mathbf{S}_{3,1,1} + 192 D_1 \mathbf{S}_{1,1,-2,1} \\
& + 768 D_1 \mathbf{S}_{1,1,1,-2} + 168 D_1 \mathbf{S}_{1,1,1,2} - 84 D_1 \mathbf{S}_{1,1,2,1} - 96 D_1 \mathbf{S}_{1,2,1,1} \\
& + \mathbf{S}_{-4} (-1008/5 D_{-2} - 1008 D_0 + 876 D_1 - 1512/5 D_3 + 864 D_1^2) \\
& + \mathbf{S}_4 (144/5 D_{-2} + 144 D_0 - 372 D_1 + 216/5 D_3) + \mathbf{S}_{-3,1} (552/5 D_{-2} - 132 D_{-1} \\
& + 552 D_0 - 272 D_1 - 264 D_2 + 828/5 D_3 - 504 D_1^2) + \mathbf{S}_{-2,-2} (192/5 D_{-2} \\
& + 96 D_{-1} + 192 D_0 - 728 D_1 + 192 D_2 + 288/5 D_3) + \mathbf{S}_{-2,2} (288/5 D_{-2} - 96 D_{-1}
\end{aligned}$$

$$\begin{aligned}
 & + 288 D_0 - 48 D_1 - 192 D_2 + 432/5 D_3 - 288 D_1^2) + \mathbf{S}_{1,-3} (624/5 D_{-2} + 168 D_{-1} \\
 & + 624 D_0 - 1504 D_1 + 336 D_2 + 936/5 D_3 - 240 D_1^2) + \mathbf{S}_{1,3} (-48/5 D_{-2} - 24 D_{-1} \\
 & - 48 D_0 + 43 D_1 + 72 D_2 + 1428/5 D_3 - 168 D_1^2) + \mathbf{S}_{2,-2} (336/5 D_{-2} + 120 D_{-1} \\
 & + 336 D_0 - 928 D_1 + 240 D_2 + 504/5 D_3 - 96 D_1^2) + \mathbf{S}_{2,2} (48/5 D_{-2} + 24 D_{-1} \\
 & + 48 D_0 - 336 D_1 + 60 D_2 + 222/5 D_3 - 24 D_1^2) + \mathbf{S}_{3,1} (-24 D_{-2} - 60 D_{-1} \\
 & - 120 D_0 + 433 D_1 - 264 D_2 - 396 D_3 + 132 D_1^2) + \mathbf{S}_{-2,1,1} (-48 D_{-2} + 120 D_{-1} \\
 & - 240 D_0 + 240 D_2 - 72 D_3 + 240 D_1^2) + \mathbf{S}_{1,-2,1} (-192/5 D_{-2} - 192 D_0 + 352 D_1 \\
 & - 288/5 D_3 + 96 D_1^2) + \mathbf{S}_{1,1,-2} (-288/5 D_{-2} - 144 D_{-1} - 288 D_0 + 1056 D_1 \\
 & - 288 D_2 - 432/5 D_3) + \mathbf{S}_{1,1,2} (-24/5 D_{-2} - 12 D_{-1} - 24 D_0 + 384 D_1 - 108 D_2 \\
 & - 1266/5 D_3 + 84 D_1^2) + \mathbf{S}_{1,2,1} (24/5 D_{-2} + 12 D_{-1} + 24 D_0 + 42 D_1 + 36 D_2 \\
 & + 186/5 D_3) + \mathbf{S}_{2,1,1} (114 D_1 + 84 D_2 + 246 D_3 - 96 D_1^2) - 174 D_1 \mathbf{S}_{1,1,1,1} \\
 & + \mathbf{S}_{-3} (1216/25 D_{-2} - 168 D_{-1} + 2336 D_0 - 4604/3 D_1 + 12 D_1 \zeta_2 - 336 D_2 \\
 & + 1884/25 D_3 - 1248/5 D_{-2}^2 - 1248 D_0^2 - 1192 D_1^2 + 24 D_1^3 + 432/5 D_3^2) \\
 & + \mathbf{S}_3 (-236/25 D_{-2} + 24 D_{-1} - 152 D_0 + 1547/3 D_1 - 12 D_1 \zeta_2 - 72 D_2 \\
 & - 11664/25 D_3 + 96/5 D_{-2}^2 + 96 D_0^2 + 28 D_1^2 - 24 D_1^3) + \mathbf{S}_{-2,1} (-1016/25 D_{-2} \\
 & + 156 D_{-1} - 936 D_0 + 388 D_1 + 336 D_2 - 1584/25 D_3 + 96 D_{-2}^2 - 144 D_{-1}^2 \\
 & + 480 D_0^2 + 552 D_1^2 - 48 D_1^3 + 96 D_2^2 - 144/5 D_3^2) + \mathbf{S}_{1,-2} (-296/25 D_{-2} \\
 & - 12 D_{-1} - 888 D_0 + 2812/3 D_1 - 24 D_1 \zeta_2 - 48 D_2 - 504/25 D_3 + 96 D_{-2}^2 \\
 & + 144 D_{-1}^2 + 480 D_0^2 + 328 D_1^2 - 96 D_2^2 - 144/5 D_3^2) + \mathbf{S}_{1,2} (36/5 D_{-2} \\
 & + 12 D_{-1} - 110 D_0 + 83 D_1 - 222 D_2 + 589/5 D_3 + 48 D_1^2 - 12 D_1^3 - 24 D_2^2 \\
 & - 60 D_3^2) + \mathbf{S}_{2,1} (-36/5 D_{-2} - 12 D_{-1} - 82 D_0 - 84 D_1 + 294 D_2 + 1031/5 D_3 \\
 & - 156 D_1^2 + 12 D_1^3 + 24 D_2^2 + 60 D_3^2) + \mathbf{S}_{1,1,1} (96 D_0 - 60 D_1 + 96 D_1^2) \\
 & + \mathbf{S}_{-2} (-904/125 D_{-2} + 24/5 D_{-2} \zeta_2 + 84 D_{-1} - 7324/3 D_0 + 24 D_0 \zeta_2 \\
 & + 2019 D_1 - 12 D_1 \zeta_2 + 672 D_1 \zeta_3 + 192 D_2 - 971/125 D_3 + 36/5 D_3 \zeta_2 \\
 & + 1032/25 D_{-2}^2 - 192 D_{-2}^3 - 144 D_{-1}^2 + 1872 D_0^2 - 960 D_0^3 + 2158/3 D_1^2 \\
 & - 24 D_1^2 \zeta_2 + 140 D_1^3 - 48 D_1^4 + 96 D_2^2 - 828/25 D_3^2) + \mathbf{S}_2 (144/5 D_{-2} \\
 & + 72 D_{-1} - 73 D_0 - 3383/4 D_1 - 12 D_1 \zeta_2 + 1176 D_1 \zeta_3 + 498 D_2 + 726/5 D_3 \\
 & + 45 D_0^2 + 202 D_1^2 - 27 D_1^3 + 24 D_2^2 + 90 D_3^2) + \mathbf{S}_{1,1} (-36 D_{-2} - 120 D_{-1} \\
 & + 55 D_0 + 2311/4 D_1 + 12 D_1 \zeta_2 - 792 D_1 \zeta_3 - 156 D_2 + 507/2 D_3 - 33 D_0^2 \\
 & + 82 D_1^2 - 75 D_1^3) + \mathbf{S}_1 (-2562/25 D_{-2} + 624/5 D_{-2} \zeta_3 - 252 D_{-1} \\
 & + 216 D_{-1} \zeta_3 + 275/6 D_0 - 15/2 D_0 \zeta_2 + 624 D_0 \zeta_3 + 149695/144 D_1
 \end{aligned}$$

---


$$\begin{aligned}
& + 25/4 D_1 \zeta_2 - 1004 D_1 \zeta_3 - 180 D_1 \zeta_4 - 30 D_2 - 48 D_2 \zeta_3 + 7112/25 D_3 \\
& - 5424/5 D_3 \zeta_3 + 72 D_{-2}^2 + 144 D_{-1}^2 - 22 D_0^2 + 63/2 D_0^3 - 381/2 D_1^2 \\
& - 9/2 D_1^2 \zeta_2 + 288 D_1^2 \zeta_3 - 335/2 D_1^3 + 141/2 D_1^4 - 72 D_2^2 + 267/5 D_3^2) \\
& - 47861/250 D_{-2} + 18/5 D_{-2} \zeta_2 + 2268/25 D_{-2} \zeta_3 + 216/5 D_{-2} \zeta_4 - 60 D_{-1} \zeta_3 \\
& + 36 D_{-1} \zeta_4 - 4729/18 D_0 - 13/2 D_0 \zeta_2 + 2655 D_0 \zeta_3 + 216 D_0 \zeta_4 \\
& + 333811/288 D_1 - 41/2 D_1 \zeta_2 - 3671/2 D_1 \zeta_3 + 36 D_1 \zeta_3 \zeta_2 - 333 D_1 \zeta_4 \\
& - 480 D_1 \zeta_5 - 1596 D_2 \zeta_3 - 36 D_2 \zeta_4 - 109639/250 D_3 + 27/5 D_3 \zeta_2 \\
& + 11982/25 D_3 \zeta_3 - 1026/5 D_3 \zeta_4 + 5274/25 D_{-2}^2 - 288 D_{-2}^2 \zeta_3 - 144 D_{-2}^3 \\
& - 144 D_{-1}^2 \zeta_3 + 247/6 D_0^2 + 6 D_0^2 \zeta_2 - 1440 D_0^2 \zeta_3 + 83/2 D_0^3 - 75/2 D_0^4 \\
& - 11753/18 D_1^2 + 14 D_1^2 \zeta_2 - 579 D_1^2 \zeta_3 + 1661/6 D_1^3 - 6 D_1^3 \zeta_2 - 103 D_1^4 \\
& + 75/2 D_1^5 - 48 D_2^2 \zeta_3 - 2256/25 D_3^2 - 1368/5 D_3^2 \zeta_3 \\
& a_{L,ns}^{(3)F}(N) = \\
& + 36 D_1 \mathbf{S}_3 - 36 D_1 \mathbf{S}_{1,2} - 36 D_1 \mathbf{S}_{2,1} + 36 D_1 \mathbf{S}_{1,1,1} + \mathbf{S}_2 (30 D_0 - 131 D_1 \\
& + 30 D_1^2) + \mathbf{S}_{1,1} (-30 D_0 + 131 D_1 - 30 D_1^2) + \mathbf{S}_1 (-82 D_0 + 785/3 D_1 \\
& - 3 D_1 \zeta_2 + 24 D_0^2 - 106 D_1^2 + 24 D_1^3) - 875/6 D_0 + 3 D_0 \zeta_2 + 14797/36 D_1 \\
& - 25/2 D_1 \zeta_2 - 12 D_1 \zeta_3 + 63 D_0^2 - 18 D_0^3 - 1253/6 D_1^2 + 3 D_1^2 \zeta_2 + 81 D_1^3 \\
& - 18 D_1^4
\end{aligned} \tag{J.0.5}$$

The following is the  $a_3$ :

$$\begin{aligned}
a_{3,ns}^{(3)}(N) &= n_f^0 \text{ contributions} \\
&+ C_F C_A n_f \frac{16}{9} a_{3,ns}^{(3)L}(N) + C_F (C_F - \frac{1}{2} C_A) n_f \frac{16}{9} a_{3,ns}^{(3)N}(N) + C_F n_f^2 \frac{16}{27} a_{3,ns}^{(3)F}(N)
\end{aligned}$$

$$\begin{aligned}
a_{3,ns}^{(3)L}(N) &= \\
& + 225 \mathbf{S}_6 - 229 \mathbf{S}_{1,5} - 209 \mathbf{S}_{2,4} - 281 \mathbf{S}_{3,3} - 338 \mathbf{S}_{4,2} - 363 \mathbf{S}_{5,1} + 186 \mathbf{S}_{1,1,4} \\
& + 401/2 \mathbf{S}_{1,2,3} + 529/2 \mathbf{S}_{1,3,2} + 300 \mathbf{S}_{1,4,1} + 481/2 \mathbf{S}_{2,1,3} + 249 \mathbf{S}_{2,2,2} + 519/2 \mathbf{S}_{2,3,1} \\
& + 637/2 \mathbf{S}_{3,1,2} + 675/2 \mathbf{S}_{3,2,1} + 389 \mathbf{S}_{4,1,1} - 343/2 \mathbf{S}_{1,1,1,3} - 191 \mathbf{S}_{1,1,2,2} \\
& - 459/2 \mathbf{S}_{1,1,3,1} - 235 \mathbf{S}_{1,2,1,2} - 246 \mathbf{S}_{1,2,2,1} - 607/2 \mathbf{S}_{1,3,1,1} - 238 \mathbf{S}_{2,1,1,2} - 256 \mathbf{S}_{2,1,2,1} \\
& - 276 \mathbf{S}_{2,2,1,1} - 681/2 \mathbf{S}_{3,1,1,1} + 171 \mathbf{S}_{1,1,1,1,2} + 202 \mathbf{S}_{1,1,1,2,1} + 225 \mathbf{S}_{1,1,2,1,1} \\
& + 258 \mathbf{S}_{1,2,1,1,1} + 249 \mathbf{S}_{2,1,1,1,1} - 195 \mathbf{S}_{1,1,1,1,1,1} + \mathbf{S}_5 (-1387/2 + 229/2 D_0 \\
& - 229/2 D_1) + \mathbf{S}_{1,4} (1387/3 - 18 D_{-1} - 93 D_0 + 93 D_1 + 18 D_2) + \mathbf{S}_{2,3} (12923/24
\end{aligned}$$



$$\begin{aligned}
 & -9 D_{-1} - 401/4 D_0 + 401/4 D_1 + 9 D_2) + \mathbf{S}_{3,2} (17861/24 + 9 D_{-1} - 529/4 D_0 \\
 & + 529/4 D_1 - 9 D_2) + \mathbf{S}_{4,1} (2669/3 + 24 D_{-1} - 150 D_0 + 150 D_1 - 24 D_2) \\
 & + \mathbf{S}_{1,1,3} (-9793/24 + 15 D_{-1} + 343/4 D_0 - 343/4 D_1 - 15 D_2) + \mathbf{S}_{1,2,2} (-5555/12 \\
 & + 3 D_{-1} + 191/2 D_0 - 191/2 D_1 - 3 D_2) + \mathbf{S}_{1,3,1} (-14011/24 - 9 D_{-1} + 459/4 D_0 \\
 & - 459/4 D_1 + 9 D_2) + \mathbf{S}_{2,1,2} (-6937/12 + 3 D_{-1} + 235/2 D_0 - 235/2 D_1 - 3 D_2) \\
 & + \mathbf{S}_{2,2,1} (-1235/2 - 3 D_{-1} + 123 D_0 - 123 D_1 + 3 D_2) + \mathbf{S}_{3,1,1} (-6519/8 - 15 D_{-1} \\
 & + 607/4 D_0 - 607/4 D_1 + 15 D_2) + \mathbf{S}_{1,1,1,2} (1609/4 - 171/2 D_0 + 171/2 D_1) \\
 & + \mathbf{S}_{1,1,2,1} (5551/12 - 101 D_0 + 83 D_1 + 27 D_2) + \mathbf{S}_{1,2,1,1} (6317/12 - 225/2 D_0 \\
 & + 261/2 D_1 - 27 D_2) + \mathbf{S}_{2,1,1,1} (1780/3 - 129 D_0 + 129 D_1) + \mathbf{S}_{1,1,1,1,1} (-1713/4 \\
 & + 195/2 D_0 - 195/2 D_1) + \mathbf{S}_4 (91463/72 - 69/4 \zeta_2 + 18 D_{-1} - 1537/6 D_0 \\
 & + 1861/6 D_1 - 18 D_2 + 91 D_0^2 - 25 D_1^2) + \mathbf{S}_{1,3} (-11813/18 + 75/4 \zeta_2 - 16 D_{-1} \\
 & + 5321/24 D_0 - 3535/12 D_1 + 13 D_2 - 18 D_{-1}^2 - 427/4 D_0^2 + 54 D_1^2 - 6 D_2^2) \\
 & + \mathbf{S}_{2,2} (-34313/36 + 39/2 \zeta_2 - 3 D_{-1} + 1481/6 D_0 - 1901/6 D_1 + 9/2 D_2 - 111 D_0^2 \\
 & + 44 D_1^2) + \mathbf{S}_{3,1} (-10337/8 + 99/4 \zeta_2 + 10 D_{-1} + 7523/24 D_0 - 4447/12 D_1 \\
 & - 10 D_2 + 18 D_{-1}^2 - 465/4 D_0^2 + 39/2 D_1^2 + 6 D_2^2) + \mathbf{S}_{1,1,2} (4981/8 - 15 \zeta_2 \\
 & - 209 D_0 + 1143/4 D_1 - 21/2 D_2 + 211/2 D_0^2 - 109/2 D_1^2) + \mathbf{S}_{1,2,1} (8453/12 \\
 & - 39/2 \zeta_2 - 1483/6 D_0 + 1927/6 D_1 - 51/2 D_2 + 229/2 D_0^2 - 39 D_1^2) \\
 & + \mathbf{S}_{2,1,1} (3877/4 - 39/2 \zeta_2 - 1787/6 D_0 + 4219/12 D_1 + 75/2 D_2 + 249/2 D_0^2 \\
 & - 63/2 D_1^2) + \mathbf{S}_{1,1,1,1} (-4969/8 + 15 \zeta_2 + 939/4 D_0 - 300 D_1 - 111 D_0^2 \\
 & + 81/2 D_1^2) + \mathbf{S}_3 (-363857/216 + 15/8 Z_{5,1} + 717/16 \zeta_2 + 182 \zeta_3 - 8 D_{-1} \\
 & + 54389/144 D_0 - 75/8 D_0 \zeta_2 - 80687/144 D_1 + 75/8 D_1 \zeta_2 + 2 D_2 + 18 D_{-1}^2 \\
 & - 3047/12 D_0^2 + 451/4 D_0^3 + 2513/24 D_1^2 - 20 D_1^3 + 6 D_2^2) + \mathbf{S}_{1,2} (163445/216 \\
 & - 3/4 Z_{5,1} - 77/2 \zeta_2 - 161 \zeta_3 - 3 D_{-1} - 5723/16 D_0 + 15/2 D_0 \zeta_2 + 27749/48 D_1 \\
 & - 15/2 D_1 \zeta_2 - 57/4 D_2 + 6715/24 D_0^2 - 263/2 D_0^3 - 3673/24 D_1^2 + 45/2 D_1^3 \\
 & - 3 D_2^2) + \mathbf{S}_{2,1} (288791/216 - 3/2 Z_{5,1} - 369/8 \zeta_2 - 209 \zeta_3 + 3 D_{-1} - 20141/48 D_0 \\
 & + 39/4 D_0 \zeta_2 + 9761/16 D_1 - 39/4 D_1 \zeta_2 + 201/4 D_2 + 2411/8 D_0^2 - 141 D_0^3 \\
 & - 2777/24 D_1^2 + 33 D_1^3 + 3 D_2^2) + \mathbf{S}_{1,1,1} (-106405/144 + 3/4 Z_{5,1} + 35 \zeta_2 + 90 \zeta_3 \\
 & + 6137/16 D_0 - 15/2 D_0 \zeta_2 - 9425/16 D_1 + 15/2 D_1 \zeta_2 - 7147/24 D_0^2 \\
 & + 285/2 D_0^3 + 3325/24 D_1^2 - 57/2 D_1^3) + \mathbf{S}_2 (17098453/10368 - 9/8 Z_{5,2} \\
 & - 57/16 Z_{5,1} - 1937/32 \zeta_2 - 4405/12 \zeta_3 - 63/2 \zeta_4 - 9 D_{-1} + 36 D_{-1} \zeta_3 \\
 & - 838553/1728 D_0 + 3/8 D_0 Z_{5,1} + 43/2 D_0 \zeta_2 + 161/2 D_0 \zeta_3 + 1509971/1728 D_1
 \end{aligned}$$

---


$$\begin{aligned}
& -3/8 D_1 Z_{5,1} - 26 D_1 \zeta_2 - 161/2 D_1 \zeta_3 + 123/4 D_2 - 36 D_2 \zeta_3 + 17929/36 D_0^2 \\
& - 69/8 D_0^2 \zeta_2 - 15545/48 D_0^3 + 1031/8 D_0^4 - 39667/144 D_1^2 + 27/8 D_1^2 \zeta_2 \\
& + 3719/48 D_1^3 - 95/8 D_1^4 + 3 D_2^2) + \mathbf{S}_{1,1} (-2535307/3456 + 9/8 Z_{5,2} + 29/16 Z_{5,1} \\
& + 1265/32 \zeta_2 + 451/2 \zeta_3 + 27/2 \zeta_4 + 15 D_{-1} - 30 D_{-1} \zeta_3 + 287723/576 D_0 \\
& - 3/8 D_0 Z_{5,1} - 41/2 D_0 \zeta_2 - 45 D_0 \zeta_3 - 540629/576 D_1 + 3/8 D_1 Z_{5,1} + 25 D_1 \zeta_2 \\
& + 117 D_1 \zeta_3 + 45/2 D_2 - 78 D_2 \zeta_3 - 1081/2 D_0^2 + 69/8 D_0^2 \zeta_2 + 5947/16 D_0^3 \\
& - 1235/8 D_0^4 + 14911/48 D_1^2 - 27/8 D_1^2 \zeta_2 - 1469/16 D_1^3 + 123/8 D_1^4) \\
& + \mathbf{S}_1 (-51352297/62208 + 27/32 Z_{5,2} + 247/96 Z_{5,1} + 21169/576 \zeta_2 + 57143/144 \zeta_3 \\
& - 9/2 \zeta_3 \zeta_2 + 503/8 \zeta_4 + 129 \zeta_5 + 29 D_{-1} + 32 D_{-1} \zeta_3 - 9 D_{-1} \zeta_4 \\
& + 1063615/1728 D_0 - 9/16 D_0 Z_{5,2} - 19/16 D_0 Z_{5,1} - 963/32 D_0 \zeta_2 - 221/2 D_0 \zeta_3 \\
& - 27/4 D_0 \zeta_4 - 4562063/3456 D_1 + 9/16 D_1 Z_{5,2} + 7/4 D_1 Z_{5,1} + 177/4 D_1 \zeta_2 \\
& + 431/2 D_1 \zeta_3 + 27/4 D_1 \zeta_4 + 7/4 D_2 + 52 D_2 \zeta_3 + 9 D_2 \zeta_4 - 18 D_{-1}^2 \\
& + 36 D_{-1}^2 \zeta_3 - 1382249/1728 D_0^2 + 3/4 D_0^2 Z_{5,1} + 197/8 D_0^2 \zeta_2 + 373/4 D_0^2 \zeta_3 \\
& + 15491/24 D_0^3 - 39/4 D_0^3 \zeta_2 - 8915/24 D_0^4 + 132 D_0^5 + 224237/432 D_1^2 \\
& - 3/8 D_1^2 Z_{5,1} - 10 D_1^2 \zeta_2 - 427/4 D_1^2 \zeta_3 - 3147/16 D_1^3 + 15/8 D_1^3 \zeta_2 \\
& + 2201/48 D_1^4 - 33/8 D_1^5 - 3 D_2^2 + 12 D_2^2 \zeta_3) + 8503399/6912 + 9/32 Z_{5,3b} \\
& + 9/16 Z_{5,3a} - 45/32 Z_{5,2} - 449/128 Z_{5,1} - 38161/768 \zeta_2 - 5223/16 \zeta_3 + 27/8 \zeta_3 \zeta_2 \\
& - 723/16 \zeta_4 - 477/4 \zeta_5 - 2 D_{-1} \zeta_3 + 9 D_{-1} \zeta_4 - 90 D_{-1} \zeta_5 + 63294971/62208 D_0 \\
& + 9/32 D_0 Z_{5,2} - 131/96 D_0 Z_{5,1} - 58693/1152 D_0 \zeta_2 - 24961/144 D_0 \zeta_3 \\
& + 9/4 D_0 \zeta_3 \zeta_2 - 229/8 D_0 \zeta_4 - 129/2 D_0 \zeta_5 - 29202533/15552 D_1 \\
& + 9/16 D_1 Z_{5,2} + 151/48 D_1 Z_{5,1} + 84685/1152 D_1 \zeta_2 + 4264/9 D_1 \zeta_3 \\
& - 9/4 D_1 \zeta_3 \zeta_2 + 245/4 D_1 \zeta_4 + 849/2 D_1 \zeta_5 - 461/2 D_2 \zeta_3 - 45/2 D_2 \zeta_4 \\
& - 450 D_2 \zeta_5 - 36 D_{-1}^2 \zeta_3 - 5839213/5184 D_0^2 + 9/16 D_0^2 Z_{5,2} + 15/8 D_0^2 Z_{5,1} \\
& + 2033/48 D_0^2 \zeta_2 + 455/3 D_0^2 \zeta_3 + 27/2 D_0^2 \zeta_4 + 1589929/1728 D_0^3 \\
& - 15/16 D_0^3 Z_{5,1} - 615/32 D_0^3 \zeta_2 - 269/4 D_0^3 \zeta_3 - 84317/144 D_0^4 \\
& + 69/16 D_0^4 \zeta_2 + 1531/6 D_0^5 - 225/4 D_0^6 + 1908389/2592 D_1^2 - 17/16 D_1^2 Z_{5,1} \\
& - 2039/96 D_1^2 \zeta_2 - 2081/12 D_1^2 \zeta_3 - 99/4 D_1^2 \zeta_4 - 121829/432 D_1^3 \\
& + 3/16 D_1^3 Z_{5,1} + 15/32 D_1^3 \zeta_2 - 73/2 D_1^3 \zeta_3 + 5593/72 D_1^4 + 27/16 D_1^4 \zeta_2 \\
& - 13/8 D_1^5 - 27/4 D_1^6 - 30 D_2^2 \zeta_3 \\
& a_{3,\text{ns}}^{(3)\text{N}}(N) = \\
& + 220 \mathbf{S}_{-6} + 230 \mathbf{S}_6 - 92 \mathbf{S}_{-5,1} - 984 \mathbf{S}_{-4,-2} - 60 \mathbf{S}_{-4,2} - 1104 \mathbf{S}_{-3,-3} + 72 \mathbf{S}_{-3,3}
\end{aligned}$$

$$\begin{aligned}
 & -672 \mathbf{S}_{-2,-4} + 96 \mathbf{S}_{-2,4} - 748 \mathbf{S}_{1,-5} - 200 \mathbf{S}_{1,5} - 940 \mathbf{S}_{2,-4} - 166 \mathbf{S}_{2,4} - 1192 \mathbf{S}_{3,-3} \\
 & - 326 \mathbf{S}_{3,3} - 988 \mathbf{S}_{4,-2} - 508 \mathbf{S}_{4,2} - 484 \mathbf{S}_{5,1} + 16 \mathbf{S}_{-4,1,1} + 576 \mathbf{S}_{-3,-2,1} \\
 & + 192 \mathbf{S}_{-3,1,-2} + 456 \mathbf{S}_{-2,-3,1} + 24 \mathbf{S}_{-2,-2,-2} + 264 \mathbf{S}_{-2,-2,2} + 192 \mathbf{S}_{-2,1,-3} \\
 & + 72 \mathbf{S}_{-2,2,-2} + 272 \mathbf{S}_{1,-4,1} + 672 \mathbf{S}_{1,-3,-2} + 144 \mathbf{S}_{1,-3,2} + 672 \mathbf{S}_{1,-2,-3} + 1024 \mathbf{S}_{1,1,-4} \\
 & + 320 \mathbf{S}_{1,1,4} + 976 \mathbf{S}_{1,2,-3} + 495 \mathbf{S}_{1,2,3} + 712 \mathbf{S}_{1,3,-2} + 311 \mathbf{S}_{1,3,2} + 4 \mathbf{S}_{1,4,1} \\
 & + 272 \mathbf{S}_{2,-3,1} + 408 \mathbf{S}_{2,-2,-2} + 96 \mathbf{S}_{2,-2,2} + 976 \mathbf{S}_{2,1,-3} + 511 \mathbf{S}_{2,1,3} + 592 \mathbf{S}_{2,2,-2} \\
 & + 612 \mathbf{S}_{2,2,2} + 61 \mathbf{S}_{2,3,1} + 200 \mathbf{S}_{3,-2,1} + 712 \mathbf{S}_{3,1,-2} + 639 \mathbf{S}_{3,1,2} + 493 \mathbf{S}_{3,2,1} \\
 & + 582 \mathbf{S}_{4,1,1} + 16 \mathbf{S}_{-3,1,1,1} - 240 \mathbf{S}_{-2,-2,1,1} - 96 \mathbf{S}_{-2,1,-2,1} - 16 \mathbf{S}_{1,-3,1,1} - 384 \mathbf{S}_{1,-2,-2,1} \\
 & - 96 \mathbf{S}_{1,-2,1,-2} - 272 \mathbf{S}_{1,1,-3,1} - 384 \mathbf{S}_{1,1,-2,-2} - 96 \mathbf{S}_{1,1,-2,2} - 976 \mathbf{S}_{1,1,1,-3} \\
 & - 497 \mathbf{S}_{1,1,1,3} - 592 \mathbf{S}_{1,1,2,-2} - 560 \mathbf{S}_{1,1,2,2} - 73 \mathbf{S}_{1,1,3,1} - 176 \mathbf{S}_{1,2,-2,1} - 592 \mathbf{S}_{1,2,1,-2} \\
 & - 524 \mathbf{S}_{1,2,1,2} - 432 \mathbf{S}_{1,2,2,1} - 157 \mathbf{S}_{1,3,1,1} - 16 \mathbf{S}_{2,-2,1,1} - 176 \mathbf{S}_{2,1,-2,1} - 592 \mathbf{S}_{2,1,1,-2} \\
 & - 664 \mathbf{S}_{2,1,1,2} - 434 \mathbf{S}_{2,1,2,1} - 422 \mathbf{S}_{2,2,1,1} - 583 \mathbf{S}_{3,1,1,1} - 32 \mathbf{S}_{1,-2,1,1,1} + 160 \mathbf{S}_{1,1,1,-2,1} \\
 & + 576 \mathbf{S}_{1,1,1,1,-2} + 570 \mathbf{S}_{1,1,1,1,2} + 354 \mathbf{S}_{1,1,1,2,1} + 334 \mathbf{S}_{1,1,2,1,1} + 408 \mathbf{S}_{1,2,1,1,1} \\
 & + 498 \mathbf{S}_{2,1,1,1,1} - 390 \mathbf{S}_{1,1,1,1,1,1} + \mathbf{S}_{-5} (-278/3 + 266 D_0 - 266 D_1) + \mathbf{S}_5 (-407 \\
 & + 208 D_0 - 208 D_1) + \mathbf{S}_{-4,1} (166/3 - 100 D_0 + 100 D_1) + \mathbf{S}_{-3,-2} (548 - 144 D_0 \\
 & + 144 D_1) + \mathbf{S}_{-3,2} (40 - 60 D_0 + 60 D_1) + \mathbf{S}_{-2,-3} (472 - 144 D_0 + 144 D_1) \\
 & + \mathbf{S}_{-2,3} (-78 - 12 D_0 + 12 D_1) + \mathbf{S}_{1,-4} (1406/3 - 224 D_0 + 224 D_1) + \mathbf{S}_{1,4} (1516/3 \\
 & - 232 D_0 + 232 D_1) + \mathbf{S}_{2,-3} (1520/3 - 200 D_0 + 200 D_1) + \mathbf{S}_{2,3} (3187/12 \\
 & - 507/2 D_0 + 507/2 D_1) + \mathbf{S}_{3,-2} (1610/3 - 152 D_0 + 152 D_1) + \mathbf{S}_{3,2} (9335/12 \\
 & - 413/2 D_0 + 413/2 D_1) + \mathbf{S}_{4,1} (1040 - 140 D_0 + 140 D_1) + \mathbf{S}_{-3,1,1} (-80/3 + 8 D_0 \\
 & - 8 D_1) + \mathbf{S}_{-2,-2,1} (-164 + 72 D_0 - 72 D_1) + \mathbf{S}_{-2,1,-2} (-156 + 24 D_0 - 24 D_1) \\
 & + \mathbf{S}_{1,-3,1} (-640/3 + 64 D_0 - 64 D_1) + \mathbf{S}_{1,-2,-2} (-316 + 72 D_0 - 72 D_1) \\
 & + \mathbf{S}_{1,-2,2} (-80 + 24 D_0 - 24 D_1) + \mathbf{S}_{1,1,-3} (-1760/3 + 176 D_0 - 176 D_1) \\
 & + \mathbf{S}_{1,1,3} (-6425/12 + 485/2 D_0 - 485/2 D_1) + \mathbf{S}_{1,2,-2} (-1040/3 + 104 D_0 - 104 D_1) \\
 & + \mathbf{S}_{1,2,2} (-2236/3 + 247 D_0 - 247 D_1) + \mathbf{S}_{1,3,1} (-6961/12 + 325/2 D_0 - 325/2 D_1) \\
 & + \mathbf{S}_{2,-2,1} (-400/3 + 40 D_0 - 40 D_1) + \mathbf{S}_{2,1,-2} (-1040/3 + 104 D_0 - 104 D_1) \\
 & + \mathbf{S}_{2,1,2} (-759 + 238 D_0 - 238 D_1) + \mathbf{S}_{2,2,1} (-1610/3 + 219 D_0 - 219 D_1) \\
 & + \mathbf{S}_{3,1,1} (-12481/12 + 325/2 D_0 - 325/2 D_1) + \mathbf{S}_{-2,1,1,1} (16 D_0 - 16 D_1) \\
 & + 160/3 \mathbf{S}_{1,-2,1,1} + \mathbf{S}_{1,1,-2,1} (160 - 32 D_0 + 32 D_1) + \mathbf{S}_{1,1,1,-2} (1120/3 - 96 D_0 \\
 & + 96 D_1) + \mathbf{S}_{1,1,1,2} (4003/6 - 243 D_0 + 243 D_1) + \mathbf{S}_{1,1,2,1} (1209/2 - 198 D_0 \\
 & + 198 D_1) + \mathbf{S}_{1,2,1,1} (4193/6 - 191 D_0 + 191 D_1) + \mathbf{S}_{2,1,1,1} (2108/3 - 204 D_0
 \end{aligned}$$

---


$$\begin{aligned}
& + 204 D_1) + \mathbf{S}_{1,1,1,1,1} (-1185/2 + 195 D_0 - 195 D_1) + \mathbf{S}_{-4} (4283/18 - 15 \zeta_2 \\
& + 252 D_{-1} - 1216/3 D_0 + 1216/3 D_1 - 252 D_2 + 62 D_0^2 - 258 D_1^2) + \mathbf{S}_4 (5921/36 \\
& - 39/2 \zeta_2 - 36 D_{-1} - 1001/3 D_0 + 1325/3 D_1 + 36 D_2 + 176 D_0^2 + 62 D_1^2) \\
& + \mathbf{S}_{-3,1} (-764/9 - 138 D_{-1} + 908/3 D_0 - 908/3 D_1 + 138 D_2 + 38 D_0^2 + 150 D_1^2) \\
& + \mathbf{S}_{-2,-2} (-253 + 18 \zeta_2 - 48 D_{-1} + 36 D_0 - 36 D_1 + 48 D_2 - 72 D_0^2 + 24 D_1^2) \\
& + \mathbf{S}_{-2,2} (-24 - 72 D_{-1} + 172 D_0 - 172 D_1 + 72 D_2 + 36 D_0^2 + 84 D_1^2) \\
& + \mathbf{S}_{1,-3} (-3088/9 + 36 \zeta_2 - 156 D_{-1} + 400/3 D_0 - 400/3 D_1 + 156 D_2 - 140 D_0^2 \\
& + 84 D_1^2) + \mathbf{S}_{1,3} (-12247/18 + 69/2 \zeta_2 + 12 D_{-1} + 5617/12 D_0 - 2921/6 D_1 \\
& + 198 D_2 - 529/2 D_0^2 + 76 D_1^2) + \mathbf{S}_{2,-2} (-1876/9 + 24 \zeta_2 - 84 D_{-1} + 148/3 D_0 \\
& - 148/3 D_1 + 84 D_2 - 92 D_0^2 + 36 D_1^2) + \mathbf{S}_{2,2} (-2329/9 + 39 \zeta_2 - 12 D_{-1} \\
& + 1172/3 D_0 - 1559/3 D_1 + 33 D_2 - 252 D_0^2 + 59 D_1^2) + \mathbf{S}_{3,1} (-27691/36 \\
& + 81/2 \zeta_2 + 30 D_{-1} + 3197/12 D_0 - 3205/6 D_1 - 282 D_2 - 193/2 D_0^2 - 12 D_1^2) \\
& + \mathbf{S}_{-2,1,1} (60 D_{-1} - 488/3 D_0 + 488/3 D_1 - 60 D_2 - 52 D_0^2 - 68 D_1^2) \\
& + \mathbf{S}_{1,-2,1} (664/9 + 48 D_{-1} - 80 D_0 + 80 D_1 - 48 D_2 + 16 D_0^2 - 32 D_1^2) \\
& + \mathbf{S}_{1,1,-2} (664/3 - 24 \zeta_2 + 72 D_{-1} - 32/3 D_0 + 32/3 D_1 - 72 D_2 + 104 D_0^2 - 8 D_1^2) \\
& + \mathbf{S}_{1,1,2} (8063/12 - 36 \zeta_2 + 6 D_{-1} - 1297/3 D_0 + 2873/6 D_1 - 171 D_2 + 284 D_0^2 \\
& - 95 D_1^2) + \mathbf{S}_{1,2,1} (2149/3 - 33 \zeta_2 - 6 D_{-1} - 711/2 D_0 + 501 D_1 + 27 D_2 + 211 D_0^2 \\
& - 67 D_1^2) + \mathbf{S}_{2,1,1} (985/2 - 39 \zeta_2 - 890/3 D_0 + 3175/6 D_1 + 165 D_2 + 184 D_0^2 \\
& - 47 D_1^2) + \mathbf{S}_{1,1,1,1} (-6931/12 + 30 \zeta_2 + 675/2 D_0 - 468 D_1 - 222 D_0^2 + 81 D_1^2) \\
& + \mathbf{S}_{-3} (-8054/27 + 10 \zeta_2 - 1124 \zeta_3 - 316 D_{-1} + 4742/9 D_0 - 15 D_0 \zeta_2 - 4742/9 D_1 \\
& + 15 D_1 \zeta_2 + 316 D_2 + 312 D_{-1}^2 - 196/3 D_0^2 + 14 D_0^3 + 324 D_1^2 - 222 D_1^3 \\
& + 72 D_2^2) + \mathbf{S}_3 (11665/36 + 15/4 Z_{5,1} + 109/8 \zeta_2 - 948 \zeta_3 + 35 D_{-1} + 23693/72 D_0 \\
& - 81/4 D_0 \zeta_2 - 35051/72 D_1 + 81/4 D_1 \zeta_2 - 245 D_2 - 24 D_{-1}^2 - 1261/6 D_0^2 \\
& + 347/2 D_0^3 - 563/12 D_1^2 + 93 D_1^3) + \mathbf{S}_{-2,1} (58 + 168 \zeta_3 + 132 D_{-1} - 2558/9 D_0 \\
& + 2558/9 D_1 - 132 D_2 - 120 D_{-1}^2 + 320/3 D_0^2 + 80 D_0^3 - 296/3 D_1^2 + 64 D_1^3 \\
& - 24 D_2^2) + \mathbf{S}_{1,-2} (4390/27 - 20 \zeta_2 + 544 \zeta_3 + 108 D_{-1} - 170/3 D_0 + 6 D_0 \zeta_2 \\
& + 170/3 D_1 - 6 D_1 \zeta_2 - 108 D_2 - 120 D_{-1}^2 - 152/3 D_0^2 - 92 D_0^3 - 416/3 D_1^2 \\
& + 76 D_1^3 - 24 D_2^2) + \mathbf{S}_{1,2} (61667/108 - 3/2 Z_{5,1} - 55 \zeta_2 + 410 \zeta_3 - 6 D_{-1} \\
& - 4379/8 D_0 + 18 D_0 \zeta_2 + 4359/8 D_1 - 18 D_1 \zeta_2 - 81 D_2 + 1567/4 D_0^2 - 264 D_0^3 \\
& - 2729/12 D_1^2 + 42 D_1^3 - 42 D_2^2) + \mathbf{S}_{2,1} (6659/108 - 3 Z_{5,1} - 193/4 \zeta_2 + 50 \zeta_3 \\
& + 6 D_{-1} - 7093/24 D_0 + 33/2 D_0 \zeta_2 + 18391/24 D_1 - 33/2 D_1 \zeta_2 + 225 D_2
\end{aligned}$$

$$\begin{aligned}
 & + 2359/12 D_0^2 - 191 D_0^3 - 913/12 D_1^2 + 16 D_1^3 + 42 D_2^2) + \mathbf{S}_{1,1,1} (-10459/24 \\
 & + 3/2 Z_{5,1} + 48 \zeta_2 - 72 \zeta_3 + 10243/24 D_0 - 15 D_0 \zeta_2 - 16003/24 D_1 + 15 D_1 \zeta_2 \\
 & - 3751/12 D_0^2 + 244 D_0^3 + 2497/12 D_1^2 - 70 D_1^3) + \mathbf{S}_{-2} (989/6 - 6 \zeta_2 + 698 \zeta_3 \\
 & + 126 \zeta_4 + 1657/6 D_{-1} - 6 D_{-1} \zeta_2 - 11054/27 D_0 + 19 D_0 \zeta_2 - 104 D_0 \zeta_3 \\
 & + 11054/27 D_1 - 19 D_1 \zeta_2 + 104 D_1 \zeta_3 - 1657/6 D_2 + 6 D_2 \zeta_2 - 266 D_{-1}^2 \\
 & + 240 D_{-1}^3 + 470/9 D_0^2 - 3 D_0^2 \zeta_2 - 28/3 D_0^3 + 2 D_0^4 - 2738/9 D_1^2 + 9 D_1^2 \zeta_2 \\
 & + 532/3 D_1^3 - 134 D_1^4 - 70 D_2^2) + \mathbf{S}_2 (-328019/576 - 9/4 Z_{5,2} - 57/8 Z_{5,1} \\
 & + 1261/48 \zeta_2 + 47/2 \zeta_3 + 63 \zeta_4 - 60 D_{-1} - 377441/864 D_0 + 3/4 D_0 Z_{5,1} + 32 D_0 \zeta_2 \\
 & + 89 D_0 \zeta_3 + 545147/864 D_1 - 3/4 D_1 Z_{5,1} - 41 D_1 \zeta_2 - 89 D_1 \zeta_3 + 228 D_2 \\
 & + 4087/18 D_0^2 - 69/4 D_0^2 \zeta_2 - 2561/24 D_0^3 + 575/4 D_0^4 + 1973/72 D_1^2 \\
 & + 15/4 D_1^2 \zeta_2 - 75/8 D_1^3 + 349/4 D_1^4 + 42 D_2^2) + \mathbf{S}_{1,1} (-17171/192 + 9/4 Z_{5,2} \\
 & + 29/8 Z_{5,1} + 691/48 \zeta_2 - 96 \zeta_3 - 27 \zeta_4 + 60 D_{-1} + 49361/96 D_0 - 3/4 D_0 Z_{5,1} \\
 & - 30 D_0 \zeta_2 - 162 D_0 \zeta_3 - 81823/96 D_1 + 3/4 D_1 Z_{5,1} + 39 D_1 \zeta_2 + 162 D_1 \zeta_3 \\
 & + 105 D_2 - 1949/6 D_0^2 + 69/4 D_0^2 \zeta_2 + 5225/24 D_0^3 - 811/4 D_0^4 + 6091/24 D_1^2 \\
 & - 27/4 D_1^2 \zeta_2 - 4271/24 D_1^3 + 95/4 D_1^4) + \mathbf{S}_1 (33485/1152 + 27/16 Z_{5,2} \\
 & + 247/48 Z_{5,1} - 995/32 \zeta_2 + 1891/24 \zeta_3 + 9 \zeta_3 \zeta_2 - 219/4 \zeta_4 - 198 \zeta_5 + 252 D_{-1} \\
 & - 156 D_{-1} \zeta_3 + 53939/96 D_0 - 9/8 D_0 Z_{5,2} - 19/8 D_0 Z_{5,1} - 797/48 D_0 \zeta_2 \\
 & - 1243/2 D_0 \zeta_3 - 63/2 D_0 \zeta_4 - 191071/192 D_1 + 9/8 D_1 Z_{5,2} + 7/2 D_1 Z_{5,1} \\
 & + 359/12 D_1 \zeta_2 + 577/2 D_1 \zeta_3 + 63/2 D_1 \zeta_4 + 168 D_2 - 720 D_2 \zeta_3 - 120 D_{-1}^2 \\
 & - 446705/864 D_0^2 + 3/2 D_0^2 Z_{5,1} + 91/4 D_0^2 \zeta_2 + 613/2 D_0^2 \zeta_3 + 1645/36 D_0^3 \\
 & - 15 D_0^3 \zeta_2 + 137/12 D_0^4 + 97 D_0^5 + 22889/216 D_1^2 - 3/4 D_1^2 Z_{5,1} \\
 & - 27/2 D_1^2 \zeta_2 - 139/2 D_1^2 \zeta_3 + 1333/72 D_1^3 + 9/4 D_1^3 \zeta_2 + 219/8 D_1^4 \\
 & + 379/4 D_1^5 + 18 D_2^2) + 221777/1152 + 9/16 Z_{5,3b} - 45/16 Z_{5,2} - 449/64 Z_{5,1} \\
 & + 1989/128 \zeta_2 + 19027/8 \zeta_3 - 81/4 \zeta_3 \zeta_2 + 1287/4 \zeta_4 + 657/2 \zeta_5 + 4759/6 D_{-1} \\
 & - 6 D_{-1} \zeta_2 - 423 D_{-1} \zeta_3 - 54 D_{-1} \zeta_4 + 475681/1152 D_0 + 9/16 D_0 Z_{5,2} \\
 & - 131/48 D_0 Z_{5,1} + 3209/192 D_0 \zeta_2 - 11105/24 D_0 \zeta_3 + 9/2 D_0 \zeta_3 \zeta_2 \\
 & - 231/2 D_0 \zeta_4 - 21 D_0 \zeta_5 - 103141/288 D_1 + 9/8 D_1 Z_{5,2} + 151/24 D_1 Z_{5,1} \\
 & - 5801/192 D_1 \zeta_2 - 4993/6 D_1 \zeta_3 - 9/2 D_1 \zeta_3 \zeta_2 + 165/4 D_1 \zeta_4 + 21 D_1 \zeta_5 \\
 & - 4759/6 D_2 + 6 D_2 \zeta_2 - 213 D_2 \zeta_3 - 135 D_2 \zeta_4 - 530 D_{-1}^2 + 360 D_{-1}^2 \zeta_3 \\
 & + 240 D_{-1}^3 - 664531/864 D_0^2 + 9/8 D_0^2 Z_{5,2} + 15/4 D_0^2 Z_{5,1} - 575/24 D_0^2 \zeta_2 \\
 & + 1491/2 D_0^2 \zeta_3 + 72 D_0^2 \zeta_4 - 49429/288 D_0^3 - 15/8 D_0^3 Z_{5,1} + 409/16 D_0^3 \zeta_2
 \end{aligned}$$

---


$$\begin{aligned}
& -477/2 D_0^3 \zeta_3 + 41495/72 D_0^4 - 51/8 D_0^4 \zeta_2 - 434 D_0^5 + 215/2 D_0^6 \\
& - 507037/432 D_1^2 - 17/8 D_1^2 Z_{5,1} + 1229/48 D_1^2 \zeta_2 + 355/2 D_1^2 \zeta_3 \\
& + 81/2 D_1^2 \zeta_4 + 227123/216 D_1^3 + 3/8 D_1^3 Z_{5,1} - 273/16 D_1^3 \zeta_2 - 413 D_1^3 \zeta_3 \\
& - 29843/36 D_1^4 + 195/8 D_1^4 \zeta_2 + 5261/12 D_1^5 - 827/2 D_1^6 - 118 D_2^2 \\
& - 180 D_2^2 \zeta_3 \\
a_{3,\text{ns}}^{(3)\text{F}}(N) = & + 121 \mathbf{S}_5 - 36 \mathbf{S}_{1,4} - 66 \mathbf{S}_{2,3} - 90 \mathbf{S}_{3,2} - 108 \mathbf{S}_{4,1} + 36 \mathbf{S}_{1,1,3} + 36 \mathbf{S}_{1,2,2} + 36 \mathbf{S}_{1,3,1} \\
& + 66 \mathbf{S}_{2,1,2} + 66 \mathbf{S}_{2,2,1} + 90 \mathbf{S}_{3,1,1} - 36 \mathbf{S}_{1,1,1,2} - 36 \mathbf{S}_{1,1,2,1} - 36 \mathbf{S}_{1,2,1,1} - 66 \mathbf{S}_{2,1,1,1} \\
& + 36 \mathbf{S}_{1,1,1,1,1} + \mathbf{S}_4 (-830/3 + 18 D_0 - 18 D_1) + \mathbf{S}_{1,3} (77 - 18 D_0 + 18 D_1) \\
& + \mathbf{S}_{2,2} (162 - 18 D_0 + 18 D_1) + \mathbf{S}_{3,1} (228 - 18 D_0 + 18 D_1) + \mathbf{S}_{1,1,2} (-77 + 18 D_0 \\
& - 18 D_1) + \mathbf{S}_{1,2,1} (-77 + 18 D_0 - 18 D_1) + \mathbf{S}_{2,1,1} (-162 + 18 D_0 - 18 D_1) \\
& + \mathbf{S}_{1,1,1,1} (77 - 18 D_0 + 18 D_1) + \mathbf{S}_3 (4643/12 - 9 \zeta_2 - 46 D_0 + 73 D_1 + 33 D_0^2 \\
& - 15 D_1^2) + \mathbf{S}_{1,2} (-1325/12 + 3 \zeta_2 + 46 D_0 - 73 D_1 - 33 D_0^2 + 15 D_1^2) \\
& + \mathbf{S}_{2,1} (-1063/4 + 6 \zeta_2 + 46 D_0 - 73 D_1 - 33 D_0^2 + 15 D_1^2) + \mathbf{S}_{1,1,1} (1325/12 - 3 \zeta_2 \\
& - 46 D_0 + 73 D_1 + 33 D_0^2 - 15 D_1^2) + \mathbf{S}_2 (-20219/54 + 67/4 \zeta_2 + 26 \zeta_3 \\
& + 853/12 D_0 - 3/2 D_0 \zeta_2 - 899/6 D_1 + 3/2 D_1 \zeta_2 - 90 D_0^2 + 45 D_0^3 + 59 D_1^2 \\
& - 12 D_1^3) + \mathbf{S}_{1,1} (4963/36 - 29/4 \zeta_2 - 12 \zeta_3 - 853/12 D_0 + 3/2 D_0 \zeta_2 + 899/6 D_1 \\
& - 3/2 D_1 \zeta_2 + 90 D_0^2 - 45 D_0^3 - 59 D_1^2 + 12 D_1^3) + \mathbf{S}_1 (205661/1296 \\
& - 235/24 \zeta_2 - 97/3 \zeta_3 + 3 \zeta_4 - 3077/36 D_0 + 19/4 D_0 \zeta_2 + 6 D_0 \zeta_3 + 4135/18 D_1 \\
& - 7 D_1 \zeta_2 - 6 D_1 \zeta_3 + 571/4 D_0^2 - 3 D_0^2 \zeta_2 - 123 D_0^3 + 54 D_0^4 - 356/3 D_1^2 \\
& + 3/2 D_1^2 \zeta_2 + 45 D_1^3 - 9 D_1^4) - 165343/576 + 27/16 Z_{5,3c} + 203/16 \zeta_2 + 123/4 \zeta_3 \\
& - 9/4 \zeta_4 - 122035/1296 D_0 + 203/24 D_0 \zeta_2 + 68/3 D_0 \zeta_3 - 3/2 D_0 \zeta_4 \\
& + 25108/81 D_1 - 187/12 D_1 \zeta_2 - 95/3 D_1 \zeta_3 + 3/2 D_1 \zeta_4 + 20129/108 D_0^2 \\
& - 41/4 D_0^2 \zeta_2 - 13 D_0^2 \zeta_3 - 785/4 D_0^3 + 9/2 D_0^3 \zeta_2 + 881/6 D_0^4 - 121/2 D_0^5 \\
& - 9913/54 D_1^2 + 7 D_1^2 \zeta_2 + 7 D_1^2 \zeta_3 + 179/2 D_1^3 - 3/2 D_1^3 \zeta_2 - 197/6 D_1^4 \\
& + 13/2 D_1^5
\end{aligned}
\tag{J.0.7}$$



# Summary

I could imagine that one gets overwhelmed by the lengthy and complicated formulae written down in this manuscript. You might be inclined to close this thesis (after reading the acknowledgements of course), put it on a shelf and let it collect dust, never to be opened again. And I agree, if I would have had no knowledge on the subjects discussed in the thesis, I would have done exactly the same. Therefore I have written the following sections specially for those curious lay(women), who are interested in the fundamentals of Nature, in an accessible manner.

## From ancient thinkers to scientists at Nikhef

Ever since ancient times people have been thinking about the building blocks of the material world. This happened both in the East<sup>1</sup> and in the West<sup>2</sup>. Although these schools of thought are now to be considered of the philosophical (metaphysical) nature, the pursuit of knowledge about the fundamental building blocks and their interactions is one of the primary topics in contemporary science. In particular, the field of particle physics is dedicated to the understanding of all the elementary processes at subatomic length scales.

To get an impression of the modern definition of an atom, let us consider a generic daily object, such as a plant, and zoom in on its surface using a fictitious microscope. At first we would identify the individual cells composed of the cell nucleus and organelles, enclosed by a membrane. By zooming further into the cell nucleus, we would uncover the chromosomes which consist out of DNA molecules. These molecules, in turn, are collections of atoms, usually stuck together by pairs of electrons (covalent bonds). Thus we arrived at the atoms. However, this is not the end of the story: the variety of atoms are composite objects containing different amounts of (electric pos-

---

<sup>1</sup>In the 8<sup>th</sup> century BCE the Indian sage Aruni hypothesised about infinitesimally small particles which mass together to form the objects that one experiences in life.

<sup>2</sup>The Greek philosophers Leucippus and Democritus argued in the 5<sup>th</sup> century BCE that all matter is made out of invisible small particles, atoms.



itively charged) protons and (electrically neutral) neutrons which together form the atomic nucleus, and electrons. The electrons are point-like particles, meaning that their spatial size is zero. Nonetheless they carry a mass and an electric charge. As such, the electrons are our first class of elementary particles. Protons and neutrons are compound objects consisting out of massive point-like quarks being glued together by the massless gluons. The latter elementary particles, alternatively known as partons, and the interactions between them, described by the theory of Quantum Chromo Dynamics (QCD), have been the subject of research in this thesis.

If our fictitious microscope were to be real, it would have worked well up til the length scale of a plant cell and perhaps the chromosomes. However, to obtain information on elementary particles one would need an experiment such as a modern particle collider. A prime example is the Large Hadron Collider (LHC) at Cern in Geneva in which hadrons (to be explained below) are collided into each other at extremely high energies, such that they break up and form new (composite) particles. From the information of these resulting particles one should be able to deduce the properties of the constituents.

In order to analyse data of the resulting particles at the physics experiments, one has to be able to match the results of the experiments onto the theoretical predictions for each of the processes, using the Standard Model (SM) of Particle Physics. The SM describes all the elementary particles and their interactions, including not only the partons, but also the leptons and their neutrinos, the gauge bosons and the Higgs particle. As such, the SM can be dissected into three sectors: one sector describing the electro-weak interactions, one sector describing the Higgs mechanism and a sector describing the strong interactions (QCD).

In QCD one can ascribe the three colours red, blue and green to the quarks and gluons<sup>3</sup>. On top of that there exist six different ‘flavours’ of quarks: up, down, charm, strange, top and bottom. Composite objects, mesons and baryons, are formed by combining two or three (anti)quarks such that one obtains colourless states<sup>4</sup>, collectively called hadrons. The nature of QCD makes it hard to perform calculations for the predictions of processes which involve partons. At low energy scales the partons are strongly coupled together, rendering it impossible to perform perturbative calculations. Only at high energy scales one is able to perform perturbative calculations for free partons. However, this does not mean that one observes free partons in nature. Partons which are freed after the collision of the initial hadron(s) combine together in a process called hadronization, such

---

<sup>3</sup>Colouring the partons is merely a tool to support the algebraic relations.

<sup>4</sup>For the baryons that colourless state is the combination of red+green+blue.

that one only observes the resulting colourless final state hadrons. The entire calculation, which starts with the initial state hadrons and ends with the hadronized final state composite particles, can be dissected into multiple subparts. The focus of this thesis is the perturbative partonic sector.

As explained in the introduction, the SM is incomplete. Although it is a self-consistent theory, it fails to incorporate gravity and does not explain observed physical phenomena such as neutrino oscillations. Therefore, to search for hints of new physics and to constrain the parameters of the SM, the existing experiments have been upgraded and new experiments are planned to be built. As a result, the experimental uncertainties (are expected to) decrease. In turn this requires more precise theoretical predictions. However, these theoretical predictions become computationally more complex at each succeeding order of precision. Even by using large clusters of supercomputers some of these calculations can last for years to evaluate. Hence there is a need for new efficient methods to obtain predictions at the required accuracy. In this thesis we invented and applied two novel algorithms which allowed us to obtain new (more precise) results for jet functions and deep inelastic scattering.

## GOJet

The first study in this thesis deals with the subtraction of soft and collinear singularities due to real radiation of jet functions in Soft-Collinear Effective Theory (SCET). SCET is an effective theory (read approximate derivative) of QCD in the case that the final state particles become collinear to each other or if a massless particle is radiated from the bunch of final state particles with a low (soft) energy<sup>5</sup>. In particular, the jet functions characterise the collinear subpart of the previously mentioned entire calculations. At the one-loop order, meaning considering first-order corrections in the expansion parameter  $\alpha_s$  to the predictions, the inclusion of an extra collinear or emitted soft particle introduces so-called (infrared) singularities to the jet functions: these are factors of infinity in the expressions of the jet functions. At first this might seem troublesome, since the predictive power of the calculations appears to be lost if they result in numerical values of infinity. However, these singularities in the jet functions cancel against singularities in other subparts of the larger overall calculations. The challenge is therefore to identify and categorise individual singular mathematical terms in the jet functions, such

---

<sup>5</sup>In spirit similar to the idea that one can approximate the shape of an apple by a ball in the case that the apple is seen from afar.

that the jet functions can be divided into genuine non-singular terms and indefinite singular terms. This procedure is called regularization.

There are many ways to regularize jet functions. However, none of them is perfect. In this thesis we have modified, applied and automated the promising, recently invented regularization procedure called Geometric Subtraction to the case of generic one-loop jet functions. Geometric, because it considers a certain set of variables of the jet functions as geometrical objects, such as triangles and boxes, and exploits geometric relations amongst them. The automated algorithm has been implemented in the MATHEMATICA package called GOJET. The algorithm has been verified on numerous known one-loop jet functions. In addition we also calculated, for the first time ever, the highly non-trivial jet function of angularities with recoil.

## Deep Inelastic Scattering

In the second study we calculated the  $n_f^2$  corrections to the four-loop Deep Inelastic Scattering (DIS) coefficient functions. First of all, DIS is a process in which a lepton and hadron collide on each other. Through the exchange of a vector boson (like a photon) the composite hadron gets altered to evolve into a new final state with a different momentum. Again, to calculate predictions for this process, the overall entire process can be divided into multiple subparts. One of those subparts, the coefficient function, deals with the interaction of a constituent quark of the initial hadron and the vector boson. Using QCD, one can calculate higher order corrections (in the expansion parameter  $\alpha_s$ ) to the coefficient functions. However, the number of processes and the complexity of the equations at this order of precision are so involved, that we had to restrict ourselves to a specific part of the calculation, namely the equations categorised by the parameter  $n_f$  at the quadratic order.

To perform the calculations, we applied, for the first time ever, three methods in the following order: we used the optical theorem to cast the initial equations, which were expressed in terms including complicated phase space integrals, into the simpler amplitude-type expressions (without the phase space integrals). Sequentially we reduced 10 000 of complicated loop-integrals into 100 of much simpler master loop-integrals<sup>6</sup>. And lastly we used a sophisticated recursive algorithm to calculate the so-called Mellin moments of the coefficient functions. By calculating 1500 Mellin moments in an efficient manner, we were able to reconstruct complete algebraic expressions for the coefficient functions (the pages-long expressions). Not only have we

---

<sup>6</sup>This was only for the confined four-loop set of integrals. For the full three-loop calculation we reduced millions of integrals into thousands of master integrals.

calculated these specific coefficient functions for the first time ever, we also were the first ones to verify four-loop splitting functions at order  $n_f^2$ . Our calculation served as a proof of concept, as we expect more coefficient- and splitting functions to be calculated using the same algorithm (albeit with more optimised reduction routines).



# Samenvatting

Ik kan me voorstellen dat een lezer overweldigd raakt door de lange en gecompliceerde formulae uitgewerkt in dit manuscript. Misschien bent u zelfs geneigd om dit proefschrift (na het lezen van de dankbetuiging natuurlijk) dicht te slaan, op een plank van uw boekenkast neer te leggen, waar het stof zal verzamelen, opdat het nooit meer geopend wordt. En om eerlijk te zijn, ben ik het helemaal met u eens! Ik zou exact hetzelfde hebben gedaan als ik geen voorkennis had over de onderwerpen die worden besproken in dit proefschrift. Derhalve heb ik de volgende paragrafen op een toegankelijke manier geschreven speciaal voor de nieuwsgierige leek, die geïnteresseerd is in de fundamenteën van de Natuur.

## Van denkers uit de klassieke oudheid tot wetenschappers op Nikhef

Sinds de oudheid denkt men al na over de bouwstenen van de fysieke wereld om ons heen. Dit gebeurde zowel in het Oosten<sup>7</sup> als in het Westen<sup>8</sup>. Hoewel deze stromingen nu worden beschouwd als filosofisch (metafysisch), is de zoektocht naar de kennis over de fundamentele bouwstenen en hun onderlinge interacties een van de primaire onderwerpen in de hedendaagse wetenschap. In het bijzonder, het domein van de deeltjes fysica is toegewijd aan het doorgronden van alle elementaire processen op subatomaire lengteschalen.

Laten wij, om een impressie te krijgen van de hedendaagse definitie van een atoom, een generiek alledaags object beschouwen, zoals een plant, en inzoomen op het oppervlak van de plant met een fictieve microscoop. In eerste instantie zouden we de individuele cellen identificeren die zijn samengesteld

---

<sup>7</sup>In de achtste eeuw v.o.j. stelde de Indiase geleerde Aruni een hypothese op over infinitesimale kleine deeltjes die samenklonteren om de objecten te vormen die men ervaart in het leven.

<sup>8</sup>De Griekse filosofen Leucippus en Democritus beredeneerden in de vijfde eeuw v.o.j. dat alle materie is opgebouwd uit onzichtbare kleine deeltjes, genaamd atomen.

uit de celkern en de organellen, omsloten door een membraan. Door verder op de celkern in te zoomen, zouden wij de chromosomen onthullen die bestaan uit DNA moleculen. Deze moleculen zijn, op hun beurt, verzamelingen van atomen die meestal aan elkaar kleven door paren van elektronen (covalente bindingen). Zodoende zijn we aangekomen bij de atomen. Echter, dit is nog niet het einde van het verhaal: de verscheidene atomen zijn objecten samengesteld uit verschillende hoeveelheden van (elektrisch positief geladen) protonen en (elektrisch neutrale) neutronen die samen de atoomkern vormen, en elektronen. De elektronen zijn puntdeeltjes, wat betekent dat ze een ruimtelijke grootte hebben die nihil is. Desalniettemin hebben zij een massa en een elektrische lading. Zodanig zijn de elektronen de eerste groep elementaire deeltjes die we tegenkomen. Protonen en neutronen zijn objecten samengesteld uit massieve puntdeeltjes, genaamd quarks, vastgelijmd door de massaloze gluonen. De laatstgenoemde groep elementaire deeltjes, ook wel bekend als partonen, en de interacties tussen hen, beschreven door de theorie van de Quantum Chromo Dynamica (QCD), zijn het onderzoeksonderwerp in dit proefschrift.

Als onze fictieve microscoop echt was, zou het slechts kunnen functioneren tot aan de lengteschaal van een plantencel en misschien de chromosomen. Echter, om informatie te kunnen vergaren over elementaire deeltjes, heeft men een experiment nodig zoals een hedendaagse deeltjesversneller. Een primair voorbeeld is de Large Hadron Collider (LHC) in Cern te Genève. Hierin worden de hadronen (verderop beschreven) tegen elkaar aan gebotst met een extreem hoge energie, zodat de deeltjes opbreken en nieuwe (samengestelde) deeltjes vormen. Vanuit de informatie over deze resulterende deeltjes is het mogelijk om de eigenschappen van de bestanddelen af te leiden

Om de data van de uitkomsten van de experimenten te analyseren, is het noodzakelijk dat de resultaten van de experimenten kunnen worden vergeleken met de theoretische voorspellingen voor elk afzonderlijk fysisch proces, gebruik makend van het Standaard Model (SM) van de deeltjesfysica. In het SM zijn alle elementaire deeltjes en hun onderlinge interacties beschreven, bijvoorbeeld voor de partonen, maar ook de leptonen en de bijbehorende neutrino's, de ijkbosonen en het Higgs deeltje. Dusdanig kan het SM worden ingedeeld in drie sectoren: een sector over de elektrozwakke wisselwerking, een sector over het Higgs mechanisme en een sector over de sterke kernkracht (QCD).

In QCD kan men de drie kleuren rood, blauw en groen toekennen aan de quarks en gluonen<sup>9</sup>. Daarenboven bestaan er zes verschillende 'smaken' aan

---

<sup>9</sup>De verschillende kleuren zijn fictief en slechts een attribuut ter ondersteuning van de wiskundige relaties.

quarks: up, down, charm, strange, top en bottom. Samengestelde objecten, de mesonen en baryonen, worden gevormd door twee of drie (anti)quarks te combineren, zodat men kleurloze toestanden verkrijgt<sup>10</sup>, die collectief de hadronen worden genoemd. QCD is complex van aard, waardoor het ingewikkeld is om berekeningen uit te voeren voor de voorspellingen van fysische processen die betrekking hebben tot de partonen. Op lage energieschalen zijn de partonen stevig samengebundeld, waardoor het onmogelijk is om storingsrekening toe te passen. Alleen op hoge energieschalen is het mogelijk om storingsrekening toe te passen voor vrijbewegende partonen. Dit betekent echter niet dat vrijbewegende partonen ook worden waargenomen in de natuur. De partonen die zijn vrijgekomen door de botsing van de initiële hadron(en), combineren samen in een proces dat hadronisatie heet, zodanig dat alleen de resulterende kleurloze hadronen worden waargenomen. De gehele berekening, die start met de inkomende hadronen en eindigt met de resulterende gehadroniseerde samengestelde deeltjes, kan worden opgedeeld in verschillende subonderdelen. De focus van dit proefschrift is de perturbatieve partonische sector.

Zoals uitgelegd in de introductie, is het SM incompleet. Hoewel de theorie zelfconsistent is, laat de theorie het na om zwaartekracht te beschrijven en slaagt de theorie er niet in om waargenomen fysische fenomenen zoals neutrino oscillaties te verklaren. En dus, om te zoeken naar hints voor nieuwe fysica en om de waarden van de parameters van het SM verder te beperken, zijn de bestaande experimenten verbeterd en zijn er plannen gemaakt om nieuwe experimenten op te zetten. Als resultaat wordt er verwacht dat de experimentele onzekerheden zullen krimpen. Als gevolg hiervan, zijn er ook nauwkeurigere theoretische voorspellingen vereist. Echter, deze theoretische voorspellingen worden wiskundig complexer met elke opvolgende orde van nauwkeurigheid. Zelfs als men grote clusters van supercomputers gebruikt om de algebraïsche relaties op te lossen, kan het jaren duren voordat sommige van deze berekeningen voltooiden. Dus is er een behoefte aan nieuwe efficiënte methodes om theoretische voorspellingen te verkrijgen met de vereiste nauwkeurigheid. In dit proefschrift hebben we twee nieuwe algoritmen bedacht en toegepast waarmee we nieuwe (preciezere) resultaten hebben kunnen verkrijgen voor jetfuncties en diepe inelastische verstrooiing.

## GOJet

In het eerste onderzoek dat wordt beschreven in dit proefschrift, gaan we in op een methode om de zogenaamde softe en collineaire singulariteiten te

---

<sup>10</sup>De kleurloze toestand voor de baryonen is de combinatie rood+groen+blauw.



verwijderen in berekeningen die ontstaan door de reële straling componenten van de jet functies in de Soft-Collineaire Effectieve Theorie (SCET). SCET is een effectieve theorie (lees afgeleide benadering) van QCD voor het geval dat uitgaande deeltjes collineair aan elkaar worden of als een massaloos deeltje wordt uitgestraald van een bundel aan uitgaande deeltjes met een lage (softe) energie<sup>11</sup>. In het bijzonder, de jet functies karakteriseren het collineaire subgedeelte van de voorgaand genoemde gehele berekening voor een theoretische voorspelling. Op een-lus orde, wat betekent dat we de eerste-orde correcties beschouwen in de uitbreidingsparameter  $\alpha_s$  van de wiskundige voorspellingen, zorgt het meetellen van een extra collineair of uitgestraald soft deeltje voor zogenoemde (infrarood) singulariteiten van de jet functies: dit zijn termen met een waarde van oneindig in de formules van de jet functies. Op het eerste gezicht lijkt dit problematisch, aangezien het voorspellend vermogen van de berekeningen verloren schijnt te gaan als de berekeningen resulteren in numerieke waarden die oneindig groot zijn. Echter, deze singulariteiten in de jet functies blijken weg te vallen tegen singulariteiten in andere subgedeelten van de grotere gehele berekening. De uitdaging ligt dus in het identificeren en categoriseren van individuele singulaire wiskundige termen in de jet functies, zodat de jet functies kunnen worden opgedeeld tussen werkelijke niet-singulaire termen en oneindige singulaire termen. Deze procedure heet regularisatie.

Er bestaan meerdere manieren om jet functies te regulariseren, maar geen van hen is perfect. In dit proefschrift hebben we een veelbelovende, pas ontworpen, regularisatie procedure genaamd Geometrische Subtractie aangepast, toegepast en geautomatiseerd voor generieke een-lus jet functies. Geometrisch, omdat een bepaalde set van variabelen van de jet functies wordt beschouwd als geometrische objecten, zoals driehoeken en dozen, opdat geometrische relaties tussen de variabelen worden uitgebuit. Het geautomatiseerde algoritme, genaamd GOJET, is geïmplementeerd in een MATHEMATICA extensie. We hebben het algoritme geverifieerd door verschillende bekende een-lus jet functies na te rekenen. Daarbovenop hebben we, voor het eerst ooit, de uiterst niet-triviale jet functie van angulariteiten met terugslag berekend.

## Diepe Inelastische Verstrooiing

In het tweede onderzoek hebben we de  $n_f^2$  correcties van de vier-lus Diepe Inelastische Verstrooiing (in het engels Deep Inelastic Scattering, afgekort als

<sup>11</sup>In essentie vergelijkbaar met het idee dat de vorm van een appel van veraf gezien kan worden benaderd door een bal.

DIS) coëfficiënten functies berekend. Ten eerste, DIS is een proces waarin een lepton en een hadron tegen elkaar aan botsen. Door het uitwisselen van een vector boson (zoals een foton) wordt de samenstelling van de ingaande hadron gewijzigd naar een nieuwe hadron met een aangepaste impuls. Zoals gebruikelijk kan de gehele berekening voor de theoretische voorspelling van dit proces worden opgesplitst in meerdere delen. Een van deze delen, de coëfficiënten functie, beschrijft de interactie tussen een parton dat onderdeel uitmaakt van de inkomende hadron en de vector boson. Door gebruik te maken van QCD is het mogelijk om hogere orde correcties (in de uitbreidingsparameter  $\alpha_s$ ) van de coëfficiënten functies te berekenen. Het aantal processen neemt echter rap toe met elke opeenvolgende orde in de uitbreidingsparameter en daarbovenop wordt de complexiteit van de vergelijkingen ingewikkelder met elke orde. Om die reden hebben wij ons op de vier-lus orde (vier ordes in de uitbreidingsparameter) moeten beperken tot een specifiek gedeelte van de berekening, namelijk de vergelijkingen die gecategoriseerd worden door de parameter  $n_f$  op de kwadratische orde.

Om de berekeningen uit te voeren, hebben we, voor het eerst ooit, drie methoden toegepast in deze volgorde: we hebben het optische theorema toegepast om de aanvankelijke vergelijkingen, die in eerste instantie waren uitgedrukt in termen van ingewikkelde fase-ruimte integralen, om te schrijven naar simpelere amplitude-achtige formules (zonder de fase-ruimte integralen). Vervolgens hebben we de 10 000 gecompliceerde lus-integralen gereduceerd naar 100 veel simpelere master-integralen<sup>12</sup>. Tenslotte hebben we een verfijnd recursief algoritme gebruikt om de zogenoemde Mellin momenten van de coëfficiënten functies te berekenen. Door 1500 Mellin momenten op een efficiënte manier te berekenen, zijn we erin geslaagd om complete algebraïsche formules voor de coëfficiënten functies te reconstrueren (de pagina's-lange formules in dit proefschrift). Niet alleen zijn wij de eersten die erin zijn geslaagd om deze specifieke coëfficiënten functies te verkrijgen, ook zijn we de eersten die de vier-lus splitsingsfuncties op orde  $n_f^2$  hebben geverifieerd. Onze berekeningen dienden als voorbeeld voor ons nieuwe algoritme. We verwachten namelijk dat er meer coëfficiënten- en splitsingsfuncties zullen worden berekend met dit algoritme (waarschijnlijk met geoptimaliseerde reductieroutines).

---

<sup>12</sup>Dit was alleen voor de beperkte set aan vier-lus integralen. Voor de volledige drie-lus berekening hebben we miljoenen integralen gereduceerd naar duizenden master-integralen.



# Acknowledgements

In the past four (+) years I went *down the loop hole*. I started with one-loop calculations for Jet Functions and then slowly built my way up to massive four-loop calculations in Deep Inelastic Scattering. I could not have done this without the support of a set of people around me, whom I would like to thank in the following.

First of all I would like to thank my supervisor Franz. I have the honour of being your first PhD student. You took me under your wing and taught me all the ins and outs of perturbative QCD, including the necessary programming skills. You always made sure that I understood the subject matter at hand and you were very patient if I required further explanations on the same topic. Even after moving to Edinburgh, having lovely twins and in midst of the pandemic you always managed to catch up with me on a weekly basis. I surely enjoyed all our conversations, both at Nikhef and during the hours-long Zoom sessions. We had plenty of fun whilst also conducting cutting-edge research, which resulted in fascinating results. I wish you the best of luck in Edinburgh, take care of the aliens<sup>13</sup>, and be nice to Peter!

Then I would like to thank my promotor Eric for guiding me throughout my academic career. My first academic baby steps were made when you taught me the intricate physics of the hydrogen atom in the bachelor. Subsequently you imparted to me the intriguing topics of gauge theories and renormalization during my academic puberty in the master. To top it off you oversaw the progression and completion of my PhD which allowed me to become an academic adult. Moreover, thank you for the occasional advice, not only on topics in physics, but also on various subjects, relevant to a 27-year old boy, in life.

I would like to thank the PhD defence committee for carefully reading my thesis.

The contents of chapter 2 and chapter 3 were the results of a team effort. The contributions of my collaborators Wouter Waalewijn and Andreas

---

<sup>13</sup>For the uninitiated: Don't worry, I do not mean extraterrestrial beings, but the mathematical objects named accordingly.

Vogt were indispensable to the completion of the projects. I would like to thank both for sharing their expertise on Jet Functions and Deep Inelastic Scattering respectively.

My liquid cheese loving, chicken grease finger licking, academic uncle Andrea Pelloni, it would have been impossible to finish this thesis without you. After Franz left, I would have had nobody to talk to about precision calculations in QCD at Nikhef, if it weren't for you. You acted as mentor and I learned a lot from you. We had a blast while working together on the DIS projects. Therefore I do not only consider you as a mentor, but arguably also as a good friend. You willingly carefully read major parts of my thesis and commented on it. This allowed me to significantly improve the quality of the manuscript. Thank you for that. I kept some nice memories from our trip to Edinburgh to visit Franz, of which our chicken wing devouring in the Black Rooster is the most memorable.

Next I would like to thank Solange. I enjoyed working together with you on the first project. We were both novices and started out clueless, but we became experts in the subtraction of Jet Functions along the way. It was helpful for me to have a such a good friend as you with whom I could share my scientific doubts. I also had fun going to the numerous workshops, graduate schools and RADCOR conference with you. You're a people person, attendees of the events liked being around you and I surely benefited by tagging along.

I would like to thank Rhorry Gauld for the introduction to VEGAS in C++. I applied it in the GOJET program. Also thanks for sharing the burden of teaching Field Theory in Particle Physics. Teaching a class during the pandemic over Zoom was suboptimal, nevertheless we prevailed. I am happy that you ended up at MPI.

Thank you Jos Vermaseren for your insightful explanations on FORM. Even more, without your creation of FORM, nobody that is in the business of performing precision calculations in particle physics would have been able to carry out his/her computation in the past 30 years. For that we are ever grateful to you.

My dear colleagues Tommaso 'Don Salvatore' Giani and Rudi 'Leeroy Jenkins' Rahn, thank you as well for proofreading parts of my thesis. Your feedback was much appreciated. Tommaso, after all these years I still have to find out if your pasta cooking skills are as good as your explanations of PDFs, so we need to do that very soon. Rudi, I'm still waiting for you to join my guild in WoW.

Coenraad 'Dumoulin' Marinissen never forget the moment we shared with a dancing Eric and 't Hooft in the lovely village of Erice on Sicily. Good luck exploiting hidden features of Kira and finishing up your thesis.

Ping Pong Master Sachin Shain Poruvelil, our ping pong matches were so intense and fierce, that my right (ping pong) arm is significantly more muscular than my left arm. All jokes aside, I am happy that Jordy flew you over to Amsterdam. We get along really well and have the same taste of humour. I must admit though, the physics discussions with you are very tough. I try to understand, but I just can't wrap my head around  $\chi$ -PT and nucleon wave functions. I hope that you will stay in the Netherlands so that we get to hang out in the future.

Ground wrestling viking, next generation 'Jimi Hendrix' Anders Rehult, you have been a very relaxed guy to share my coffees with. You were always chill, tranquil and optimistic, which resulted in me being zen as well (at least during the coffee breaks). I was positively stunned by your solo guitar performance at Nikhef, keep it up! We share a common appreciation for judo, well ne-waza judo for you (Basically Just Judo right). So maybe we will ever face off each other on the tatami?

My dear friend Guanghui 'Frikandel' Zhou. I feel honoured that you consider me your best friend in the Netherlands. I have fond memories of our after-hours discussions about the Netherlands, China, the US (including its political climate), India, the UK,..., and all the other countries in the world. I enjoyed guiding you in the Netherlands, which culminated in my paranimfship for your defence. If I ever visit China, I will surely give you a call (or send a WeChat text).

I would like to wish the recently started PhD students Ustad Vaisakh Khan, Jelle 'I am' Groot and his Majesty Robin van Bijleveld good luck on their academic journeys ahead. The next four years you will explore uncharted territories in the realm of particle physics. Enjoy each moment, because time flies when you're having fun.

Mens sana in corpore sano: A sportive shoutout to my hockey team the 'Strijders' van Pinoké Heren 19 and judo team Pleizier, to provide me such pleasant environments where I can commit to an active lifestyle.

Next up is my dear friend Shri Pawan Kumar Gupta from the geodesic surfing group (alternatively known as gravitational waves) at Nikhef. I enjoyed all the wonderful discussions we had over the past four years. Not only did you educate me on Indian politics, but you also reignited my interest in black holes. We became buddies and even hang out in the weekends. We visited each others places and we relaxed on the beach. Let's not become strangers and stay in touch!

Now some special shoutouts to the following persons: Max 'vakantie-man' Jaarsma you should try another cola flavour once in a while; Giacomo 'Casanova' Magni forget about Berlusconi, he got canceled; both Eleftheria Malami of Athens and Tanjona 'I like to move it' Rabemananjara enjoy your

lagers in Germany; Jaco ter Hoeve of Citium<sup>14</sup> sorry for my occasional humming in the office; Pieter 'tie knotting apprentice' Braat next time you are on BNN give me a shoutout; Ruben the original Jaarsma thank you for introducing me to the PhD council; office mate Guoxing Wang we had a laugh in the old office; guys from across the street Ricardo 'El Trailero' Espíndola, Zoroastrian magus Bahman Najian and the 678<sup>th</sup> Jeremy van der Heijden you know how to party; All the master students of the theory group of the last four years, thank you for the engaging conversations at the soccer table.

Not to forget the Nikhef theory group graduates like Pedro, Rabah, Lorenzo, Gillian and Jorinde. Thank you for the social interaction!

Furthermore I would like to thank the staff members of the Nikhef theory group. You provide a very encouraging environment and also a pleasingly open atmosphere for the students. I am thankful to Robert for allowing me to enter Nikhef as a visitor while I am finishing up my projects and thesis. Moreover, I am grateful to the Nikhef management team for the additional support in the final stages of the thesis.

Mnème cutie- $\pi$  Stapel, you truly are a muse. I could not have done this without you by my side. You have been supporting me from the start of my PhD, you encouraged me in the most dispiriting moments, and you lauded me for every success. It was a delight to have you as a master-student-member of our group during my last year at Nikhef. You provided that energy boost, that not only I, but the whole group required after the dreary pandemic years. You make me proud time and time again, first as a fellow theoretical physicist and now as a fancy banker. However my dear Wolf of the Zuidas, I have one request: Please always check your signs in order to prevent a next financial crisis!

And last, but very certainly not least, I would like to express my sincere thanks to my family for inspiring me and encouraging me to excel in physics. All the mousie's, mausa's, mamoe's, kaka's, dada, uncles, aunts, cousins and even little nieces, thank you for your continuous support. In particular I would like to thank my parents, who have been in my corner since day one. Your imparted wisdom and lessons have been my guiding principles in life, and you are both an example to live up to. Dad, you inspired my curiosity for the unknown physical mechanisms in the Universe, from the smallest scales to the large cosmological horizon and beyond. However, you will have to excuse me for not being able to proof your hypothesised existence of anti-gravity. Mom, thank you for rehearsing my lessons during primary and high school, as you can tell, it payed off. And believe it or not, but I used some of your teaching tips during the tutorials which I supervised, which resulted

---

<sup>14</sup>You might have to google this.

## Acknowledgements

---

in astonishing performances of the attendees (well, for most of them). There aren't enough words to express my gratitude to you both, but foremost I hope that I have made you proud.





# Bibliography

- [1] A. Basdew-Sharma, F. Herzog, S. Schrijnder van Velzen and W. J. Waalewijn, *One-loop jet functions by geometric subtraction*, *JHEP* **10** (2020) 118 [2006.14627].
- [2] A. Basdew-Sharma, *Towards DIS at  $N_4$ LO*, *SciPost Phys. Proc.* **8** (2022) 153 [2108.00459].
- [3] A. Basdew-Sharma, A. Pelloni, F. Herzog and A. Vogt, *Four-loop large- $n_f$  contributions to the non-singlet structure functions  $F_2$  and  $F_L$* , *JHEP* **03** (2023) 183 [2211.16485].
- [4] S. Amoroso et al., *Les Houches 2019: Physics at TeV Colliders: Standard Model Working Group Report*, in *11th Les Houches Workshop on Physics at TeV Colliders: PhysTeV Les Houches*, 3, 2020, 2003.01700.
- [5] G. Altarelli and G. Parisi, *Asymptotic Freedom in Parton Language*, *Nucl. Phys. B* **126** (1977) 298.
- [6] E. G. Floratos, D. A. Ross and C. T. Sachrajda, *Higher Order Effects in Asymptotically Free Gauge Theories: The Anomalous Dimensions of Wilson Operators*, *Nucl. Phys. B* **129** (1977) 66.
- [7] A. Gonzalez-Arroyo, C. Lopez and F. J. Yndurain, *Second Order Contributions to the Structure Functions in Deep Inelastic Scattering. 1. Theoretical Calculations*, *Nucl. Phys. B* **153** (1979) 161.
- [8] G. Curci, W. Furmanski and R. Petronzio, *Evolution of Parton Densities Beyond Leading Order: The Nonsinglet Case*, *Nucl. Phys. B* **175** (1980) 27.
- [9] W. Furmanski and R. Petronzio, *Singlet Parton Densities Beyond Leading Order*, *Phys. Lett. B* **97** (1980) 437.

- 
- [10] E. G. Floratos, C. Kounnas and R. Lacaze, *Higher Order QCD Effects in Inclusive Annihilation and Deep Inelastic Scattering*, *Nucl. Phys. B* **192** (1981) 417.
  - [11] R. Hamberg and W. L. van Neerven, *The Correct renormalization of the gluon operator in a covariant gauge*, *Nucl. Phys. B* **379** (1992) 143.
  - [12] S. Moch, J. A. M. Vermaseren and A. Vogt, *The Three loop splitting functions in QCD: The Nonsinglet case*, *Nucl. Phys. B* **688** (2004) 101 [[hep-ph/0403192](#)].
  - [13] A. Vogt, S. Moch and J. A. M. Vermaseren, *The Three-loop splitting functions in QCD: The Singlet case*, *Nucl. Phys. B* **691** (2004) 129 [[hep-ph/0404111](#)].
  - [14] J. Davies, A. Vogt, B. Ruijl, T. Ueda and J. A. M. Vermaseren, *Large- $n_f$  contributions to the four-loop splitting functions in QCD*, *Nucl. Phys. B* **915** (2017) 335 [[1610.07477](#)].
  - [15] S. Moch, B. Ruijl, T. Ueda, J. A. M. Vermaseren and A. Vogt, *Four-Loop Non-Singlet Splitting Functions in the Planar Limit and Beyond*, *JHEP* **10** (2017) 041 [[1707.08315](#)].
  - [16] S. Moch, B. Ruijl, T. Ueda, J. A. M. Vermaseren and A. Vogt, *Low moments of the four-loop splitting functions in QCD*, *Phys. Lett. B* **825** (2022) 136853 [[2111.15561](#)].
  - [17] A. Accardi et al., *A Critical Appraisal and Evaluation of Modern PDFs*, *Eur. Phys. J. C* **76** (2016) 471 [[1603.08906](#)].
  - [18] E. D. Bloom et al., *High-Energy Inelastic  $e p$  Scattering at 6-Degrees and 10-Degrees*, *Phys. Rev. Lett.* **23** (1969) 930.
  - [19] M. Breidenbach, J. I. Friedman, H. W. Kendall, E. D. Bloom, D. H. Coward, H. C. DeStaebler et al., *Observed behavior of highly inelastic electron-proton scattering*, *Phys. Rev. Lett.* **23** (1969) 935.
  - [20] H1 collaboration, *Measurement of neutral and charged current cross-sections in positron proton collisions at large momentum transfer*, *Eur. Phys. J. C* **13** (2000) 609 [[hep-ex/9908059](#)].
  - [21] H1 collaboration, *Measurement of neutral and charged current cross-sections in electron - proton collisions at high  $Q^2$* , *Eur. Phys. J. C* **19** (2001) 269 [[hep-ex/0012052](#)].

- [22] H1 collaboration, *Measurement and QCD analysis of neutral and charged current cross-sections at HERA*, *Eur. Phys. J. C* **30** (2003) 1 [hep-ex/0304003].
- [23] H1 collaboration, *First measurement of charged current cross sections at HERA with longitudinally polarised positrons*, *Phys. Lett. B* **634** (2006) 173 [hep-ex/0512060].
- [24] H1 collaboration, *Measurement of the Inclusive  $ep$  Scattering Cross Section at Low  $Q^2$  and  $x$  at HERA*, *Eur. Phys. J. C* **63** (2009) 625 [0904.0929].
- [25] H1 collaboration, *Measurement of the Proton Structure Function  $F(L)(x, Q^{*2})$  at Low  $x$* , *Phys. Lett. B* **665** (2008) 139 [0805.2809].
- [26] H1 collaboration, *A Precision Measurement of the Inclusive  $ep$  Scattering Cross Section at HERA*, *Eur. Phys. J. C* **64** (2009) 561 [0904.3513].
- [27] ZEUS collaboration, *Measurement of the proton structure function  $F_2$  and  $\sigma_{\text{tot}}(\gamma^* p)$  at low  $q^{*2}$  and very low  $x$  at HERA*, *Phys. Lett. B* **407** (1997) 432 [hep-ex/9707025].
- [28] ZEUS collaboration, *Measurement of the proton structure function  $F(2)$  at very low  $Q^{*2}$  at HERA*, *Phys. Lett. B* **487** (2000) 53 [hep-ex/0005018].
- [29] ZEUS collaboration, *ZEUS results on the measurement and phenomenology of  $F(2)$  at low  $x$  and low  $Q^{*2}$* , *Eur. Phys. J. C* **7** (1999) 609 [hep-ex/9809005].
- [30] ZEUS collaboration, *Measurement of the neutral current cross-section and  $F(2)$  structure function for deep inelastic  $e + p$  scattering at HERA*, *Eur. Phys. J. C* **21** (2001) 443 [hep-ex/0105090].
- [31] ZEUS collaboration, *Measurement of high  $Q^{*2}$  charged current  $e + p$  deep inelastic scattering cross-sections at HERA*, *Eur. Phys. J. C* **12** (2000) 411 [hep-ex/9907010].
- [32] ZEUS collaboration, *Measurement of high  $Q^{*2}$   $e - p$  neutral current cross-sections at HERA and the extraction of  $x F(3)$* , *Eur. Phys. J. C* **28** (2003) 175 [hep-ex/0208040].

- 
- [33] ZEUS collaboration, *Measurement of high  $Q^2$  charged current cross-sections in  $e^-p$  deep inelastic scattering at HERA*, *Phys. Lett. B* **539** (2002) 197 [[hep-ex/0205091](#)].
- [34] ZEUS collaboration, *High  $Q^{*2}$  neutral current cross-sections in  $e+p$  deep inelastic scattering at  $s^{*2}(1/2) = 318\text{-GeV}$* , *Phys. Rev. D* **70** (2004) 052001 [[hep-ex/0401003](#)].
- [35] ZEUS collaboration, *Measurement of high  $Q^{*2}$  charged current cross-sections in  $e+p$  deep inelastic scattering at HERA*, *Eur. Phys. J. C* **32** (2003) 1 [[hep-ex/0307043](#)].
- [36] A. J. Buras, E. G. Floratos, D. A. Ross and C. T. Sachrajda, *Asymptotic Freedom Beyond the Leading Order*, *Nucl. Phys. B* **131** (1977) 308.
- [37] E. G. Floratos, D. A. Ross and C. T. Sachrajda, *Higher Order Effects in Asymptotically Free Gauge Theories. 2. Flavor Singlet Wilson Operators and Coefficient Functions*, *Nucl. Phys. B* **152** (1979) 493.
- [38] W. A. Bardeen, A. J. Buras, D. W. Duke and T. Muta, *Deep Inelastic Scattering Beyond the Leading Order in Asymptotically Free Gauge Theories*, *Phys. Rev. D* **18** (1978) 3998.
- [39] W. L. van Neerven and E. B. Zijlstra, *Order  $\alpha_s^{*2}$  contributions to the deep inelastic Wilson coefficient*, *Phys. Lett. B* **272** (1991) 127.
- [40] E. B. Zijlstra and W. L. van Neerven, *Contribution of the second order gluonic Wilson coefficient to the deep inelastic structure function*, *Phys. Lett. B* **273** (1991) 476.
- [41] E. B. Zijlstra and W. L. van Neerven, *Order  $\alpha_s^{*2}$  correction to the structure function  $F_3(x, Q^{*2})$  in deep inelastic neutrino - hadron scattering*, *Phys. Lett. B* **297** (1992) 377.
- [42] S. Moch, J. A. M. Vermaseren and A. Vogt, *The Longitudinal structure function at the third order*, *Phys. Lett. B* **606** (2005) 123 [[hep-ph/0411112](#)].
- [43] J. A. M. Vermaseren, A. Vogt and S. Moch, *The Third-order QCD corrections to deep-inelastic scattering by photon exchange*, *Nucl. Phys. B* **724** (2005) 3 [[hep-ph/0504242](#)].

- [44] S. Moch, J. A. M. Vermaseren and A. Vogt, *Third-order QCD corrections to the charged-current structure function  $F(3)$* , *Nucl. Phys. B* **813** (2009) 220 [0812.4168].
- [45] J. Davies, A. Vogt, S. Moch and J. A. M. Vermaseren, *Non-singlet coefficient functions for charged-current deep-inelastic scattering to the third order in QCD*, *PoS DIS2016* (2016) 059 [1606.08907].
- [46] B. Ruijl, T. Ueda, J. A. M. Vermaseren, J. Davies and A. Vogt, *First Forcer results on deep-inelastic scattering and related quantities*, *PoS LL2016* (2016) 071 [1605.08408].
- [47] D. Bonocore, E. Laenen and R. Rietkerk, *Unitarity methods for Mellin moments of Drell-Yan cross sections*, *JHEP* **05** (2016) 079 [1603.05252].
- [48] G. 't Hooft and M. J. G. Veltman, *Regularization and Renormalization of Gauge Fields*, *Nucl. Phys. B* **44** (1972) 189.
- [49] K. G. Chetyrkin and F. V. Tkachov, *Integration by Parts: The Algorithm to Calculate beta Functions in 4 Loops*, *Nucl. Phys. B* **192** (1981) 159.
- [50] S. G. Gorishnii, S. A. Larin, L. R. Surguladze and F. V. Tkachov, *Mincer: Program for Multiloop Calculations in Quantum Field Theory for the Schoonschip System*, *Comput. Phys. Commun.* **55** (1989) 381.
- [51] H. Strubbe, *Manual for Schoonschip: A CDC 6000 / 7000 program for symbolic evaluation of algebraic expressions*, *Comput. Phys. Commun.* **8** (1974) 1.
- [52] J. A. M. Vermaseren, *New features of FORM*, [math-ph/0010025](#).
- [53] J. Kuipers, T. Ueda, J. A. M. Vermaseren and J. Vollinga, *FORM version 4.0*, *Comput. Phys. Commun.* **184** (2013) 1453 [1203.6543].
- [54] S. A. Larin, F. V. Tkachov and J. A. M. Vermaseren, *The FORM version of MINCER*, .
- [55] S. A. Larin and J. A. M. Vermaseren, *Two Loop QCD Corrections to the Coefficient Functions of the Deep Inelastic Structure Functions  $F - 2$  and  $F - L$* , *Z. Phys. C* **57** (1993) 93.

- 
- [56] S. A. Larin, P. Nogueira, T. van Ritbergen and J. A. M. Vermaseren, *The Three loop QCD calculation of the moments of deep inelastic structure functions*, *Nucl. Phys. B* **492** (1997) 338 [[hep-ph/9605317](#)].
- [57] T. Ueda, B. Ruijl and J. A. M. Vermaseren, *Forcer: a FORM program for 4-loop massless propagators*, *PoS LL2016* (2016) 070 [[1607.07318](#)].
- [58] S. Laporta and E. Remiddi, *The Analytical value of the electron ( $g-2$ ) at order  $\alpha^3$  in QED*, *Phys. Lett. B* **379** (1996) 283 [[hep-ph/9602417](#)].
- [59] S. Laporta, *High precision calculation of multiloop Feynman integrals by difference equations*, *Int. J. Mod. Phys. A* **15** (2000) 5087 [[hep-ph/0102033](#)].
- [60] J. Klappert, F. Lange, P. Maierhöfer and J. Usovitsch, *Integral reduction with Kira 2.0 and finite field methods*, *Comput. Phys. Commun.* **266** (2021) 108024 [[2008.06494](#)].
- [61] A. V. Smirnov and F. S. Chuharev, *FIRE6: Feynman Integral REduction with Modular Arithmetic*, *Comput. Phys. Commun.* **247** (2020) 106877 [[1901.07808](#)].
- [62] A. V. Kotikov, *Differential equations method: New technique for massive Feynman diagrams calculation*, *Phys. Lett. B* **254** (1991) 158.
- [63] A. V. Kotikov, *Differential equations method: The Calculation of vertex type Feynman diagrams*, *Phys. Lett. B* **259** (1991) 314.
- [64] A. V. Kotikov, *Differential equation method: The Calculation of  $N$  point Feynman diagrams*, *Phys. Lett. B* **267** (1991) 123.
- [65] A. V. Kotikov, *New method of massive Feynman diagrams calculation*, *Mod. Phys. Lett. A* **6** (1991) 677.
- [66] A. V. Kotikov, *New method of massive Feynman diagrams calculation. Vertex type functions*, *Int. J. Mod. Phys. A* **7** (1992) 1977.
- [67] E. Remiddi, *Differential equations for Feynman graph amplitudes*, *Nuovo Cim. A* **110** (1997) 1435 [[hep-th/9711188](#)].
- [68] T. Gehrmann and E. Remiddi, *Differential equations for two loop four point functions*, *Nucl. Phys. B* **580** (2000) 485 [[hep-ph/9912329](#)].

- [69] C. Anastasiou and K. Melnikov, *Higgs boson production at hadron colliders in NNLO QCD*, *Nucl. Phys. B* **646** (2002) 220 [[hep-ph/0207004](#)].
- [70] C. Anastasiou, L. J. Dixon, K. Melnikov and F. Petriello, *High precision QCD at hadron colliders: Electroweak gauge boson rapidity distributions at NNLO*, *Phys. Rev. D* **69** (2004) 094008 [[hep-ph/0312266](#)].
- [71] C. Anastasiou, S. Beerli, S. Bucherer, A. Daleo and Z. Kunszt, *Two-loop amplitudes and master integrals for the production of a Higgs boson via a massive quark and a scalar-quark loop*, *JHEP* **01** (2007) 082 [[hep-ph/0611236](#)].
- [72] J. M. Henn, *Multiloop integrals in dimensional regularization made simple*, *Phys. Rev. Lett.* **110** (2013) 251601 [[1304.1806](#)].
- [73] C. W. Bauer, S. Fleming and M. E. Luke, *Summing Sudakov logarithms in  $B \rightarrow X_s \gamma$  in effective field theory*, *Phys. Rev.* **D63** (2000) 014006 [[hep-ph/0005275](#)].
- [74] C. W. Bauer, S. Fleming, D. Pirjol and I. W. Stewart, *An Effective field theory for collinear and soft gluons: Heavy to light decays*, *Phys. Rev.* **D63** (2001) 114020 [[hep-ph/0011336](#)].
- [75] C. W. Bauer and I. W. Stewart, *Invariant operators in collinear effective theory*, *Phys. Lett.* **B516** (2001) 134 [[hep-ph/0107001](#)].
- [76] C. W. Bauer, D. Pirjol and I. W. Stewart, *Soft collinear factorization in effective field theory*, *Phys. Rev.* **D65** (2002) 054022 [[hep-ph/0109045](#)].
- [77] M. Beneke, A. Chapovsky, M. Diehl and T. Feldmann, *Soft collinear effective theory and heavy to light currents beyond leading power*, *Nucl. Phys. B* **643** (2002) 431 [[hep-ph/0206152](#)].
- [78] T. Kinoshita, *Mass singularities of Feynman amplitudes*, *J. Math. Phys.* **3** (1962) 650.
- [79] T. D. Lee and M. Nauenberg, *Degenerate Systems and Mass Singularities*, *Phys. Rev.* **133** (1964) B1549.
- [80] S. Catani and M. H. Seymour, *A General algorithm for calculating jet cross-sections in NLO QCD*, *Nucl. Phys. B* **485** (1997) 291 [[hep-ph/9605323](#)].



- 
- [81] S. Catani and M. H. Seymour, *The Dipole formalism for the calculation of QCD jet cross-sections at next-to-leading order*, *Phys. Lett. B* **378** (1996) 287 [[hep-ph/9602277](#)].
- [82] S. Frixione, Z. Kunszt and A. Signer, *Three jet cross-sections to next-to-leading order*, *Nucl. Phys. B* **467** (1996) 399 [[hep-ph/9512328](#)].
- [83] R. Frederix, S. Frixione, F. Maltoni and T. Stelzer, *Automation of next-to-leading order computations in QCD: The FKS subtraction*, *JHEP* **10** (2009) 003 [[0908.4272](#)].
- [84] A. Gehrmann-De Ridder, T. Gehrmann and E. W. N. Glover, *Antenna subtraction at NNLO*, *JHEP* **09** (2005) 056 [[hep-ph/0505111](#)].
- [85] A. Gehrmann-De Ridder, T. Gehrmann, E. W. N. Glover and G. Heinrich, *Infrared structure of  $e^+ e^- \rightarrow 3$  jets at NNLO*, *JHEP* **11** (2007) 058 [[0710.0346](#)].
- [86] J. Currie, E. W. N. Glover and S. Wells, *Infrared Structure at NNLO Using Antenna Subtraction*, *JHEP* **04** (2013) 066 [[1301.4693](#)].
- [87] W. T. Giele and E. W. N. Glover, *Higher order corrections to jet cross-sections in  $e^+ e^-$  annihilation*, *Phys. Rev. D* **46** (1992) 1980.
- [88] S. Catani and M. Grazzini, *An NNLO subtraction formalism in hadron collisions and its application to Higgs boson production at the LHC*, *Phys. Rev. Lett.* **98** (2007) 222002 [[hep-ph/0703012](#)].
- [89] R. Boughezal, C. Focke, W. Giele, X. Liu and F. Petriello, *Higgs boson production in association with a jet at NNLO using jettness subtraction*, *Phys. Lett. B* **748** (2015) 5 [[1505.03893](#)].
- [90] J. Gaunt, M. Stahlhofen, F. J. Tackmann and J. R. Walsh, *N-jettiness Subtractions for NNLO QCD Calculations*, *JHEP* **09** (2015) 058 [[1505.04794](#)].
- [91] I. Moulst, L. Rothen, I. W. Stewart, F. J. Tackmann and H. X. Zhu, *N-jettiness subtractions for  $gg \rightarrow H$  at subleading power*, *Phys. Rev. D* **97** (2018) 014013 [[1710.03227](#)].
- [92] R. Boughezal, A. Isgrò and F. Petriello, *Next-to-leading-logarithmic power corrections for N-jettiness subtraction in color-singlet production*, *Phys. Rev. D* **97** (2018) 076006 [[1802.00456](#)].

- [93] F. Herzog, *Geometric IR subtraction for final state real radiation*, *JHEP* **08** (2018) 006 [1804.07949].
- [94] G. F. Sterman, *An Introduction to quantum field theory*. Cambridge University Press, 8, 1993.
- [95] R. K. Ellis, W. J. Stirling and B. R. Webber, *QCD and collider physics*, vol. 8. Cambridge University Press, 2, 2011, 10.1017/CBO9780511628788.
- [96] PARTICLE DATA GROUP collaboration, *Review of Particle Physics*, *PTEP* **2022** (2022) 083C01.
- [97] B. De Wit, E. Laenen and J. Smith, *Field Theory in Particle Physics (To Appear)*.
- [98] M. Nakahara, *Geometry, topology and physics*, Graduate student series in physics. Hilger, Bristol, 1990.
- [99] H. D. Politzer, *Reliable Perturbative Results for Strong Interactions?*, *Phys. Rev. Lett.* **30** (1973) 1346.
- [100] D. J. Gross and F. Wilczek, *Ultraviolet Behavior of Nonabelian Gauge Theories*, *Phys. Rev. Lett.* **30** (1973) 1343.
- [101] W. E. Caswell, *Asymptotic Behavior of Nonabelian Gauge Theories to Two Loop Order*, *Phys. Rev. Lett.* **33** (1974) 244.
- [102] O. V. Tarasov, A. A. Vladimirov and A. Y. Zharkov, *The Gell-Mann-Low Function of QCD in the Three Loop Approximation*, *Phys. Lett. B* **93** (1980) 429.
- [103] S. A. Larin and J. A. M. Vermaseren, *The Three loop QCD Beta function and anomalous dimensions*, *Phys. Lett. B* **303** (1993) 334 [hep-ph/9302208].
- [104] P. A. Baikov, K. G. Chetyrkin and J. H. Kühn, *Five-Loop Running of the QCD coupling constant*, *Phys. Rev. Lett.* **118** (2017) 082002 [1606.08659].
- [105] T. Luthe, A. Maier, P. Marquard and Y. Schröder, *Towards the five-loop Beta function for a general gauge group*, *JHEP* **07** (2016) 127 [1606.08662].

- 
- [106] F. Herzog, B. Ruijl, T. Ueda, J. A. M. Vermaseren and A. Vogt, *The five-loop beta function of Yang-Mills theory with fermions*, *JHEP* **02** (2017) 090 [[1701.01404](#)].
- [107] T. Luthe, A. Maier, P. Marquard and Y. Schroder, *The five-loop Beta function for a general gauge group and anomalous dimensions beyond Feynman gauge*, *JHEP* **10** (2017) 166 [[1709.07718](#)].
- [108] K. G. Chetyrkin, G. Falcioni, F. Herzog and J. A. M. Vermaseren, *Five-loop renormalisation of QCD in covariant gauges*, *JHEP* **10** (2017) 179 [[1709.08541](#)].
- [109] R. Tarrach, *The Pole Mass in Perturbative QCD*, *Nucl. Phys. B* **183** (1981) 384.
- [110] O. Nachtmann and W. Wetzel, *The Beta Function for Effective Quark Masses to Two Loops in QCD*, *Nucl. Phys. B* **187** (1981) 333.
- [111] S. Moch and J. A. M. Vermaseren, *Deep inelastic structure functions at two loops*, *Nucl. Phys. B* **573** (2000) 853 [[hep-ph/9912355](#)].
- [112] T. Giani, *Towards a new generation of Parton Distribution Functions: from high-precision collider data to lattice Quantum Chromodynamics*, Ph.D. thesis, Edinburgh U., 2021. [10.7488/era/1515](#).
- [113] M. D. Schwartz, *Quantum Field Theory and the Standard Model*. Cambridge University Press, 3, 2014.
- [114] J. C. Collins, *Renormalization: An Introduction to Renormalization, The Renormalization Group, and the Operator Product Expansion*, vol. 26 of *Cambridge Monographs on Mathematical Physics*. Cambridge University Press, Cambridge, 1986, [10.1017/CBO9780511622656](#).
- [115] V. A. Smirnov, *Analytic tools for Feynman integrals*, vol. 250. Springer, 2012, [10.1007/978-3-642-34886-0](#).
- [116] R. N. Lee, *Presenting LiteRed: a tool for the Loop InTEgrals REDuction*, [1212.2685](#).
- [117] J. Usovitsch, *Factorization of denominators in integration-by-parts reductions*, [2002.08173](#).
- [118] A. V. Smirnov and V. A. Smirnov, *How to choose master integrals*, *Nucl. Phys. B* **960** (2020) 115213 [[2002.08042](#)].

- [119] Y. L. Dokshitzer, D. Diakonov and S. Troian, *Hard Processes in Quantum Chromodynamics*, *Phys. Rept.* **58** (1980) 269.
- [120] G. Parisi and R. Petronzio, *Small Transverse Momentum Distributions in Hard Processes*, *Nucl. Phys. B* **154** (1979) 427.
- [121] G. Curci, M. Greco and Y. Srivastava, *QCD Jets From Coherent States*, *Nucl. Phys. B* **159** (1979) 451.
- [122] J. C. Collins and D. E. Soper, *Back-To-Back Jets in QCD*, *Nucl. Phys. B* **193** (1981) 381.
- [123] J. Kodaira and L. Trentadue, *Summing Soft Emission in QCD*, *Phys. Lett. B* **112** (1982) 66.
- [124] G. T. Bodwin, *Factorization of the Drell-Yan Cross-Section in Perturbation Theory*, *Phys. Rev. D* **31** (1985) 2616.
- [125] J. C. Collins, D. E. Soper and G. F. Sterman, *Transverse Momentum Distribution in Drell-Yan Pair and W and Z Boson Production*, *Nucl. Phys. B* **250** (1985) 199.
- [126] J. C. Collins, D. E. Soper and G. F. Sterman, *Factorization of Hard Processes in QCD*, *Adv. Ser. Direct. High Energy Phys* **5** (1989) 1 [[hep-ph/0409313](#)].
- [127] X. Liu and F. Petriello, *Resummation of jet-veto logarithms in hadronic processes containing jets*, *Phys. Rev. D* **87** (2013) 014018 [[1210.1906](#)].
- [128] X. Liu and F. Petriello, *Reducing theoretical uncertainties for exclusive Higgs-boson plus one-jet production at the LHC*, *Phys. Rev. D* **87** (2013) 094027 [[1303.4405](#)].
- [129] A. Banfi, G. P. Salam and G. Zanderighi, *Principles of general final-state resummation and automated implementation*, *JHEP* **03** (2005) 073 [[hep-ph/0407286](#)].
- [130] A. Banfi, H. McAslan, P. F. Monni and G. Zanderighi, *A general method for the resummation of event-shape distributions in  $e^+e^-$  annihilation*, *JHEP* **05** (2015) 102 [[1412.2126](#)].
- [131] C. W. Bauer and A. V. Manohar, *Shape function effects in  $B \rightarrow X_s \gamma$  and  $B \rightarrow X_u \ell \bar{\nu}$  decays*, *Phys. Rev.* **D70** (2004) 034024 [[hep-ph/0312109](#)].

- 
- [132] T. Becher and M. Neubert, *Toward a NNLO calculation of the  $\bar{B} \rightarrow X_s \gamma$  decay rate with a cut on photon energy. II. Two-loop result for the jet function*, *Phys. Lett. B* **637** (2006) 251 [[hep-ph/0603140](#)].
- [133] T. Becher and M. D. Schwartz, *Direct photon production with effective field theory*, *JHEP* **02** (2010) 040 [[0911.0681](#)].
- [134] T. Becher and G. Bell, *The gluon jet function at two-loop order*, *Phys. Lett. B* **695** (2011) 252 [[1008.1936](#)].
- [135] R. Brüser, Z. L. Liu and M. Stahlhofen, *Three-Loop Quark Jet Function*, *Phys. Rev. Lett.* **121** (2018) 072003 [[1804.09722](#)].
- [136] P. Banerjee, P. K. Dhani and V. Ravindran, *Gluon jet function at three loops in QCD*, *Phys. Rev.* **D98** (2018) 094016 [[1805.02637](#)].
- [137] A. Hornig, C. Lee and G. Ovanessian, *Effective Predictions of Event Shapes: Factorized, Resummed, and Gapped Angularity Distributions*, *JHEP* **05** (2009) 122 [[0901.3780](#)].
- [138] T. Becher and G. Bell, *NNLL Resummation for Jet Broadening*, *JHEP* **11** (2012) 126 [[1210.0580](#)].
- [139] G. Bell, A. Hornig, C. Lee and J. Talbert,  *$e^+e^-$  angularity distributions at NNLL' accuracy*, *JHEP* **01** (2019) 147 [[1808.07867](#)].
- [140] A. J. Larkoski, D. Neill and J. Thaler, *Jet Shapes with the Broadening Axis*, *JHEP* **04** (2014) 017 [[1401.2158](#)].
- [141] M. Procura, W. J. Waalewijn and L. Zeune, *Joint resummation of two angularities at next-to-next-to-leading logarithmic order*, *JHEP* **10** (2018) 098 [[1806.10622](#)].
- [142] T. T. Jouttenus, *Jet Function with a Jet Algorithm in SCET*, *Phys. Rev. D* **81** (2010) 094017 [[0912.5509](#)].
- [143] J. Chay, C. Kim and I. Kim, *Factorization of the dijet cross section in electron-positron annihilation with jet algorithms*, *Phys. Rev.* **D92** (2015) 034012 [[1505.00121](#)].
- [144] S. D. Ellis, C. K. Vermilion, J. R. Walsh, A. Hornig and C. Lee, *Jet Shapes and Jet Algorithms in SCET*, *JHEP* **11** (2010) 101 [[1001.0014](#)].

- [145] Z.-B. Kang, F. Ringer and I. Vitev, *The semi-inclusive jet function in SCET and small radius resummation for inclusive jet production*, *JHEP* **10** (2016) 125 [1606.06732].
- [146] L. Dai, C. Kim and A. K. Leibovich, *Fragmentation of a Jet with Small Radius*, *Phys. Rev. D* **94** (2016) 114023 [1606.07411].
- [147] H.-n. Li, Z. Li and C.-P. Yuan, *QCD resummation for jet substructures*, *Phys. Rev. Lett.* **107** (2011) 152001 [1107.4535].
- [148] Y.-T. Chien and I. Vitev, *Jet Shape Resummation Using Soft-Collinear Effective Theory*, *JHEP* **12** (2014) 061 [1405.4293].
- [149] P. Cal, F. Ringer and W. J. Waalewijn, *The jet shape at NLL'*, *JHEP* **05** (2019) 143 [1901.06389].
- [150] S. Fleming, A. H. Hoang, S. Mantry and I. W. Stewart, *Top Jets in the Peak Region: Factorization Analysis with NLL Resummation*, *Phys. Rev. D* **77** (2008) 114003 [0711.2079].
- [151] A. H. Hoang, C. Lepenik and M. Stahlhofen, *Two-Loop Massive Quark Jet Functions in SCET*, *JHEP* **08** (2019) 112 [1904.12839].
- [152] D. Krohn, M. D. Schwartz, T. Lin and W. J. Waalewijn, *Jet Charge at the LHC*, *Phys. Rev. Lett.* **110** (2013) 212001 [1209.2421].
- [153] W. J. Waalewijn, *Calculating the Charge of a Jet*, *Phys. Rev. D* **86** (2012) 094030 [1209.3019].
- [154] T. Kasemets, W. J. Waalewijn and L. Zeune, *Calculating Soft Radiation at One Loop*, *JHEP* **03** (2016) 153 [1512.00857].
- [155] G. Bell, R. Rahn and J. Talbert, *Automated Calculation of Dijet Soft Functions in Soft-Collinear Effective Theory*, *PoS RADCOR2015* (2016) 052 [1512.06100].
- [156] G. Bell, R. Rahn and J. Talbert, *Generic dijet soft functions at two-loop order: correlated emissions*, *JHEP* **07** (2019) 101 [1812.08690].
- [157] G. Bell, R. Rahn and J. Talbert, *Generic dijet soft functions at two-loop order: uncorrelated emissions*, 2004.08396.
- [158] G. Bell, B. Dehnadi, T. Mohrmann and R. Rahn, *Automated Calculation of  $N$ -jet Soft Functions*, *PoS LL2018* (2018) 044 [1808.07427].

- 
- [159] I. Moulst, I. W. Stewart, F. J. Tackmann and W. J. Waalewijn, *Employing Helicity Amplitudes for Resummation*, *Phys. Rev.* **D93** (2016) 094003 [1508.02397].
- [160] A. Budhraj, A. Jain and M. Procura, *One-loop angularity distributions with recoil using Soft-Collinear Effective Theory*, *JHEP* **08** (2019) 144 [1903.11087].
- [161] T. Becher and M. Neubert, *Drell-Yan Production at Small  $q_T$ , Transverse Parton Distributions and the Collinear Anomaly*, *Eur. Phys. J. C* **71** (2011) 1665 [1007.4005].
- [162] J.-y. Chiu, A. Jain, D. Neill and I. Z. Rothstein, *The Rapidity Renormalization Group*, *Phys. Rev. Lett.* **108** (2012) 151601 [1104.0881].
- [163] J. Collins, *Foundations of perturbative QCD*, vol. 32. Cambridge University Press, 11, 2013.
- [164] M. G. Echevarria, A. Idilbi and I. Scimemi, *Factorization Theorem For Drell-Yan At Low  $q_T$  And Transverse Momentum Distributions On-The-Light-Cone*, *JHEP* **07** (2012) 002 [1111.4996].
- [165] T. Becher and G. Bell, *Analytic Regularization in Soft-Collinear Effective Theory*, *Phys. Lett. B* **713** (2012) 41 [1112.3907].
- [166] J.-Y. Chiu, A. Jain, D. Neill and I. Z. Rothstein, *A Formalism for the Systematic Treatment of Rapidity Logarithms in Quantum Field Theory*, *JHEP* **05** (2012) 084 [1202.0814].
- [167] M. Ritzmann and W. J. Waalewijn, *Fragmentation in Jets at NNLO*, *Phys. Rev. D* **90** (2014) 054029 [1407.3272].
- [168] T. Hahn, *CUBA: A Library for multidimensional numerical integration*, *Comput. Phys. Commun.* **168** (2005) 78 [hep-ph/0404043].
- [169] C. F. Berger, T. Kucs and G. F. Sterman, *Event shape / energy flow correlations*, *Phys. Rev.* **D68** (2003) 014012 [hep-ph/0303051].
- [170] A. V. Manohar and I. W. Stewart, *The Zero-Bin and Mode Factorization in Quantum Field Theory*, *Phys. Rev. D* **76** (2007) 074002 [hep-ph/0605001].

- [171] I. W. Stewart, F. J. Tackmann and W. J. Waalewijn, *Factorization at the LHC: From PDFs to Initial State Jets*, *Phys. Rev. D* **81** (2010) 094035 [0910.0467].
- [172] A. Accardi et al., *Electron Ion Collider: The Next QCD Frontier: Understanding the glue that binds us all*, *Eur. Phys. J. A* **52** (2016) 268 [1212.1701].
- [173] R. Abdul Khalek et al., *Science Requirements and Detector Concepts for the Electron-Ion Collider: EIC Yellow Report*, *Nucl. Phys. A* **1026** (2022) 122447 [2103.05419].
- [174] LHeC STUDY GROUP collaboration, *A Large Hadron Electron Collider at CERN: Report on the Physics and Design Concepts for Machine and Detector*, *J. Phys. G* **39** (2012) 075001 [1206.2913].
- [175] LHeC, FCC-HE STUDY GROUP collaboration, *The Large Hadron–Electron Collider at the HL-LHC*, *J. Phys. G* **48** (2021) 110501 [2007.14491].
- [176] P. Bolzoni, F. Maltoni, S.-O. Moch and M. Zaro, *Higgs production via vector-boson fusion at NNLO in QCD*, *Phys. Rev. Lett.* **105** (2010) 011801 [1003.4451].
- [177] F. A. Dreyer and A. Karlberg, *Vector-Boson Fusion Higgs Production at Three Loops in QCD*, *Phys. Rev. Lett.* **117** (2016) 072001 [1606.00840].
- [178] J. Currie, T. Gehrmann, E. W. N. Glover, A. Huss, J. Niehues and A. Vogt,  *$N^3LO$  corrections to jet production in deep inelastic scattering using the Projection-to-Born method*, *JHEP* **05** (2018) 209 [1803.09973].
- [179] J. Sanchez Guillen, J. Miramontes, M. Miramontes, G. Parente and O. A. Sampayo, *Next-to-leading order analysis of the deep inelastic  $R = \sigma_{\text{sig}}\text{-L} / \sigma_{\text{sig}}\text{-total}$* , *Nucl. Phys. B* **353** (1991) 337.
- [180] E. B. Zijlstra and W. L. van Neerven, *Order  $\alpha_s^{**2}$  QCD corrections to the deep inelastic proton structure functions  $F_2$  and  $F(L)$* , *Nucl. Phys. B* **383** (1992) 525.
- [181] J. Blümlein, P. Marquard, C. Schneider and K. Schönwald, *The massless three-loop Wilson coefficients for the deep-inelastic structure functions  $F_2, F_L, xF_3$  and  $g_1$* , 2208.14325.



- 
- [182] S. Moch, B. Ruijl, T. Ueda, J. A. M. Vermaseren and A. Vogt, *DIS coefficient functions at four loops in QCD and beyond*, in *16th DESY Workshop on Elementary Particle Physics: Loops and Legs in Quantum Field Theory 2022*, 8, 2022, 2208.11067.
- [183] S. Moch, B. Ruijl, T. Ueda, J. A. M. Vermaseren and A. Vogt, *to appear*, .
- [184] B. Ruijl, T. Ueda and J. A. M. Vermaseren, *Forcer, a FORM program for the parametric reduction of four-loop massless propagator diagrams*, *Comput. Phys. Commun.* **253** (2020) 107198 [1704.06650].
- [185] J. A. Gracey, *Large  $n_f$  methods for computing the perturbative structure of deep inelastic scattering*, in *4th International Workshop on Software Engineering and Artificial Intelligence for High-energy and Nuclear Physics*, 9, 1995, hep-ph/9509276.
- [186] L. Mankiewicz, M. Maul and E. Stein, *Perturbative part of the nonsinglet structure function  $F_2$  in the large  $n_f$  limit*, *Phys. Lett. B* **404** (1997) 345 [hep-ph/9703356].
- [187] J. A. M. Vermaseren, *Harmonic sums, Mellin transforms and integrals*, *Int. J. Mod. Phys. A* **14** (1999) 2037 [hep-ph/9806280].
- [188] E. Remiddi and J. A. M. Vermaseren, *Harmonic polylogarithms*, *Int. J. Mod. Phys. A* **15** (2000) 725 [hep-ph/9905237].
- [189] W. L. van Neerven and A. Vogt, *NNLO evolution of deep inelastic structure functions: The Singlet case*, *Nucl. Phys. B* **588** (2000) 345 [hep-ph/0006154].
- [190] S. A. Larin, T. van Ritbergen and J. A. M. Vermaseren, *The Next next-to-leading QCD approximation for nonsinglet moments of deep inelastic structure functions*, *Nucl. Phys. B* **427** (1994) 41.
- [191] S. Moch and M. Rogal, *Charged current deep-inelastic scattering at three loops*, *Nucl. Phys. B* **782** (2007) 51 [0704.1740].
- [192] S. Moch, J. A. M. Vermaseren and A. Vogt, *Three-loop results for quark and gluon form-factors*, *Phys. Lett. B* **625** (2005) 245 [hep-ph/0508055].
- [193] S. Moch, J. A. M. Vermaseren and A. Vogt, *Nonsinglet structure functions at three loops: Fermionic contributions*, *Nucl. Phys. B* **646** (2002) 181 [hep-ph/0209100].

- [194] P. Nogueira, *Automatic Feynman graph generation*, *J. Comput. Phys.* **105** (1993) 279.
- [195] B. Ruijl, T. Ueda and J. Vermaseren, *FORM version 4.2*, 1707.06453.
- [196] J. A. M. Vermaseren, “The minos database facility.” <https://www.nikhef.nl/~form/maindir/others/minos/minos.html>.
- [197] P. Maierhöfer, J. Usovitsch and P. Uwer, *Kira—A Feynman integral reduction program*, *Comput. Phys. Commun.* **230** (2018) 99 [1705.05610].
- [198] R. Boughezal, M. Czakon and T. Schutzmeier, *NNLO fermionic corrections to the charm quark mass dependent matrix elements in  $\bar{B} \rightarrow X_s \gamma$* , *JHEP* **09** (2007) 072 [0707.3090].
- [199] J. Blümlein and C. Schneider, *The Method of Arbitrarily Large Moments to Calculate Single Scale Processes in Quantum Field Theory*, *Phys. Lett. B* **771** (2017) 31 [1701.04614].
- [200] R. N. Lee, A. V. Smirnov and V. A. Smirnov, *Solving differential equations for Feynman integrals by expansions near singular points*, *JHEP* **03** (2018) 008 [1709.07525].
- [201] X. Liu, Y.-Q. Ma and C.-Y. Wang, *A Systematic and Efficient Method to Compute Multi-loop Master Integrals*, *Phys. Lett. B* **779** (2018) 353 [1711.09572].
- [202] B. Mistlberger, *Higgs boson production at hadron colliders at  $N^3\text{LO}$  in QCD*, *JHEP* **05** (2018) 028 [1802.00833].
- [203] J. Ablinger, J. Blümlein, P. Marquard, N. Rana and C. Schneider, *Automated Solution of First Order Factorizable Systems of Differential Equations in One Variable*, *Nucl. Phys. B* **939** (2019) 253 [1810.12261].
- [204] F. Moriello, *Generalised power series expansions for the elliptic planar families of Higgs + jet production at two loops*, *JHEP* **01** (2020) 150 [1907.13234].
- [205] I. Dubovyk, A. Freitas, J. Gluza, K. Grzanka, M. Hidding and J. Usovitsch, *Evaluation of multi-loop multi-scale Feynman integrals for precision physics*, 2201.02576.

- 
- [206] M. Fael, F. Lange, K. Schönwald and M. Steinhauser, *Singlet and nonsinglet three-loop massive form factors*, *Phys. Rev. D* **106** (2022) 034029 [2207.00027].
- [207] M. Hidding, *DiffExp, a Mathematica package for computing Feynman integrals in terms of one-dimensional series expansions*, *Comput. Phys. Commun.* **269** (2021) 108125 [2006.05510].
- [208] X. Liu and Y.-Q. Ma, *AMFlow: A Mathematica package for Feynman integrals computation via auxiliary mass flow*, *Comput. Phys. Commun.* **283** (2023) 108565 [2201.11669].
- [209] T. Armadillo, R. Bonciani, S. Devoto, N. Rana and A. Vicini, *Evaluation of Feynman integrals with arbitrary complex masses via series expansions*, *Comput. Phys. Commun.* **282** (2023) 108545 [2205.03345].
- [210] J. Moser, *The order of a singularity in Fuchs' theory*, *Mathematische Zeitschrift* **72** (1959) 379.
- [211] R. N. Lee, *Reducing differential equations for multiloop master integrals*, *JHEP* **04** (2015) 108 [1411.0911].
- [212] R. N. Lee, *Libra: A package for transformation of differential systems for multiloop integrals*, *Comput. Phys. Commun.* **267** (2021) 108058 [2012.00279].
- [213] O. Gituliar and V. Magerya, *Fuchsia: a tool for reducing differential equations for Feynman master integrals to epsilon form*, *Comput. Phys. Commun.* **219** (2017) 329 [1701.04269].
- [214] M. Prausa, *epsilon: A tool to find a canonical basis of master integrals*, *Comput. Phys. Commun.* **219** (2017) 361 [1701.00725].
- [215] C. Sabbah, *Lieu des pôles d'un système holonome d'équations aux différences finies*, *Bulletin de la Société Mathématique de France* **120** (1992) 371.
- [216] M. Jamin and R. Miravitllas, *Absence of even-integer  $\zeta$ -function values in Euclidean physical quantities in QCD*, *Phys. Lett. B* **779** (2018) 452 [1711.00787].
- [217] P. A. Baikov and K. G. Chetyrkin, *The structure of generic anomalous dimensions and no- $\pi$  theorem for massless propagators*, *JHEP* **06** (2018) 141 [1804.10088].

- [218] J. Davies and A. Vogt, *Absence of  $\pi^2$  terms in physical anomalous dimensions in DIS: Verification and resulting predictions*, *Phys. Lett. B* **776** (2018) 189 [1711.05267].
- [219] W. L. van Neerven and A. Vogt, *Nonsinglet structure functions beyond the next-to-next-to-leading order*, *Nucl. Phys. B* **603** (2001) 42 [hep-ph/0103123].
- [220] F. Herzog, S. Moch, B. Ruijl, T. Ueda, J. A. M. Vermaseren and A. Vogt, *Five-loop contributions to low- $N$  non-singlet anomalous dimensions in QCD*, *Phys. Lett. B* **790** (2019) 436 [1812.11818].
- [221] F. Herzog and B. Ruijl, *The  $R^*$ -operation for Feynman graphs with generic numerators*, *JHEP* **05** (2017) 037 [1703.03776].
- [222] J. A. Gracey, *Anomalous dimension of nonsinglet Wilson operators at  $O(1/N(f))$  in deep inelastic scattering*, *Phys. Lett. B* **322** (1994) 141 [hep-ph/9401214].
- [223] T. Gehrmann and E. Remiddi, *Numerical evaluation of harmonic polylogarithms*, *Comput. Phys. Commun.* **141** (2001) 296 [hep-ph/0107173].
- [224] S. Moch, J. A. M. Vermaseren and A. Vogt, *Higher-order corrections in threshold resummation*, *Nucl. Phys. B* **726** (2005) 317 [hep-ph/0506288].
- [225] G. Das, S.-O. Moch and A. Vogt, *Soft corrections to inclusive deep-inelastic scattering at four loops and beyond*, *JHEP* **03** (2020) 116 [1912.12920].
- [226] S. Moch and A. Vogt, *On non-singlet physical evolution kernels and large- $x$  coefficient functions in perturbative QCD*, *JHEP* **11** (2009) 099 [0909.2124].
- [227] G. Grunberg, *Large- $x$  structure of physical evolution kernels in Deep Inelastic Scattering*, *Phys. Lett. B* **687** (2010) 405 [0911.4471].
- [228] A. A. Almasy, G. Soar and A. Vogt, *Generalized double-logarithmic large- $x$  resummation in inclusive deep-inelastic scattering*, *JHEP* **03** (2011) 030 [1012.3352].
- [229] S. Moch and A. Vogt, *Threshold Resummation of the Structure Function  $F(L)$* , *JHEP* **04** (2009) 081 [0902.2342].

- 
- [230] J. Davies, C. H. Kom, S. Moch and A. Vogt, *Resummation of small- $x$  double logarithms in QCD: inclusive deep-inelastic scattering*, *JHEP* **08** (2022) 135 [2202.10362].
- [231] A. Retey and J. A. M. Vermaseren, *Some higher moments of deep inelastic structure functions at next-to-next-to-leading order of perturbative QCD*, *Nucl. Phys. B* **604** (2001) 281 [hep-ph/0007294].
- [232] A. Vogt, F. Herzog, S. Moch, B. Ruijl, T. Ueda and J. A. M. Vermaseren, *Anomalous dimensions and splitting functions beyond the next-to-next-to-leading order*, *PoS* **LL2018** (2018) 050 [1808.08981].
- [233] E. Panzer, *Algorithms for the symbolic integration of hyperlogarithms with applications to Feynman integrals*, *Comput. Phys. Commun.* **188** (2015) 148 [1403.3385].
- [234] A. I. Davydychev and M. Kalmykov, *New results for the epsilon expansion of certain one, two and three loop Feynman diagrams*, *Nucl. Phys. B* **605** (2001) 266 [hep-th/0012189].
- [235] A. I. Davydychev and M. Kalmykov, *Some remarks on the epsilon expansion of dimensionally regulated Feynman diagrams*, *Nucl. Phys. B Proc. Suppl.* **89** (2000) 283 [hep-th/0005287].
- [236] M. Kalmykov and A. Sheplyakov, *lsjk - a C++ library for arbitrary-precision numeric evaluation of the generalized log-sine functions*, *Comput. Phys. Commun.* **172** (2005) 45 [hep-ph/0411100].
- [237] S. A. Larin and J. A. M. Vermaseren, *The  $\alpha_s^{**3}$  corrections to the Bjorken sum rule for polarized electroproduction and to the Gross-Llewellyn Smith sum rule*, *Phys. Lett. B* **259** (1991) 345.
- [238] S. A. Larin, *The Renormalization of the axial anomaly in dimensional regularization*, *Phys. Lett. B* **303** (1993) 113 [hep-ph/9302240].
- [239] N. N. Bogoliubov and O. S. Parasiuk, *On the Multiplication of the causal function in the quantum theory of fields*, *Acta Math.* **97** (1957) 227.
- [240] K. Hepp, *Proof of the Bogolyubov-Parasiuk theorem on renormalization*, *Commun. Math. Phys.* **2** (1966) 301.
- [241] W. Zimmermann, *Convergence of Bogolyubov's method of renormalization in momentum space*, *Commun. Math. Phys.* **15** (1969) 208.

- [242] D. A. Akyeampong and R. Delbourgo, *Dimensional regularization, abnormal amplitudes and anomalies*, *Nuovo Cim. A* **17** (1973) 578.
- [243] K. G. Chetyrkin, A. L. Kataev and F. V. Tkachov, *New Approach to Evaluation of Multiloop Feynman Integrals: The Gegenbauer Polynomial  $x$  Space Technique*, *Nucl. Phys. B* **174** (1980) 345.